

# University of Southampton Research Repository

Copyright © and Moral Rights for this thesis and, where applicable, any accompanying data are retained by the author and/or other copyright owners. A copy can be downloaded for personal non-commercial research or study, without prior permission or charge. This thesis and the accompanying data cannot be reproduced or quoted extensively from without first obtaining permission in writing from the copyright holder/s. The content of the thesis and accompanying research data (where applicable) must not be changed in any way or sold commercially in any format or medium without the formal permission of the copyright holder/s.

When referring to this thesis and any accompanying data, full bibliographic details must be given, e.g.

Thesis: Author (Year of Submission) "Full thesis title", University of Southampton, name of the University Faculty or School or Department, PhD Thesis, pagination.

Data: Author (Year) Title. URI [dataset]

# University of Southampton

Faculty of Medicine

Human Development and Health

**Does accelerated epigenetic ageing predict accelerated future musculoskeletal ageing?**

by

**Nicholas Rubek Fuggle MBBS BSc MRCP(UK) PGCert HBE**

**Student number: 30652707**

ORCID ID: 0000-0001-5463-2255

Thesis for the degree of Doctor of Philosophy

September 2021

# University of Southampton

## Abstract

Faculty of Medicine  
Human Development and Health  
Thesis for the degree of Doctor of Philosophy

### **Does accelerated epigenetic ageing predict accelerated future musculoskeletal ageing?**

By  
**Nicholas Rubek Fuggle**

The ability to predict those at risk of more rapid musculoskeletal ageing is vital if therapeutic strategies are to be successful. Precise description of the ageing musculoskeletal phenotype combined with the mapping of epigenetic changes, specifically those within the DNA methylome, enable precise age prediction and 'epigenetic clocks' have been formulated to capture 'biological' ageing. With this in mind, the broad aims of my thesis are:

- To describe the longitudinal change in bone microarchitecture and muscle strength
- To investigate the association between baseline epigenetic age acceleration and musculoskeletal outcomes
- To identify novel epigenetic marks which are associated with key musculoskeletal indices of grip strength and bone mineral density through Epigenome-Wide Association Study

This thesis is focused on the Hertfordshire Cohort Study (HCS); a group of community-dwelling, older adults in which baseline blood samples are available for epigenetic analysis. In 2017 I led a musculoskeletal phenotyping pass of the cohort including grip dynamometry, dual-energy X-ray absorptiometry (DXA) and High Resolution peripheral quantitative computed tomography (HR-pQCT) to complement the same assessments which had previously been performed in 2011-12. Longitudinal change in HR-pQCT parameters, grip strength and hip bone mineral density was analysed and the determinants of HR-pQCT parameter change were examined. Using DNA from whole blood leukocytes at HCS baseline (1998-2004) DNA methylation was measured and epigenetic age acceleration calculated (HorvathAge, GrimAge and PhenoAge). The relationship between epigenetic age acceleration at baseline (1998-2004) and musculoskeletal phenotype was examined. In additional exploratory analyses an epigenome-wide approach was utilised to elucidate specific CpG sites associated with cross-sectional grip strength and total femoral neck bone mineral density.

Baseline values of HR-pQCT parameters and greater decline in trabecular Bone Mineral Density (BMD) were associated with fracture and change in trabecular BMD was associated with a single-nucleotide polymorphism (SNP) in the *WNT16* gene ( $\beta = -0.28$  (-0.50,-0.07),  $p=0.011$ ). Greater epigenetic age acceleration, as calculated via the new iterations of the epigenetic clocks (in particular GrimAge), was associated with lower maximum grip strength ( $\beta = -1.25$  (-2.24,-0.26),  $p<0.02$ ) and gait speed ( $\beta = (-0.04$  (-0.09,-0.00),  $p<0.05$ ) at multiple time points in males. In epigenome-wide analyses, methylation of a CpG site proximal to *ECE1* was associated with maximum grip strength (adjusted  $p<0.05$ ) and biologically plausible pathways including those governing the regulation of the actin cytoskeleton were significantly associated with total femoral neck bone mineral density ( $p<0.05$ ).

These findings are largely hypothesis building and require further investigation and replication. However, they do add to our current understanding of skeletal changes associated with ageing, the ability of epigenetic clocks to predict future musculoskeletal phenotypes and identify novel loci of methylation which are associated with musculoskeletal ageing.

# Table of Contents

<b>Table of Contents</b> .....	<b>iii</b>
<b>List of Figures</b> .....	<b>ix</b>
<b>List of Photographs</b> .....	<b>xii</b>
<b>Appendix Tables and Figures</b> .....	<b>xiii</b>
<b>Research Thesis: Declaration of Authorship</b> .....	<b>xvi</b>
<b>My contribution to this work</b> .....	<b>xvii</b>
<b>Acknowledgements</b> .....	<b>xix</b>
<b>Definitions and Abbreviations</b> .....	<b>xx</b>
<b>Chapter 1 Introduction</b> .....	<b>1</b>
1.1 Summary of the project .....	1
1.1.1 Introduction .....	1
1.2 Musculoskeletal ageing .....	1
1.2.1 Sarcopenia .....	1
1.2.2 Osteoporosis .....	4
1.2.3 Fractures .....	7
1.3 Literature review process .....	8
1.4 Skeletal scanning .....	9
1.4.1 Dual X-ray Absorptiometry .....	10
1.4.2 Development of High Resolution Peripheral Quantitative Computed Tomography .....	11
1.5 Epigenetic ageing .....	17
1.5.1 Ageing .....	17
1.5.2 Epigenetics .....	17
1.5.3 Methylation .....	18
1.5.4 Epigenetic clocks .....	20
1.5.5 Associations of epigenetic age acceleration with clinical outcomes .....	22
1.5.6 Musculoskeletal EWAS .....	25
1.6 Aims and purpose .....	27

1.7	Potential outcomes and wider impact.....	27
<b>Chapter 2</b>	<b>Methods.....</b>	<b>29</b>
2.1	Hertfordshire Cohort Study .....	29
2.2	Procedures .....	32
2.2.1	Height and weight measurements .....	32
2.2.2	Gait speed .....	33
2.2.3	JAMAR Grip Strength Dynamometry .....	33
2.2.4	Questionnaires.....	33
2.2.5	Dual X-ray absorptiometry.....	34
2.2.6	High resolution peripheral quantitative computed tomography (HR-pQCT)..	35
2.2.7	Peripheral quantitative Computed Tomography (pQCT) .....	38
2.3	Genetic analyses for bone microarchitecture .....	38
2.4	Epigenetic preparation and analyses.....	39
2.4.1	Overview of epigenetic methods.....	39
2.4.2	450k Methylation arrays.....	41
2.4.3	EPIC (850k) Methylation arrays .....	41
2.4.4	Quality Control of array data .....	42
2.4.5	Methylation clocks.....	50
2.4.6	Statistical analyses .....	51
<b>Chapter 3</b>	<b>Results.....</b>	<b>61</b>
3.1	Description of change in musculoskeletal parameters with ageing and associations with fracture and genetic loci .....	61
3.1.1	Participant characteristics .....	62
3.1.2	Associations between bone microarchitecture and previous fracture .....	63
3.1.3	Associations between baseline values and changes in tibial HR-pQCT parameters and previous fracture .....	66
3.1.4	Selected loci in relation to tibial HR-pQCT parameters that were associated with previous fracture .....	69
3.1.5	Description of change in maximum grip strength from HBS11-12 to HBS17..	71
3.1.6	Description of change in total femoral BMD from HBS11-12 to HBS17.....	71
3.1.7	Associations of grip strength and total femoral BMD with fracture .....	71
3.1.8	Sensitivity analyses .....	72

3.1.9	Results summary .....	72
3.2	Associations between epigenetic age acceleration and musculoskeletal parameters .....	74
3.2.1	The cohort .....	74
3.2.2	Epigenetic age .....	77
3.2.3	Epigenetic age acceleration .....	80
3.2.4	Epigenetic age acceleration vs muscle outcomes.....	81
3.2.5	Epigenetic age acceleration vs DXA bone mineral density outcomes .....	87
3.2.6	Epigenetic age acceleration vs HR-pQCT .....	89
3.2.7	Epigenetic age vs body composition .....	90
3.2.8	Sensitivity analyses.....	91
3.2.9	Results summary .....	92
3.3	EWAS of maximum grip strength and total femoral neck BMD .....	94
3.3.1	Demographics.....	94
3.3.2	EWAS model description .....	96
3.3.3	Inflation .....	99
3.3.4	EWAS results: maximum grip strength .....	99
3.3.5	Pathway and gene ontology for maximum grip strength .....	102
3.3.6	Total femoral neck bone mineral density .....	104
3.3.7	Summary results.....	111
<b>Chapter 4</b>	<b>Discussion.....</b>	<b>113</b>
4.1	Change in musculoskeletal parameters with ageing .....	113
4.1.1	Change in bone microarchitecture.....	113
4.1.2	Change in grip strength .....	114
4.1.3	Change in bone mineral density at the femoral neck .....	114
4.1.4	Associations of musculoskeletal ageing parameters with odds of fracture ..	115
4.2	Epigenetic Age Acceleration.....	116
4.2.1	Differences in epigenetic clocks between 450k array and 850k array .....	117
4.2.2	Observed differences between clocks .....	118

4.2.3	GrimAge acceleration and muscle outcome in males .....	119
4.2.4	Epigenetic age acceleration and increased tissue measures in females.....	121
4.2.5	Associations of epigenetic age acceleration with bone outcomes .....	121
4.3	Epigenome-wide association studies (EWAS).....	123
4.3.1	Maximum grip strength EWAS.....	123
4.3.2	Total femoral neck bone mineral density EWAS .....	130
4.4	Strengths and weaknesses.....	133
4.5	Overall implications of this research .....	134
4.5.1	Findings in relation to osteoporosis .....	135
4.5.2	Findings in relation to sarcopenia.....	136
4.6	Summary of findings .....	136
4.7	Future work.....	137
4.8	Conclusion.....	138
	<b>Outputs from doctoral research period .....</b>	<b>140</b>
4.8.1	Publications.....	140
4.8.2	Conference abstracts .....	142
	<b>List of References .....</b>	<b>191</b>



## List of Tables

<b>Table 1:</b> The characteristics of the Horvath, GrimAge and PhenoAge epigenetic clocks.....	21
<b>Table 2:</b> Sample name and XY difference for the 7 sex detection outliers. ....	46
<b>Table 3:</b> Lowest (most extreme) mean absolute deviation scores for methylation and corresponding samples.....	50
<b>Table 4:</b> EWAS model and covariates included in adjustment .....	57
<b>Table 5:</b> Descriptive statistics for participant characteristics in 2011-2012 <sup>220</sup> .....	63
<b>Table 6:</b> Descriptive statistics for <i>tibial</i> HR-pQCT parameters at baseline (2011-2012) and for changes in parameters from EPOSA to HBS17 <sup>220</sup> .....	65
<b>Table 7:</b> Odds ratios for previous fracture per standard deviation difference in both baseline values and changes in parameters <sup>220</sup> .....	68
<b>Table 8:</b> Selected loci in relation to tibial HR-pQCT parameters that were associated with previous fracture <sup>220</sup> .....	70
<b>Table 9:</b> Baseline demographic data.....	75
<b>Table 10:</b> Baseline lifestyle data. ....	76
<b>Table 11:</b> EPOSA and HBS17 musculoskeletal and body composition outcomes. ....	77
<b>Table 12:</b> Summary statistics for chronological age, HorvathAge, PhenoAge and GrimAge .....	78
<b>Table 13:</b> Epigenetic age acceleration summary statistics .....	80
<b>Table 14:</b> Epigenetic age acceleration Z-scores summary statistics.....	81
<b>Table 15:</b> Regression coefficients and p-values for associations between GrimAge Acceleration and maximum grip strength and gait speed measured at HCS baseline (1998-2004), EPOSA (2011-12) and HBS17 (2017).....	82
<b>Table 16:</b> Summary and descriptive statistics for the 334 participants included in the epigenome- wide analyses.....	96
<b>Table 17:</b> EWAS models and covariates included in adjustment .....	97

<b>Table 18:</b> Levels of genomic inflation for each model in each EWAS. ....	99
<b>Table 19:</b> The five CpG sites with the lowest p-values (and thus highest significance) for the model 2 EWAS of maximum grip strength. ....	100
<b>Table 20:</b> The five CpG sites with the lowest p-values (and thus highest significance) for the model 3 EWAS of maximum grip strength. ....	101
<b>Table 21:</b> The five CpG sites with the lowest p-values (and thus highest significance) for the model 4 EWAS of maximum grip strength .....	101
<b>Table 22:</b> The five most significant molecular function gene ontologies for maximum grip strength model 4.....	104
<b>Table 23:</b> The five CpG sites with the lowest p-values (and thus highest significance) for the model 2 EWAS of total hip bone mineral density. ....	105
<b>Table 24:</b> The five CpG sites with the lowest p-values (and thus highest significance) for the model 3 EWAS of total hip bone mineral density. ....	105
<b>Table 25:</b> The five CpG sites with the lowest p-values (and thus highest significance) for the model 4 EWAS of total hip bone mineral density. ....	105
<b>Table 26:</b> The <i>biological function</i> gene ontology for the genes associated with CpG sites with a $p < 1 \times 10^{-5}$ in model 2 EWAS for total femoral neck BMD.....	109
<b>Table 27:</b> The <i>human phenotype</i> gene ontology for the genes associated with CpG sites with a $p < 1 \times 10^{-5}$ in model 2 EWAS for total femoral neck BMD.....	109
<b>Table 28:</b> showing the mean (and standard deviation) chronological, HorvathAge, PhenoAge and GrimAge for epidemiological studies. ....	118

## List of Figures

<b>Figure 1:</b> The lifecourse trends and trajectories for grip strength in males and females. ....	3
<b>Figure 2:</b> Graph mapping bone mass over the lifecourse for males and females. ....	5
<b>Figure 3:</b> Age-specific incidence of radiographic vertebral, hip, and wrist (distal forearm) fractures in men and women. ....	6
<b>Figure 4:</b> Bone structure. ....	9
<b>Figure 5:</b> Timeline of skeletal scanning modalities. ....	10
<b>Figure 6:</b> Flow diagram of study participant structure of the Hertfordshire Cohort Study. ....	31
<b>Figure 7:</b> Timeline depicting the timings of follow-up visits and methylation samples, questionnaire data and musculoskeletal measures ....	32
<b>Figure 8:</b> This plot depicts the difference between median X and Y chromosome intensities in the 450k array. Dashed lines represent 5 standard deviations from the mean XY difference. Females should appear within the left cluster and males in the right cluster. As can be seen there are no mismatches and no sex difference outliers. .....	43
<b>Figure 9:</b> Plot demonstrating the methylation intensity signals in the 450k array against unmethylation intensity signals. ....	44
<b>Figure 10:</b> Schematic demonstrating the quality control process and exclusion of samples from the 450k dataset .....	45
<b>Figure 11:</b> Plot depicting the difference between median X and Y chromosome intensities in the 850k array. ....	47
<b>Figure 12:</b> Plot demonstrating the methylation intensity signals in the 850k array against unmethylation intensity signals. ....	48
<b>Figure 13:</b> Schematic demonstrating the quality control process and exclusion of samples from the 850k dataset .....	50
<b>Figure 14:</b> Timelines for the HRpQCT, maximum grip strength and DXA BMD parameters examined in this chapter. ....	61

<b>Figure 15:</b> Odds of fracture for level and change of musculoskeletal parameters. ....	67
<b>Figure 16:</b> A histogram depicting the distribution of frequency density of HorvathAge (DNAMAge in years) in the 450k and 850k arrays combined. ....	79
<b>Figure 17:</b> A histogram depicting the distribution of frequency density of HorvathAge (DNAMAge in years) in the 450k and 850k arrays separately.....	79
<b>Figure 18:</b> Schema showing the timing of the clock exposure and musculoskeletal outcomes for this section .....	81
<b>Figure 19:</b> Mean and 95% confidence intervals for maximum grip strength against GrimAge acceleration quartiles in males at EPOSA (2011-12). ....	83
<b>Figure 20:</b> Mean and 95% confidence intervals for gait speed against GrimAge acceleration quartiles in males at HBS17 (2017) .....	84
<b>Figure 21:</b> Musculoskeletal variable Z-scores at EPOSA and HBS17 timepoints in males, associations with GrimAge acceleration. ....	84
<b>Figure 22:</b> Change in musculoskeletal variable Z-scores at EPOSA and HBS17 timepoints in males and females, associations with GrimAge acceleration.....	85
<b>Figure 23:</b> Schema showing the timing of the clock exposure and musculoskeletal outcomes for this section .....	87
<b>Figure 24:</b> Schema showing the timing of the clock exposure and musculoskeletal outcomes for this section .....	90
<b>Figure 25:</b> Schema showing the timing of the clock exposure and musculoskeletal outcomes for this section .....	90
<b>Figure 26:</b> A directed acyclic graph demonstrating the relationship between GrimAge acceleration, fat mass and change in total femoral neck bone mineral density .....	93
<b>Figure 27:</b> Schema showing the timing of the clock exposure and musculoskeletal outcomes for this section .....	94
<b>Figure 28:</b> Histogram of maximum grip strength. ....	98
<b>Figure 29:</b> Histogram of dietary calcium intake. ....	98
<b>Figure 30:</b> Manhattan plot for the EWAS of maximum grip strength in model 2 .....	100

<b>Figure 31:</b> Network analysis of human phenotype gene ontology (for model 4 maximum grip strength EWAS CpG sites with $p < 1 \times 10^{-5}$ (n=10 genes)).	104
<b>Figure 32</b> The KEGG phospholipase D signalling pathway with proteins expressed from genes associated with the top 100 CpG sites associated with femoral neck BMD EWAS model 2 (highlighted in red).	107
<b>Figure 33:</b> The KEGG actin cytoskeleton regulation pathway with proteins expressed from genes associated with the top 100 CpG sites associated with femoral neck BMD EWAS model 2 (highlighted in red).	108
<b>Figure 34:</b> Manhattan plot demonstrating the level of significance for the association between human phenotypes and the genes associated with the top 100 CpG sites associated with femoral neck BMD EWAS model 2.	110
<b>Figure 35:</b> Schematic demonstrating the flow between an association between reduced methylation at cg00960509 and higher grip strength.	124
<b>Figure 36:</b> Schema depicting the hypothesised mechanism of association between lower methylation at cg00960509 and higher grip strength.	125
<b>Figure 37:</b> The purine metabolic pathway.	128

## List of Photographs

**Photograph 1:** A Hertfordshire Cohort participant undergoing a whole-body DXA in 2017 ..... 35

**Photograph 2:** A Hertfordshire Cohort participant undergoing a radial HR-pQCT in 2017 ..... 36

## Appendix Tables and Figures

<b>Appendix 1:</b> Literature review of change in bone microarchitecture. Note that not all papers quoted in this table directly relate to the research aims of this doctoral thesis but all were examined as part of a wider literature review. ....	147
<b>Appendix 2:</b> 2017 Hertfordshire Bone Study (HBS17) participant information leaflet.....	153
<b>Appendix 3:</b> Consent form for the 2017 Hertfordshire Bone Study (HBS17).....	154
<b>Appendix 4:</b> Ethical approval for 2017 visit of the Hertfordshire Bone Study (HBS17) .....	155
<b>Appendix 5:</b> HBS17 Questionnaire and physical performance data collection sheet.....	157
<b>Appendix 6:</b> Descriptive statistics for radial HR-pQCT parameters at baseline (2011-2012) and for changes in parameters from EPOSA to HBS17 <sup>220</sup> .....	165
<b>Appendix 7:</b> Odds ratios for previous fracture per standard deviation difference in both baseline values and changes in parameters at the radius <sup>220</sup> .....	166
<b>Appendix 8:</b> Odds ratios for previous fracture per standard deviation difference in both baseline values and changes in parameters for fully-adjusted models and those additionally adjusted for bisphosphonate usage. ....	167
<b>Appendix 9:</b> Odds of fracture associated with Z-scores of baseline and percentage change in grip strength and baseline and percentage change in femoral neck BMD. ....	168
<b>Appendix 10:</b> Histograms for epigenetic age acceleration distribution for HorvathAge acceleration, PhenoAge acceleration and GrimAge acceleration within the 450k (left) and 850k (right) arrays.....	169
<b>Appendix 11:</b> Density plots depicting the distribution of epigenetic age and chronological age (A) and epigenetic age acceleration measures (B).....	170
<b>Appendix 12:</b> Regression coefficients and p-values for associations between <b>PhenoAge</b> Acceleration and maximum grip strength and gait speed measured at HCS baseline (1998-2004), EPOSA (2011-12) and HBS17 (2017).....	171

<b>Appendix 13:</b> Regression coefficients and p-values for associations between <b>HorvathAge</b> Acceleration and maximum grip strength and gait speed measured at HCS baseline (1998-2004), EPOSA (2011-12) and HBS17 (2017).....	172
<b>Appendix 14:</b> Regression coefficients and p-values for associations between epigenetic age acceleration measures and percentage and absolute change in gait speed between EPOSA (2011-12) and HBS17 (2017). .....	173
<b>Appendix 15:</b> Regression coefficients and p-values for associations between epigenetic age acceleration measures and percentage and absolute change in gait speed from HCS baseline (1998-2004) to EPOSA (2011-12, upper table) or HBS17 (2017, lower table). .....	174
<b>Appendix 16:</b> GrimAge acceleration associations with total spine, total femoral and total femoral neck BMD .....	175
<b>Appendix 17:</b> PhenoAge acceleration associations with total spine, total femoral and total femoral neck BMD .....	176
<b>Appendix 18:</b> HorvathAge acceleration associations with total spine, total femoral and total femoral neck BMD.....	177
<b>Appendix 19:</b> Epigenetic age acceleration associations with total femoral neck BMD at baseline (BL), EPOSA and HBS17 and percentage change between baseline and HBS17 and EPOSA and HBS17 in sex-stratified analyses fully- adjusted for age, height and BMI, social class, physical activity, dietary calcium, ever smoking regularly and alcohol consumption. Change analyses were additionally adjusted for follow-up time. Fully-adjusted models with the additional adjusted of bisphosphonate usage are shown on the right.....	178
<b>Appendix 20:</b> Epigenetic age acceleration associations with total femoral BMD at baseline (BL), EPOSA and HBS17 and percentage change between baseline and HBS17 and EPOSA and HBS17 in sex-stratified analyses fully- adjusted for age, height and BMI, social class, physical activity, dietary calcium, ever smoking regularly and alcohol consumption. Change analyses were additionally adjusted for follow-up time. Fully-adjusted models with the additional adjusted of bisphosphonate usage are shown on the right. BL = baseline.....	179
<b>Appendix 21:</b> Age acceleration associations with bone microarchitecture outcomes (trabecular density, volumetric BMD and cortical thickness).....	180



<b>Appendix 22:</b> Age acceleration associations with pQCT cortical thickness at the 14%, 38% and 66% slices.....	181
<b>Appendix 23:</b> Age acceleration associations with change in bone microarchitecture .....	182
<b>Appendix 24:</b> Associations between epigenetic age acceleration variable and appendicular lean mass (ALM) at the EPOSA (2011-12) and HBS17 (2017) timepoints. ....	183
<b>Appendix 25:</b> Associations between epigenetic age acceleration variable and total fat mass at the EPOSA (2011-12) and HBS17 (2017) timepoints.....	184
<b>Appendix 26:</b> Table demonstrating the associations between PhenoAge acceleration and musculoskeletal outcomes with the outlier for PhenoAge included (on the left) and excluded (on the right). The outlier was a male so only sex-specific, male analyses are shown for unadjusted and fully adjusted analyses. Statistically significant results are highlighted in red. ....	185
<b>Appendix 27:</b> Genome browser output demonstrating the location of the cg00960509 and the geographic location in a CpG island associated the 5' end of the gene <i>ECE1</i> on chromosome 1.....	187
<b>Appendix 28:</b> Genome browser output demonstrating the location of the cg02389067 lying in a CpG island at in the promoter region at the 5' end of <i>GNA13</i> on chromosome 17 .....	188
<b>Appendix 29:</b> Genes associated with the 100 CpG sites with the lowest p-values associated with the maximum grip strength in model 2 EWAS .....	189
<b>Appendix 30:</b> Genes associated with the 100 CpG sites with the lowest p-values associated with the maximum grip strength in model 4 EWAS. ....	190

# Research Thesis: Declaration of Authorship

**Print name:** Dr Nicholas Rubek Fuggle

**Title of thesis:** Does accelerated epigenetic ageing predict accelerated future musculoskeletal ageing?

I declare that this thesis and the work presented in it is my own and has been generated by me as the result of my own original research.

I confirm that:

1. This work was done wholly or mainly while in candidature for a research degree at this University
2. Where any part of this thesis has previously been submitted for a degree or any other qualification at this University or any other institution, this has been clearly stated; where I have consulted the published work of others, this is always clearly attributed; where I have quoted from the work of others, the source is always given. With the exception of such quotations, this thesis is entirely my own work
3. I have acknowledged all main sources of help
4. Where the thesis is based on work done by myself jointly with others, I have made clear exactly what was done by others and what I have contributed myself
5. Parts of this work have been published as:

**Fuggle NR**, Westbury LD, Bevilacqua G, Titcombe P, Ó Breasail M, Harvey NC, Dennison EM, Cooper C, Ward KA. Level and change in bone microarchitectural parameters and their relationship with previous fracture and established bone mineral density loci. *Bone*. 2021 Jun;147:115937. doi: 10.1016/j.bone.2021.115937. Epub 2021 Mar 22. PMID: 33766802.

**Signature:**

**Date:** 1<sup>st</sup> September 2021

## **My contribution to this work**

I have been involved in this project from conception to completion. I composed the ethics application including study protocol, participant information leaflet, consent forms and study questionnaires and submitted them to the East of England, Cambridgeshire and Hertfordshire, Research Ethics Committee. This provided me with further experience of laying the foundations for a research project and honing the primary research questions to be answered.

I successfully applied to the Dunhill Medical Trust for a research fellowship in order to fund this doctoral research project, which included the preparation of the grant application form and financial costings for the project.

Together with Professor Kate Ward, who at that point was primarily based at the MRC Elsie Widdowson Laboratory in Cambridge, I arranged the logistics of participant attendance and performed the physical performance assessments, DXA and HRpQCT scanning and supervised the team of research assistants. Through this I gained experience in the operation of the scanning technology and downstream processing.

I arranged the preparation of the DNA samples and plate preparation. I coordinated the shipping to Professor Michael Kobor at the University of British Columbia, including legal and financial arrangements, for methylation microarray.

A substantial proportion of my development during this doctoral research project has been in the arena of bioinformatics including the utilisation of STATA and R, the management of datasets within these statistical programmes, familiarisation with bioinformatic packages and commands and the conducting of the analyses themselves. I would like to particularly acknowledge the training provided on the University of Bristol Epigenetic Epidemiology Course and the advice provided by Dr Chris Bell and Professor John Holloway's group (especially Negusse Kitaba and Faisal Rezwan). In particular, Negusse Kitaba assisted greatly in performing methylation pre-processing, normalisation and EWAS of the EPIC array data.

I have also trained and developed in my epidemiology and statistical skills through the London School of Hygiene and Tropical Medicine Post-Graduate Certificate in Epidemiology which I am undertaking and through the supervision and teaching of statisticians within the MRC Lifecourse Epidemiology Centre, in particular Leo Westbury. Genomic data were previously processed by Dr Phillip Titcombe and Leo Westbury.

These gained experiences and expertise have equipped me to continue to pursue a career in academia.

## Acknowledgements

I would like to thank my supervisors Professors Cyrus Cooper, Elaine Dennison, Keith Godfrey and Christopher Bell. Their insight, instruction and training have been integral to my development and have made this project possible.

I would like to thank Professor Kate Ward for her oversight, supervision and training when collecting the data at the MRC Elsie Widdowson Laboratory at the University of Cambridge, and Micheal O'Breasail for his training and assistance in performing the skeletal scanning and Gregorio Bevilaqua for his assistance in preparing the scan data for analysis.

In addition to Dr Christopher Bell, I would like to thank Professor John Holloway, Faisal Rezwan and Negusse Kitaba for their bioinformatic expertise, teaching and assistance in formulating and performing the methylation analyses. Thank you to Leo Westbury for his statistical supervision and Phillip Titcombe for his previous work on the genomic data within the Hertfordshire Cohort.

Thank you to Professor Karen Lillycrop and the Epigen Consortium for hosting me at their meetings which have taught me so much about the bioinformatics of methylation analyses.

Thank you to the members of the Hertfordshire Cohort Study for attending the research visits in 2017 and for their immense contribution over the last 20 years.

Finally, I would like to thank my family for their support and encouragement.

## Definitions and Abbreviations

450k array	A methylation microarray measuring methylation at 450,000 CpG sites
850k array	A methylation microarray measuring methylation at 850,000 CpG sites
<i>ACE</i>	Angiotensin-converting Enzyme gene
<i>AHRR</i>	Aryl-Hydrocarbon Receptor Repressor gene
BMC	Bone mineral content
BMD	Bone mineral density
BMI	Body Mass Index
CaMOS	Canadian Multicentre Osteoporosis Study
CI	Confidence interval
CpG	Cytosine (C) adjacent to a Guanine (G) bound by a phosphate backbone (p)
CNTNAP2	Contactin Associated Protein 2
DNA	Deoxyribonucleic acid
DNMT	DNA methyltransferase enzymes
DXA	Dual X-ray Absorptiometry
<i>ECE1</i>	Endothelin converting enzyme-1 gene
eNOS	Endothelial nitric oxide synthase (also known as Nos3)
EPIC array	see 850k array
ET	Endothelin
ETA	Endothelin receptor A
ETB	Endothelin receptor B (including B1 and B2)
EWAS	Epigenome-Wide Association Study
EWGSOP2	European Working Group on Sarcopenia (definition version 2)

FDR	False discovery rate
FRAX®	Fracture risk assessment tool
<i>GNA13</i>	G Protein Subunit Alpha-13 gene
HBS17	Hertfordshire Bone Study 2017
HCS	Hertfordshire Cohort Study
HR-pQCT	High Resolution Peripheral Quantitative Computed Tomography
ICD-10-CM	International Classification of Disease-10 – Clinical Modification
IGF2	Insulin-like growth factor-2
KEGG	Kyoto Encyclopaedia of Genes and Genomes
MAPK	Mitogen-activated protein kinase
microSv	MicroSievert (a measure of radiation)
MRC	Medical Research Council
MRI	Magnetic-resonance imaging
MrOS	Osteoporotic Fractures in Men study
MSFU	Musculoskeletal follow-up (a pass of the Hertfordshire Cohort)
NO	Nitric oxide
NSHD	National Survey of Health and Disease
OFELY	Os des Femmes de Lyon (Bones of Women in Lyon) study
OR	Odds ratio
pQCT	Peripheral Quantitative Computed Tomography
<i>PLAG</i>	Pleomorphic adenoma gene
QCT	Quantitative Computed Tomography
RhoA	Ras Homolog Family Member A

RNAseq	Ribonucleic acid sequencing
RXR $\alpha$	Retinoid X receptor alpha
SD	Standard deviation
<i>SDK1</i>	Sidekick Cell Adhesion Molecule-1 gene
SNP	Single nucleotide polymorphism
SPA	Single Photon Absorptiometry
STRAMBO	Structure of the Aging Men's Bones study
TET	Ten-eleven translocation enzymes
TILDA	The Irish Longitudinal Study on Ageing
vBMD	Volumetric bone mineral density
WHO	World Health Organisation
<i>WNT-16</i>	Wingless-type integration family member 16 gene



# Chapter 1 Introduction

## 1.1 Summary of the project

### 1.1.1 Introduction

The deteriorating effect of ageing on bones and muscles is a cause of significant concern for the population at large and is due to grow with the rapid expansion of the elderly population<sup>1</sup>. The ability to predict those at risk of more pronounced musculoskeletal ageing is vital if therapeutic strategies are to be successful<sup>2</sup>. Therefore, a thorough understanding of changes in bone microarchitecture, grip strength and bone mineral density over time as an individual ages, and the identification of biomarkers, including epigenetic clocks<sup>3</sup>, that capture 'biological' age have the potential for significant clinical application<sup>4,5</sup>. Further exploration of the DNA methylation profiles has the potential to shape hypotheses and provide mechanistic insights which could lead to new therapeutic approaches.

## 1.2 Musculoskeletal ageing

Ageing affects all tissues including muscle and bone leading ultimately to the ageing diseases of the musculoskeletal system; sarcopenia and osteoporosis, both of which increase the risk of fractures.

### 1.2.1 Sarcopenia

The etymology of sarcopenia is from the Greek 'sarx' for muscle and 'penia' meaning 'loss'. It is a condition characterized by progressive, age-related muscle weakness<sup>6</sup> and, in September 2016, sarcopenia gained 'disease-status' as it was assigned an ICD-10-CM code (M62.84)<sup>7</sup>. Sarcopenia leads to a significant burden to the UK health economy with a recent health economic analysis estimating that sarcopenia is responsible for approximately £2.5 billion of healthcare costs each year<sup>8</sup>.

It is defined by the European Working Group on Sarcopenia (EWGSOP) as the presence of low muscle mass, reduced muscle strength and impaired physical performance<sup>9</sup>, with the most recent European definition (EWGSOP2) stating that sarcopenia is confirmed by the combination of low grip

strength and low lean mass, and sarcopenia is categorised as severe if there is additional muscle function impairment as judged by gait speed<sup>6</sup>.

A recent meta-analysis including over 50,000 individuals estimated that the global prevalence of sarcopenia was 10% in men and women<sup>10</sup>, which is concerning from a global and national health perspective as the condition is associated with a greatly increased risk of frailty, disability, premature death and falls, which, in turn, increase the risk of fracture. The incidence increases with age<sup>11</sup> with estimates of 1.6% in European individuals over a period of 4.3 years (aged 40-79 years)<sup>12</sup>, 3.4% in Chinese older adults over 4 years (mean age 72 years)<sup>13</sup> and 3.7% in English older adults (85 years)<sup>14</sup>. Indeed, another Chinese study including 4500 participants (mean age 62 years) described a steadily increasing percentage prevalence by age for < 65 years, 65–74, 75–84 and ≥ 85 years of 11.2%, 26.5%, 50.5% and 65.2%, respectively<sup>15</sup>.

Although there are different facets to sarcopenia (being strength, function and mass) we will focus largely on grip strength and gait speed, as these parameters are available at all timepoints of the Hertfordshire Cohort Study. Indeed, both are included as key elements of ‘intrinsic capacity’, a concept developed by the World Health Organisation in 2015 to consider healthy ageing not simply as the absence or presence of disease, but as the ability of an individual to perform the tasks or functions they value<sup>16</sup>.

The performance of muscle changes across the lifecourse. For example, grip strength peaks in the fourth decade (30-40 years) before a plateau or very gradual decline until the seventh decade (60-70 years) when the decline is more rapid<sup>17</sup>. This is depicted in **Figure 1** which shows the results of a meta-analysis of studies from across the lifespan and the amalgamated lifecourse trends for grip strength in the UK<sup>17</sup>.

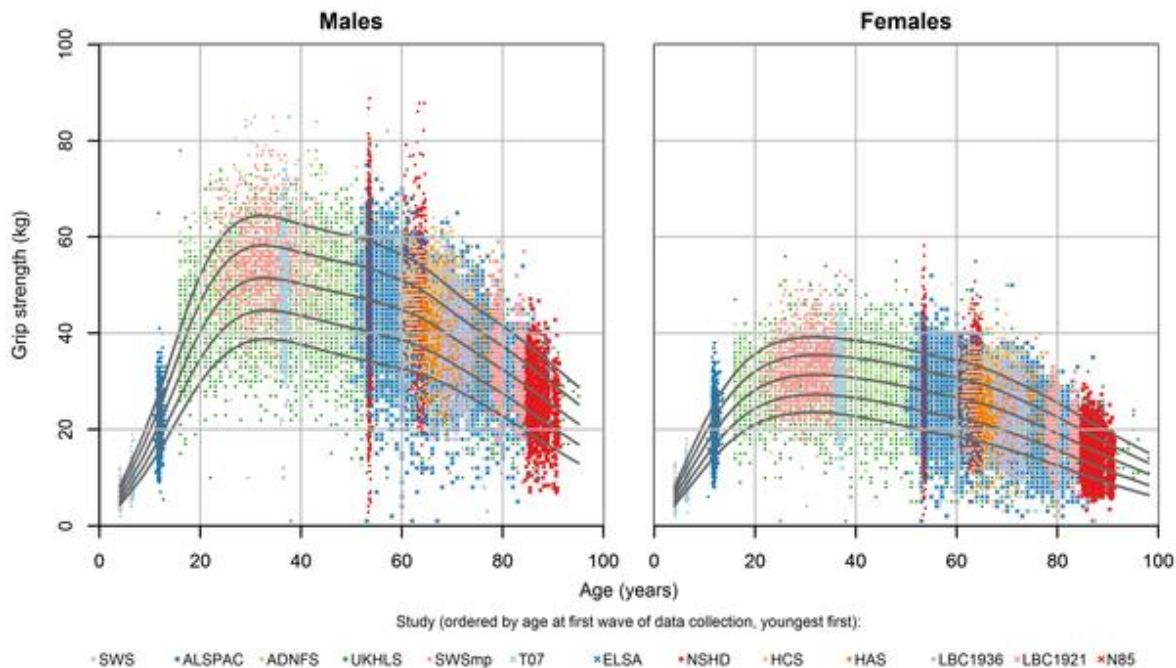


**Figure 1:** The lifecourse trends and trajectories for grip strength in males and females.

Lines are drawn for the 10<sup>th</sup>, 25<sup>th</sup>, 50<sup>th</sup>, 75<sup>th</sup> and 90<sup>th</sup> centiles. Coloured dots represent each of the constituent studies included in the meta-analysis (reproduced from Dodds and colleagues under the terms of the Creative Commons Attribution License <sup>17</sup>).

Body composition is also important to consider in individuals with sarcopenia, not least because lean mass is included in some definitions of the disease<sup>6,18,19</sup>, but also because the metabolic and inflammatory changes associated with obesity and excessive adipose tissue can lead to reduced muscle function and muscle mass<sup>20</sup>. The term to describe this subset of sarcopenia is ‘sarcopenic obesity’ and has been associated with various health outcomes including death<sup>21</sup>.

Falls are one of the key clinical sequelae for sarcopenia with a meta-analysis incorporating 45,000 individuals from 33 studies showing that sarcopenic individuals had an increased odds of falls compared to non-sarcopenic controls (for cross-sectional studies: OR 1.60 (95% CI 1.37,1.86)  $p < 0.001$ ), for prospective studies: OR 1.89 (95% CI 1.33,2.68),  $p < 0.001$ )<sup>22</sup>. Pertinently, this study also showed an increased risk of fractures in sarcopenic individuals (for cross-sectional studies OR 1.84 (95% CI 1.30,2.62)  $p = 0.001$ ; for prospective studies: OR 1.71 (95% CI 1.44,2.03),  $p = 0.011$ ) compared with non-sarcopenic individuals.

The reason for the increased risk of fractures in individuals with sarcopenia may be due to a heightened risk of falls (and therefore trauma) risk, but there may also be interplay within the muscle and bone unit. The Mechanostat hypothesis states that the forces applied through bone via muscular contraction and relaxation lead to bone remodelling in order to cope with these stresses<sup>23,24</sup>. If muscle strength is poor, this hypothesis would suggest that bone strength is also reduced. Thus, sarcopenia and osteoporosis are potentially related.

### 1.2.2 Osteoporosis

Osteoporosis is a disease characterized by the deterioration of bone microarchitecture leading to reduced bone mineral density (BMD), increased bone fragility and a greatly increased risk of fracture<sup>25</sup> as a result of even minor trauma. Bone mass is assessed using dual X-ray absorptiometry (DXA) with World Health Organization criteria defining osteopenia as a BMD between -1.0 and -2.5 standard deviations for a young healthy adult (T-score). Osteoporosis is defined as a BMD of  $\leq -2.5$  standard deviations<sup>26</sup>.

In 2010, there were 22 million females and 5.5 million males living with osteoporosis in Europe<sup>27</sup> and the disease accounts for approximately 3% of healthcare costs<sup>27</sup>. The impact of fragility fractures is estimated to increase by 23% by 2030<sup>28</sup>, due largely to the growing elderly population with over 65 year olds comprising a quarter of the total population.

Bone mass, which influences the occurrence of osteoporosis, mirrors the changes seen in muscle strength across the lifecourse, with the lifetime peak in the middle of the 4<sup>th</sup> decade and declines from approximately the 7<sup>th</sup> decade onwards<sup>29,30</sup>. The one substantial difference is the sudden, rapid decline in bone mass seen for women immediately after the age of 50 due to the menopause<sup>29</sup> (**Figure 2**). The decline in bone mass is mirrored by an increase in the prevalence of fracture, which is particularly observed as an exponential rise in hip and radiographic vertebral fractures in females, as seen **Figure 3**<sup>31</sup>.

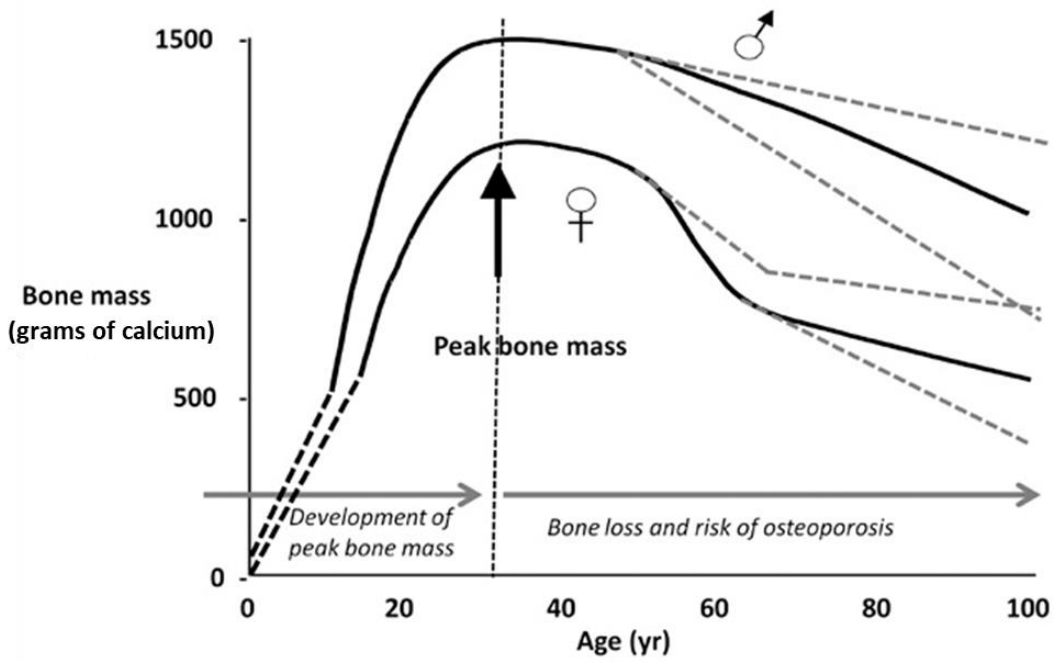


**Figure 2:** Graph mapping bone mass over the lifecourse for males and females.

Bone mass reaches peak at approximately the fourth decade and, after a period of plateau, declines into older age. Particularly marked decline is observed in females following the menopause (reproduced from Cooper and colleagues with permission, License number: 5185430644725<sup>30</sup>). g/Ca = grams of calcium, yr = years

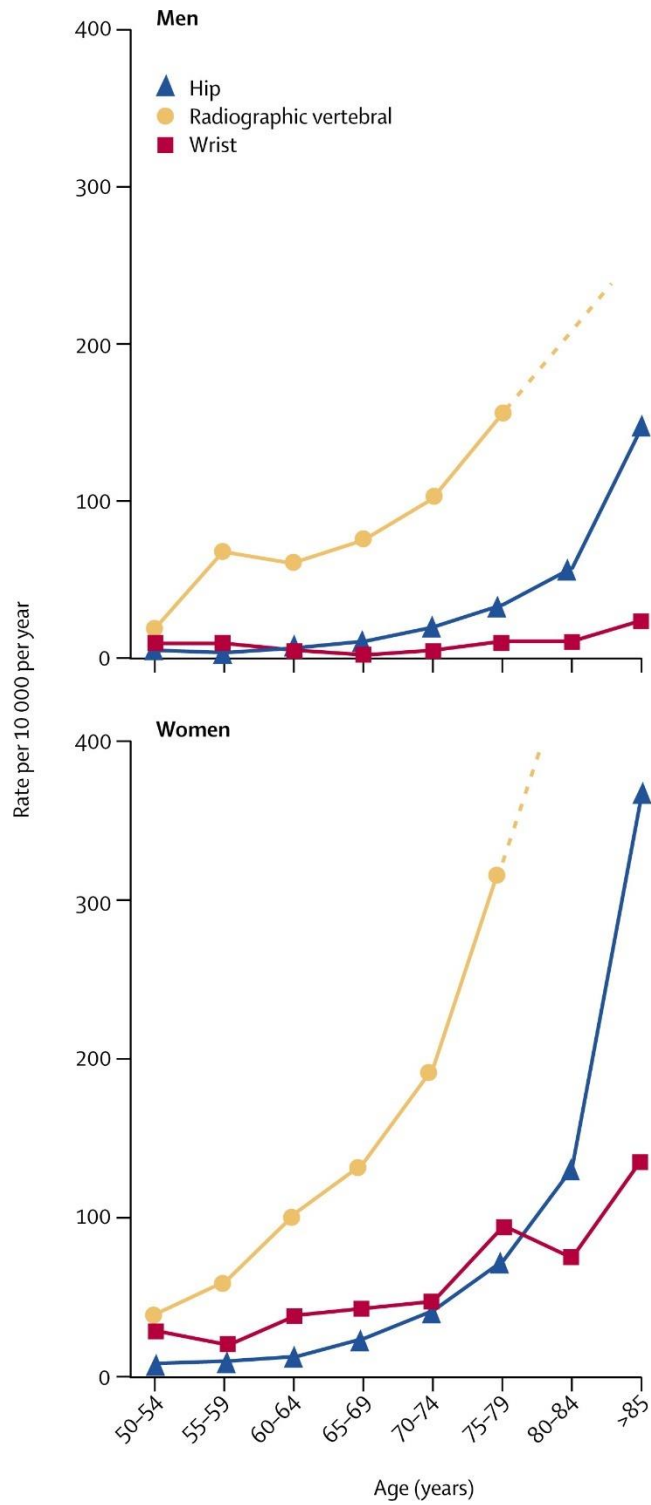


**Figure 3:** Age-specific incidence of radiographic vertebral, hip, and wrist (distal forearm) fractures in men and women.

(reproduced from Sambrook and colleagues with permission, License number: 5185430893577 <sup>31</sup>)

### 1.2.3 Fractures

Both osteoporosis and sarcopenia are associated with a huge burden to the health service through the clinical sequelae that manifest as a result of these conditions including poor health outcomes, premature death and fractures<sup>32,33</sup>.

Fragility fractures are common in the United Kingdom with about half of women and a fifth of men, over the age of 50, experiencing a fragility fracture during their lifetime<sup>34</sup>. In Europe, in 2010, there were an estimated 3.5 million fragility fractures with 610,000 hip fractures, 520,000 vertebral fractures, 560,000 forearm fractures and 1.8 million “other fractures” (comprising fractures of the pelvis, rib, humerus, tibia, fibula, clavicle, scapula, sternum and other femoral fractures<sup>27</sup>).

They are also a major source of mortality and morbidity in the elderly. For example, approximately a third of hip fracture patients die within a year<sup>34</sup> and patients continue to have an increased mortality for up to 10-years post-fracture<sup>35</sup>.

In the UK there are approximately 200,000 osteoporosis-related fractures per year<sup>36</sup> which have a substantial impact on quality of life with 50% of hip fracture patients losing the ability to live independently<sup>37</sup>. In the US, fragility fractures lead to greater than 432,000 hospital admissions and 180,000 nursing home admissions per annum<sup>38</sup>.

The incidence of fractures is increasing<sup>27,31,39</sup>, and by 2050, it is estimated that fragility fractures will affect more than a quarter of those aged 60 or greater with a concurrent rise in the prevalence of hip fracture increasing from 1.66 million in 1990 to 6.26 million in 2050<sup>40,41</sup>.

There are of course additional financial implications of fragility fractures. The yearly European economic cost of osteoporosis-related fractures was estimated at €37 billion<sup>27</sup> with 66% of the cost attributable to incident fractures, 29% to prevalent fractures and 5% to associated pharmacological costs. In the United States alone, the cost of fragility fractures has been estimated to rise to \$25.3 billion by 2025<sup>42</sup>. Given the shift in the demographic landscape of fractures with the increasingly elderly skew of the population<sup>43</sup>, the above costs are likely to increase further. More recent health economic analyses are therefore required to elucidate the modern-day financial impact of fragility fractures.

Effective therapies exist to reduce the risk of fracture<sup>44</sup>. However, at-risk individuals must first be identified. This can either be through secondary prevention (after an initial fracture), by using fracture prediction clinical tools (for example the FRAX algorithm<sup>25,45</sup>) or by using skeletal scanning

modalities which provide metrics of bone health, the most commonly employed of which is bone mineral density<sup>46</sup>.

### **1.3 Literature review process**

Literature searches were regularly performed throughout the doctoral research period via PubMed to identify relevant manuscripts and scope the related literature. Although a formal systematic review was not performed, the structure of the literature searches for each of the aims is described below.

Searches on PubMed included the following terms for the investigation of HR-pQCT change (“bone microarchitecture” OR “HR-pQCT” OR “High Resolution peripheral Quantitative Computed Tomography” OR “cortical” or “trabecular”) AND/OR (“longitudinal” OR “change”).

For the examination of the body of literature on epigenetic clocks and musculoskeletal ageing the following terms were employed via PubMed: (“epigenetic age acceleration” OR “epigenetic age” OR “methylation age acceleration” OR “methylation age” OR “clock” OR “epigenetic clock” OR “methylation clock” OR “DNAm clock” OR “biological clock”) AND/OR (“musculoskeletal” OR “muscle” OR “bone” OR “sarcopenia” OR “osteoporosis” OR “grip” OR “grip strength” OR “bone mineral density” OR “BMD” OR “DXA” OR “bone microarchitecture” OR “HR-pQCT” OR “gait” OR “body composition” OR “aging” OR “ageing”).

For the examination of the literature for epigenome-wide association studies of grip strength and bone mineral density. Searches were performed on PubMed for (“EWAS” OR “epigenome-wide” OR “epigenome-wide association study” OR “methylation” OR “GWAS” OR “genome-wide association study”) AND (“grip strength” OR “sarcopenia” OR “strength” OR “BMD” or “bone mineral density” OR “osteoporosis”). Additional searches for relevant outcomes including “grip strength” and “bone mineral density” were performed using the National Human Genome Research Institute and European Bioinformatics Institute GWAS catalog and the MRC Integrative Epidemiology Unit EWAS catalog.

After reviewing titles and abstracts full manuscript reviews were performed and relevant information and data collected. References were examined for further relevant titles and literature which were then reviewed.



## 1.4 Skeletal scanning

An important element of this thesis is the characterisation of change in bone microarchitecture with time. Bone is a complex tissue composed of a collagen scaffold, onto which calcium hydroxyapatite is laid providing rigidity to the structure. Cortical bone is the strong outer shell which is tunnelled by vascular canals or pores and provides the bone with strength to support the body and allow movement. It is composed of an outer layer, the periosteum, and an inner layer, the endosteum which boundaries the trabecular compartment.

Trabecular (or spongy) bone is a honeycomb, porous, cellular network which constitutes the inner compartment of the bone responsible for haematopoiesis and is the metabolic powerhouse. The structure of bone can be seen in **Figure 4**.

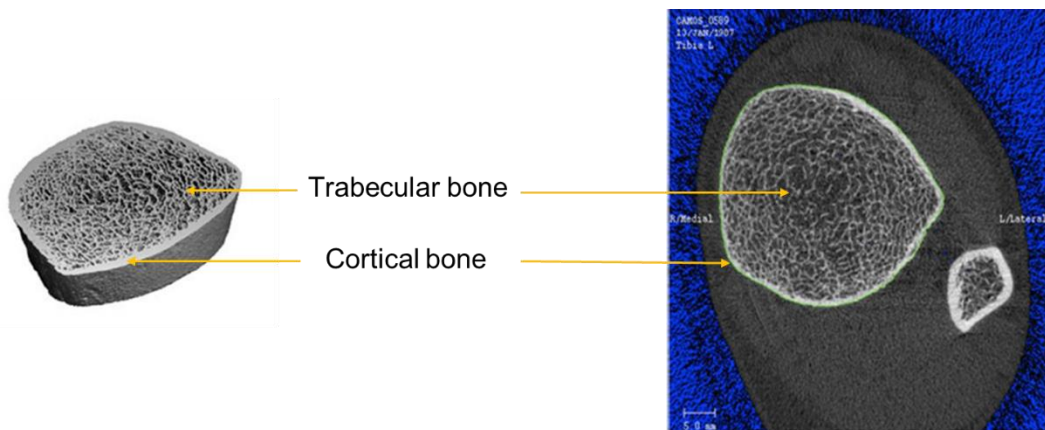


**Figure 4:** Bone structure.

On the left is a three-dimensional reconstruction of an HR-pQCT scan image of the tibia. On the right is a two-dimensional slice taken from an HR-pQCT of the tibia (and fibula). The trabecular and cortical compartments are labelled. On the two-dimensional slice, pores can be seen within the cortex (adapted from Paccou and colleagues<sup>47</sup>).

Bone cells include osteoblasts, responsible for bone formation, osteoclasts, responsible for the bone resorption (the removal of defective or old bone) and osteocytes, which are osteoblasts which have become fixed within the bone matrix and play a role in cell communication and bone regulation (including coordinating bone homeostasis and response to mechanical stressors).

Imaging of the skeleton allows us to identify and track changes in bone as an individual ages and there have been substantial developments in the field over the past century (as seen in the timeline below, **Figure 5**). The predominant scanning modality is DXA which allows visualisation of bone, but also provides measures of body composition, including muscle and fat.

Recently there have been particular step-changes in research scanning modalities which have enabled further analysis of skeletal properties and particularly bone microarchitecture through high resolution imaging. The use of this technology is a feature of this thesis.

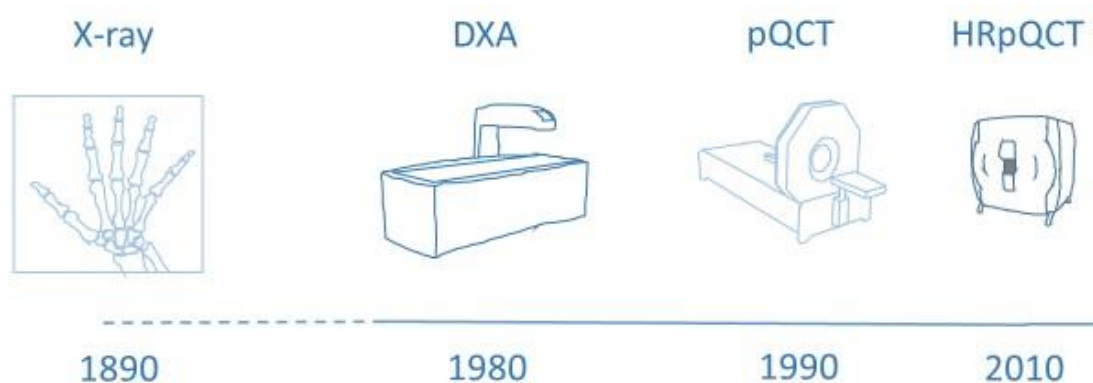


**Figure 5:** Timeline of skeletal scanning modalities.

DXA (Dual X-ray Absorptiometry). pQCT (Peripheral Quantitative Computed Tomography). HR-pQCT (High Resolution pQCT)

#### 1.4.1 Dual X-ray Absorptiometry

There has been great progress in the field of skeletal scanning, as seen in the timeline in **Figure 5**. The assessment of bone mineral density harks back to the late 19<sup>th</sup> Century with observations published on the osteopenic appearances of dental radiographs and later progressed to use absorptiometry. The origin of the latter lies in the *in vivo*, single photon absorptiometry (SPA) work of Cameron and Sorenson in 1963<sup>48</sup>.

Dual X-ray Absorptiometry (DXA) has since become the gold-standard measure for bone mineral density due to the scientific demonstration of a strong correlation with biomechanical bone strength via finite element analysis<sup>49</sup>, correlation with the clinical outcome of fracture risk<sup>50</sup> and the relatively low radiation burden<sup>51</sup>. It is also a viable measure for muscle mass in the assessment

of sarcopenia<sup>52</sup>, when appendicular (arm and leg) lean mass is employed, and also fat mass in measures of body composition. Indeed, DXA-measured body composition has been extensively validated<sup>53-55</sup> and used in epidemiological cohort study<sup>56,57</sup>.

The quantitative measures which can be derived from 2D densitometry include bone area (cm<sup>2</sup>), bone mineral content (BMC) (grams) and areal bone mineral density (BMD) (g/cm<sup>2</sup>), with the last being the most widely used parameter in clinical practice. Areal BMD is calculated using pixel by pixel attenuation values of a test material (in this case bone) against a control phantom<sup>58</sup>.

Material BMD refers to the mineralization of a small volume of organic bone matrix. The small volume is due to the necessity to exclude marrow, lacunae, canaliculi and osteonal canals from the sample. This can be performed invasively via bone biopsy, or, more recently (for cortical bone), via the virtual bone biopsy afforded by High Resolution Peripheral Quantitative Computed Tomography (HR-pQCT) which will be described further below.

#### **1.4.2 Development of High Resolution Peripheral Quantitative Computed Tomography**

As previously attested, DXA is the current gold standard, though it does have some limitations. These include the lack of compartmental (and volumetric) bone mineral density, the fact that bone mineral density measurements are size dependent (as they are calculated using a two-dimensional projection of a three-dimensional structure with no adjustment for the depth of the object) and the measures of bone mineral density are susceptible to changes in body composition.

In order to counter these issues and to provide additional measures of bone structure, morphometry and biomechanics, other 'non-DXA' scanning techniques have developed and are employed (largely in the research setting) including HR-pQCT.

##### **1.4.2.1 High-Resolution pQCT**

The most recent member of the QCT family is the high resolution peripheral QCT (XtremeCT, Scanco Medical, Bruttisellen, Switzerland). The enhanced spatial resolution afforded by this modality is in excess of that provided by standard pQCT, QCT or magnetic resonance imaging (MRI)<sup>59</sup>. It has a low radiation dose (3-5 microSv depending on the scanner<sup>60</sup>) and, due to semi-automated contouring and segmentation, provides densitometry, morphometry and biomechanic measures through finite element analysis (including stiffness and elastic modulus<sup>61,62</sup>).

Although cross-sectional studies utilising this modality exist, longitudinal studies focused on a mixed-sex, older population are lacking. This can be seen demonstrated in **Appendix 1** and section below which summarises the relevant HR-pQCT, bone microarchitecture literature.

*The process of literature review for this section is described in section 1.3.*

#### **1.4.2.1.1 Density**

Due to the nature of the imaging technique, HR-pQCT provides a three-dimensional measure of bone mineral density and thus, whereas DXA BMD is a two-dimensional areal measure, HR-pQCT BMD is volumetric. This can be captured in the bone as a whole (total volumetric BMD) or in the individual cortical and trabecular compartments.

A rich area of research in this area is the cross-sectional examination of females either side of the menopause, in order to describe the bone microarchitectural changes occurring in response to this change in physiology.

While some studies have demonstrated a significantly lower bone mineral density (BMD) in post-menopausal compared to healthy pre-menopausal or perimenopausal females<sup>63</sup> (a 36.3% lower volumetric BMD,  $p < 0.001$ <sup>64</sup> and  $291 \text{ mg/cm}^3$  (perimenopausal) vs  $331 \text{ mg/cm}^3$  (post-menopausal),  $p < 0.01$ <sup>65</sup>). When examining longitudinal change of bone microarchitecture in these groups significant differences for change in total BMD over 6 years of follow-up are not observed<sup>65</sup> (0.8% loss per year (perimenopausal) vs 1.1% loss per year (post-menopausal),  $p = 0.28$ <sup>65</sup>). Furthermore, a study across the lifecourse did demonstrate a significant reduction in total density at the tibia over 3 years of follow-up in a subgroup of post-menopausal females (0.42% loss per year) but moderate annual increases in pre-menopausal females (0.28% gain per year), young men (aged 20-49 years, 0.13% gain per year) and older men (aged over 50 years, 0.15% gain per year)<sup>66</sup>. This may be because post-menopausal females were compared to perimenopausal females in the study (by Burt and colleagues) where no significant differences were observed<sup>65</sup> and a younger group of females was included in the study by Shanbhogue and colleagues (aged as young as 21 years)<sup>66</sup>.

In the absence of long-term longitudinal studies across the lifecourse, a recent review has combined the results of previous studies to map the differences between bone microarchitecture of normal young adults (aged 20-30 years) and older adults (of age 80). This described that in females there was a 33% reduction in total volumetric BMD between these two ages, with a 22% reduction for males<sup>60</sup>. Reductions were also observed in cortical (females 16%, males 11%) and trabecular (females 29%, males 17%) BMD.

#### **1.4.2.1.2 Cortical parameters**

To recap, the cortex is the dense, hard, outer layer of long bones with microarchitectural descriptions including thickness and density of the cortex and cortical porosity (which measures the degree to which the cortex is affected by pores in the bone).

Cortical porosity (measured by percentage of the total cortex) is higher in post-menopausal compared to pre-menopausal females (3.2% vs 12.9%,  $p < 0.001$ )<sup>67</sup> and higher in osteoporotic compared to osteopenic individuals (2.1% vs 8.1%,  $p < 0.001$ )<sup>67</sup>. The rate of development of cortical porosity does not differ significantly between younger (aged 21-49 years) and older (aged over 50 years) men (4.73%/year vs 2.77%/year,  $p > 0.05$ ) (in a longitudinal lifecourse study of bone microarchitecture)<sup>66</sup>. Tibial cortical porosity increases faster in perimenopausal females compared to postmenopausal females ((increasing at 9%/year vs increasing at 6%/year,  $p < 0.05$ )<sup>65</sup>.

Cortical thickness in post-menopausal females is 41.4% lower compared to pre-menopausal females ( $p < 0.001$ ) and 18.1% lower for those with post-menopausal osteoporosis compared to post-menopausal osteopenia ( $p < 0.01$ )<sup>63,67</sup>. In younger women and men cortical thickness increases by 0.06%/year and 0.37%/year over 3 years of follow-up<sup>66</sup>.

In the comparison review of young adults (aged 20-30 years) and older adults (aged 80) cortical thickness reduced (females 33%, males 20%) and cortical porosity increased substantially (females 303%, males 185%) in the older adults<sup>60</sup>.

#### **1.4.2.1.3 Trabecular parameters**

Again, to recap, the trabecular compartment refers to bone filled with trabeculae, which is spongy, marrow-filled and resides at the distal ends of long bones and also in the vertebrae and pelvis. It can be described according to the number of trabeculae, trabecular thickness, and degree of separation of trabecular elements.

Trabecular separation is observed to be 12.3% higher in osteoporotic compared to osteopenic individuals ( $p < 0.01$ )<sup>63</sup> and a 20.4% lower trabecular number is seen in post-menopausal females compared to pre-menopausal females ( $p < 0.001$ )<sup>63</sup>. Early in the lifecourse trabecular thickness was observed to increase in growth curves over 2 years of follow-up in a longitudinal study of children and adolescents<sup>68</sup>.

A comparison review revealed reductions in trabecular number (females 19%, males 4%) and trabecular thickness (females 17%, males 9%)<sup>60</sup> for older adults compared to young, healthy adults.

#### 1.4.2.1.4 Association with fracture

When examining the relationship between bone microarchitecture and fracture, the literature is divided into studies examining the phenotype of individuals who have sustained fractures previously and those who sustain fractures in the future (thus representing the ability of the technique to demonstrate the capacity to predict fractures).

Volumetric BMD was predictive of future fracture beyond the Fracture Risk Assessment Tool (FRAX<sup>®</sup>) over 5 years in the GERICO cohort of post-menopausal women (AUC 0.78 vs 0.71,  $p=0.015$ )<sup>69</sup>, as was tibial total BMD (OR 2.1), radial total BMD (OR 2.1) and radial trabecular BMD (OR 2.0) in the CaMOS cohort<sup>70</sup>. Cortical thickness at the tibia was also predictive in the CaMOS study (OR 2.2)<sup>70</sup> though trabecular parameters at the radius had greater predictability over 10 year of follow-up in the OFELY cohort (for each quartile decrease in trabecular BMD, Hazard Ratio (HR) for fracture = 1.39,  $p=0.001$ )<sup>71</sup> and trabecular parameters had a greater association with future fracture in a group taking denosumab<sup>72</sup>. An additional finding from the CaMOS study was that baseline values rather than rate of change were more associated with future fractures in post-menopausal women<sup>70</sup>.

In males, trabecular number appeared to be the strongest baseline predictor of fracture in the STRAMBO cohort of 825 males aged 60 to 87 years (over 8 years of prospective follow-up)<sup>73</sup> (HR=1.63 per SD decrease,  $p<0.001$ ) and the MrOS study (1794 males, mean age 84.4 years) (HR=1.68 per SD decrease,  $p<0.05$ )<sup>74</sup>. In a cohort of Swedish males the fracture prediction from tibial cortical area was independent of DXA-measured areal BMD (HR=2.05 per SD decrease,  $p<0.05$ ), but trabecular number was not (HR=1.23 per SD decrease,  $p>0.05$ )<sup>75</sup>, which may be due to the fact that this Swedish study focused on tibial rather than radial HR-pQCT

Associations with prior fracture (which will be the subject of the analyses within this project given the available fracture outcomes in the HCS) have been explored in males and females. In older men prior fracture was associated with reduced cortical thickness (OR=2.13,  $p<0.001$ ), reduced cortical BMD (OR=2.16,  $p<0.001$ ) and increased cortical porosity (OR=1.75,  $p<0.001$ ), in the Swedish arm of the MrOS study<sup>76</sup> and vertebral fractures were associated with cortical density (OR=1.39,  $p<0.05$ ) and cortical thickness (OR=1.61,  $p<0.05$ ) in the STRAMBO study (independent of areal BMD)<sup>77</sup>. In the GLOW study of females who had sustained fractures, cluster-analysis identified a phenotype of trabecular impairment (lower trabecular density and number) which was associated with fracture ( $p<0.01$ )<sup>78</sup>.

A recent systematic review of bone microarchitecture associations with fracture included 40 studies with individuals of 10-85 years, and demonstrated that significantly poorer bone parameters were observed in those with a history of fracture<sup>79</sup>, highlighting the potential of HR-pQCT to identify phenotypic changes in bone microarchitecture for those sustaining fractures.

#### **1.4.2.1.5 Post-fracture change**

The changes associated with fracture have been investigated at the radius following wrist fracture, and demonstrated increases in cortical (21% increase) and trabecular thickness (55% increase) for the wrist on the fracture side at 1 year of follow-up in post-menopausal women<sup>80</sup>.

#### **1.4.2.1.6 Changes across the lifecourse**

The description of change across the lifecourse appear to vary between studies and anatomical regions (radius and tibia). In the CaMOS cohort bone volume parameters at the radius were stable until the age of 50 years, when a reduction was observed. However, in the same study, a linear deterioration was seen at the tibia<sup>81</sup>. In a different study, including 132 adults aged 20-79 years, a linear reduction was also observed,<sup>82</sup> likely due to the fact that the CaMOS study included over 600 individuals and so was better powered to identify non-linear associations.

When specifically examining the cortex, parameters appear to plateau until the age of 50 for women (likely due to the menopause) and 60 for men, after which an accelerated decline is observed for BMD and rapid increase in porosity<sup>82-84</sup>.

However, this approach of mapping change across the lifecourse appears to over-estimate the change in parameters compared to more rigorous longitudinal studies.

#### **1.4.2.1.7 Longitudinal literature**

There are three previous studies describing longitudinal change in bone microarchitecture.

A 5-year follow-up study in the CaMOS cohort of mixed sex 20-80 year olds (n=466) described (quoting the results for the 70-79 year old subgroup who are most similar to the HCS at the time HR-pQCT was performed) reduced volumetric bone mineral density(-0.5%/year males, -0.9%/year females), increases in trabecular area (0.3%/year males, 0.1%/year females) and cortical porosity (2.8%/year males, 10%/year females), with reductions in cortical BMD (-0.2%/year males, -0.6%/year females), thickness (-1.2%/year males, -0.8%/year females) and area (-1.3%/year males, -0.9%/year females)<sup>85</sup>.

Kawalilak and colleagues examined a subset of post-menopausal women (n=51, mean age 77 years) in the CaMOS cohort and, over 1 year follow-up described, at the radius, significant decreases in total volumetric BMD (-1.7%), trabecular number (-6.4%) and increases in trabecular thickness (6.0%) and separation (8.6%). At the tibia, there were reductions in cortical area (-4.5%), density (-1.9%), and thickness (-4.4%) with increases in trabecular area (0.4%)<sup>86</sup>. Shanbhogue and colleagues

performed a study in the Danish Civil registry including 3 years of follow-up in 260 adults (females mean age 46 years, males mean age 55 years)<sup>66</sup>. In the subgroup, which was most similar to the HCS, post-menopausal females had reduced trabecular BMD (-0.2%/year) and cortical BMD (0.4%/year) at the radius and reduced cortical BMD at the tibia (-0.6%/year), with milder deterioration observed in males of the same age.

The HR-pQCT phenotyping of the HCS cohort, due to the age group, length of follow-up (approximately 5 years) and size (approximately 220 individuals) therefore has the potential to add to the current literature and expand our knowledge of bone microarchitecture changes in community-dwelling older adults.

#### **1.4.2.1.8 Changes associated with interventions**

Medications to treat osteoporosis include anti-resorptive bisphosphonates. These have been shown to significantly increase cortical area, reduce trabecular area and increase total volumetric density<sup>86</sup> as well as to increase cortical density and thickness<sup>86,87</sup> in order to reduce fracture risk. Sedentary time, as measured by accelerometry has been shown to be detrimental to bone microarchitecture in cross-sectional studies<sup>88</sup>.

#### **1.4.2.1.9 HR-pQCT literature review conclusion**

As demonstrated from the above literature review, the aim of our study 'To evaluate the change in bone microarchitecture from 2011-12 to 2017' is a novel endeavour and will contribute to the wider literature. The studies included are summarised in **Appendix 1** table.



## **1.5 Epigenetic ageing**

### **1.5.1 Ageing**

Ageing is defined as the ‘increasing frailty of an organism with time that reduces the ability of that organism to deal with stress’. It is a process which is intimately related to a multitude of disease processes and, as such, is an exciting area of research as it is both a problem and opportunity. The problem is that unhealthy ageing can lead to increasing frailty and dependence and is a burden on the national health and social care services. The opportunity is that healthy ageing could maintain the independent function of individuals and allow continued contribution to society.

As suggested by the increased susceptibility to many diseases with increasing age, ageing affects all tissues. It is characterized by cardinal cellular features including altered telomere length, deterioration in the function of antioxidants, reduced somatic repair, alterations in stress response and chronic inflammation.

Some individuals age at a faster rate, with a more rapid trajectory towards dependence than others. Thus, there appears to be a dichotomy between chronological and biological age. Given ‘problem’ and ‘opportunity’ presented above, it would be valuable to be able to predict those at risk of a faster rate of ageing or accelerated aging so that interventions could be made to reduce the rate of decline.

In this thesis we will investigate the relationship between elements of musculoskeletal ageing and novel epigenetic biomarkers followed by methylation loci across the genome.

### **1.5.2 Epigenetics**

Epigenetics is the study of changes which occur in an organism due to changes in expression of the genetic code rather than changes to the genetic code itself (termed ‘genetics’). In other words, epigenetic mechanisms impact upon the function of DNA without changing the DNA sequence<sup>89</sup>. It is important to recognise that epigenetic changes, in contrast to genetic changes, can vary according to different cell types and therefore can demonstrate significant tissue-specificity<sup>90</sup>. There are different types of epigenetic mechanisms: histone modification, non-coding RNAs and DNA methylation. The latter is the focus of this doctoral thesis but I will introduce the first two mechanism now to provide context.

Histones are basic proteins which act as spools around which DNA is wrapped and, as such, fulfil the function of both efficiently packing, and providing protection to, DNA strands<sup>91</sup>. A nucleosome is a unit formed of DNA wound around a histone (octamer) core and is the subunit of chromatin (the name given to the overall complex of DNA and protein). Histones possess N-terminal tails of amino acids which are usually positively charged but can undergo neutralisation via post-translational modifications leading to reduced binding to (negatively charged) DNA<sup>91,92</sup>. This results in unwinding of DNA and provides a platform for transcription factors to bind and express genes. An example of post-translational modification is acetylation of lysine<sup>93</sup> residues by the enzyme histone acetyl transferase (HAT) which leads to active transcription<sup>94</sup>. In contrast, the enzyme histone deacetylase (HDAC) converts acetylated lysine residues to lysine and thereby reduces transcription<sup>94</sup>.

Gene expression can also be negatively regulated by non-coding ribonucleic acids (RNAs). These silencing RNAs include microRNAs and short-interfering (si)RNAs which are usually 20-50 nucleotides in length and act in the cytoplasm to block the transcription of messenger (m)RNA (via combination with the enzymatic, RNA-induced Silencing Complex (RISC))<sup>95</sup>. There are also long non-coding RNAs which are larger at over 200 nucleotides in length and modulate the structure and function of chromatin in order to control the transcription of genes and influence RNA translation<sup>96</sup> (for example playing a key role in X-chromosome inactivation<sup>97</sup>).

### **1.5.3 Methylation**

Methylation of the fifth carbon of the aromatic ring of cytosine bases (forming 5-methylcytosine) can theoretically affect any cytosine in the genome<sup>98</sup> but frequently occurs where a cytosine abuts a guanine base (named a CpG site with 'C' standing for cytosine, 'G' standing for guanine and 'p' referring to the phosphate backbone of DNA which joins the two bases).

The purposes of DNA methylation are the subject of ongoing research but findings so far suggest that the process plays a role in genomic imprinting (where DNA methylation is differentially present in the paternal and maternal germlines leading to differential gene expression in those genes inherited from each parent), X chromosome inactivation<sup>99</sup> and, potentially, in the regulation of gene expression.

CpG sites are under-represented in the mammalian genome with 5-fold fewer than would be expected by chance alone<sup>89</sup>. This under-representation may be due to the fact that a methylated cytosine can undergo deamination to become thymine and thereby predispose to mutation<sup>100</sup>. CpG sites cluster in regions known as CpG islands<sup>101</sup>. These islands are bordered by CpG shores (which extend for <2 kilobases), which in turn are bordered by CpG shelves (which extend for <2 kilobases).

Over 50% of genes in vertebrate genomes have CpG islands<sup>102</sup> and most CpG islands remain unmethylated in somatic cells<sup>102</sup> (over 90% in normal cells and tissues<sup>101</sup>). On the contrary, the majority (80%) of CpG sites (as a whole) are methylated in human embryonic stem cells<sup>103</sup>.

This emphasises that the process of DNA methylation is dynamic. Cytosine methylation is performed by DNA methyltransferases (DNMT), a family of enzymes with various functions including the maintenance of DNA methylation through mitotic division (DNMT1)<sup>104</sup> and de novo methylation at particular sites (DNMT3A, DNMT3B)<sup>105</sup>. Demethylation is performed by demethylases including ten eleven translocation (which converts 5-methylcytosine to 5-hydroxymethylcytosine)<sup>106,107</sup>, activation-induced cytidine deaminase and thymine DNA glycosylase<sup>108</sup>. The dynamic process of cytosine methylation and demethylation is important when we consider the potential impact on gene expression.

CpG islands are found in transcription start sites and, less commonly, in the body of genes<sup>102</sup>. Methylation of cytosines has been shown to be more prevalent in the promoter regions of silenced genes compared to those genes which are actively transcribed<sup>109</sup> and methylated cytosines have been demonstrated to block the binding of transcription factors (required for gene expression)<sup>110,111</sup>. These associated discoveries suggest that the presence of methylation at transcription start site CpG islands is associated with silenced genes. However, it is not established whether the methylation of CpG islands initiates gene silencing or is a method of 'locking in' the repression of the gene<sup>89,102,112</sup>.

CpG sites also occur within gene bodies, although most gene bodies are 'CpG-poor'<sup>102</sup> and those that do occur are often methylated<sup>102</sup>. CpG islands also occur within gene bodies<sup>113</sup>; however, methylation at these locations within the body does not appear to repress gene transcription<sup>114</sup> and, in fact, methylation appears to be positively correlated with gene expression<sup>113</sup>. The differential relationship between methylation and gene expression at these two genomic locations (promoter regions and gene bodies) is important to consider when contextualising the findings from epigenome-wide association studies.

Global alterations in methylation levels can occur across the genome in response to particular environmental exposures and nutritional stimuli<sup>102</sup>. Hypermethylation can occur with age and loss of methylation has the potential to lead to genomic instability, unregulated gene expression and cancer<sup>115</sup>.

With technological advancement, including methylation micro-arrays, methylation at particular loci could be investigated and environmental exposures were demonstrated to affect methylation

either via direct manipulation of DNMTs and TETs <sup>116</sup>. Associations have since been demonstrated between air pollution and hypomethylation of Mitogen-Activated Protein Kinase (MAPK) and Angiotensin Converting Enzyme (ACE) leading to asthma, emphysema and lung ageing, cigarette smoking and hypomethylation of AHRR and Contactin Associated Protein-2 (CNTNAP2) leading to cancer, cardiovascular disease and chronic respiratory conditions and nutritional exposures leading to hypermethylation of insulin-like growth factor-2 (IGF2), Retinoid X Receptor- $\alpha$  (RXR $\alpha$ ) and Pleomorphic Adenoma (PLAG) leading to aberrant development<sup>116</sup>.

There are data to suggest that methylation can accumulate across the lifecourse in response to environmental triggers <sup>117</sup>. The potential reasons for this ‘epigenetic drift’ include impairment of methylation maintenance with age (due to malfunctioning, less effective DNMTs) <sup>118</sup> together with alterations in epigenetic profile due to environmental exposures. Indeed there is evidence from twin studies to support the hypothesis that increased variation in methylation with ageing is due to environmental stimuli <sup>119</sup>. In this study of 230 monozygotic twin pairs, older twins had greater between-twin variation in methylation than younger twins.

There are therefore various possible causes of age-associated, stochastic methylation related to environmental exposures and specifically programmed age-related methylation at designated sites to manifest a designated function, or a combination of the two.

Regardless of the cause of methylation changes with age, the increased variability of methylation associated with ageing has led to interest in the ability of ‘the methylome’ to correlate with chronological age in so-called ‘Epigenetic Clocks’.

#### 1.5.4 Epigenetic clocks

Epigenetic clocks are ageing biomarkers produced from methylation datasets. These tools have been developed using statistical techniques, such as elastic net regression. This method of statistical regularization is derived from Ridge regression and Lasso regression and is therefore useful for models containing many parameters which may be highly correlated. By adding a penalty to the sum of the squared residuals it performs better than linear regression which may over-fit to training data (and thereby underperform in the testing dataset).

Elastic net regression was employed in order to identify the optimal combination of CpG sites (from methylation arrays) to correlate with chronological age. There are 3 main permutations which are summarised in **Table 1** below.

Clock	Array type	Number of CpG sites	Tissue type	Correlation with chronological age
-------	------------	---------------------	-------------	------------------------------------

<b>HorvathAge, 2013</b>	27k/450k array	353	Multiple tissues	96% correlation 3.6 year mean absolute difference
<b>Horvath GrimAge</b>	450k/850k arrays	1030	Whole blood leukocytes	Not applicable
<b>Horvath PhenoAge</b>	450k/850k arrays	513	Whole blood leukocytes	71% correlation

**Table 1:** The characteristics of the Horvath, GrimAge and PhenoAge epigenetic clocks.

The HorvathAge clock <sup>120</sup> (the earliest of the clocks used in this thesis) was designed as a multi-tissue clock, being trained on 51 different cell and tissue-types. Of the 353 CpG sites, 193 positively correlate with chronological age and 160 negatively correlate with chronological age with a resultant 0.96 correlation with chronological age and a mean absolute difference of 3.6 years.

The initial utility of methylation age as a correlate of chronological age has been added to by the discovery that the residual of known chronological age and methylation age (age predicted from methylation datasets) can provide methylation age acceleration. This parameter has been examined in association with health and disease phenotypes. The concept of age acceleration originates in studies of material science, but in human biology it simply refers to the residual of the regression of chronological age and a calculated biological age. Age acceleration is positive if the predicted biological age is greater than the chronological age, and negative (or age decelerated) if the predicted biological age is less than the chronological age.

There are some specific features of epigenetic clocks which are important to note with regard to changes across the lifecourse, sexual dimorphism and longevity. The profile of the clocks through the lifecourse has been investigated with longitudinal studies (using the Horvath clock) and suggest that methylation age is stable throughout adulthood<sup>121</sup> with increases in ‘ticking rate’ during periods of rapid growth, for example in childhood<sup>122</sup>. There are significant differences in epigenetic age acceleration between the sexes, with men consistently being ‘more accelerated’ than women (consistent with epidemiological findings regarding life expectancy)<sup>123,124</sup>. Long-living individuals (e.g. centenarians) are age decelerated compared to controls<sup>125</sup> and, even the offspring of semi-supercentenarians have lower epigenetic age than their age-matched controls<sup>125</sup>.

Since Horvath's initial DNA methylation 'HorvathAge' clock, further methylation clocks have been devised, and with these the notion of first- and second-generation clocks has come into being. First generation clocks had set out with the original intention of predicting chronological age but are hampered by the fact that the CpG sites selected were correlative with age, rather than necessarily causal. This led to the production of the aforementioned second-generation methylation clocks (including GrimAge and PhenoAge) which aim to utilise CpG sites which could be more causative in the ageing process.

The GrimAge<sup>126</sup> instrument aimed to improve the prediction of lifespan and was designed using a two-stage approach. The first stage involved developing methylation-based surrogates of 88 plasma proteins and whittling down to the 13 methylation models which were most highly correlated with the levels of a subset of 12 plasma proteins and a model of smoking packyears ( $r > 0.35$ )<sup>126</sup>. The second stage involved regressing time to death (based on all-cause mortality) on the above models and, using a Cox elastic net regression, the models for smoking packyears and the 7 plasma proteins (adrenomedullin, beta-2-microglobulin, cystatin C, GDF-15, leptin, PAI-1, and tissue inhibitor metalloproteinase 1) were selected<sup>126</sup>. This process resulted in the GrimAge clock which uses methylation from 1030 CpG sites to predict time to death (all-cause mortality) and so give a measure of lifespan.

The PhenoAge<sup>127</sup> clock aimed to correlate with clinical characteristics which are known features of phenotypic aging. It too was created via a two-step process in which, in step one, a weighted composite score produced from 10 clinical characteristics (including albumin, creatinine, serum glucose, C-reactive protein, lymphocyte percentage, mean red cell volume, red cell distribution width, alkaline phosphatase, white cell count and age). In the second step elastic net regression was used to identify CpG sites which best correlated with previous biomarkers that had been identified as composite score. The resultant PhenoAge clock was composed of 513 CpG sites and significantly outperformed previous predictors of cancer, 'healthspan', physical functioning and Alzheimer's disease<sup>127</sup>.

### **1.5.5 Associations of epigenetic age acceleration with clinical outcomes**

*The process of literature review for this section is described in section 1.3.*

The Horvath clocks have been investigated in cohort studies and associations demonstrated with mortality<sup>128-130</sup>, cancer incidence<sup>131</sup>, lung cancer<sup>132</sup> (though a non-significant effect of smoking on age acceleration<sup>132,133</sup>) and a host of other cancer outcomes, diseases of ageing and mental health phenomena. However, there is a relative paucity of studies investigating associations with musculoskeletal diseases of ageing.

In a cross-sectional, observational study of 1820 older individuals in their early 60s in Germany, Horvath methylation age acceleration was significantly associated with a comprehensive frailty measure, 'The Frailty Index'<sup>134</sup>. This index is based on 34 deficits in health status (including the presence of 11 diseases, self-rated health, 6 symptoms and difficulties in performing 16 particular activities of daily living). Each of these scores a single 'deficit' in the Frailty Index with the maximum being 34. There was an approximate increase of half a deficit per 6 years of epigenetic age acceleration ( $p=0.0004$ ).

The relationship between peripheral blood epigenetic age acceleration and frailty (according to the Fried Criteria<sup>135</sup>) has also been investigated in the Lothian Birth Cohort 1936 (composed of individuals living in Lothian currently who were born in 1936)<sup>136</sup>. This study found that a greater Extrinsic Epigenetic Age Acceleration (EEAA) (which incorporates the changes in white cell composition associated with age) was associated with a higher risk of being frail (for one year increase in epigenetic age, RR 1.06, 95% CI 1.02-1.10). No associations were noted with Horvath or Intrinsic Epigenetic Age Acceleration (IEAA) (age acceleration adjusted for white cell composition).

Physical activity has been investigated in both the Women's Health Initiative, which found a weak correlation between EEAA and physical inactivity (assessed by self-report)<sup>137</sup> and in the Lothian cohort, which found that neither EEAA or IEAA were associated with sedentary or walking behaviour (which had been objectively measured)<sup>138</sup>.

Increased epigenetic age acceleration was associated with reduction in balance, motor coordination, self-reported physical limitation, cognitive abilities, self-rated health, facial ageing but not grip strength<sup>139</sup>. It should be noted that effect sizes were modest.

Marioni and colleagues<sup>140</sup> investigated the associations between the Horvath epigenetic clock-based age acceleration and four mortality-linked markers of fitness including general cognitive ability, gait speed, lung function and grip strength. Epigenetic age acceleration from blood was acquired, and the above markers were assessed, in 920 members of the Lothian Birth Cohort at age 70, age 73 (in 299 participants) and age 76 (in 273 participants). Significant cross-sectional associations (after adjustment for leukocyte composition, height and smoking status) were observed between age acceleration and cognitive ability ( $\beta = -0.07$ ,  $p=0.024$ ), grip strength ( $\beta = -0.05$ ,  $p<0.01$ ), Forced Expiratory Volume in one second (FEV1) ( $\beta = -0.06$ ,  $p<0.01$ ) though not with 6-metre gait speed ( $\beta = 0.03$ ,  $p=0.45$ ). There was no significant change in DNA methylation age acceleration over time (supporting previous data suggesting that it is stable in adulthood<sup>121</sup>) and only longitudinal change in FEV1 was associated with baseline age acceleration, though with a

clinically insignificant effect size ( $\beta = 7.8 \times 10^{-4}$ ,  $p = 0.05$ ). The lack of association may have been due to insufficient tissue specificity, the relatively short follow-up time (6 years) and a potential lack of statistical power.

Simpkin and colleagues<sup>141</sup> investigated associations between Horvath age acceleration and three measures of physical capability; grip strength, standing balance time and chair rise speed. Participants were drawn from females enrolled in the National Survey for Health and Development (NSHD) and included 152 who had blood samples. Age at baseline was 53 years and follow-up was performed at age 60-64 years. Baseline epigenetic age acceleration was significantly associated with a greater decrease in grip strength from baseline to follow-up (0.42kg decrease in grip strength per year increase in age acceleration, 95% CI 0.82kg;  $p = 0.03$ ) though this was not then demonstrated in replicate work in The Avon Longitudinal Study of Parents and Children (ALSPAC) cohort. No associations were observed with standing balance time or chair rise speed.

HorvathAge acceleration was investigated in 48 monozygotic twins in Finland with the finding that an increase in Horvath age acceleration was associated with a reduction in grip strength ( $\beta = -5.3$ , SE 1.9,  $p = 0.01$ ), though no association was observed with knee extension or 10m gait speed<sup>142</sup>.

Since the above studies<sup>140-142</sup> which focused on the first-generation epigenetic clocks, further studies have been performed to examine the second-generation iterations, which appear to show stronger associations with the ageing muscle phenotype.

McCrory and colleagues found significant associations between GrimAge acceleration and grip strength and gait speed in 490 community-dwelling older adults who were part of The Irish Longitudinal Study of Ageing (TILDA)<sup>143</sup>. Maddock and colleagues found significant associations for GrimAge and PhenoAge in a meta-analysis of studies including the National Survey for Health and Disease (NSHD) over 13 years of follow-up<sup>144</sup>

Although a few associations have been established with grip strength, none of the associations with muscle outcomes have been particularly strong. It is pertinent, therefore, that Horvath has recently co-authored a paper which reports the development (using elastic net regression) of a clock to provide a biological age of human skeletal muscle tissue<sup>145</sup>. Whereas the original Horvath clock contained 353 CpG sites, this new muscle clock is composed of 200 CpG sites (16 of which overlap with the original clock). This suggests that there may be utility in more 'tissue-specific' clock development (using bone tissue) and (as bone tissue collection is outside the purview of the current project) in whole blood biomarkers correlated to musculoskeletal outcomes.

It is also relevant that no studies to date have reported associations between epigenetic age acceleration and bone outcomes, especially as a recent study has demonstrated that CpG methylation in peripheral blood monocytes has a causative effect (as established by Mendelian



Randomisation) Mendelian randomisation is a technique used in observational epidemiology which employs genetic information as a proxy (or instrumental variable) for non-genetic information which allows testing for causal effects in the presence of confounding on BMD measured in 118 Caucasian women (with extremes of bone mineral density)<sup>146</sup>. One study in 32 individuals with osteoporosis and 16 controls found no association between bone parameters and HorvathAge acceleration<sup>147</sup>. This may be due to a lack of power or the use of a first-generation rather than second-generation epigenetic clock.

In our study we examined the associations between 10- and 17-year musculoskeletal outcomes (including grip strength, gait speed, DXA-measured bone mineral density (at the hip, femur and lumbar spine), bone microarchitecture and body composition) and age acceleration variable acquired from each of these epigenetic clocks (Horvath, GrimAge and PhenoAge).

### **1.5.6 Musculoskeletal EWAS**

*The process of literature review for this section is described in section 1.3.*

#### **1.5.6.1 Bone mineral density**

Epigenome-wide association studies have been performed in various tissues examining relationships with osteoporosis and fracture. Some studies have focussed on the methylation profile of femoral head tissue collected from hip fractures compared to hip replacements. One particular paper identified differential methylation of the HOX genes on 27k methylation array<sup>148</sup>. An alternative approach was taken by Reppe and colleagues<sup>149</sup>, examining associations between osteoporosis and methylation (via 450k array) at 2529 CpG sites in 100 genes previously identified to be associated with bone mineral density in post-menopausal women<sup>149,150</sup>. In 84 postmenopausal women, CpG methylation at 63 sites differed significantly between osteoporotic and non-osteoporotic post-menopausal women at a 10% FDR. These included CpG sites within the tenascin XB gene (a protein which supports the structure and maintenance of bone, muscle and connective tissues), glycogen synthase 1 in muscle. Five of these CpG sites at a 5% FDR level explaining 14% of the BMD variation including Matrix Extracellular Phosphoglycoprotein (MEPE, responsible for phosphate uptake and bone mineralisation), Sclerostin (SOST), Wnt Inhibitory factor 1 (WIF1) and Dickkopf Wnt Signalling pathway inhibitor 1 (DKK1), the latter 3 all being Wnt pathway inhibitors.

Cheishvili and colleagues compared of 22 osteoporotic postmenopausal women against 22 non-osteoporotic controls and found 1233 differentially methylated CpG sites (using 450k array) with an FDR of 5% in peripheral blood leukocytes. They then subdivided the osteoporotic group into early and advanced osteoporosis (using a T-score threshold of  $\geq 3.0$  for advanced disease) and selected a panel of 5 of the most significantly associated, biologically plausible genes to create a polygenic risk score to predict the development of early osteoporosis<sup>151</sup>. Interestingly the panel of genes included Programmed Cell Death Protein 1 (PDCD1), which plays a role in T- and B- cell regulation.

A study investigating the differential methylation of human mesenchymal stem cells acquired from the femoral neck of those undergoing hip replacement for hip fracture and those undergoing hip replacement for osteoarthritis found differential methylation in gene pathways enriched for human mesenchymal stem cell growth and osteoblast differentiation<sup>152</sup>. However, it should be recognised that differential methylation signatures in bone tissue which has recently fractured may be influenced by the trauma itself and not be purely representative of the osteoporotic disease process.

A large, collaborative EWAS of peripheral blood leukocyte methylation and BMD, including a 4616 individual discovery dataset identified one CpG site, cg23196985, associated with BMD in females. However, this association was not reproduced in the 901 individual validation dataset<sup>153</sup>.

#### **1.5.6.2 Grip strength**

Compared to bone mineral density, there is a relative paucity of grip strength epigenome-wide association studies. Soerensen and colleagues investigated associations between grip strength and differentially methylated CpG sites in blood samples from a cohort of 672 twins from the Study of Middle Aged Danish Twins (MADT) and the Longitudinal Study of Aging Danish Twins (LSADT)<sup>154</sup>. They found that no CpG sites met statistical significance (adjusted for sex, age, height, cell composition); however, two CpG sites associated with *COL6A1* and *CACNA1B* genes respectively were suggestive of association and downstream pathway enrichment analysis implicated a role of the immune system. Two further EWAS studies of grip strength have demonstrated no significant associations; one in 172 female twins<sup>155</sup> and the other in the Lothian Birth Cohort<sup>140</sup>.

In our study we examined the epigenome-wide associations between methylation at CpG sites and maximum grip strength and total femoral neck (which are available cross-sectionally). Future work will include examination of bone microarchitecture epigenome-wide association.

## **1.6 Aims and purpose**

Using data collected on Hertfordshire Cohort Study (HCS) participants the following aims will be addressed:

- To describe the longitudinal change in bone microarchitecture, grip strength and femoral neck bone mineral density, in a cohort of community-dwelling older adults in the United Kingdom, and investigate their relationship with fracture, and the relationship between bone microarchitecture and genetic loci related to bone health.
- To investigate the association between baseline epigenetic age acceleration and musculoskeletal outcomes
- To identify novel epigenetic patterns and individual epigenetic marks which are associated with key musculoskeletal indices of grip strength and hip bone mineral density through Epigenome-wide Association Study (EWAS).

## **1.7 Potential outcomes and wider impact**

The robust description of the landscape of musculoskeletal ageing is necessary if the impacts of interventions are to be accurately evaluated. This includes the phenotyping of bone microarchitecture changes with age and assessment of the key parameters of musculoskeletal ageing: grip strength and bone mineral density.

In the search for effective biomarkers of musculoskeletal ageing, epigenetic clocks, with their potential to measure biological ageing, demand examination. We hope that the outcome of the analyses presented in this thesis will might help to determine the extent to which epigenetic age can be used to predict future musculoskeletal outcomes. Clinically, this could be extremely useful to identify at-risk individuals earlier in the lifecourse and allow for earlier intervention leading to significantly improved outcomes. In the era of personalized medicine this could be a biomarker used in primary care and health checks, to identify at-risk individuals who are likely to benefit most from intervention.

Scientifically, the in-depth exploration of biological DNA methylation ageing in the musculoskeletal system may identify commonalities with other age-related diseases. Furthermore, the identification of specific blood-derived CpG sites, which are associated with bone and muscle outcomes, could provide integrative knowledge with respect to multisystem inflammatory and other disease-related co-morbidities, could generate hypotheses for future research and could ultimately assist with identifying novel therapeutic strategies for musculoskeletal ageing.

## Chapter 2 Methods

The methods employed in this doctoral thesis are set out in detail below.

The study was sited in the Hertfordshire Cohort Study, a group of community-dwelling older adults who have undergone extensive phenotyping over the last (approximately) 20 years. Phenotyping visits were performed at baseline (1998-2004), EPOSA (2011-12) and HBS17 (2017) and phenotyping data collected in these passes, together with DNA methylation arrays of bloods taken at baseline, were used to answer the specific aims of this project.

In order to describe the longitudinal change in bone microarchitecture, grip strength and femoral neck BMD, measurements taken from HR-pQCT, grip dynamometry and femoral neck DXA (the first of the stated Aims) respectively were used at EPOSA (2011-12) and HBS17 (2017) follow-up. The relationship between these parameters and fracture history was examined.

In order to investigate the association between baseline epigenetic age acceleration and musculoskeletal outcomes (the second of the stated Aims) epigenetic clocks (and thence epigenetic age acceleration) were calculated from DNA methylation array data acquired from baseline (1998-2004) bloods. Cross-sectional associations (based on musculoskeletal phenotype at baseline (1998-2004) and longitudinal associations (based on musculoskeletal phenotype at EPOSA (2011-12) and HBS17 (2017)) between baseline epigenetic age acceleration and grip strength, gait speed, DXA bone mineral density, bone microarchitecture and elements of body composition.

In order to investigate the epigenome-wide (DNA methylation) associations for cross-sectional grip strength and BMD at the femoral neck (the third of the stated Aims), DNA methylation array data on blood samples from baseline (1998-2004) were used and examined for relationships with grip dynamometry and DXA-measured BMD, also at baseline (1998-2004).

### 2.1 Hertfordshire Cohort Study

This study is sited in a community dwelling cohort of older adults, the Hertfordshire Cohort Study. The origin of this cohort is described below. A detailed exposition of the cohort is presented in the recent cohort summary paper, 'The Hertfordshire Cohort Study: an overview'<sup>156</sup>. In brief, due to concerns over the health of the British public, in 1911, birth and early life information was collected in Hertfordshire with the aim of using the collected data to improve paediatric health. These data

were collated by local midwives and health visitors under the direction of Ethel Margaret Burnside, the 'Lady Director of the Midwives and Chief Health Visitor' in the county at the time.

The information collected included the weight at birth, whether the child was breast-fed or bottle-fed, childhood conditions and the weight at 1 year, and was transcribed into ledgers which were stored in the council buildings. Births were recorded until 1948, though the data collection was potentially affected by the advent of the Second World War.

The ledgers were discovered by researchers from the forerunner to the MRC Lifecourse Epidemiology Unit, who aimed to study the developmental origins of health and disease, and focused on the cohort born between 1931-1939. There were 42,974 births recorded during this period, including 39,764 live births (thus, non-live births were excluded). Of those, deaths during childhood, records with missing information (e.g. birth weight or weight at 1 year), or with insufficient tracing information were excluded and tracing through the National Health Service Central Registry was attempted for 24,130 and was successful for 21,063. Of these, 8,650 were found to be still living in the county and 7,113 were registered with a Hertfordshire General Practice surgery<sup>156</sup>. Letters of invitation were sent to General Practitioners, to acquire permission to contact the potential participants, and this led to 6,099 being invited to participate. Of these 3,225 (53%) agreed to take part and 2,997 were visited. Those in the East Hertfordshire area were identified for specialist musculoskeletal phenotyping (1,482 visited at home), and of these, 966 attended the baseline clinic as can be seen in **Figure 6**. From this point on, the focus was on collecting long-term longitudinal data and all participants who attended a phenotyping pass of the cohort were invited for the following pass. Participants were unable to attend due to illness or undisclosed reasons were noted to have withdrawn from the study for face to face visits though mortality data is still being collected for all cohort members.

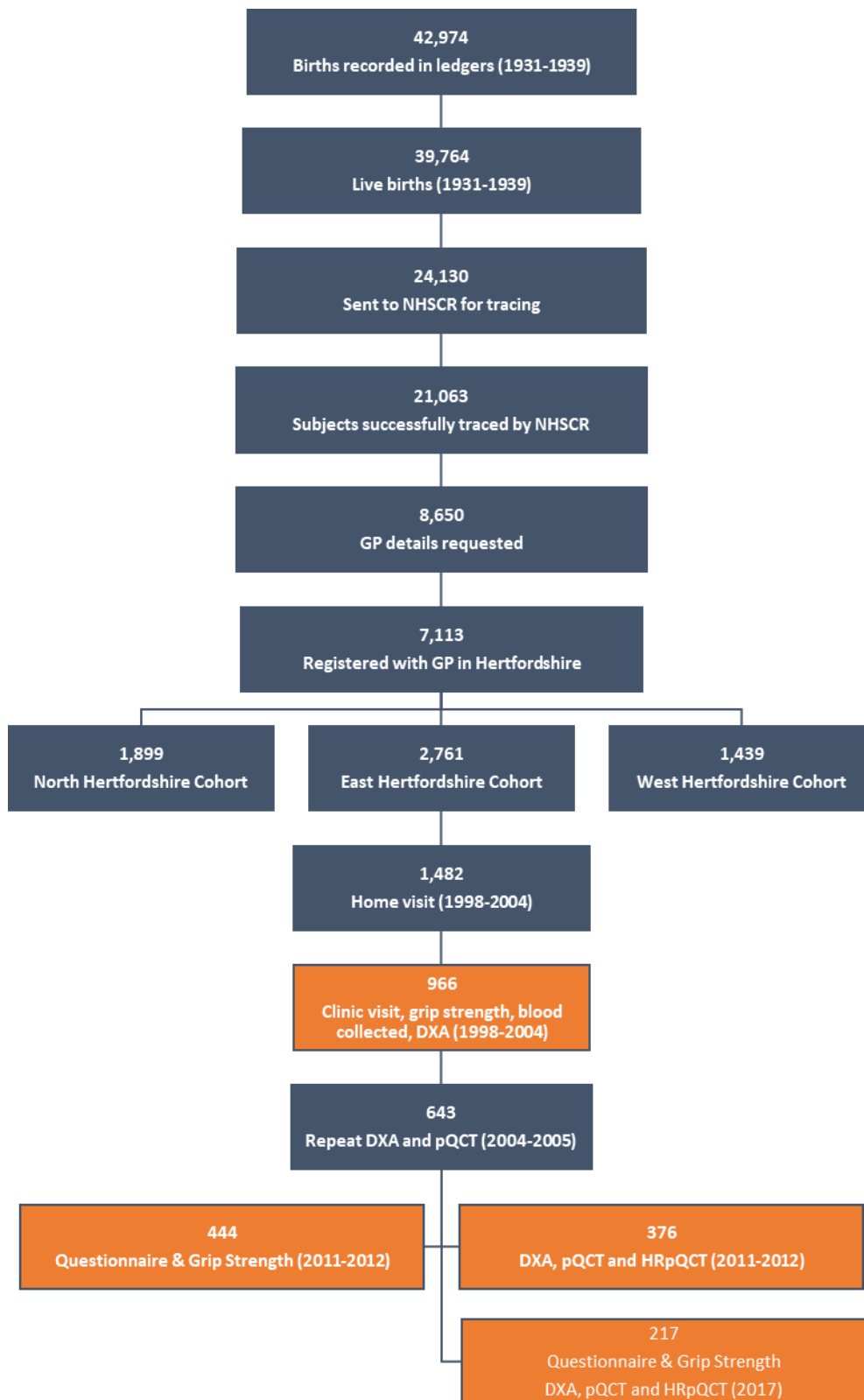
The first research clinic visits included assessment through lifestyle questionnaires, physical performance measures, grip strength, dual X-ray absorptiometry for bone mineral density and phlebotomy. These blood samples were processed, DNA extracted and stored at -80°C. It is these samples which underwent DNA methylation array analysis as part of the current study.

In 2011-12, 444 participants agreed to take part in the European Project on OsteoArthritis (EPOSA) study, which included osteoarthritis assessments, as well as physical performance, grip strength and repeat lifestyle questionnaires. Bone parameters were also assessed in 376 of these participants as part of the Hertfordshire Bone Study, using DXA, peripheral quantitative computed tomography (pQCT) and High Resolution-pQCT (HR-pQCT).

In 2017, together with a research team, I repeated these phenotyping measurements on 217 of the Hertfordshire Bone Study participants. The figure below (**Figure 6**) depicts the development of the cohort and **Figure 7** shows the timeline of the measures relevant to this thesis.

**Figure 6:** Flow diagram of study participant structure of the Hertfordshire Cohort Study.

Passes of the cohort relevant to this study are highlighted in orange.



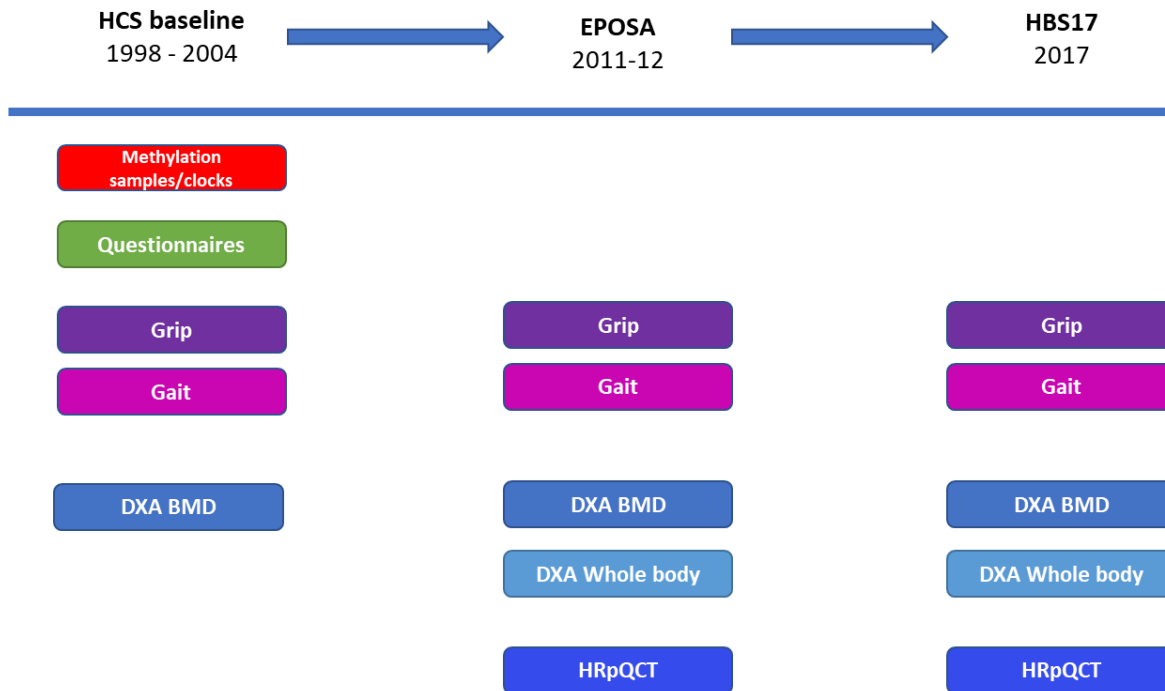


**Figure 7:** Timeline depicting the timings of follow-up visits and methylation samples, questionnaire data and musculoskeletal measures

## 2.2 Procedures

The procedures which are relevant to the current thesis are described below. All procedures were carried out by trained fieldworkers and researchers. HCS baseline research visits were carried out in Hertfordshire and the EPOSA (2011-12) and HBS17 (2017) follow-up visits were completed at the Elsie Widdowson Laboratory in Cambridge.

### 2.2.1 Height and weight measurements

These measurements were performed at HCS baseline (1998-2004), EPOSA (2011-12) and by me as part of a team at HBS17 (2017).

Height was measured using a wall-mounted stadiometer. The subject was asked to remove their shoes and stand on the floor with their back to the wall. They were asked to stand as tall and straight as possible (to avoid lordosis) with their feet together. The wall-mounted head plate was lowered and placed on the top of the subject's scalp with the participant's head in the Frankfurt Plane (a theoretical, horizontal line running from the external auditory meatus to the lower border of the orbit).

When measuring weight, the scales were zeroed and shoes, heavy items in pockets and jewellery were removed prior to weighing.



Height, weight and body mass index (BMI) were used in our analyses.

### **2.2.2 Gait speed**

An 8-foot walking course was marked out using a tape measure. Participants were asked to “Walk to the other line at the end, at your usual walking pace, as if you were walking to the shops.” Participants were allowed to use assistive devices if required. The timer was started on the “Go” of “One, two, three, Go” and stopped as the participant passed through the finish line. This was measured at the HCS baseline (1998-2004), EPOSA (2011-12) and by me as part of a team at HBS17 (2017) research clinics.

### **2.2.3 JAMAR Grip Strength Dynamometry**

Whilst seated in a chair the participants were asked to position their elbows at right angles and their wrists in a neutral position with their hands gripping the dynamometer comfortably. The dynamometer was adjusted for size if necessary and the participant was encouraged to squeeze the instrument “as hard as possible” and the result recorded to the nearest 1kg. The grip strength of the right and left hands was measured alternately, three times on each side. This was measured at the HCS baseline (1998-2004), EPOSA (2011-12) and by me as part of a team at HBS17 (2017) research clinics.

### **2.2.4 Questionnaires**

Participants took part in a researcher-administered questionnaire at each visit (including those performed for HBS17 at which I was part of the field-work team) which included information on: medical history, medication history, fracture history, activities of daily living, smoking and detailed alcohol intake, social set-up and history, nutrition via a food frequency questionnaire (including dietary calcium) and measures of physical activity were assessed using an established questionnaire<sup>157</sup>. Fracture history was assessed by the following question, “Have you sustained a fracture since the age of 45 years old?”. The answer to this question at the EPOSA (2011-12) follow-up was used for analyses in this thesis. Bisphosphonate usage was captured via questionnaire at each timepoint (baseline, EPOSA, HBS17).

The participant information leaflet, consent form, ethical approval, study questionnaires and physical performance data collection sheets from HBS17 are included in the appendices (**Appendix 2, Appendix 3, Appendix 4, Appendix 5**)

### **2.2.5 Dual X-ray absorptiometry**

The procedure was explained prior to the commencement of scanning and communication continued during the scan. The participants were asked to keep still and not to talk during the scan to minimize movement artefact.

A dressing gown was provided and any clothing containing metal removed together with metal jewellery, glasses or any object which could cause artefact via attenuation of the X-ray beam. The participant was asked to lie on the scanner bed within a white rectangle marked on the mattress (which indicated the margins, or outer limits, of the scan area).

The same methods were used at HCS baseline (1998-2004), EPOSA (2011-12) and HBS17 (2017). I was part of the fieldwork team performing this scan at HBS17.

#### **2.2.5.1 Whole body scan**

Whole body scans, providing measures of body composition (including lean mass and fat mass) were measured at EPOSA (2011-12) and HBS17 (2017) follow-up visits, but not at HCS baseline where bone images only were collected.

The legs were strapped together to ensure that positioning was optimal with the legs straight and toes pointed inwards. This prevents overlap of the skeleton in the final scan. The hands were positioned palm down on the bed on either side of the body ensuring that, if possible, the whole body lay within the white triangle markings of the scan margin. If the arms could not be placed inside the white rectangle then the participant was requested to hold them flat against the body with the lateral border of the little finger against the bed and the palms facing inwards against the lateral aspect of the thighs (**Photograph 1**).

#### **2.2.5.2 Femur scan**

For scans of the femur, the hips were internally rotated and the feet strapped to a foot brace. The scanning arm was positioned so that a red cross marker was overlying the hip and once in the correct position the hip region was scanned. If the position was found to be incorrect during the scan, the procedure was halted, the patient repositioned and the femur re-scanned.

This process was then repeated on the contralateral side. It should be noted that hips which had undergone surgical replacement were excluded from femur DXA assessment.

#### **2.2.5.3 Lateral spine scan**

At the EPOSA (2011-12) follow-up visit lateral spine DXA was performed with the participant lying in the left lateral position in order to identify vertebral fractures. These fractures were defined as 'previous fractures' in downstream analysis.

#### 2.2.5.4 DXA scanner

It should be noted that the HCS baseline scans (1998-2004) were performed using a QDR 4500 densitometer (Hologic®), the EPOSA DXA scans in 2011-12 were performed using a Lunar Prodigy DXA scanner (GE Healthcare) and scans at HBS17 were performed using a Lunar iDXA (GE Healthcare). Hologic and GE Healthcare modalities have been previously compared and precision errors were found to be low<sup>158</sup>. A previous review of the correlation between the two GE Healthcare modalities noted that, although the majority of parameters were similar and highly correlated, there were small but significant differences in regional bone estimates, fat mass in the arms, lean total mass and percentage fat in the arms and legs in a cohort of approximately 90 adults aged 20-74 years<sup>159</sup>.



**Photograph 1:** A Hertfordshire Cohort participant undergoing a whole-body DXA in 2017

#### 2.2.6 High resolution peripheral quantitative computed tomography (HR-pQCT)

##### 2.2.6.1 HR-pQCT preparation

The same instrument was used at EPOSA and HBS17 visits (XtremeCT, Scanco Medical). HR-pQCT measurements were made at the non-dominant distal radius and tibia unless contra-indicated due to a previous fracture. The height and position of the chair were adjusted to ensure the maximal

comfort of the participant and, once again, participants were politely asked to remain, “as still as possible”, and not to talk during the procedure in order to prevent movement artefact.

Scans were performed according to the manufacturer’s guidance <sup>160</sup>.

The methods for this piece of apparatus were the same at EPOSA (2011-12) and HBS17 (2017) and I was part of the fieldwork team performing this scan at HBS17.



**Photograph 2:** A Hertfordshire Cohort participant undergoing a radial HR-pQCT in 2017

### **2.2.6.2 Tibial HR-pQCT**

A cast was placed on the lower limb and foam moulds were placed around to ensure a comfortable and snug fit and the leg placed within the gantry of the scanner. Once in position the gantry was closed and chair wheels were locked into place in order to reduce movement artefact.

A ‘scout view’ scan was performed to allow a reference line to be set along the tibial plateau in 2011-12 scans or set along the 2011-12 reference line in the 2017 scans (to ensure the same region was scanned at both time points). Scanning time was approximately 3 minutes.

### **2.2.6.3 Radial HR-pQCT**

Similar to the tibial scan, the forearm was placed within a cast and foam used to ensure a good fit. The arm was extended and placed into the gantry of the scanner with chair wheels locked into place (**Photograph 2**).

A scout view was performed one third to half-way along the radial end plate in 2011-12 or along the 2011-12 reference line for scans performed in 2017 (again, to ensure that the same region was scanned at both time points). Again, scanning time was approximately 3 minutes.

### **2.2.6.4 Motion artefact**

Scans were performed and reviewed immediately afterwards. If motion artefact was identified (e.g. by streaking or distortion of the image) the scan was repeated one further time.

### **2.2.6.5 Scan image analyses**

A length of 9mm was scanned with 110 slices and 750 projections were performed across 180°. Scans image analyses was commenced according to manufacturer's protocol, followed by segmentation (a line being drawn around the outline of the bony cortex) to assist with identification of bony margins. Density was assessed compared to phantom cylinders (composed of resin and hydroxyapatite) which had been scanned at the beginning of each study day, and values ascertained for trabecular and cortical microarchitecture outcomes.

Using previously described methods (in which scans are manually graded for image quality on a five-point scale)<sup>161</sup>, scans exhibiting substantial motion artefact despite the efforts described above (chair locking etc.) were excluded from analyses but all other scans of sufficient quality were included. Manufacturer standard evaluation and cortical porosity scripts were used for image analysis<sup>64,69,83,162-164</sup> and extended cortical analysis was performed for all scans<sup>165</sup>.

Overlap between EPOSA and HBS17 HR-pQCT scans was established via the Scanco Medical 'slice-match method' and comparison for scans was not performed if the overlap was less than 75%<sup>166</sup> (values were therefore set to missing for 7 scans at the radius and 2 scans at the tibia). Median overlap between the scans included in the analyses was 93% (lower quartile=87%, upper quartile=96%) for the radius and 95% (lower quartile=92%, upper quartile=97%) for the tibia. Short term precision values for cortical and trabecular BMD have been previously demonstrated to range between 0.3 to 1.2 (percentage root mean squared coefficient of variation)<sup>167</sup>.

These analyses were performed with Dr Gregorio Bevilacqua under the supervision of Professor Kate Ward.

### **2.2.7 Peripheral quantitative Computed Tomography (pQCT)**

At the EPOSA (2011-12) follow-up pQCT scans of the tibia were performed using a Stratec 2000XL instrument, version 6.00. The non-dominant leg was scanned (provided that it had not previously sustained a fracture) following initial scout views to identify the cortical endplate reference point as an established landmark. Slices of scans were taken at the 4%, 14% and 38% positions. Cortical thickness was the only parameter used in our analyses. These scans were performed by researchers from the University of Southampton and the University of Cambridge.

## **2.3 Genetic analyses for bone microarchitecture**

### *2.5 SNP genotyping*

Single Nucleotide Polymorphism (SNP) genotyping was previously carried out by colleagues at the Genetic laboratory of the Department of Internal Medicine (Population Genomics) at Erasmus Medical Center in Rotterdam using the Infinium Global Screening Array (v1). Raw .idat files had been uploaded to Illumina Genome Studio 2.0.0 and analysed using genotyping Module 2.0.0. Data were processed using Illumina hard cut-off technical specifications<sup>168</sup>. The packages *bcftools* and PLINK 1.9 beta<sup>169</sup> were used to prepare the quality assured genotype data for imputation according to Sangerspecifications. Data were uploaded in Variant Call Format (a bioinformatic text file) to Sanger servers, pre-phased using the *EAGLE2* pipeline and imputed using UK10K + 1000 Genome Phase 3<sup>170</sup> (comprehensive descriptions of common genetic variation acquired via whole genome sequencing). This was performed by Dr Phillip Titcombe (statistician).

### *2.5 Choice of SNPs for analyses*

A genome-wide meta-analysis performed by Estrada and colleagues identified 64 SNPs that were associated with DXA bone mineral density (at the femoral neck or lumbar spine) or associated with fracture<sup>171</sup>. In total, 61 of these 64 SNPs were available in the HCS and were examined in relation to femoral neck and lumbar spine BMD at HCS commencement (1998-2004). The following loci were associated with both femoral neck and lumbar spine BMD in HCS and so were used in analyses of bone microarchitecture: rs1053051 (*TMEM263*); rs7812088 (*ABCF2*); rs10226308 (*TXNDC3*); and rs3801387 (*WNT16*).

## 2.4 Epigenetic preparation and analyses

### 2.4.1 Overview of epigenetic methods

The microarrays used in this project include the Illumina Human Methylation 450K array and the Illumina Human Methylation 850K (EPIC) array. These are both two-colour arrays, with red and green channels, which establish the level of cytosine methylation at approximately 450,000 and 850,000 loci across the genome respectively.

They use bisulphite converted DNA, which differentiates methylated from unmethylated cytosine through a process of converting unmethylated cytosines to uracil. In this project we utilised DNA from peripheral blood leukocytes.

The bisulphite converted DNA initially undergoes whole genome amplification, fragmentation (by which the DNA is cleaved to an optimal length of 300-600 base pairs) and hybridization, whereby the DNA attaches to the probes on the array via allele-specific annealing.

Methylation arrays contain 12 samples per chip and are composed of microwells which contain 3micron beads. These beads are coated with allele-specific, ~50 base pair oligonucleotides, one bead corresponding to the methylated cytosine locus and the other bead corresponding to the unmethylated cytosine (bisulphite converted to uracil) locus. After allele-specific annealing the fragments undergo single-base extension using hapten-labeled dideoxynucleotides including dideoxycytosine triphosphate (ddCTP) and dd-guanine-TP (ddGTP) labelled with biotin and dd-uracil-TP (ddUTP) and dd-adenosine-TP (ddATP) labelled with 2,4-dinitrophenol. After staining, the chips are scanned with fluorescence intensity measured on a scale from 0 to 1.

At each cytosine locus two intensity signals are measured; the amount of methylated DNA, and the amount of unmethylated DNA. The intensities then undergo a process of quantile normalisation (whereby the quantiles of different measures are aligned) which is applied to the methylated and unmethylated intensities separately, and, for probes on the sex chromosomes, applied separately to males and females in the dataset.

The  $\beta$ -value or methylation ratio is then calculated as methylated DNA/(unmethylated DNA + methylated DNA) and quality control can then be performed. It is important to remove low-quality samples that cannot be corrected by normalisation as this improves the down-stream result<sup>172</sup>.

The sex of a sample can be predicted by using copy number information from the X and Y chromosomes to produce an 'XY difference' which is used to identify sex mismatches and sex outliers.

Median methylation and unmethylation for each array is then plotted to identify methylation outliers; which are either significantly hypomethylated or hypermethylated indicating a low quality of the sample or array data for that sample.

To evaluate elements of the array process a number of control probes are included on the chips to examine staining (measuring the efficiency of the staining step of the array), extension (measuring the efficiency of extension of A,U,G or C nucleotides), hybridization (assessed using synthetic targets as opposed to the amplified sample DNA) and bisulphate conversion (testing methylation at a site which is known to be methylated).

Sample quality is also assessed via the proportion of probes which are bound per sample with samples bound to less than 1% of the total number of probes excluded. The quality of the chip for the sample is also inspected with those samples with a high proportion of wells with less than 3 beads being excluded.

Probe quality is assessed for bead number (as described above for sample quality) and for methylation signal, with those probes with a high proportion of background signal measurement adjudged to have failed to reach the necessary quality standard to be included in down-stream analysis.

Other probe exclusions include; cross-reacting to multiple sites on the genome, probes binding to non-CpG sites, probes affected by common SNPs and probes on sex chromosomes. Other sample exclusions include those with low mean absolute deviation (MAD) scores.

Houseman's method is a bioinformatic technique for predicting the proportion of different leukocytes in a blood sample. This is used to establish a cellular population which can be used as a covariate in down-stream, epigenome-wide analyses.

After normalisation and quality control is complete, the resulting dataset of  $\beta$ -values can be used to examine the relationships between a predictor (methylation level at a CpG site) and an outcome, in this case grip strength and total femoral neck BMD.

The limma package was used in these analyses which, for a given outcome, fits a linear model to the methylation level for each CpG site (corresponding to a probe on the array)<sup>173</sup>. Beyond this simple linear regression, limma uses statistical algorithms to enhance differential expression analyses through quantitative weighting and information borrowing as described below<sup>173</sup>:



*Quantitative weighting* - limma uses a 'robust' (rather than 'least squares') regression model which performs a residual analysis and down-weights, or even removes, outlying (and therefore less-reliable) samples.

*Information borrowing* - Gene-expression studies have some elements which run in parallel. For example, strong correlations existing between methylation at different loci, and strong correlations between overall methylation levels within individual samples. Limma uses a specialised statistical technique (parametric empirical Bayes) to borrow this information, allowing the residual variance of each CpG site linear model to be moderated accordingly. This results in enhanced reliability of the inferences made, particularly from studies with smaller sample sizes.

#### **2.4.2 450k Methylation arrays**

The methylation arrays were performed as part of the 'EURHealthAging' collaboration. This was a European consortium which was established with the aim of investigating the relationship between early development and longevity (and aging). The arrays were performed externally and the methods used are described below.

Genome-wide DNA methylation levels were measured using Illumina Human Methylation 450K array (Illumina) which enables the simultaneous quantitative measurement of the methylation status at 485,577 CpG sites<sup>174</sup>. In two batches, 500ng samples of DNA (per participant) were bisulphite converted using the Zymo EZ-96 DNA-methylation kit (Zymo© Research, Irvine, CA, USA). Samples were then hybridized to the arrays according to the manufacturer's specification.

#### **2.4.3 EPIC (850k) Methylation arrays**

Epigenetic analyses were performed in collaboration with the Institute of Developmental Sciences (University of Southampton) with all laboratory preparation performed by Dr Nikki Graham. Baseline (1998-2004) samples of whole blood leukocyte DNA samples were removed from -80°C storage and the amount of DNA was assessed using Qubit. Samples of 50µl at a concentration of 20ng/ µl were loaded onto a 96 well-plate and shipped to the University of British Columbia for methylation array analyses.

Genome-wide DNA methylation profiles were assessed by Illumina Infinium HumanMethylationEPIC BeadChip 850k methylation array<sup>175</sup>. Whole blood leukocyte genomic DNA were bisulphite converted (by which process unmethylated cytosines are converted to uracil) using Zymo DNA Methylation-Gold Kit (©Zymo Research Corp., USA), denatured, amplified and

fragmented before being hybridized to the chip arrays. Primer extension, staining, coating and finally imaging with the Illumina BeadArray reader were performed.

#### **2.4.4 Quality Control of array data**

I performed quality controls performed for the 450k array using R version 3.5.1/3.6.1 and R packages including *BiocManager*, *SmartSVA*, *Illuminaio*, *limma*, *DNAcopy*, *preprocessCore*, *devtools*, *knitr*, *markdown*, *champ*, *minfi* and *meffil*. Using *Meffil*<sup>176</sup> and *minfi*<sup>177</sup>, the .idat files were used to produce a sample sheet and perform background correction, dye bias correction, sex prediction and cell count estimates using the Houseman method<sup>178</sup>. Each sample was then normalised to the cell type reference dataset. I produced a quality control report at this stage.

##### **2.4.4.1 Quality control report for 450k array**

*Sex mismatches*: In order to separate males from females, the difference between the total median intensities for probes known to lie on the X and Y chromosomes (XY difference) are used. Sex mismatches are defined as those in which the predicted sex using the median intensities method above do not match the sex as documented in the phenotyping file<sup>177</sup>. Sex outliers are those individuals for whom the XY difference is greater than 0.1 or less than -0.1. As can be seen in **Figure 8**, there were no sex mismatches and no sex detection outliers.

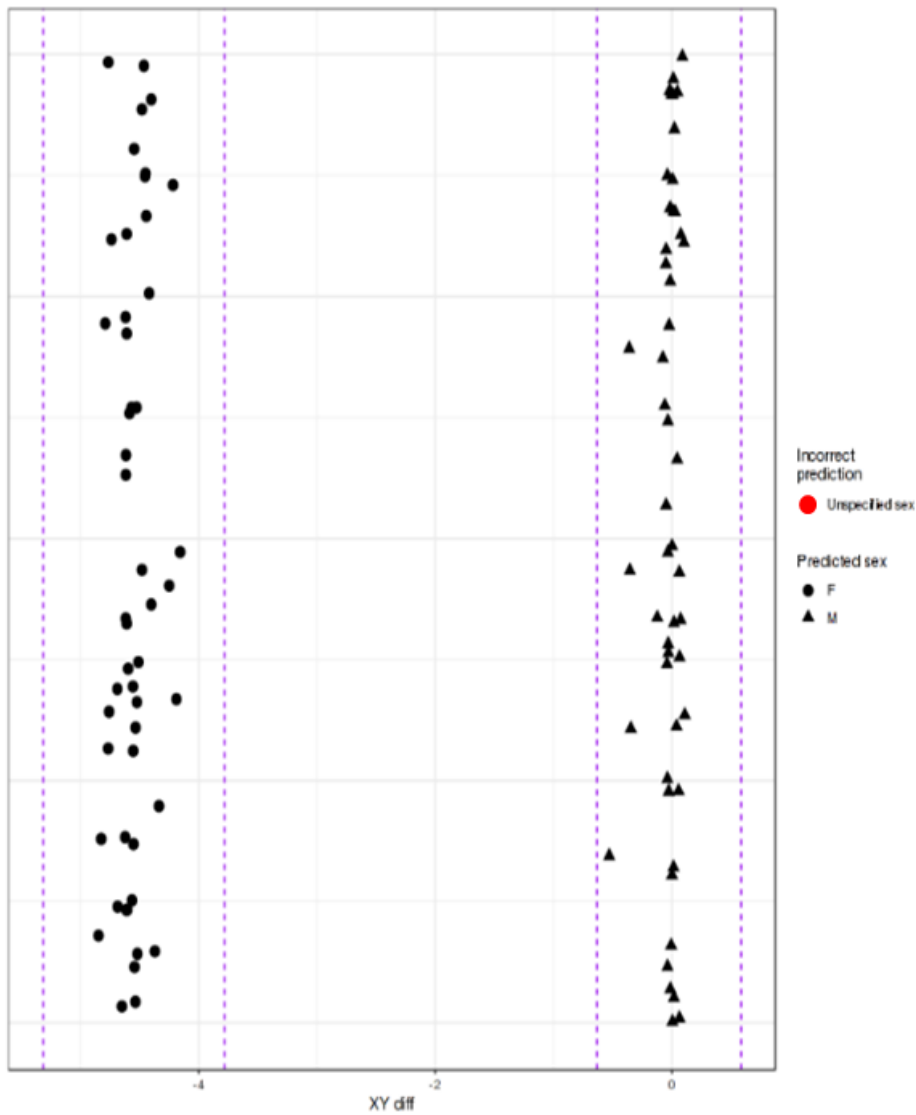


**Figure 8:** This plot depicts the difference between median X and Y chromosome intensities in the 450k array. Dashed lines represent 5 standard deviations from the mean XY difference. Females should appear within the left cluster and males in the right cluster. As can be seen there are no mismatches and no sex difference outliers.

*Methylated vs unmethylated:* In order to examine the quality of the samples it is necessary to compare the median methylation intensity to the median unmethylation intensity. Outliers are defined as those beyond 3 standard deviations of the expected (according to regression). There was 1 outlier for this comparison, as seen in red in the **Figure 9** below.

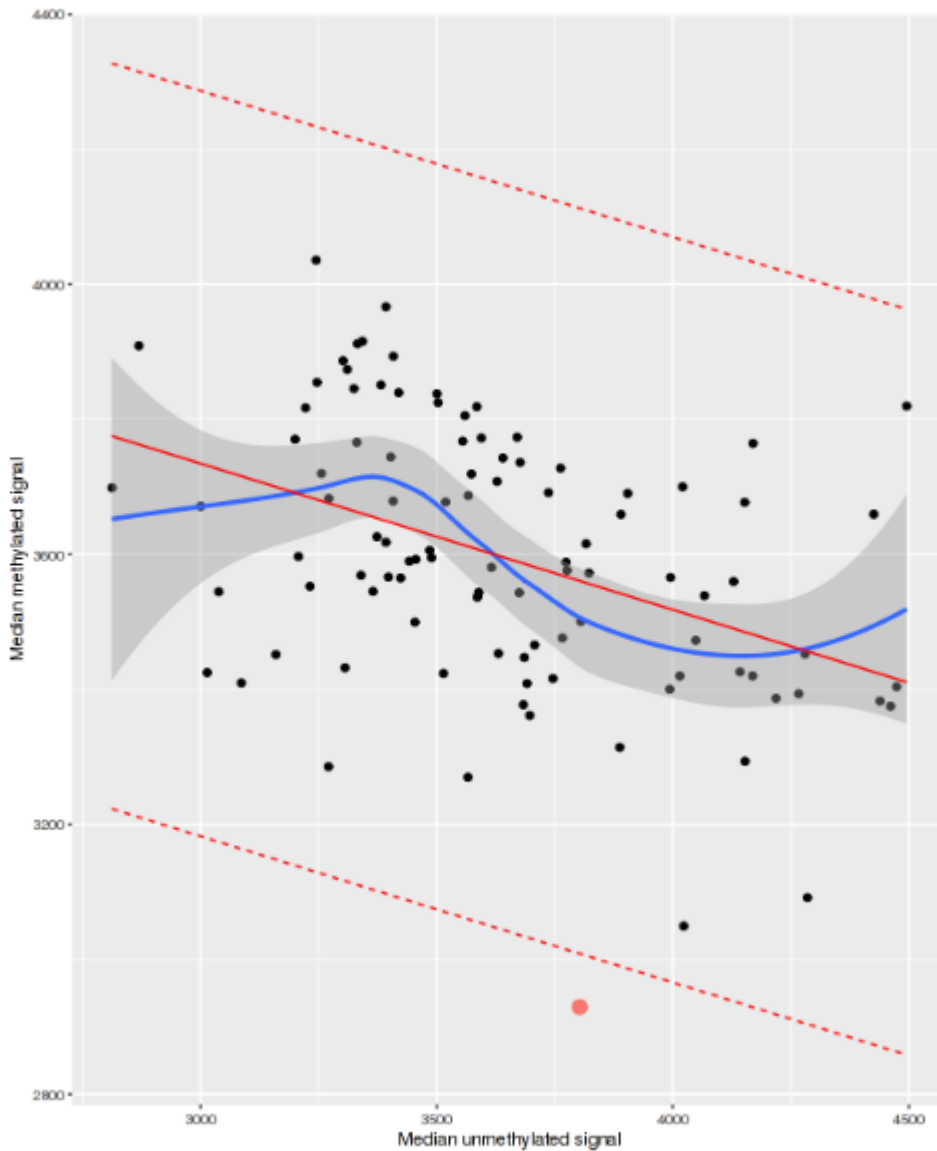


**Figure 9:** Plot demonstrating the methylation intensity signals in the 450k array against unmethylation intensity signals.

The outlier is coloured red. The red dashed line represents 3 standard deviations from the expected (according to regression).

*Control probes:* The 450k array contains control probes which can be used to evaluate elements of sample processing including staining (measuring the efficiency of the staining step of the array), extension (measuring the efficiency of extension of A,U,G or C dideoxynucleotides), hybridization (assessed using synthetic targets as opposed to the amplified sample DNA) and bisulphate conversion (testing methylation at a site which is known to be methylated). Control probes are therefore internal controls for the process of DNA methylation array and samples failing these controls are excluded, however, there were no outliers in this respect.

*Sample detection and bead number:* Sample detection is used to identify inadequate samples in which the fraction of probes which are detected in less than 1% of the total probes. There were no samples with a high proportion of undetected probes, indicating good sample quality. No samples reached the threshold for a high proportion of probes with a low bead number (defined as less than 3 beads).

*CpG detection p-values and Low bead number per CpG:* To explore the quality of the probes the proportion of samples that did not pass the detection p-value was calculated. There were 256 probes with only background signal in a high proportion of samples. Additionally, 233 CpG sites had a low bead number in a high proportion of samples.

*Estimates of cellular composition:* the proportional leukocyte constituents of the samples were assessed using Houseman's method (a bioinformatic technique which uses DNA methylation signatures to predict the white blood cell proportions in a sample of blood)<sup>178</sup>.

As a result of the above one sample was removed, leaving 99 samples for further analyses as shown in **Figure 10**.

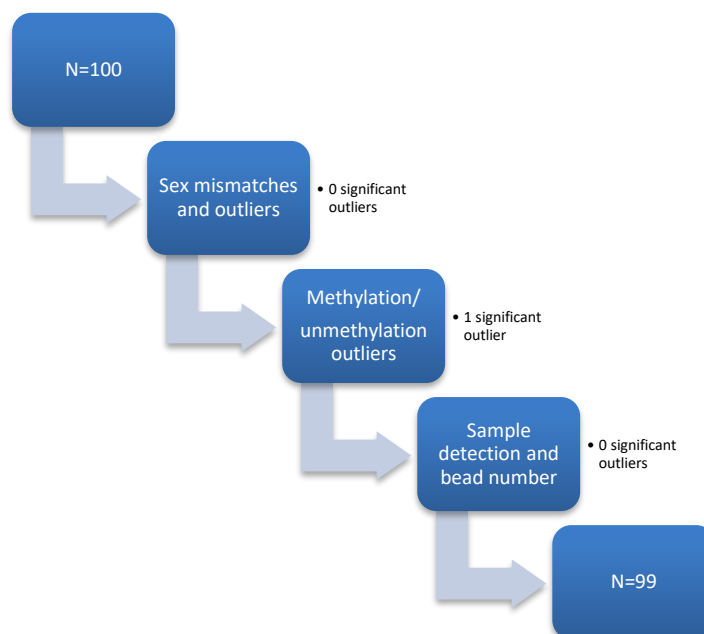


**Figure 10:** Schematic demonstrating the quality control process and exclusion of samples from the 450k dataset

#### 2.4.4.2 Quality control report for 850k array

I performed quality control for the 850k (EPIC) arrays on 356 samples (which included 11 replicates).

*Sex mismatches:* As can be seen in **Table 2** and **Figure 11** below, there were no sex mismatches and 7 sex detection outliers, 3 of which were excluded (samples 965011, 865547 and 866191) as their XY difference was  $>0.1$  or  $<-0.1$ .

*Methylated vs unmethylated:* There was 1 outlier for this comparison, as seen in **Figure 12** (sample 17605C).

Sample name	Predicted sex	Declared sex	XY difference
965011	F	F	-4.85
865379	M	M	0.07
1345422C	M	M	0.07
855027	M	M	0.09
1345422	M	M	0.09
865547	M	M	0.11
866191	M	M	0.51

**Table 2:** Sample name and XY difference for the 7 sex detection outliers.

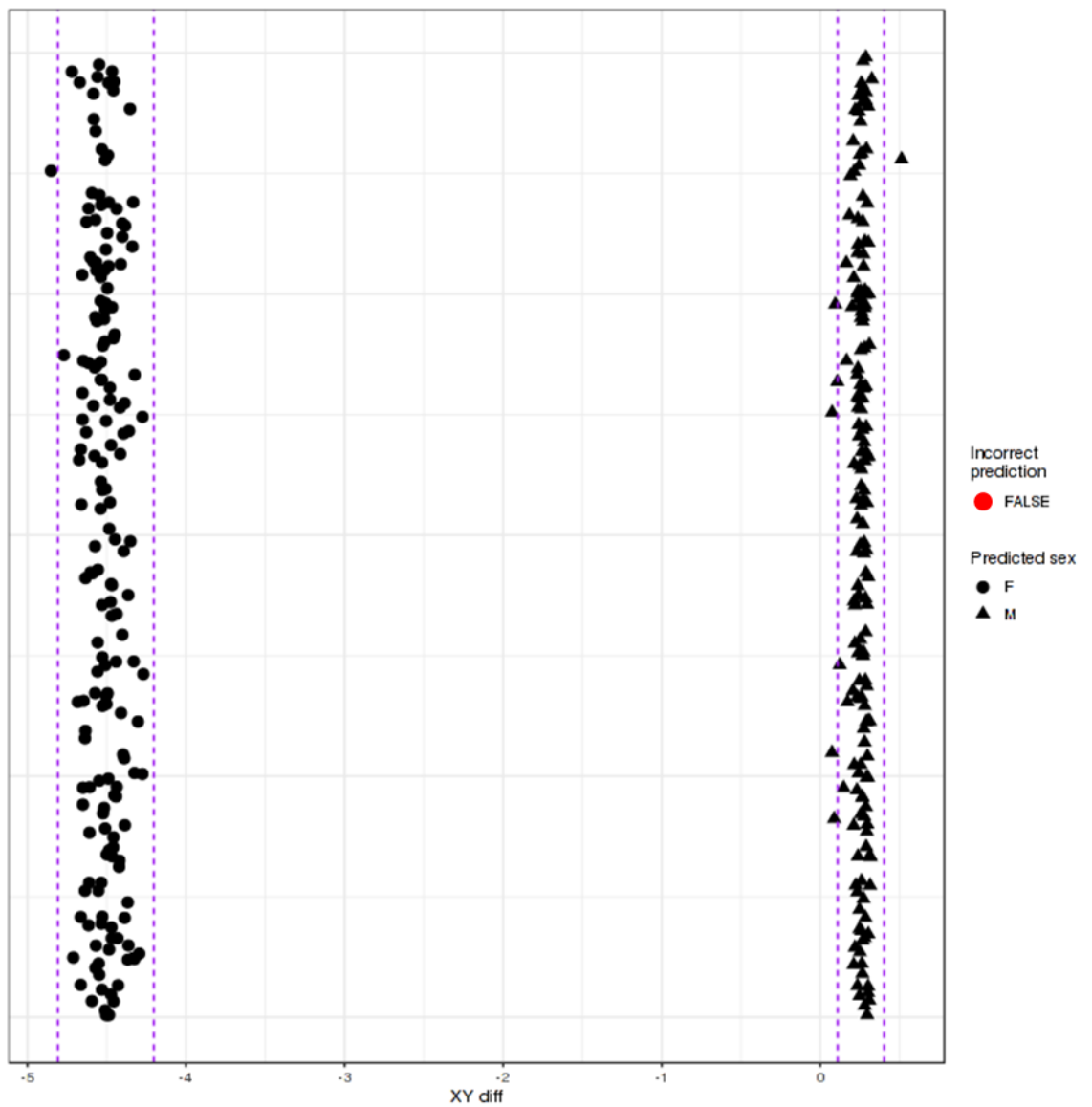


**Figure 11:** Plot depicting the difference between median X and Y chromosome intensities in the 850k array.

Dashed lines represent 3 standard deviations from the mean XY difference. Females should appear within the left cluster and males in the right cluster. As can be seen there were no mismatches and 7 sex difference outliers.

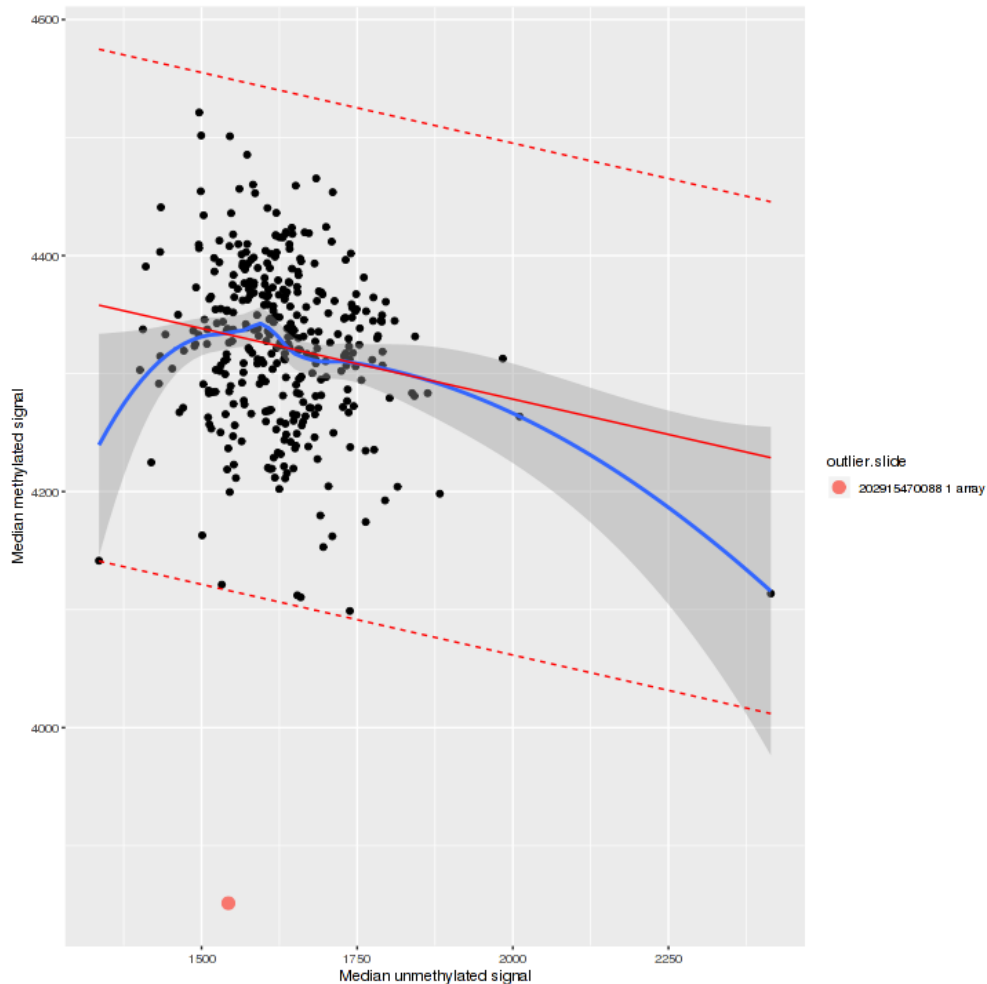


**Figure 12:** Plot demonstrating the methylation intensity signals in the 850k array against unmethylation intensity signals.

The outlier is the red-coloured dot. The red dashed line represents 3 standard deviations from the expected (according to regression).

*Control probes:* The 850k array contains control probes which can be used to evaluate elements of sample processing including staining (measuring the efficiency of the staining step of the array), extension (measuring the efficiency of extension of A,U,G or C dideoxynucleotides), hybridization (assessed using synthetic targets as opposed to the amplified sample DNA) and bisulphate conversion (testing methylation at a site which is known to be methylated). Control probes are therefore internal controls for the process of DNA methylation array and samples failing these controls are excluded. There was one outlier in this respect (sample 866146).

*Sample detection and bead number:* There were no samples with a high proportion of undetected probes, indicating good sample quality. No samples reached the threshold for a high proportion of probes with a low bead number.



*CpG probe Quality Control:* This process seeks to exclude probes from the EPIC (850k array) which have been experimentally shown to be suboptimal for the measurement of epigenome-wide methylation. The following elements were excluded from the analysis: probes with a detection p-value >0.01 in at least one sample (this was the case for n=13,259 probes), probes with less than 3 beads in at least 5% of samples (n= 5928 probes), multi-hit probes (or cross-hybridizing probes) as identified in Nordlund and colleagues (n=49)<sup>179</sup> which are known to bind to more than one site across the genome, non-CpG probes (n=2766), probes affected by SNPs as identified by Zhou and colleagues (n=94,136)<sup>180</sup>, probes on the X or Y chromosome (n= 16,349) and previously identified cross-reactive probes from the EPIC array (n=43,000)<sup>175</sup>. Thus, a total of 733,638 probes were used for downstream analysis.

*Technical variation:* This refers to batch effects and systematic variation in the dataset which is introduced, for example, by different technicians<sup>181</sup>. Some technical variation was detected using singular value decomposition analysis (via *champ* package<sup>182</sup>) and thus *COMBAT* (an adjustment for batch effects where the batch covariate is known) was applied to account for variation between slides<sup>183</sup>.

*Mean absolute deviation (MAD) scores<sup>184</sup>:* This score uses the mean absolute deviation of CpG methylation levels for each probe on the array across all individuals. If the score is positive it indicates that the sample sits within a cluster and is therefore not an outlier, however, if the MAD score is less than a -5 threshold, the sample is defined as an outlier and is excluded. Sample MAD scores were calculated with 9 outliers identified (see **Table 3** below). MAD scores were also used to exclude replicates, with the replicate with the lowest MAD score being excluded.

Sample	MAD score
176028	-5.53
176057C	-5.45
176184	-5.67
785040	-7.06
795028	-9.21
855072	-40.85
935487	-9.97
1347102	-6.47
1407727	-5.37

**Table 3:** Lowest (most extreme) mean absolute deviation scores for methylation and corresponding samples.

The last character of 'C' indicates a replicate sample.

*Estimates of cellular composition:* the proportional leukocyte constituents of the samples were assessed using Houseman's method (a bioinformatic technique which uses DNA methylation signatures to predict the white blood cell proportions in a sample of blood)<sup>178</sup>.

*Final dataset:* The final 850k methylation dataset (excluded 22 participants and) was therefore comprised of a total of 334 participants (with the process depicted in **Figure 13**)

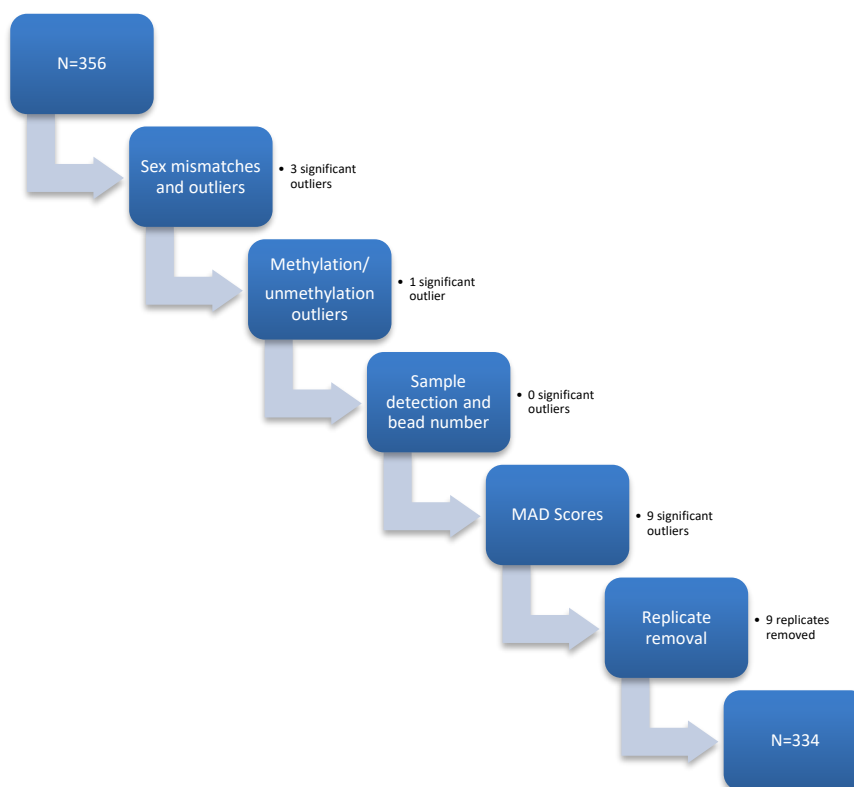


**Figure 13:** Schematic demonstrating the quality control process and exclusion of samples from the 850k dataset

#### 2.4.5 Methylation clocks

I trimmed the methylation, beta datasets to include the necessary CpG sites for clock analysis and any absent CpG measures were replaced with 'NA'. The latter was particularly important for the 850k array due to the absence of some necessary CpG sites in this array version. I produced a

sample sheet with columns headed 'Sample ID', 'Female', 'Age' and 'Tissue' as per the instructions at <https://dnamage.genetics.ucla.edu/>. I uploaded the methylation datasets (labelled with 'Sample ID') to the Horvath website, in combination with the sample sheet. Analyses were initially run 'un-Normalized' but once initial results were produced, the 'Normalized' analyses were selected.

This provided epigenetic ages and age acceleration for the Horvath epigenetic clock<sup>3</sup>, including age acceleration according to the residual from the regression of chronological against methylation age (HorvathAge), the PhenoAge clock<sup>127</sup> (PhenoAge) designed for stronger association with phenotypic measures of aging, and the GrimAge clock<sup>126</sup> (GrimAge) which is designed to predict time to death.

The output of the Horvath website included the following epigenetic age acceleration measures: HorvathAge acceleration, PhenoAge acceleration and GrimAge acceleration.

Analyses were performed on IRIDIS4 (the University of Southampton High Performing Computer Facility) using PUTTY (secure shell and telnet software) to communicate with the nodes of the supercomputer and R version 3.5.1.

#### **2.4.6 Statistical analyses**

In this section the statistical approaches used in each of the analyses are documented. The calculation of percentage change and the approach to combining the 450k and 850k epigenetic age acceleration datasets are laid out. The covariates employed as adjustments are listed and justified and the regression models and epigenome-wide association study methods are described. I used Stata (version 15.1) to perform statistical analyses to address the first two aims, and R (version 3.5.1) to perform the epigenome-wide association studies.

##### **2.4.6.1 Calculation of percentage change**

Percentage change in musculoskeletal variables (including bone microarchitecture outcomes, grip strength and femoral neck BMD) was calculated as the follow-up value minus the baseline value, all divided by baseline value with the result multiplied by 100 (to provide a percentage) ( $[(\text{follow-up value} - \text{baseline value}) / \text{baseline value}] \times 100$ ). Annualised percentage change was calculated by dividing percentage change by the follow-up time in years.

#### **2.4.6.2 Combining 450k and 850k array epigenetic age acceleration datasets**

Relationships between epigenetic measures for age and age acceleration were examined using scatterplots; histograms were used to examine the distribution of measures. The difference between 450k and 850k array results were examined for consistency and, because of systematic and significant differences in the epigenetic ages acquired from each array type (450k and 850k) (as seen in the Results chapter) epigenetic age acceleration measures were converted to array-specific Fisher-Yates z-scores to allow for a combined analysis. A z-score of zero would correspond to an average value of the epigenetic measure, compared to other values of the same array.

#### **2.4.6.3 Power calculation**

In the overall sample of size 362, there was 80% power at the 5% significance level to detect a regression coefficient of 0.15 for a standardized continuous predictor in relation to a standardized continuous outcome using simple linear regression. This is a novel area but similar sample sizes have been used in recent studies<sup>138</sup>.

#### **2.4.6.4 Justification of covariates**

The covariates used in bone and muscle analyses have been extensively studied as determinants of bone and muscle outcomes.

The incidence rates of osteoporosis, sarcopenia and fractures, as well as levels of bone mineral density and muscle parameters (including grip strength) have been shown to vary significantly with increasing age and between the sexes<sup>34,185-187</sup>.

BMI ( $\text{kg}/\text{m}^2$ ) as a measure of adiposity and height (cm) as a measure of body anthropometry are associated with bone and muscle health via the mechanical strain placed on the musculoskeletal system by higher body mass, skeletal size associated with increased height, inflammatory mediators released by fat tissue and hormonal alterations associated with increased adiposity<sup>188-190</sup>.

Dietary intake of calcium (measured in grams per day), as a key, elemental building block of bone tissue, is known to play a role in maintaining peak BMD<sup>191</sup> and mediating the risk of fracture and bone mineral density loss<sup>192,193</sup>. Protein intake has been shown to influence the risk of sarcopenia and be associated with muscle outcomes<sup>194,195</sup>, associations which are likely driven by the fact that stimulates muscle synthesis<sup>191</sup>.

Physical activity (measured in minutes per day) is beneficial to both bone and muscle. Indeed, prolonged immobilisation leads to bone loss<sup>191</sup> and reduced muscle mass, strength and function<sup>196</sup>, whereas physical activity attenuates bone loss<sup>197</sup> and maintains muscle function into older age<sup>198</sup>.

Smoking is well established to be detrimental to bone health due to reduced body weight, catabolism and inflammation leading to reduced bone density<sup>199</sup> and increased risk of fracture<sup>200</sup>. It is also associated with detrimental effects on muscle and reduced muscle mass<sup>190</sup>. In our analyses we used a categorical variable of 'ever smoking' (which was answered as 'yes' or 'no').

Alcohol consumption (measured in units per week) has a deleterious effect on musculoskeletal health via interruptions of protein and calcium metabolism and direct toxic effects on osteoblasts and muscle tissue<sup>191</sup> leading to, for example, increased risk of fracture with higher alcohol consumption<sup>201</sup>.

Social status has effects on many facets of health including bone health<sup>202,203</sup> and ageing diseases of muscle<sup>204,205</sup>. Social class was defined as either manual or non-manual.

#### **2.4.6.5 Investigation of longitudinal bone microarchitecture, grip and femoral neck BMD**

##### **2.4.6.5.1 Associations with fracture**

The outcome in this analysis was fracture (defined according to a yes/no answer to the question "have you sustained a fracture since the age of 45 years?" at the EPOSA (2011-12) follow-up or the presence of a vertebral fracture on a lateral spine DXA image at the EPOSA follow-up) as a dichotomous outcome.

The predictors in this analysis were continuous variables including the baseline level and longitudinal change in bone microarchitecture parameters (units for these measures are as follows: area (mm<sup>2</sup>), density (mg/cm<sup>3</sup>), thickness (µm), separation (µm), trabecular number (mm<sup>-1</sup>), porosity (%), diameter (mm)), grip strength (kg) and femoral neck bone mineral density (g/cm<sup>2</sup>) measured at EPOSA follow-up and the change between EPOSA and HBS17 (2017) follow-up).

The covariates used for these analyses have been previously identified as potential confounders for the relationship between bone structure (incorporating microarchitecture and bone mineral density), grip strength and fracture and included sex, age, height, BMI, dietary calcium, physical activity, smoking history (ever vs never), alcohol consumption and social class.

In these analyses a logistic regression model was utilised to investigate the association between baseline levels and longitudinal changes in musculoskeletal parameters (bone microarchitecture parameters, grip strength and total femoral neck BMD) in relation to fracture. Fisher-Yates z-scores were derived for each musculoskeletal parameter and used in these models to enable the comparison of effect sizes. Therefore, these analyses resulted in odds ratios for previous fracture per standard deviation difference in baseline values and percentage changes in each predictor.

A p-value <0.05 was regarded as statistically significant.

Additional sensitivity analyses (using the above methods) were performed to investigate the effect of bisphosphonates. Bisphosphonate usage, acquired from questionnaires at the time of bone scans, was included as a covariate in the fully-adjusted models (incorporating sex, age, height, BMI, dietary calcium, physical activity, smoking history (ever vs never), alcohol consumption and social class).

#### **2.4.6.5.2 Associations with SNPs**

The predictors in this analysis were the SNPs and the outcomes in this analysis were continuous variables including the baseline level and longitudinal change in bone microarchitecture parameters (units for these measures are as follows: area (mm<sup>2</sup>), density (mg/cm<sup>3</sup>), thickness (mm), separation (mm), trabecular number (mm<sup>-1</sup>), porosity (%), diameter (mm)), grip strength (kg) and femoral neck bone mineral density (g/cm<sup>2</sup>) measured at EPOSA follow-up and the change between EPOSA and HBS17 (2017) follow-up).

The covariates used for these analyses included age and sex.

In these analyses a linear regression model was utilised to investigate the association between individual SNPs and continuous bone microarchitecture parameters (including baseline level and longitudinal change). Normality of bone microarchitecture outcomes was confirmed via visual inspection of histograms, linearity of relationship was confirmed graphically, Q-Q plots were used to test for normality of residuals and plots of residuals against the fitted values (outcomes values estimated by the model) were examined to check the constant variance assumption of the residuals.

A p-value <0.05 was regarded as statistically significant.

#### **2.4.6.6 Investigations of epigenetic age acceleration**

The predictors in these analyses were epigenetic age acceleration (GrimAge Acceleration, PhenoAge Acceleration and HorvathAge Acceleration) measured in years.

The outcomes were continuous, normally distributed (confirmed via histograms) and included the following:

- Maximum grip strength (kg) (measured at HCS baseline, EPOSA and HBS17)
- Gait speed (m/s) (measured at EPOSA and HBS17)
- Total spinal and femoral neck BMD ( $\text{g}/\text{cm}^2$ ) (measured at HCS baseline, EPOSA and HBS17)
- HR-pQCT outcomes (total volumetric BMD ( $\text{mg}/\text{cm}^3$ ), trabecular density ( $\text{mg}/\text{cm}^3$ ) and cortical thickness( $\mu\text{m}$ )) (measured at EPOSA and HBS17)
- pQCT cortical thickness (mm) (this outcome was used to further examine the association observed with cortical thickness in the HR-pQCT dataset) (measured at EPOSA)
- Appendicular lean mass (grams) (measured at EPOSA and HBS17)
- Total fat mass (grams) (measured at EPOSA and HBS17)

Covariates were measured at HCS baseline (199-2004) and for each musculoskeletal outcome are described below and longitudinal change outcomes were additionally adjusted for follow-up time.

All analyses were stratified by sex

Covariates for **grip strength** and **gait speed** analyses included:

- Model 1: none (unadjusted model)
- Model 2: age, height and BMI
- Model 3: age, height, BMI, social class, physical activity, prudent diet, ever smoked and alcohol consumption

Covariates included in **HR-pQCT**, **total spinal BMD** and **total femoral neck BMD** (via DXA) and **pQCT** analyses included:

- Model 1: none (unadjusted model)
- Model 2: adjusted - age, height, BMI, social class, physical activity, dietary calcium, ever smoked and alcohol consumption

Covariates included in **appendicular lean mass** and **total fat mass** analyses:

- Model 1: none (unadjusted model)
- Model 2: adjusted - age, height, occupational social class, physical activity, prudent diet, ever smoked and alcohol consumption

Linear regression models were used to examine the association between age acceleration predictors and continuous, normally-distributed musculoskeletal and body composition outcomes. Normality of musculoskeletal outcomes was confirmed via visual inspection of histograms, linearity of relationship with epigenetic age acceleration measures was confirmed graphically, Q-Q plots were used to test for normality of residuals and plots of residuals against the fitted values (outcomes values estimated by the model) were examined to check the constant variance assumption of the residuals. Note that, due to the strong relationship between BMI and both appendicular lean mass and total fat mass, BMI was not used as a covariate in these linear regression models to avoid multicollinearity problems.

A p-value <0.05 was regarded as statistically significant.

Some associations between predictors and outcomes were examined graphically using quartiles of the predictor (epigenetic age acceleration) in order to inspect the change in outcomes between the highest and lowest quartile.

Additional sensitivity analyses using the above methods were performed for the effect of medications on bone outcomes (by including bisphosphonate usage at the time of bone scans as a covariate in fully-adjusted models). Sensitivity analyses were also performed to investigate potential effects of outliers in epigenetic age acceleration which were identified from histograms. For this, the statistical method described above was repeated but with outliers excluded, to investigate whether the outlying epigenetic age acceleration values were driving associations which were statistically significant.

#### **2.4.6.7 Epigenome-wide association study**

I performed epigenome-wide association study (EWAS) analyses with supervision and direction from Dr Negusse Kitaba and Dr Faisal Rezwan. Beta values from autosomal CpG sites in the 850k array were used for EWAS using Meffil<sup>176</sup> and Minfi<sup>177</sup>. Beta value files were used together with phenotyping dataset from the baseline of the HCS (1998-2004) to allow cross-sectional analyses.

Maximum grip strength (measured in kg) and total femoral neck BMD (measured by DXA) were the continuous, normally-distributed outcomes of interest. The predictor in this analysis was DNA methylation at each CpG site, measured as a beta-value between 0 and 1.

To identify differentially methylated CpG sites, a robust multiple regression model (a linear regression model in which samples with outlying methylation levels are down-weighted) was applied using the R Bioconductor package *limma*<sup>173</sup> on methylation beta values adjusting for covariates.



The four EWAS models which were used are listed in **Table 4**, all of which were adjusted for cell count composition of the sample (including B lymphocytes, CD4+ T lymphocytes, CD8+ T lymphocytes, monocytes, natural killer cells) and array.

Analyses performed with no further adjustments (beyond cell composition and array) (Model 1) and a model with adjustment for age and sex (Model 2) which was used for the primary epigenome-wide analyses.

Sensitivity analyses were performed with epigenome-wide analyses adjusting for age, sex, height and weight for height residual (as a measure of adiposity) (Model 3) and a model with adjustment for age, sex, height, weight for height residual, occupational social class (manual vs non-manual labour), physical activity (Dallosso score<sup>157</sup>), diet (prudent diet score for grip strength analyses and dietary calcium for BMD analyses), smoking status (ever having smoked regularly) and alcohol consumption (an ordinal variable of units/week) (Model 4).

EWAS model	Adjustments			
1	Cell composition Array			
2	Cell composition Array	Age Sex		
3	Cell composition Array	Age Sex	Height Weight for height residual	
4	Cell composition Array	Age Sex	Height Weight for height residual	Occupational social class Physical activity Diet Smoking status Alcohol consumption

**Table 4:** EWAS model and covariates included in adjustment

Further models were performed for sensitivity including a model with adjustment for age, sex, height and weight for height residual (as a measure of adiposity) (Model 3) and a model with adjustment for age, sex, height, weight for height residual, occupational social class (manual vs non-manual labour), physical activity (Dallosso score<sup>157</sup>), diet (prudent diet score for grip strength analyses and dietary calcium for BMD analyses), smoking status (ever having smoked regularly) and alcohol consumption (an ordinal variable of units/week) (Model 4).

The level of significance was set at the Mansell threshold (a threshold of  $p < 9 \times 10^{-8}$  which was experimentally established to adequately control the false positive rate for EPIC (850k) array DNA methylation studies)<sup>206</sup>. Inflation, a parameter which assesses for the systematic biases within a

dataset by dividing the observed chi-squared test statistic by the expected chi-squared test statistic, was calculated by lambda statistics and visualised via Quantile-Quantile-plots (QQ-plots). As with previous analyses, R version 3.5.1 was used. Differentially methylated regions (DMRs) were identified using *dmrcate*<sup>207</sup>.

Adjustment for multiple testing was performed using Benjamini-Hochberg procedure with a false discovery rate less than 0.05 (FDR<0.05). The Benjamini-Hochberg procedure aims to reduce the number of false positives (or type 1 errors) in which the null hypothesis (that there is no association between methylation at a CpG site and the outcome of interest) is incorrectly rejected. It operates by placing the p-values for each CpG sites in ascending order, then ranking the p-values (from lowest to highest) and determining the Benjamini-Hochberg critical value for each p-value (calculated as (p-value rank x FDR)/ the number of tests performed)<sup>208</sup>. The threshold is then set at the largest p-value which is less than the critical value. It then selects the lowest p-value at which the null hypothesis would be rejected to be the adjusted p-value. Due the fact that this adjusted p-value has to come from the original list of p-values, multiple p-values will be rejected at the same adjusted p-value threshold meaning that multiple, different p-values can have the same adjusted p-value.

Pathway and gene ontology enrichment was also carried out using *missMethyl*<sup>209</sup> and *Enrichr*<sup>210</sup> on subsets of genes. Two subsets were used:

1. Limited subset: A subset of genes associated with CpG sites with a p-value (for significance of association in EWAS) of  $<1 \times 10^{-5}$
2. Extended subset: A subset of genes associated with the CpG sites with the lowest 100 p-values (for significance of association in EWAS).

It should be noted that these two approaches to producing a gene set for enrichment analysis provide a focused view (via the limited subset) and a wider view (via the extended subset) of the pathways or gene ontologies associated with the gene list derived from differential methylation analyses. Thresholds for defining gene sets for enrichment analyses are arbitrary<sup>211</sup>, and the above approaches represent a compromise, as the analyses would be most robust if all genes in the gene list were associated with CpG sites which had met the pre-set threshold for statistical significance<sup>206</sup>. Additionally, some CpG sites are unclassified, and therefore the number of significant CpG sites did not correspond exactly with the number of genes included in pathway and gene ontology analyses.

Pathway analysis was carried out by mapping genes associated with significantly associated CpG sites to the Kyoto Encyclopaedia of Genes and Genomes (KEGG) 2021, a biological database with manually drawn metabolic, signalling and cellular process pathway maps. These pathways include

rectangles (indicating the protein product of a gene) and interactions between these are represented by arrows or lines<sup>212-214</sup>.

Gene ontology enrichment analysis was performed using GO consortium tools for Biological Processes, Molecular Functions and Cellular Components<sup>215,216</sup>.

Human phenotype ontology was performed using the Human Phenotype Ontology project (HPO), a collection of health, medical and disease phenotypes<sup>217</sup>. This project aims to provide an ontology of medically relevant phenotypes including 1779 terms (each describing a clinical abnormality) with 3096 genes labelled as associated with these phenotypic terms.

Both gene ontology and pathway analysis identify, for a given set of genes, which gene ontology terms or pathways are over-represented, compared to the expected representation. In this context, odds ratio is the odds that a particular term (gene ontology term or pathway term) appears in a list of differentially methylated genes divided by the odds that the same term appears in a list of all genes of a given gene set. The p-value in these analyses is derived from the Fisher's exact test<sup>218</sup>. For both pathway analysis and gene ontology analysis a significance cut-off was defined as an adjusted p-value < 0.05 (adjusted for the number of statistical tests performed).

This enrichment approach is a particularly useful tool in smaller datasets which may lack the statistical power to demonstrate significant associations with individual CpG sites and loci.



## Chapter 3 Results

### 3.1 Description of change in musculoskeletal parameters with ageing and associations with fracture and genetic loci

As described in the methods section, the longitudinal bone microarchitecture data from the HCS are a unique resource which includes the HR-pQCT scans performed on participants at the EPOSA (2011-12) and the HBS17 (2017) follow-up visits. In this chapter the changes seen in bone microarchitecture are described and the associations with fracture and specific, known genetic loci<sup>219</sup> are examined. These findings have been published in the journal *Bone* in 2021<sup>220</sup> and some figures and tables are drawn from this publication.

Furthermore, grip strength change and DXA-measured bone mineral density change over the same time period (EPOSA to HBS17) are also described, as these represent important musculoskeletal outcomes that will be considered in future chapters.

The timings of the measurements made are summarized in **Figure 14**, and have been reported in detail in Chapter 2.

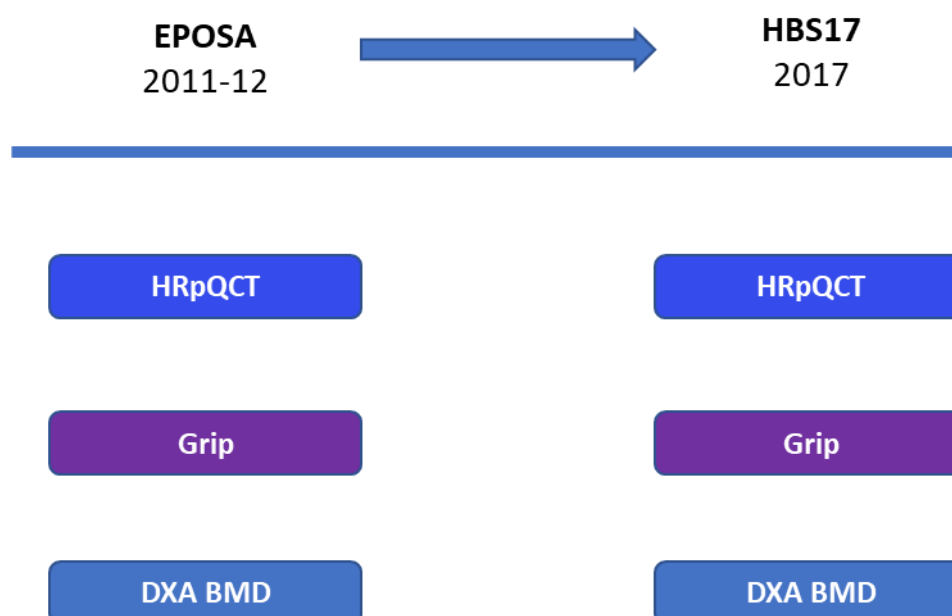


**Figure 14:** Timelines for the HRpQCT, maximum grip strength and DXA BMD parameters examined in this chapter.

### **3.1.1 Participant characteristics**

This investigation incorporated a subset of 214 HCS participants (115 males and 99 females) with a mean age of 76.0 (2.5) years at the first (EPOSA) HR-pQCT scans (in 2011-2012). Males were taller and had greater weight than females but BMI was roughly equal across the sexes. Dietary calcium intake was just over 8 grams per week. Males were more likely to have ever smoked and were more likely to be moderate or high drinkers. Approximately half of participants were from a manual social class and bisphosphonates were used by 3.7% of males and just over a fifth (20.7%) of females.

In terms of fracture outcomes, 27 (25.2%) males and 32 (33.3%) females had sustained a previous vertebral (6 in males and 6 in females) or self-reported fracture since the age 45. The median follow-up time between the first HR-pQCT scan (EPOSA) and second scan (HBS17) scans was 5.2 (4.8, 5.4) years. The characteristics of the study population are presented in **Table 5**.

**Table 5:** Descriptive statistics for participant characteristics in 2011-2012<sup>220</sup>

Participant characteristic	Mean (standard deviation), n(%) or median (lower quartile, upper quartile)	
	Males (n=115)	Females (n=99)
Age (years)	75.8 (2.5)	76.2 (2.6)
Height (cm)	173.3 (6.5)	160.4 (5.7)
Weight (kg)	83.1 (13.0)	72.4 (12.5)
BMI (kg/m <sup>2</sup> )	27.7 (4.0)	28.1 (4.5)
Weekly dietary calcium (g)*	8.3 (2.2)	8.0 (2.9)
Physical activity in last 2 weeks (min/day) **	195.0 (128.6, 291.4)	207.9 (150.0, 287.1)
Ever smoked	61 (56.5%)	39 (40.2%)
Weekly alcohol units (M: Males; F: Females)		
Very low (0/<1 M&F)	24 (22.2%)	48 (49.5%)
Low (1-10M,1-7F)	48 (44.4%)	39 (40.2%)
Moderate (11-21M,8-14F)	17 (15.7%)	8 (8.2%)
High (>21M, >14F)	19 (17.6%)	2 (2.1%)
Social class (manual)*	59 (53.6%)	53 (53.5%)
Bisphosphonate use (1998-2004 to 2012)*	4 (3.7%)	20 (20.6%)
Self-reported fracture since aged 45 years	24 (22.4%)	30 (30.9%)
Vertebral fracture	6 (5.3%)	6 (6.1%)
Any fracture (self-reported or vertebral)	27 (25.2%)	32 (33.3%)
*Ascertained using information at initial phase of the Hertfordshire Cohort Study (1998-2004)		
**Derived using the Longitudinal Ageing Study Amsterdam Physical Activity Questionnaire		

### 3.1.2 Associations between bone microarchitecture and previous fracture

Bone microarchitecture was assessed at both the radius and tibia; however, although the patterns of association were similar for each, the associations between tibial parameters and previous fracture were substantially stronger at the tibia than at the radius.

Baseline values and annual percentage changes (calculated as:  $([\text{follow-up value} - \text{baseline value}]/\text{baseline value}) \times 100$  per year of follow-up) in tibial HR-pQCT parameters are presented in **Table 6**. Although annual percentage changes in parameters were small at all sites, many of these longitudinal changes in bone microarchitecture differed significantly from zero ( $p < 0.05$ ). We observed decreases in trabecular density (females only), cortical area, density and thickness, and total volumetric bone mineral density and increases in cortical pore diameter (males only), trabecular area and cortical porosity.

Radial HR-pQCT parameters are presented in **Appendix 6**. At the radius, there were statistically significant decreases in total volumetric bone mineral density, trabecular number (females only), cortical area, cortical density and cortical thickness, and increases in trabecular area, trabecular separation (females only), cortical porosity (males only) and cortical pore diameter (females only).



Parameter [Median (lower quartile, upper quartile) values shown]	Males (n=115)			Females (n=99)		
	Baseline	Annual change (%)	P-value	Baseline	Annual change (%)	P-value
Trabecular area (mm <sup>2</sup> )	743 (648, 838)	<b><u>0.1 (0.0, 0.2)</u></b>	<b><u>&lt;0.001</u></b>	620 (542, 707)	<b><u>0.2 (0.0, 0.3)</u></b>	<b><u>&lt;0.001</u></b>
Total volumetric bone density (mg/cm <sup>3</sup> )	294 (262, 343)	<b><u>-0.5 (-1.0, -0.2)</u></b>	<b><u>&lt;0.001</u></b>	252 (219, 276)	<b><u>-0.8 (-1.5, -0.3)</u></b>	<b><u>&lt;0.001</u></b>
Trabecular density (mg/cm <sup>3</sup> )	196 (170, 215)	-0.1 (-0.3, 0.2)	0.180	167 (149, 199)	<b><u>-0.3 (-0.8, 0.2)</u></b>	<b><u>0.012</u></b>
Trabecular number (mm <sup>-1</sup> )	2.5 (2.2, 2.7)	-0.1 (-1.0, 1.1)	0.444	2.3 (2.0, 2.5)	-0.2 (-1.7, 1.4)	0.213
Trabecular thickness (mm)	0.066 (0.058, 0.072)	0.0 (-1.1, 1.0)	1.000	0.064 (0.054, 0.071)	0.0 (-1.3, 1.2)	1.000
Trabecular separation (mm)	0.34 (0.30, 0.38)	0.1 (-1.1, 1.1)	0.501	0.37 (0.34, 0.43)	0.3 (-1.3, 2.0)	0.300
Cortical area (mm <sup>2</sup> )	129 (116, 153)	<b><u>-0.7 (-1.5, 0.0)</u></b>	<b><u>&lt;0.001</u></b>	83 (74, 98)	<b><u>-1.3 (-2.4, -0.4)</u></b>	<b><u>&lt;0.001</u></b>
Cortical density (mg/cm <sup>3</sup> )	836 (803, 873)	<b><u>-0.6 (-1.0, -0.3)</u></b>	<b><u>&lt;0.001</u></b>	763 (721, 807)	<b><u>-0.7 (-1.2, -0.2)</u></b>	<b><u>&lt;0.001</u></b>
Cortical porosity (%)	8.8 (7.3, 10.6)	<b><u>2.5 (0.5, 4.8)</u></b>	<b><u>&lt;0.001</u></b>	9.9 (7.9, 12.2)	<b><u>1.5 (-0.1, 3.3)</u></b>	<b><u>&lt;0.001</u></b>
Cortical thickness (mm)	1.2 (1.1, 1.4)	<b><u>-0.4 (-1.1, 0.1)</u></b>	<b><u>&lt;0.001</u></b>	0.9 (0.8, 1.1)	<b><u>-1.1 (-2.0, -0.1)</u></b>	<b><u>&lt;0.001</u></b>
Cortical pore diameter (mm)	0.17 (0.16, 0.18)	<b><u>0.2 (-0.7, 1.3)</u></b>	<b><u>0.031</u></b>	0.18 (0.17, 0.19)	0.1 (-0.9, 0.9)	0.602

P-values correspond to tests that median annual percentage changes were zero and were calculated from sign tests

Median annual percentage changes that were significantly different from zero (p<0.05) are highlighted in bold (underlined for increases and italic for decreases)

**Table 6:** Descriptive statistics for *tibial* HR-pQCT parameters at baseline (2011-2012) and for changes in parameters from EPOSA to HBS17<sup>220</sup>

### 3.1.3 Associations between baseline values and changes in tibial HR-pQCT parameters and previous fracture

Associations between baseline values and annual percentage changes in tibial HR-pQCT parameters (**Table 7**), grip strength and femoral neck BMD in relation to previous fracture are presented in **Figure 15**. Using baseline scans (from EPOSA, 2011-12) alone increased odds of previous fracture were observed for: higher trabecular area (OR 2.18 (1.27,3.73),  $p<0.01$ ); lower total volumetric bone density (OR 0.53 (0.34,0.84)  $p<0.01$ ); lower cortical area (OR 0.53 (0.30,0.95),  $p<0.04$ ), lower cortical density (OR 0.56 (0.36,0.88),  $p<0.02$ ) and lower cortical thickness (OR 0.45 (0.27,0.77),  $p<0.01$ ); and greater declines in trabecular density (OR 0.50 (0.34,0.75),  $p<0.002$ ). These relationships remained significant in fully-adjusted models. At the radius, baseline cortical pore diameter was significantly associated with greater odds of fracture (OR 0.63 (0.44,0.92),  $p<0.005$ ). Associations between baseline values and annual percentage changes in radial HR-pQCT parameters in relation to previous fracture are presented in **Appendix 7**.

To provide some interpretation to these findings, if we take tibial total volumetric bone density as an example of a baseline measure, we found that for every SD increase in total volumetric bone density there was a 47% reduction in the odds of previous fracture (any fracture since the age of 45 years or vertebral fracture on lateral spinal DXA).

If we take change in trabecular density as an example of a change measure, per SD increase in trabecular density change there is a reduction in the odds of previous fracture by 50%. It should be noted here that higher values of the change parameter reflect reduced decline in that parameter (as annualised percentage change is calculated as  $([\text{follow-up value} - \text{baseline value}]/\text{baseline value}) \times 100$  per year of follow-up. Thus, reduced decline in trabecular density is associated with a lower odds of previous fracture.

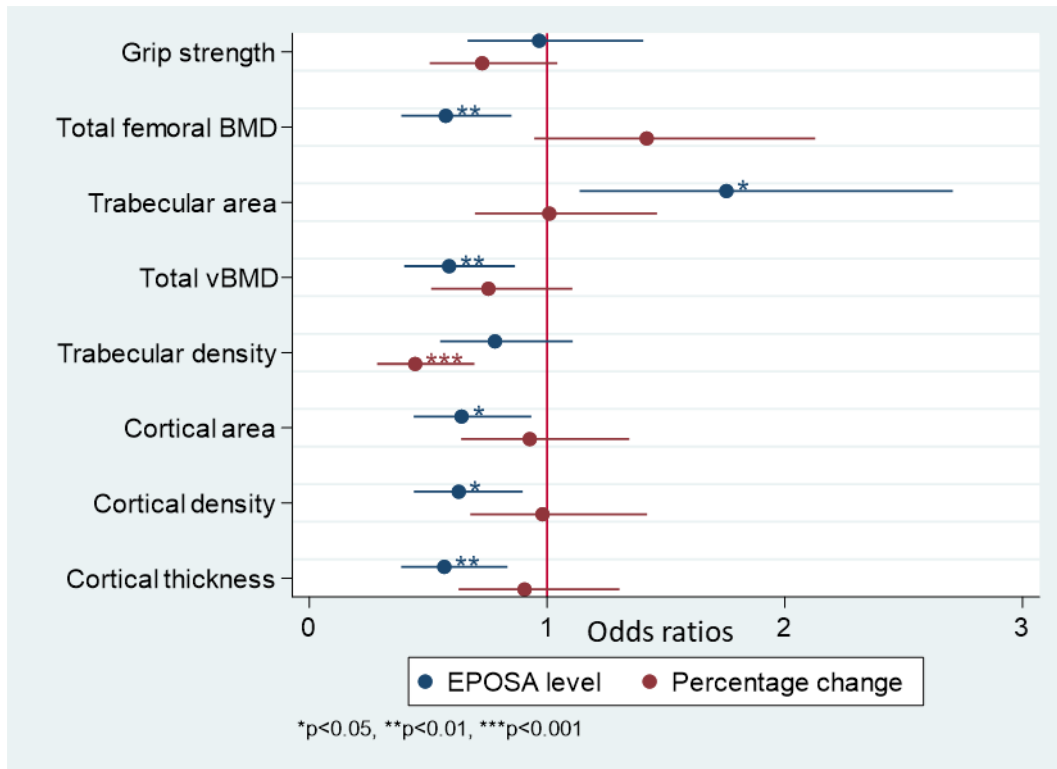


**Figure 15:** Odds of fracture for level and change of musculoskeletal parameters.

Fully-adjusted odds ratios for previous fracture per standard deviation difference in baseline values and changes in maximum grip strength, total femoral BMD (measured via DXA) and key tibial HR-pQCT parameters.

Odds ratios were adjusted for sex, age, height, BMI, dietary calcium, physical activity, smoking history (ever vs never), alcohol consumption and social class

Odds ratios greater than one: higher baseline values in 2011-2012 or reduced declines in musculoskeletal variables from 2011-2012 to 2017 were associated with greater risk of previous fracture

Odds ratios less than one: higher baseline values in 2011-2012 or reduced declines in musculoskeletal variables from 2011-2012 to 2017 were associated with lower risk of previous fracture

**Table 7:** Odds ratios for previous fracture per standard deviation difference in both baseline values and changes in parameters<sup>220</sup>

HR-pQCT tibia parameter (SD)	Baseline values in 2011-2012				Annual percentage change from 2011-2012 to 2017			
	Sex-adjusted		Fully-adjusted*		Sex-adjusted		Fully-adjusted*	
	Odds ratio (95% CI)	P-value	Odds ratio (95% CI)	P-value	Odds ratio (95% CI)	P-value	Odds ratio (95% CI)	P-value
Trabecular area	<b><i>1.70 (1.15,2.51)</i></b>	<b><i>0.007</i></b>	<b><i>2.18 (1.27,3.73)</i></b>	<b><i>0.005</i></b>	1.11 (0.80,1.56)	0.525	1.01 (0.71,1.44)	0.945
Total volumetric bone density	<b><i>0.58 (0.39,0.84)</i></b>	<b><i>0.004</i></b>	<b><i>0.53 (0.34,0.84)</i></b>	<b><i>0.007</i></b>	0.72 (0.52,1.01)	0.059	0.75 (0.53,1.07)	0.117
Trabecular density	0.79 (0.56,1.10)	0.168	0.72 (0.49,1.06)	0.099	<b><i>0.56 (0.40,0.80)</i></b>	<b><i>0.001</i></b>	<b><i>0.50 (0.34,0.75)</i></b>	<b><i>0.001</i></b>
Trabecular number	0.92 (0.66,1.27)	0.602	0.96 (0.64,1.43)	0.836	0.99 (0.72,1.36)	0.951	0.91 (0.64,1.29)	0.584
Trabecular thickness	0.80 (0.58,1.10)	0.168	0.69 (0.48,1.00)	0.052	0.83 (0.60,1.15)	0.256	0.88 (0.62,1.27)	0.502
Trabecular separation	1.12 (0.81,1.55)	0.504	1.10 (0.74,1.64)	0.626	1.03 (0.75,1.41)	0.872	1.13 (0.79,1.60)	0.515
Cortical area	<b><i>0.52 (0.32,0.84)</i></b>	<b><i>0.008</i></b>	<b><i>0.53 (0.30,0.95)</i></b>	<b><i>0.032</i></b>	0.86 (0.62,1.20)	0.377	0.98 (0.68,1.40)	0.908
Cortical density	<b><i>0.51 (0.34,0.76)</i></b>	<b><i>0.001</i></b>	<b><i>0.56 (0.36,0.88)</i></b>	<b><i>0.011</i></b>	0.93 (0.67,1.28)	0.641	1.00 (0.70,1.42)	0.987
Cortical porosity	1.09 (0.79,1.50)	0.618	0.96 (0.67,1.37)	0.808	<b><i>0.71 (0.51,1.00)</i></b>	<b><i>0.048</i></b>	0.73 (0.51,1.05)	0.090
Cortical thickness	<b><i>0.48 (0.31,0.74)</i></b>	<b><i>0.001</i></b>	<b><i>0.45 (0.27,0.77)</i></b>	<b><i>0.004</i></b>	0.82 (0.59,1.15)	0.255	0.91 (0.64,1.30)	0.597
Cortical pore diameter	0.85 (0.61,1.17)	0.317	0.71 (0.49,1.03)	0.070	0.82 (0.59,1.15)	0.253	0.82 (0.56,1.20)	0.309

HR-pQCT: High resolution peripheral quantitative computed tomography; CI: Confidence interval

\*Adjusted for sex, age, height, BMI, dietary calcium, physical activity, smoking history (ever vs never), alcohol consumption and social class

Odds ratio of less than one for annual percentage change in parameter shows that reduced declines are related to lower risk of previous fracture

Significant associations (p<0.05) are given in italics

#### **3.1.4 Selected loci in relation to tibial HR-pQCT parameters that were associated with previous fracture**

Although the focus of this thesis centred around epigenetic rather than genetic markers, we considered relationships between selected genetic loci and baseline values and annual percentage changes in tibial bone microarchitecture parameters (which were associated with previous fracture) here. These are presented in **Table 8**. Few loci significant associations were observed, though rs3801387 (*WNT16*) was related to change in trabecular density ( $p=0.011$ ) and rs7812088 (*ABCF2*) there was a borderline association with baseline values of trabecular area ( $p=0.072$ ). However, the remaining associations were weak ( $p>0.09$ ). To contextualise the result for rs3801387 (*WNT16*), we found that for each extra G allele at that locus there was a 0.28 standard deviation reduction in decline (or, more simply, a gain) of trabecular density.

**Table 8:** Selected loci in relation to tibial HR-pQCT parameters that were associated with previous fracture<sup>220</sup>

HR-pQCT tibia parameter (z-scores)	rs1053051 ( <i>TMEM263</i> ):		rs7812088 ( <i>ABCF2</i> ):		rs10226308 ( <i>TXNDC3</i> ):		rs3801387 ( <i>WNT16</i> ):	
	per extra T allele		AG compared to GG		per extra G allele		per extra G allele	
	Estimate (95% CI)	P-value	Estimate (95% CI)	P-value	Estimate (95% CI)	P-value	Estimate (95% CI)	P-value
<b>Baseline values</b>								
Trabecular area	-0.07 (-0.24,0.10)	0.426	-0.28 (-0.59,0.03)	0.072	0.07 (-0.17,0.30)	0.584	-0.02 (-0.23,0.18)	0.810
Total volumetric bone density	0.13 (-0.03,0.30)	0.112	0.18 (-0.13,0.48)	0.251	0.02 (-0.21,0.25)	0.856	0.03 (-0.17,0.23)	0.767
Cortical area	0.06 (-0.07,0.18)	0.385	0.10 (-0.13,0.33)	0.384	-0.03 (-0.21,0.15)	0.734	0.01 (-0.14,0.16)	0.879
Cortical density	0.04 (-0.12,0.20)	0.636	0.00 (-0.28,0.29)	0.974	0.06 (-0.15,0.28)	0.560	0.03 (-0.16,0.21)	0.784
Cortical thickness	0.09 (-0.06,0.24)	0.244	0.21 (-0.07,0.49)	0.136	-0.06 (-0.27,0.15)	0.571	0.01 (-0.17,0.20)	0.874
<b>Annual percentage changes</b>								
Trabecular density	0.08 (-0.11,0.26)	0.397	-0.10 (-0.43,0.23)	0.543	0.22 (-0.04,0.47)	0.092	<b><i>-0.28 (-0.50,-0.07)</i></b>	<b><i>0.011</i></b>

Estimates shown are standard deviation differences in HR-pQCT parameters according to each loci

Associations were adjusted for age and sex

Significant associations ( $p < 0.05$ ) are given in italics

### **3.1.5 Description of change in maximum grip strength from HBS11-12 to HBS17**

Next we compared maximum grip strength at the 2011-12 follow-up visit and the 2017 follow-up visit. This was performed in 215 individuals across a mean follow-up time of 5.1 years (SD 0.34).

#### *Percentage change in maximum grip strength*

Percentage change in maximum grip strength was calculated for males and females at the same timepoints with a mean percentage loss of 13.3% (SD 15.3) in males and 10.2% (SD 23.9) in females. For reference, the absolute change in grip strength was a 4.1kg (SD 4.8) loss across the sexes (a loss of 5.2kg in males and 3.0kg in females). This results in a 0.80kg/year loss over the mean 5.1 years of follow-up.

### **3.1.6 Description of change in total femoral BMD from HBS11-12 to HBS17**

Across the same follow-up time as above we also calculated the percentage change in total femoral BMD (defined as the minimum total femoral BMD from the left or right).

#### *Percentage change in total femoral BMD*

Percentage change in total femoral BMD was calculated for males and females at the same timepoints with a mean percentage loss of 2.0% (SD 3.8) in males and 3.5% (SD 5.1) in females.

### **3.1.7 Associations of grip strength and total femoral BMD with fracture**

Odds ratios were calculated via unadjusted and adjusted (for the covariates described above) models for baseline grip and BMD and percentage change in these variables. These findings are shown in **Appendix 9**.

Neither baseline grip strength nor percentage change in grip strength were associated with fracture; however, baseline DXA BMD was significantly associated with fracture in both unadjusted and adjusted models (OR 0.01, 95% CI 0.00 to 0.25,  $p=0.003$ ). This suggests that, for each unit increase in BMD ( $\text{g}/\text{cm}^2$ ) there is a 99% decrease in the odds of previous fracture. This can be a little difficult to interpret as a unit increase in  $\text{g}/\text{cm}^2$  is large. Thus, by using Z-scores of BMD, the odds of fracture reduced by 46% per standard deviation increase in BMD (OR 0.54).

### **3.1.8 Sensitivity analyses**

Sensitivity analyses were performed to investigate the effect of taking bisphosphonates on the associations observed for bone outcomes (bone microarchitecture and DXA BMD). These did not substantially alter the results (as seen in **Appendix 8** and **Appendix 9**). The reason for this lack of effect may be that adjustment for bisphosphonate is an overadjustment as it identifies those with poorer bone health, the same group we are attempting to identify through HR-pQCT or DXA imaging.

### **3.1.9 Results summary**

In this chapter we have described the change in bone microarchitecture, maximum grip strength and DXA-measured total femoral neck BMD (as primary tenets of musculoskeletal ageing) over the approximately 5 years of follow-up for a group of older adults in the UK. Large losses of nearly 20% were observed in maximum grip strength; however reductions for total femoral neck BMD were smaller at 2.2% for males and 3.9% for females. The greater loss in BMD for females is as expected and is likely due to the post-menopausal lack of protection from sex hormones. It is worth considering our findings in the context of previous findings in the HCS which examined pQCT (the precursor to HR-pQCT which provides a 2-dimensional cross-section of bone parameters together with muscle area) between a follow-up visit at 2004-05 and EPOSA (2011-12). Here, sex differences were also observed, particularly in the cortical area with greater declines in females than males at both the radius ( $p=0.006$ ) and the tibia ( $p<0.001$ )<sup>221</sup>.

Deteriorations in bone microarchitecture parameters were less marked with maximal changes being an approximate 2% rise in cortical porosity and 1% reduction in cortical area. However, although the remaining changes were less than 1%, they were in a biologically plausible direction and many were significant. Indeed, we observed increases in trabecular area and density with decreases in cortical area, thickness and density as bone is resorbed from the endocortical surface with increasing age. Increases in cortical porosity were also seen together with increasing cortical pore diameter. In the next chapter we will investigate whether these age-related changes are related to epigenetic age acceleration as a measure of biological ageing.

When we examined the associations between baseline levels and percentage change of these parameters of musculoskeletal ageing, and fracture (one of the most important musculoskeletal outcomes), we found that baseline level was more consistently predictive of fracture than change between the two timepoints. To expand, higher trabecular area and lower cortical density, area and thickness were significantly associated with a greater odds of fracture, as were lower levels of the



more global measures of total volumetric BMD (via HR-pQCT) and total femoral neck BMD (via DXA). The only measure for which change was significantly associated with fracture was loss of trabecular density.

In terms of genetic loci and associations with bone microarchitecture, we saw one significant association with rs3801387 (*WNT16*) which was related to loss of trabecular density ( $\beta=-0.28$  (-0.50,-0.07),  $p=0.011$ ). This has biological significance which will be explored in the discussion chapter.

## 3.2 Associations between epigenetic age acceleration and musculoskeletal parameters

This chapter addresses the associations between HCS baseline (1998-2004) epigenetic age acceleration (including those calculated via HorvathAge, GrimAge and PhenoAge clocks) as the predictor for selected musculoskeletal outcomes. The outcome measures are drawn from the baseline HCS visit (cross-sectionally to when blood samples were collected), the EPOSA visit (2011-12) and the HBS17 visit (2017). Muscle parameters included maximum grip strength and gait speed, bone measures included DXA bone mineral density (BMD) at the total femur, femoral neck (FN) and anterior-posterior lumbar spine (AP spine) and HR-pQCT outcomes (note that HRpQCT scans were performed at the EPOSA (2011-12) and HBS17 (2017) visits alone) and body composition including DXA-measured appendicular lean mass and total fat mass (note that whole body DXA was performed at the EPOSA (2011-12) and HBS17 (2017) visits alone).

The methods describing how the clocks were produced and musculoskeletal outcomes were measured are included in the methods chapter.

### 3.2.1 The cohort

The demographics of all those included in this study at HCS baseline (1998-2004) are shown in **Table 9** for 425 participants, 213 males and 212 females. The mean age of the males was 64.1 years (SD 2.6) and mean age of the females was 65.9 (SD 2.7). Mean weight and height were higher in males than females and mean BMI was approximately equal across the sexes. Physical activity scores were similar across the sexes as was dietary calcium intake. Males had a higher mean maximum grip strength than females. BMD was higher in males than females at the total spine, total femoral compartment and femoral neck.

Mean (SD)	Males (n=213)	Females (n=212)
Age (years)	64.1 (2.6)	65.9 (2.7)
Height (cm)	174.7 (6.6)	161.3 (5.7)
Weight (kg)	81.0 (11.3)	70.1 (12.7)
BMI (kg/m <sup>2</sup> )	26.6 (3.6)	26.9 (4.5)
Physical activity (Dallosso)	64.5 (14.2)	62.0 (13.8)
Dietary calcium intake (mg)	8584.6 (2144.4)	8003.2 (2492.6)
Grip strength (kg)	44.9 (7.0)	27.6 (5.0)
Gait speed (m/s)	NA	1.0 (0.1)
Total spinal BMD (g/cm <sup>2</sup> )	1.1 (0.2)	1.0 (0.2)
Total femoral BMD (g/cm <sup>2</sup> )	1.0 (0.1)	0.9 (0.1)
Femoral neck BMD (g/cm <sup>2</sup> )	0.9 (0.1)	0.8 (0.1)

**Table 9:** Baseline demographic data.

This table depicts the mean and standard deviation for age, body anthropometry, physical activity, calcium intake, maximum grip strength and gait speed, non-fat mass and bone mineral density (BMD) measures. These measures are taken from baseline visits (1998-2004)

As seen in **Table 10** males were more likely to have ever smoked and more likely to drink heavily (very high alcohol consumption accounted for 11.3% of males and 0% of females). Occupational social class distribution was equal across the sexes for non-manual and manual occupational social class. Musculoskeletal and body composition outcomes at EPOSA and HBS17 are seen in **Table 11**.

n(%)	Males	Females
Ever smoked		
No	89 (41.8%)	139 (65.6%)
Yes	124 (58.2%)	73 (34.4%)
Weekly alcohol consumption		
Non-drinker	3 (1.4%)	31 (14.6%)
Very Low (0/<1 M&F)	22 (10.3%)	62 (29.2%)
Low (1-10M,1-7F)	86 (40.4%)	93 (43.9%)
Moderate (11-21M,8-14F)	53 (24.9%)	23 (10.8%)
High (22-35M, 15-21F)	25 (11.7%)	3 (1.4%)
Very High (>35 M >21 F)	24 (11.3%)	0 (0.0%)
Social class		
I-IIINM	91 (44.6%)	91 (42.9%)
IIIM-V	113 (55.4%)	121 (57.1%)

**Table 10:** Baseline lifestyle data.

This table depicts the total (and percentage) for categorical variables including ever smoking, weekly alcohol consumption (M=male, F=female), occupational social class (I-IIINM (NM=non-manual), IIIM – V (M=manual)). These measures are taken from baseline visits (1998-2004)

Mean (SD)	Males	Females
<b>EPOSA (2011-12)</b>		
Age (years)	75.6 (2.5)	75.9 (2.6)
Grip strength (kg)	36.2 (7.3)	21.2 (6.0)
Gait speed (m/s)	0.8 (0.2)	0.7 (0.2)
Total lean mass (kg)	53.6 (5.3)	38.5 (4.4)
Total fat mass (kg)	24.9 (8.4)	29.7 (9.2)
<b>HBS17 (2017)</b>		
Age (years)	81.0 (2.5)	81.4 (2.6)
Grip strength (kg)	31.7 (7.8)	19.4 (5.3)
Gait speed (m/s)	0.7 (0.2)	0.7 (0.2)
Total lean mass (kg)	51.7 (6.0)	39.6 (4.9)
Total fat mass (kg)	26.4 (8.5)	29.6 (8.5)

**Table 11:** EPOSA and HBS17 musculoskeletal and body composition outcomes.

This table depicts mean age, maximum grip strength and gait speed at the EPOSA follow-up (2011-12) for a total of 399 participants (199 males and 200 females) and total lean and total fat mass for 344 participants (179 males and 165 females)

Below are included the mean age, maximum grip strength and gait speed and total lean and total fat mass at the HBS17 follow-up (2017) for a total of 205 participants (108 males and 97 females)

### 3.2.2 Epigenetic age

Epigenetic age variables were calculated using clocks derived from methylation data as described in the methods chapter. The epigenetic ages were then used to calculate the epigenetic age acceleration measures.

The three epigenetic ages were calculated and can be seen in **Table 12**. This dataset includes 425 participants and the mean chronological age was 65.0 (SD 2.8) years. The mean age for the HorvathAge

was similar at 65.8 years but the mean epigenetic ages for the second-generation clocks were younger at 56.4 years for PhenoAge and 58.4 years for GrimAge. The standard deviations for epigenetic ages (Horvath Age = 4.6 years, PhenoAge = 4.8 years, GrimAge = 5.6 year) were greater than for chronological age (2.8 years) as were the ranges.

Variable	n	Mean	Std. Dev.	Min	Max
Chronological age	425	65.0	2.8	59.2	70.8
HorvathAge	425	65.8	4.6	47.6	77.0
PhenoAge	425	56.4	4.8	26.3	69.3
GrimAge	425	58.4	5.6	48.2	82.5

**Table 12:** Summary statistics for chronological age, HorvathAge, PhenoAge and GrimAge (including number of observations (n), mean, standard deviation, minimum and maximum ages)

The distributions of HorvathAge, as an example of epigenetic age, is shown in the histogram below (**Figure 16**) with separate histograms for HorvathAge in 450k and 850k array samples shown below (**Figure 17**) and a density plot for the distribution of each epigenetic age and chronological age included in **Appendix 11**.

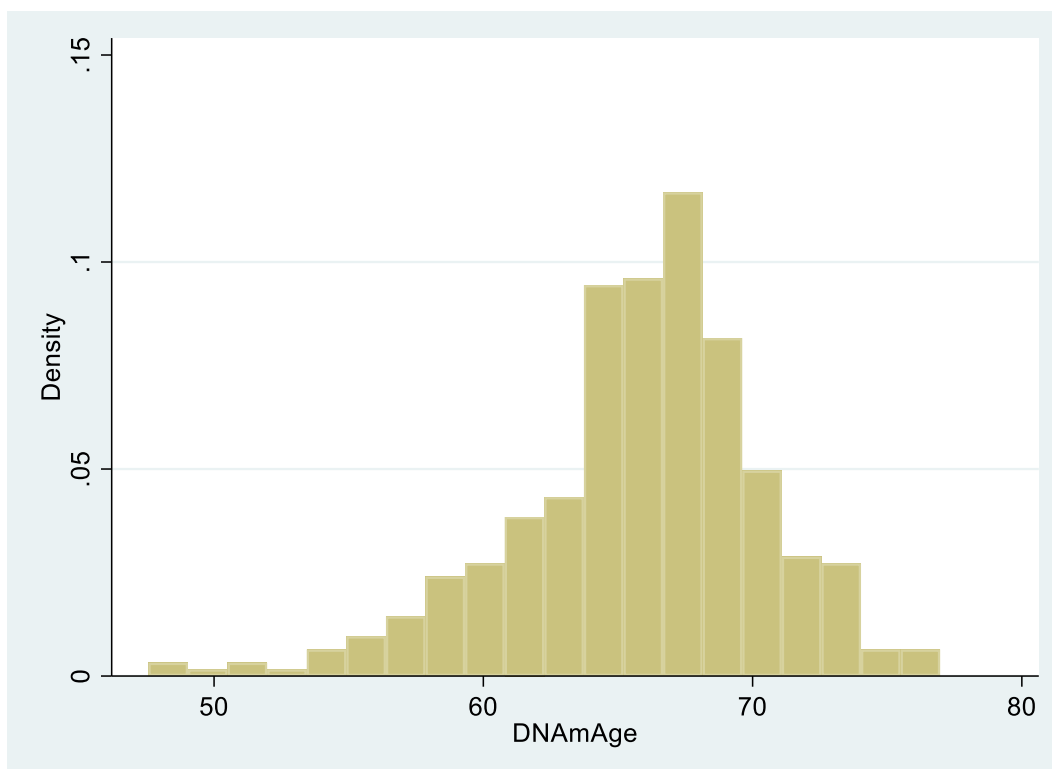


**Figure 16:** A histogram depicting the distribution of frequency density of HorvathAge (DNAMAge in years) in the 450k and 850k arrays combined.

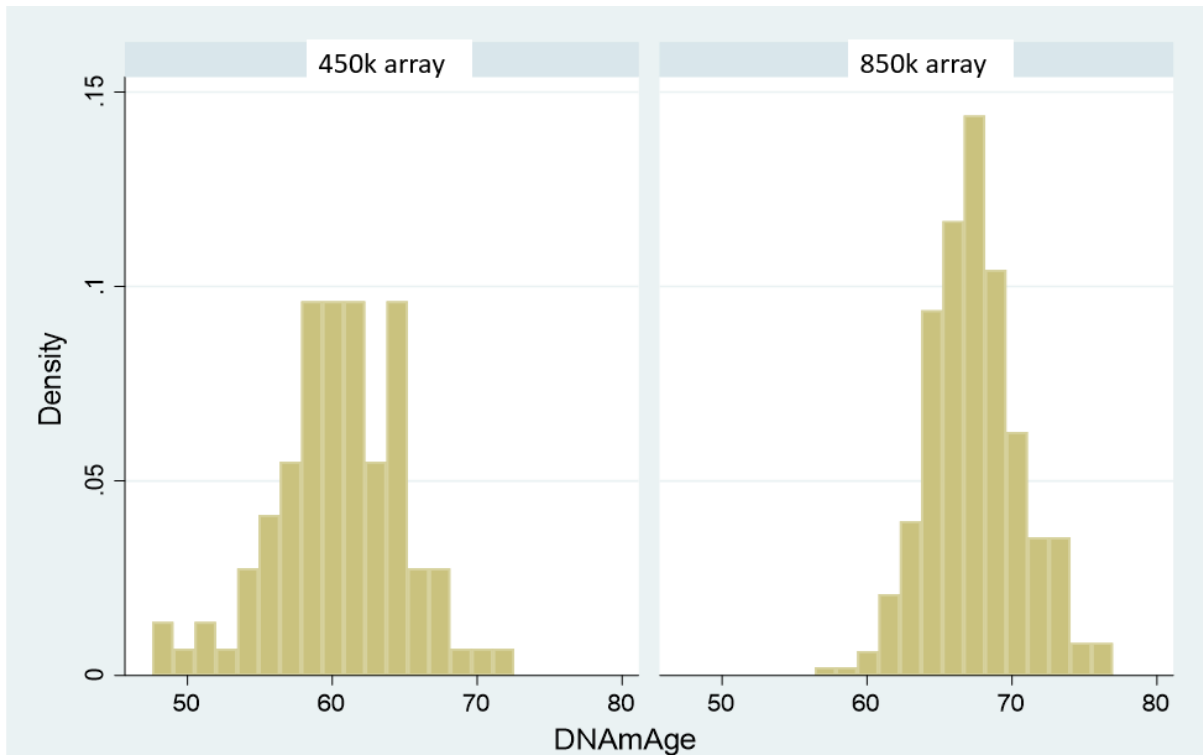


**Figure 17:** A histogram depicting the distribution of frequency density of HorvathAge (DNAMAge in years) in the 450k and 850k arrays separately.

There is a significant difference in the HorvathAge distributions for each array, with participants included appearing to be significantly younger. This was confirmed by Student's t-test with no significant difference for chronological age ( $p=0.09$ ) but significant differences seen between the distributions for 450k and 850k arrays for HorvathAge ( $p<0.0001$ ), PhenoAge ( $p<0.0001$ ) and GrimAge ( $p<0.0001$ ). For this reason, Z-scores for epigenetic age acceleration were produced so that 450k and 850k datasets could be combined.

### 3.2.3 Epigenetic age acceleration

Epigenetic age acceleration measures were produced from the residual of a regression of chronological age and predicted epigenetic age. Thus, a positive epigenetic age acceleration is indicative of accelerated epigenetic aging and a negative epigenetic age acceleration is indicative of decelerated epigenetic aging.

In **Table 13** are the means and standard deviations for raw (non-Z-score) epigenetic age acceleration measures. As expected, the mean epigenetic age acceleration for all variables tends towards 0. For PhenoAgeAcc the standard deviation was higher (4.5) as was the range (-28.8 to 14.9) that it was for HorvathAgeAcc (SD 3.3 and range 14.7 to 9.1) or GrimAgeAcc (SD 3.7 and range -7.7 to 14.4). Density plots for the distribution of each epigenetic age acceleration measure are included in **Appendix 11**.

Histograms of the distribution of HorvathAge acceleration, GrimAge acceleration and PhenoAge acceleration for both 450k and 850k arrays are shown in **Appendix 10** but show a similar shift in distribution between array types to that seen for the epigenetic age measures themselves.

Variable	Obs	Mean	Std. Dev.	Min	Max
HorvathAge acceleration	425	4.10e <sup>-9</sup>	3.3	-14.7	9.1
PhenoAge acceleration	425	-4.49e <sup>-9</sup>	4.5	-28.8	14.9
GrimAge acceleration	425	1.09e <sup>-9</sup>	3.7	-7.7	14.4

**Table 13:** Epigenetic age acceleration summary statistics

(including mean, standard deviation and maximum and minimum values for HorvathAge acceleration, PhenoAge acceleration and GrimAge acceleration)

Below is a table of the Z-scores (**Table 14**) for epigenetic age acceleration measures with standardized means of 0, standard deviations of 1 and ranges of 6.6 for HorvathAge acceleration, 8.5 for PhenoAge acceleration and 5.6 for GrimAge acceleration. In the subsequently described analyses, the age acceleration measures refer to these Z-scores for age acceleration.



Variable	Obs	Mean	Std. Dev.	Min	Max
HorvathAge acceleration	425	0	1.0	-3.5	3.1
PhenoAge acceleration	425	0	1.0	-5.4	3.1
GrimAge acceleration	425	0	1.0	-2.0	3.6

**Table 14:** Epigenetic age acceleration Z-scores summary statistics

(including mean, standard deviation, minimum and maximum)

### 3.2.4 Epigenetic age acceleration vs muscle outcomes

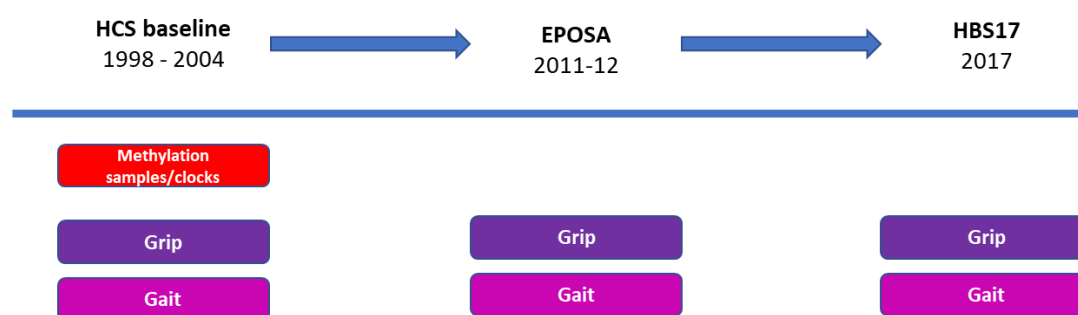


**Figure 18:** Schema showing the timing of the clock exposure and musculoskeletal outcomes for this section

The results of linear regression models investigating the association between epigenetic age acceleration variables and outcomes related to muscle strength (maximum grip strength) and muscle function (gait speed) are depicted in **Table 15**. The results shown are for sex-stratified, unadjusted models (model 1) and those adjusted for age, height and BMI (model 2) and those adjusted additionally for social class, physical activity, prudent diet, ever smoked regularly and alcohol consumption (model 3).

Note that at the HCS baseline (1998-2004) only a small subset of the population (n=98) had gait speed measured and all of these were female. The timeline of the measures utilised in these analyses are summarised in **Figure 18**.

#### 3.2.4.1 GrimAge acceleration findings

The specific findings for regressions of maximum grip strength and gait speed with GrimAge acceleration are shown in **Table 15**.

Grip	Model 1				Model 2				Model 3			
	Males		Females		Males		Females		Males		Females	
	beta	p	beta	p	beta	p	beta	p	beta	p	beta	p
Baseline	-1.43 (-2.39,-0.47)	0.004	-0.14 (-1.00,0.73)	0.756	-0.76 (-1.62,0.10)	0.085	-0.09 (-0.97,0.79)	0.837	-0.97 (-1.98,0.04)	0.059	0.14 (-0.83,1.10)	0.782
EPOSA	-1.93 (-2.96,-0.90)	0	-0.00 (-1.08,1.07)	0.993	-1.25 (-2.24,-0.26)	0.014	0.27 (-0.82,1.35)	0.627	-1.05 (-2.23,0.12)	0.078	0.69 (-0.47,1.86)	0.243
HBS17	-1.35 (-2.96,0.25)	0.098	0.79 (-0.49,2.07)	0.224	-0.69 (-2.14,0.76)	0.348	1.06 (-0.20,2.31)	0.099	-0.60 (-2.32,1.12)	0.491	1.38 (-0.07,2.82)	0.061
Gait	Model 1				Model 2				Model 3			
	Males		Females		Males		Females		Males		Females	
	beta	p	beta	p	beta	p	beta	p	beta	p	beta	p
Baseline	NA	NA	-0.02 (-0.06,0.02)	0.27	NA	NA	-0.01 (-0.05,0.02)	0.507	NA	NA	-0.02 (-0.06,0.02)	0.43
EPOSA	-0.02 (-0.05,0.00)	0.067	-0.04 (-0.08,-0.01)	0.017	-0.01 (-0.04,0.01)	0.338	-0.03 (-0.06,0.01)	0.117	-0.01 (-0.04,0.02)	0.423	-0.02 (-0.06,0.02)	0.357
HBS17	-0.06 (-0.10,-0.02)	0.002	-0.03 (-0.07,0.01)	0.183	-0.05 (-0.08,-0.01)	0.021	-0.02 (-0.06,0.03)	0.461	-0.04 (-0.09,-0.00)	0.047	-0.01 (-0.06,0.05)	0.781

**Table 15:** Regression coefficients and p-values for associations between GrimAge Acceleration and maximum grip strength and gait speed measured at HCS baseline (1998-2004), EPOSA (2011-12) and HBS17 (2017).

Model 1 is unadjusted, Model 2 is adjusted for age, height and BMI and Model 3 is adjusted additionally for social class, physical activity, prudent diet, ever smoked regularly and alcohol consumption. Red highlighting indicates a statistically significant result ( $p < 0.05$ ).

### 3.2.4.1.1 Grip

GrimAge acceleration was significantly associated with maximum grip strength at baseline and EPOSA in males in unadjusted models and at the EPOSA timepoint in models adjusted for age, height and BMI ( $\beta = -1.25$  (-2.24,-0.26),  $p < 0.02$ ). This suggests that for each standard deviation increase in GrimAge acceleration Z-score, there is a 1.25kg reduction in maximum grip strength in males. See **Figure 19** and **Figure 21**.

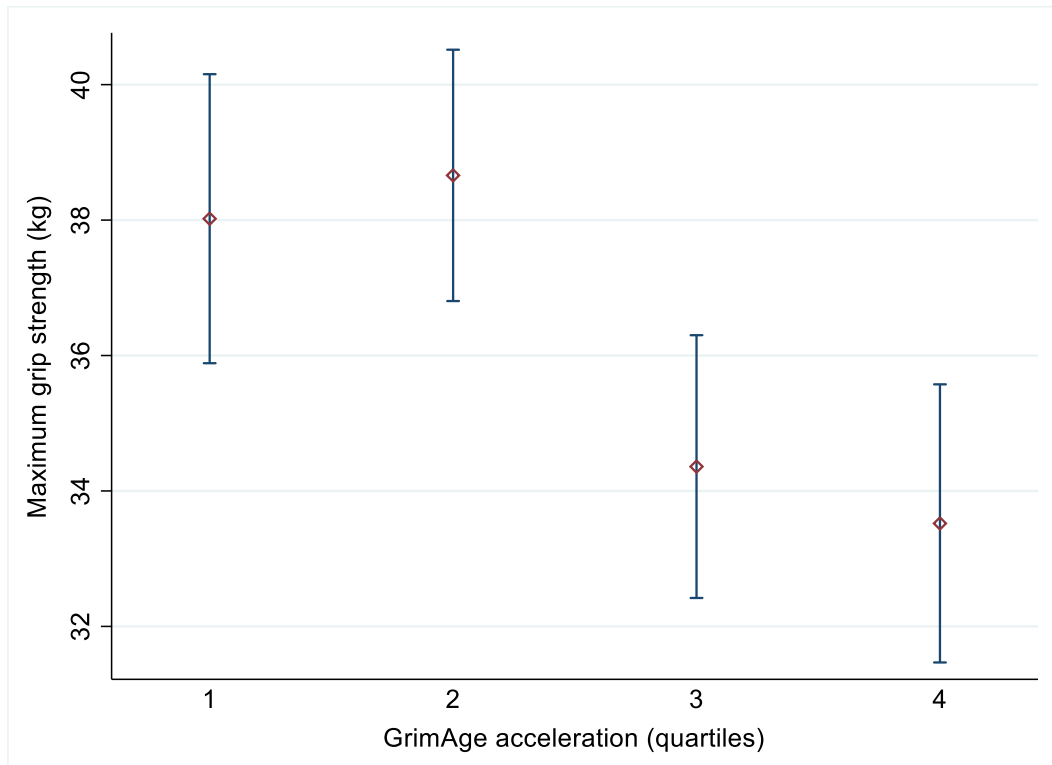


**Figure 19:** Mean and 95% confidence intervals for maximum grip strength against GrimAge acceleration quartiles in males at EPOSA (2011-12).

### 3.2.4.1.2 Gait

In unadjusted models for gait speed we observed associations in the male subgroup at HBS17, and significant associations persisted into model 2 (adjusted for age, height and BMI) at the HBS17 time points, and into the fully adjusted model 3 (adjusted for age, height, BMI, social class, physical activity, prudent diet, ever smoked regularly and alcohol consumption) ( $\beta = -0.04$  (-0.09,-0.00),  $p < 0.05$ ). To contextualise, for males we found that for each standard deviation increase in GrimAge acceleration Z-score, there is a 0.04m/s reduction in gait speed. This trend is seen in quartiles of GrimAge acceleration in **Figure 20**. In the female subgroup the only significant association for gait speed was at the EPOSA timepoint in unadjusted analyses, and was not robust to adjustment for covariates.

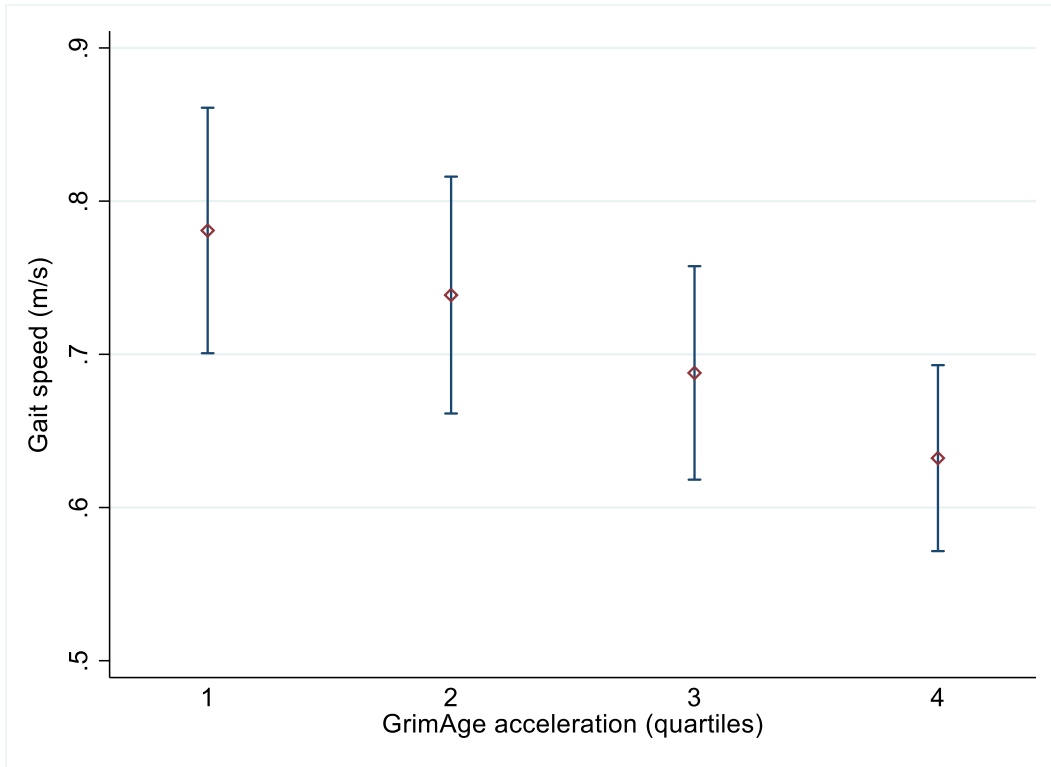


**Figure 20:** Mean and 95% confidence intervals for gait speed against GrimAge acceleration quartiles in males at HBS17 (2017)

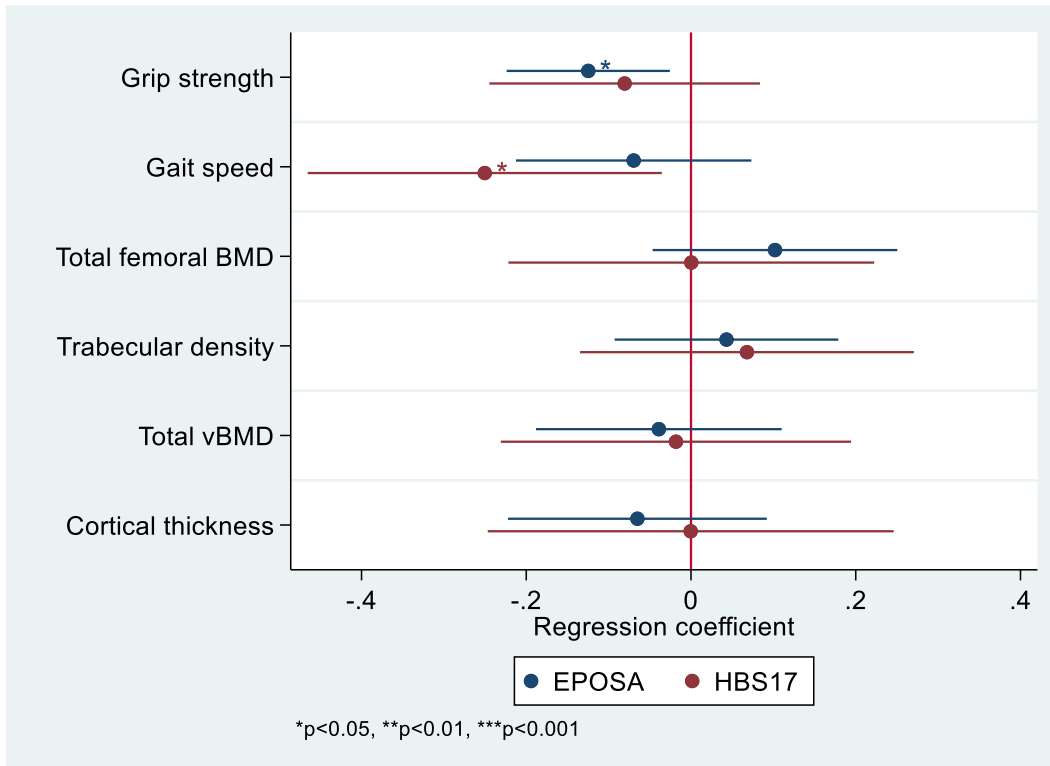


**Figure 21:** Musculoskeletal variable Z-scores at EPOSA and HBS17 timepoints in males, associations with GrimAge acceleration.

Adjusted for age, height and BMI.

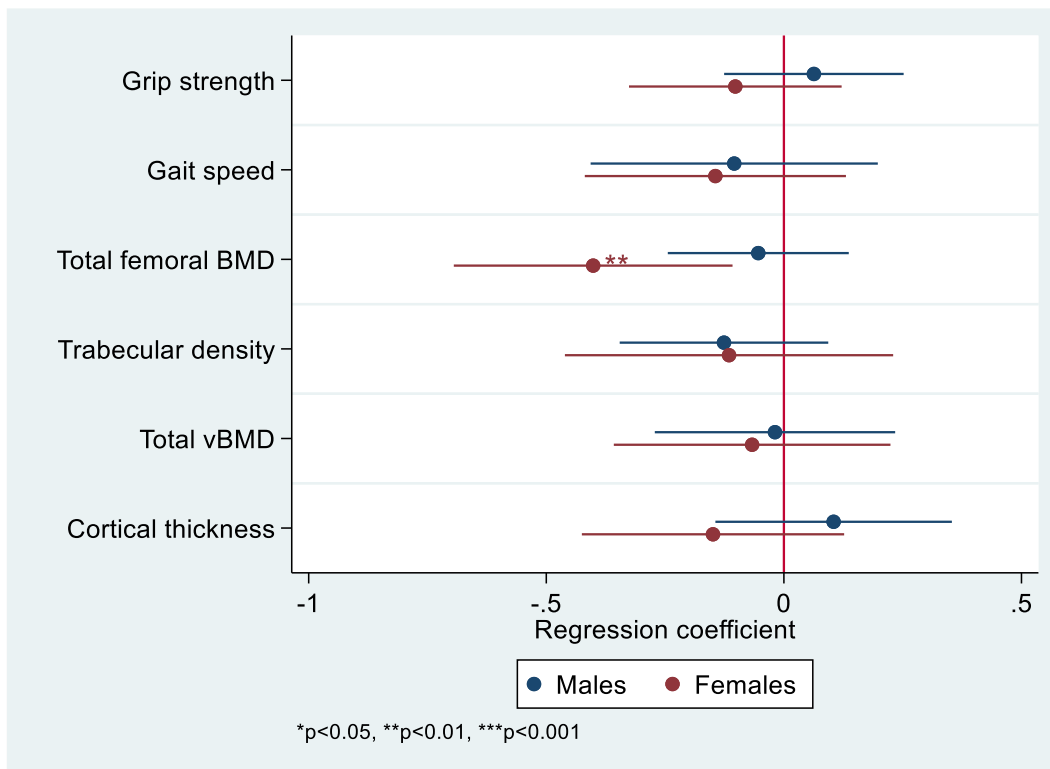


**Figure 22:** Change in musculoskeletal variable Z-scores at EPOSA and HBS17 timepoints in males and females, associations with GrimAge acceleration.

Adjusted for age, height and BMI.

### 3.2.4.2 PhenoAge acceleration findings

The specific findings for regressions of maximum grip strength and gait speed with PhenoAge acceleration are shown in **Appendix 12**.

Significant associations at the EPOSA timepoint were observed in males between PhenoAge acceleration and grip strength in unadjusted models, and those adjusted for age, height and BMI ( $\beta = -1.05$  (-1.94,-0.16),  $p < 0.03$ ). This suggests that, per standard deviation increase in PhenoAge acceleration Z-score, there is a 1.05kg loss in maximum grip strength.

PhenoAge acceleration was significantly associated with gait speed at the HBS17 in males in unadjusted models ( $\beta = -0.04$  (-0.07,-0.01),  $p < 0.01$ ) and in fully-adjusted models ( $\beta = -0.04$  (-0.07,-0.00),  $p = 0.04$ ). To provide context, this suggests that for each standard deviation increase in HorvathAge

acceleration Z-score, there was an association with a 0.04 m/s slower gait speed in the males tested at the HBS17 timepoint.

#### **3.2.4.3 HorvathAge acceleration findings**

The specific findings for regressions of maximum grip strength and gait speed with HorvathAge acceleration are shown in **Appendix 13**.

No significant associations at any timepoint were observed between HorvathAge acceleration and maximum grip strength. HorvathAge acceleration was significantly associated with cross-sectional gait speed at baseline in the female members of the cohort who had the gait speed at this timepoint in unadjusted and fully-adjusted models (n=98) ( $\beta = -0.03$  (-0.06,-0.00),  $p < 0.03$ ). To provide context, this suggests that for each standard deviation increase in HorvathAge acceleration Z-score, there was a cross-sectional association with a 0.03 m/s slower gait speed in the females tested.

#### **3.2.4.4 Epigenetic age acceleration vs Change in maximum grip strength**

Associations for absolute change and percentage change in grip strength were examined for all three epigenetic age acceleration measures at three time intervals; from HCS baseline (1998-2004) to EPOSA (2011-12), from HCS baseline (1998-2004) to HBS17 (2017) and from EPOSA (2011-12) to HBS17 (2017).

No significant associations were observed in unadjusted or fully-adjusted models for the HCS baseline to EPOSA or HCS baseline to HBS17 time intervals. There were significant associations for absolute change in females for the EPOSA to HBS17 time intervals, for PhenoAge acceleration ( $\beta = 0.98$  (0.11,1.85),  $p < 0.03$ ) and HorvathAge acceleration ( $\beta = 0.98$  (0.10,1.86),  $p = 0.03$ ) in models adjusted for age, height and BMI; however, these were not robust to full adjustment.

#### **3.2.4.5 Epigenetic age acceleration vs Change in gait speed**

It should be noted that HCS baseline measures of gait speed were limited to a small subset of the HCS baseline population and so numbers of participants for analyses including this timepoint will lack statistical power.

At the HCS baseline to EPOSA time interval (n=77, only females) the only significant finding was between GrimAge acceleration and percentage gait speed change in females ( $\beta=-5.32$  (-10.33,-0.31) $p<0.05$ ); however, this was not robust to adjustment for covariates.

No significant associations were observed for epigenetic age acceleration measures and either absolute or percentage change in gait speed between HCS baseline to HBS17 (n=41, only females) or EPOSA to HBS17 (n=175, 90 males, 85 females). These results can be seen in **Appendix 14** and **Appendix 15**.

### 3.2.5 Epigenetic age acceleration vs DXA bone mineral density outcomes

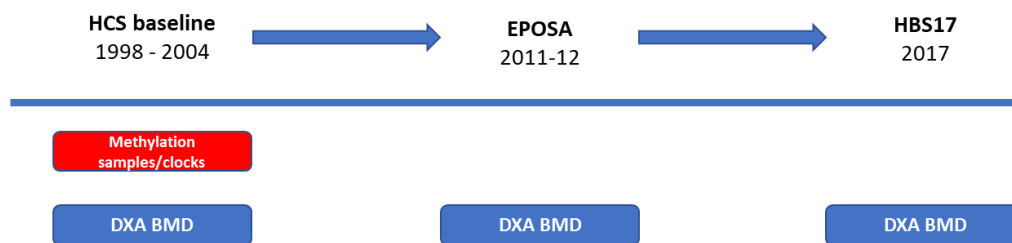


**Figure 23:** Schema showing the timing of the clock exposure and musculoskeletal outcomes for this section

The DXA BMD outcomes investigated in association with GrimAge, PhenoAge and HorvathAge acceleration variables, were total spinal BMD, total femoral BMD and total femoral neck BMD. These were measured at HCS baseline, EPOSA and HBS17 (**Figure 23**). The results are shown in **Appendix 16**, **Appendix 17** and **Appendix 18**.

#### 3.2.5.1 Total spinal BMD

Total spinal BMD at baseline was associated with GrimAge acceleration in unadjusted models in females; however, this association was not robust to adjustment for covariates. No associations were observed for total spine BMD with PhenoAge acceleration or HorvathAge acceleration.

#### 3.2.5.2 Total femoral BMD

No significant associations were observed between cross-sectional or longitudinal values of total femoral BMD and GrimAge acceleration, PhenoAge acceleration or HorvathAge acceleration.

### 3.2.5.3 Change in total femoral BMD

In males, in fully-adjusted models, significant associations were observed between GrimAge acceleration and percentage change in total femoral BMD between baseline and HBS17 ( $\beta = -2.68$  (-5.03,-0.33),  $p < 0.03$ ). In females, a significant association was observed between baseline GrimAge acceleration and percentage change from EPOSA to HBS17 ( $\beta = -1.67$  (-3.29,-0.06),  $p < 0.05$ , in the fully-adjusted model) (**Figure 22**). This suggests that for each standard deviation increase in GrimAge acceleration Z-score there is a 1.7% gain in total femoral BMD over the period of follow-up.

No significant associations with change in total femoral BMD were seen for PhenoAge acceleration or HorvathAge acceleration.

### 3.2.5.4 Total femoral neck BMD

Significant associations with total femoral neck BMD were seen in females for PhenoAge acceleration and baseline ( $\beta = 0.02$  (0.00, 0.03),  $p < 0.02$ ) and EPOSA ( $\beta = 0.02$  (0.00, 0.04),  $p < 0.03$ ) timepoints and for HorvathAge at baseline ( $\beta = 0.02$  (0.01, 0.03),  $p < 0.01$ ), EPOSA ( $\beta = 0.02$  (0.00, 0.04),  $p < 0.05$ ) and HBS17 ( $\beta = 0.04$  (0.01, 0.07),  $p < 0.02$ ) timepoints. Note that the direction of association is opposite to that expected and the effect sizes are small (indicating that for every standard deviation increase in PhenoAge acceleration or HorvathAge acceleration there is a increase of between 0.01 to 0.04g/cm<sup>2</sup> in total femoral neck BMD, depending on the timepoint of the measurement.

No significant associations were observed with total femoral neck BMD and GrimAge acceleration.

### 3.2.5.5 Change in Total femoral neck BMD

Percentage change in total femoral neck BMD from baseline to EPOSA was significantly associated with GrimAge acceleration in males ( $\beta = 1.86$ (0.02,3.70),  $p < 0.05$ ) in fully-adjusted analyses indicating a 1.9% reduction in BMD for every standard deviation increase in GrimAge acceleration..



### 3.2.6 Epigenetic age acceleration vs HR-pQCT

Bone microarchitecture was assessed (at the EPOSA 2011-12 timepoint) at the tibia and radius using the variables of trabecular density (to assess the trabecular compartment), volumetric BMD (vBMD) and cortical thickness (to assess the cortical compartment).

There were no significant associations in the fully-adjusted models except between HorvathAge acceleration and tibial cortical thickness in females ( $\beta = 35.56$  (6.91,64.21),  $p < 0.02$ ) with higher age acceleration being associated with higher cortical thickness (a 35.56 $\mu\text{m}$  increase per standard deviation increase in HorvathAge acceleration Z-score). This can be seen in **Appendix 21**.

In order to examine further the above association between HorvathAge acceleration and tibial cortical thickness, we investigated tibial cortical thickness on pQCT slices at the tibia (from the EPOSA 2011-12 timepoint).

HorvathAge acceleration was significantly associated with tibial cortical thickness at the 14% ( $\beta = 0.09$  (0.03,0.15),  $p = 0.004$ ) and 38% ( $\beta = 0.11$  (0.01,0.21),  $p = 0.03$ ) slices in females alone. This can be seen in **Appendix 22**. This was smaller than the association observed for HR-pQCT but was still significant.

Associations between epigenetic age acceleration variables (from HCS baseline in 1998-2004) and percentage change in HR-pQCT variables between EPOSA (2011-12) and HBS17 (2017) were examined (**Figure 24**). The resulting beta coefficients and p-values are presented from unadjusted and fully-adjusted models (age, height, BMI, social class, physical activity, dietary calcium, smoking, alcohol, fracture and follow-up time). Greater GrimAge acceleration ( $\beta = -1.09$  (-2.15,-0.02),  $p < 0.05$ ) and HorvathAge acceleration ( $\beta = -1.17$  (-1.99,-0.36),  $p < 0.01$ ) were significantly associated with reduced decline in radial trabecular density over the period of follow-up, in males only. No other associations were observed for percentage change in HR-pQCT variables. A selection of these results can be seen in

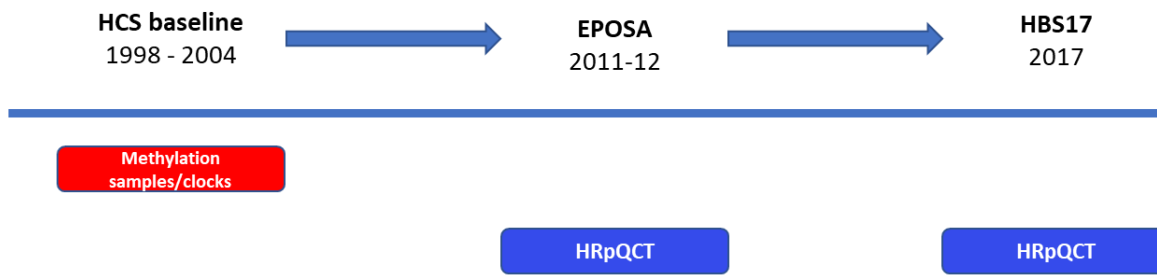


**Figure 24:** Schema showing the timing of the clock exposure and musculoskeletal outcomes for this section

### 3.2.7 Epigenetic age vs body composition

The results of linear regression models investigating the association between epigenetic age acceleration variables and outcomes related to body composition as measured by DXA (at the EPOSA and HBS17 timepoints, **Figure 25**) including appendicular (arm and leg) lean (muscle) mass and are depicted in the **Appendix 24**. The results shown are for sex-stratified, unadjusted models and those adjusted for age, height, social class, physical activity, prudent diet, ever smoked regularly and alcohol consumption. Note that models with body composition as the outcome did not include BMI due to collinearity.

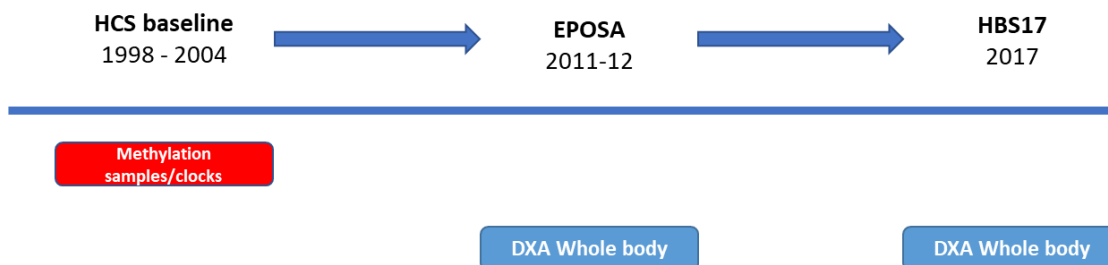


**Figure 25:** Schema showing the timing of the clock exposure and musculoskeletal outcomes for this section

#### 3.2.7.1 Appendicular Lean mass

At the EPOSA (2011-12) timepoint, associations between GrimAge acceleration and lean mass were only observed in females and were robust to adjustment ( $\beta = 118.84$  (1.23,236.45),  $p < 0.05$ ). This suggests that for every standard deviation increase in GrimAge acceleration Z-score, there is a increase of 119 grams of appendicular lean mass in females.

Note that the associations with lean mass are counter to the expected direction, with greater GrimAge acceleration being associated with greater lean mass. Neither HorvathAge acceleration

nor PhenoAge acceleration were significantly associated with appendicular lean mass. No significant associations were observed at the HBS17 (2017) timepoint.

### 3.2.7.2 Total fat mass

Once again, at the EPOSA (2011-12) timepoint, associations between GrimAge acceleration and total fat mass were only observed in females and were robust to adjustment ( $\beta= 2.2$  (0.38,4.08)  $p<0.02$ ). Again, the direction of association indicated that greater GrimAge acceleration was associated with greater fat mass (with a 2.2kg increase in fat mass for each standard deviation increase in GrimAge acceleration Z-score). At the same timepoint, PhenoAge acceleration was significantly associated with total fat mass in unadjusted and adjusted models ( $\beta= 1.5$  (0.28,2.75)  $p<0.02$ ). No significant associations were observed at the HBS17 (2017) timepoint (**Appendix 25**).

### 3.2.8 Sensitivity analyses

Sensitivity analyses were performed to investigate the effect of taking bisphosphonates on the associations observed between epigenetic age acceleration and bone outcomes (bone microarchitecture and DXA BMD). These did not substantially alter the results as seen in **Appendix 19**, **Appendix 20** and **Appendix 22**). For tibial cortical thickness, the significance for fully-adjusted analyses ( $\beta=35.6\mu\text{m}$   $p=0.02$ ) was attenuated by adjustment for bisphosphonate usage ( $\beta=27.7\mu\text{m}$   $p=0.08$ ) suggesting some influence of the medication in these analyses. However, this was not replicated in pQCT analyses for tibial cortical thickness (**Appendix 22**).

Similar to the previous results chapter, the reason for this lack of effect may be that adjustment for bisphosphonate is an overadjustment as it identifies those with poorer bone health, the same group we are attempting to identify through skeletal imaging.

An outlier for PhenoAge was identified via histograms (**Appendix 10** and **Appendix 11**). PhenoAge acceleration associations which had been observed to be significant with all participants included were repeated with the outlying individual excluded. Excluding this outlier did not substantially affect the adjusted results (as seen in **Appendix 26**), except for attenuating the association between PhenoAge acceleration and total fat mass in males at the EPOSA timepoint ( $\beta=1513\text{g}$   $p=0.02$  with outlier included,  $\beta=68\text{g}$ ,  $p=0.90$  with outlier excluded) and a borderline significant result for appendicular lean mass at the HBS17 timepoint ( $\beta=-131\text{g}$   $p=0.06$  with outlier included,  $\beta=-162\text{g}$ ,  $p=0.049$  with outlier excluded).

From the main analyses few associations with PhenoAge acceleration were significant, though it does appear that the outlier was driving the association with total fat mass in males.

### 3.2.9 Results summary

The key findings from this chapter included that the HCS appears to be a biologically young cohort when using the GrimAge and PhenoAge clocks.

We also found that epigenetic age acceleration was significantly lower for those samples analysed with the 450k array than the EPIC (850k array). This had an impact on our analyses and necessitated the conversion of epigenetic age acceleration raw values to Z-scores, which were then used for downstream regressions.

For muscle outcomes, GrimAge acceleration at baseline significantly predicted future grip strength (EPOSA) and gait speed (HBS17) with higher acceleration predicting lower outcomes in males alone. The same relationship was observed for PhenoAge acceleration which was associated with future gait speed (HBS17), again in males. For the HorvathAge acceleration measure, only cross-sectional (HCS baseline) associations were observed for gait speed in females alone.

For bone outcomes, counter-intuitive significant relationships were observed in females alone. PhenoAge acceleration and HorvathAge acceleration were consistently associated with total femoral neck BMD across timepoints; however the association was such that greater age acceleration was linked to higher total femoral neck BMD. The same direction of associations was observed for cortical thickness and was consistent across scan modalities (including HR-pQCT and pQCT at the EPOSA timepoint). This asks important questions of which facets of biological ageing are being captured by the epigenetic clocks, particularly in the female sex. It is important to consider the role treatment may have played in altering bone microarchitecture, as the general practitioners of those individuals noted (on DXA BMD) to be osteoporotic at HCS baseline and EPOSA were informed of the results. This may have led to treatment which may have influenced our results. However, the influence of anti-resorptive therapy was shown not to be significant in sensitivity analyses.

Body composition associations too were mainly observed in females with greater epigenetic age acceleration associated with higher appendicular lean mass and higher fat mass. In particular, GrimAge acceleration was associated with higher appendicular lean mass and total fat mass. PhenoAge acceleration was associated with higher fat mass in males; however, sensitivity analyses suggest that this association was being driven by an outlier for PhenoAge acceleration.

Change in outcomes was generally not predicted by epigenetic age acceleration except for bone measures including total femoral BMD change between HCS baseline (1998-2004) and HBS17 (2017) in males, and between EPOSA (2011-12) and HBS17 (2017) in females (as discussed above). For bone microarchitecture, greater loss of radial trabecular density (at EPOSA) was predicted by higher HorvathAge acceleration at baseline in males. However, it is note-worthy that change in

trabecular density was the only variable associated with fracture in our descriptive analysis in the previous results section and may indicate a particular role for this parameter in fracture associated with biological ageing.

In females, it may be the case that bone relationships were, in part, driven by adiposity. For example, given that higher GrimAge acceleration was associated with higher percentage change in BMD at the femoral neck and that higher GrimAge acceleration was associated with higher fat mass (as seen in the directed acyclic graph in **Figure 26**) it may be the association between GrimAge acceleration and BMD change in females is mediated by adiposity. The counter to this is that measures of adiposity (BMI) were included as covariates for analyses of GrimAge acceleration and BMD and the association still persisted.

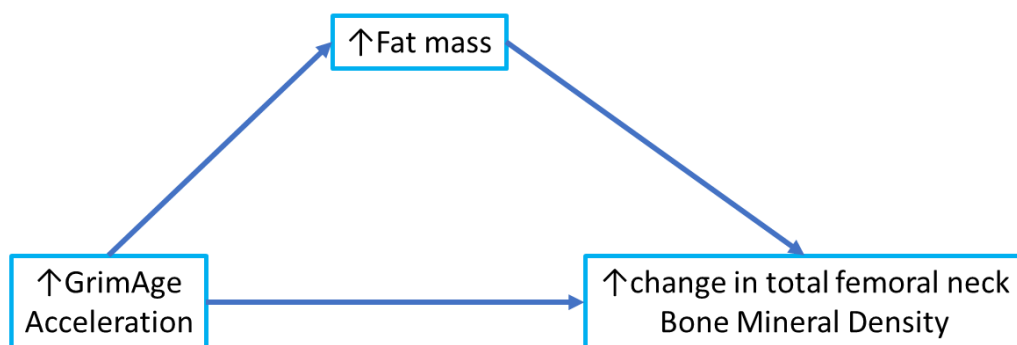


**Figure 26:** A directed acyclic graph demonstrating the relationship between GrimAge acceleration, fat mass and change in total femoral neck bone mineral density

The implications of these findings will be discussed further in the Discussion chapter.

### 3.3 EWAS of maximum grip strength and total femoral neck BMD

In this results chapter the associations between methylation levels at CpG sites across the EPIC array and two of the key parameters in assessing musculoskeletal ageing; maximum grip strength (a key constituent of sarcopenia) and total femoral neck bone mineral density (BMD) (a key determinant of fragility fractures) are examined.

The methods for ascertaining these outcomes are described in the Methods chapter, but to briefly re-cap:

- **maximum grip strength** was measured using a dynamometer, with three readings taken from each hand and the maximum grip strength recorded (in kilograms)
- **total femoral neck BMD** was measured using dual X-ray absorptiometry (DXA) of the femoral neck and refers to the minimum BMD recorded in either hip (right or left) in  $\text{g}/\text{cm}^2$

These measures were recorded at the baseline HCS visit (1998-2004) at the same time as the blood samples were collected for DNA extraction and, latterly, methylation array. The associations examined are therefore cross-sectional (**Figure 27**).

Analyses for the 334 participants included epigenome-wide association study for differential methylation at CpG sites, followed by pathway analysis and gene ontology of the most significant CpG sites.

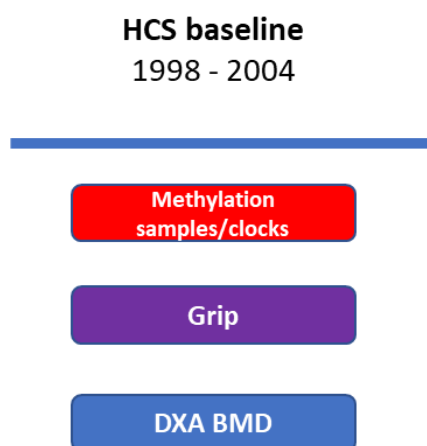


**Figure 27:** Schema showing the timing of the clock exposure and musculoskeletal outcomes for this section

#### 3.3.1 Demographics

The demographics of this subset of the HCS population are depicted in **Table 16**. The subset included 167 males and 167 females with a mean age of 64.2 (SD 2.6) and 65.9 (SD 2.8) years

respectively. Males demonstrated greater grip strength with a mean maximum grip of 44.8kg (SD 7.0) compared to 27.3kg (SD 4.8) for females. Males were also taller and heavier in terms of weight. However, measures of adiposity such as BMI and weight for height residual (mean weight-for-height residual -0.1 for both males and females) did not differ significantly across the sexes.

In terms of lifestyle factors, men were more likely to have ever smoked and tended to drink more alcohol. Physical activity did not differ substantially across the sexes with mean Dallosso scores of 63.8 (SD 14.4) for males and 61.8 (SD 13.6) for females.

For diet, dietary calcium consumption was similar for males and females at 8000-9000mg and mean prudent diet score was lower for males at -0.6 (SD 1.9) than for females at 1.0 (SD 1.7).

Just over half of participants had a background of working in a manual occupational social class.

Participant characteristic [Mean (SD) or N(%)]	Male (n=167)	Female (n=167)
Maximum baseline grip strength (kg)	44.8 (7.0)	27.3 (4.8)
Femoral neck est. BMD (g/cm <sup>2</sup> )	0.86 (0.12)	0.76 (0.11)
Age at HCS baseline clinic (years)	64.2 (2.6)	65.9 (2.8)
Age at HCS baseline DXA scan (years)	64.7 (2.6)	66.6 (2.8)
Height (cm)	174.3 (6.7)	161.3 (6.1)
Weight (kg)	81.4 (11.5)	70.0 (13.2)
BMI (kg/m <sup>2</sup> )	26.8 (3.6)	26.9 (4.7)
Weight-for-height residual	-0.1 (0.9)	-0.1 (1.0)
Ever smoked regularly	92 (55.1%)	61 (36.5%)
Alcohol consumption bands (units per week)		
Non-drinker	2 (1.2%)	25 (15.0%)
V Low (0/<1 M&F)	18 (10.8%)	49 (29.3%)
Low (1-10M,1-7F)	67 (40.1%)	73 (43.7%)
Moderate (11-21M,8-14F)	44 (26.3%)	18 (10.8%)
F High (22-35M, 15-21F)	17 (10.2%)	2 (1.2%)
High (>35 M >21 F)	19 (11.4%)	0 (0.0%)
Dallosso physical activity score	63.8 (14.4)	61.8 (13.6)
Dietary calcium (mg)	8695.6 (2147.6)	8028.0 (2468.8)
Prudent diet score	-0.6 (1.9)	1.0 (1.7)
Occupational social class (manual)	90 (56.3%)	92 (55.1%)

**Table 16:** Summary and descriptive statistics for the 334 participants included in the epigenome-wide analyses.

### 3.3.2 EWAS model description

Four EWAS models were performed as listed in **Table 17**, all of which were adjusted for cell count composition of the sample (including B lymphocytes, CD4+ T lymphocytes, CD8+ T lymphocytes, monocytes, natural killer cells) and array. The models included a model which contained no further adjustments (Model 1), a model with adjustment for age and sex (Model 2).

Further models were performed for sensitivity including a model with adjustment for age, sex, height and weight for height residual (as a measure of adiposity) (Model 3) and a model with adjustment for age, sex, height, weight for height residual, occupational social class (manual vs non-manual labour), physical activity (Dallosso score<sup>157</sup>), diet (prudent diet score for grip strength analyses and dietary calcium for BMD analyses), smoking status (ever having smoked regularly) and alcohol consumption (an ordinal variable of units/week) (Model 4).



EWAS model	Adjustments			
1	Cell composition Array			
2	Cell composition Array	Age Sex		
3	Cell composition Array	Age Sex	Height Weight for height residual	
4	Cell composition Array	Age Sex	Height Weight for height residual	Occupational social class Physical activity Diet Smoking status Alcohol consumption

**Table 17:** EWAS models and covariates included in adjustment

In terms of outcomes, maximum grip strength was log transformed (due to the bimodal distribution of grip across the sexes, with grip being higher in males than females leading to the two peaks seen in **Figure 28**).

In terms of covariates, the majority had a normal distribution except for dietary calcium intake which required log transformation due to right skewing of the distribution (see **Figure 29**).

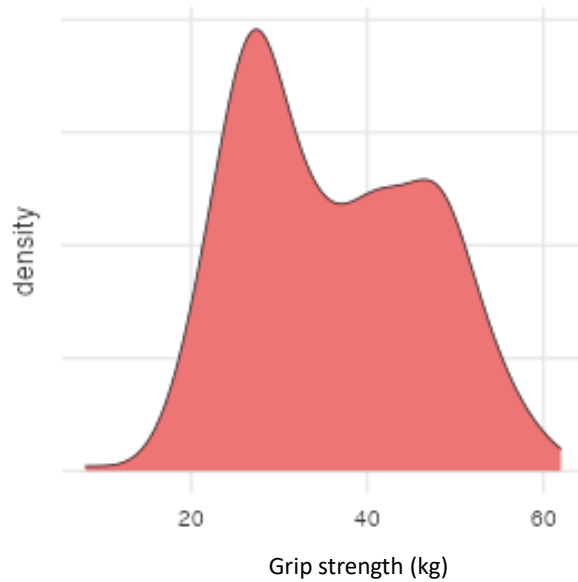


**Figure 28:** Histogram of maximum grip strength.

This figure shows the distribution of maximum grip strength (kg) at HCS baseline against frequency density. There is a bimodal distribution with peaks at approximately 27 and 47 due to the sex-specific distribution for females and males respectively. For this reason, maximum grip strength was log-transformed for some analyses.

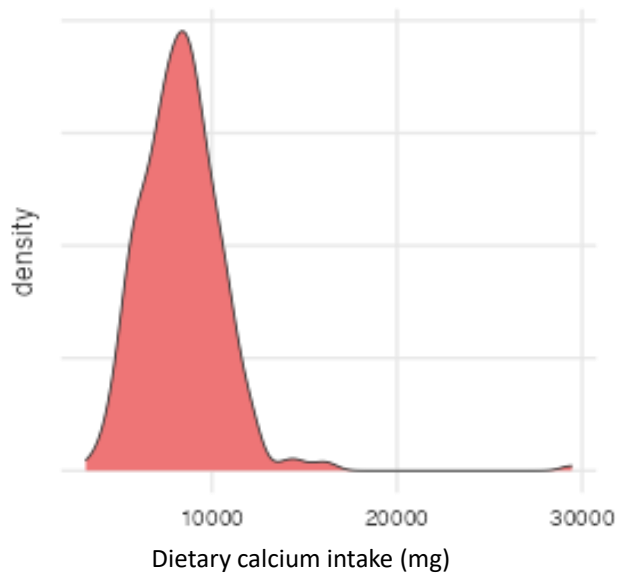


**Figure 29:** Histogram of dietary calcium intake.

This figure depicts the distribution of dietary calcium intake (mg) at HCS baseline against frequency density. The distribution is significantly skewed to the right.

### 3.3.3 Inflation

Levels of genomic inflation were calculated for each EWAS model and are shown in **Table 18**. This is a parameter which assesses the systematic biases within a dataset by dividing the observed chi-squared test statistic by the expected chi-squared test statistic and was calculated by lambda statistics (and visualised via Quantile-Quantile-plots (QQ-plots)). A lambda of 1.4 is seen in model 1 for maximum grip strength and a lambda of 1.16 is observed in model 1 for total hip bone mineral density. Otherwise, lambdas for all other models are <1.1 and are therefore acceptable<sup>222</sup>.

Model	1	2	3	4
Maximum grip strength	1.439	1.058	1.009	1.032
Total femoral neck mineral density	1.164	1.033	1.025	1.095

**Table 18:** Levels of genomic inflation for each model in each EWAS.

Moderate inflation is observed in model 1 for maximum grip strength but otherwise levels of inflation are acceptable.

### 3.3.4 EWAS results: maximum grip strength

#### 3.3.4.1 Model 2

For 334 participants, in the model which adjusted for age, sex, cell composition and array there were two CpG sites which reached the false discovery rate (FDR) less than 0.05 including cg08073934 (log<sub>2</sub> fold-change = 0.0004, adjusted p-value = 0.02) lying in a north shore region associated with the gene *SDK1* on chromosome 7. This can be interpreted as a 0.0004 log<sub>2</sub> fold-change in expression for each kilogram increase in grip strength, which equates to a 0.0003% increase in methylation (beta-value) for each kilogram increase in grip strength ( as  $2^{0.0004} = 1.0003$ ).

The locus cg00960509 was also significantly associated with grip strength (log<sub>2</sub> fold-change = -0.0006, adjusted p-value = 0.02), lying in a CpG island associated with the 5' end of the gene *ECE1* on chromosome 1 (see **Appendix 27**).The log<sub>2</sub> fold-change here can be interpreted as a -0.0006 log<sub>2</sub> fold-change in expression for each kilogram increase in grip strength, which equates to a 0.0004% decrease in methylation (beta-value) for each kilogram increase in grip strength ( as  $2^{-0.0006} = 1.0003$ ). These results can be seen in **Table 19** and **Figure 30**.

CpG site	p-value	Adjusted p-value	Gene name
cg08073934	5.31E-08	0.02	<i>SDK1</i>
cg00960509	6.59E-08	0.02	<i>ECE1</i>
cg19333996	3.62E-07	0.08	<i>KIAA1549</i>
cg26541517	6.57E-07	0.11	<i>SIAH3</i>
cg06316092	2.01E-06	0.23	unclassified

**Table 19:** The five CpG sites with the lowest p-values (and thus highest significance) for the model 2 EWAS of maximum grip strength.

Red highlighting indicates statistical significance (adjusted p-value < 0.05). Model 2 adjusting for age, sex, cell composition and array.

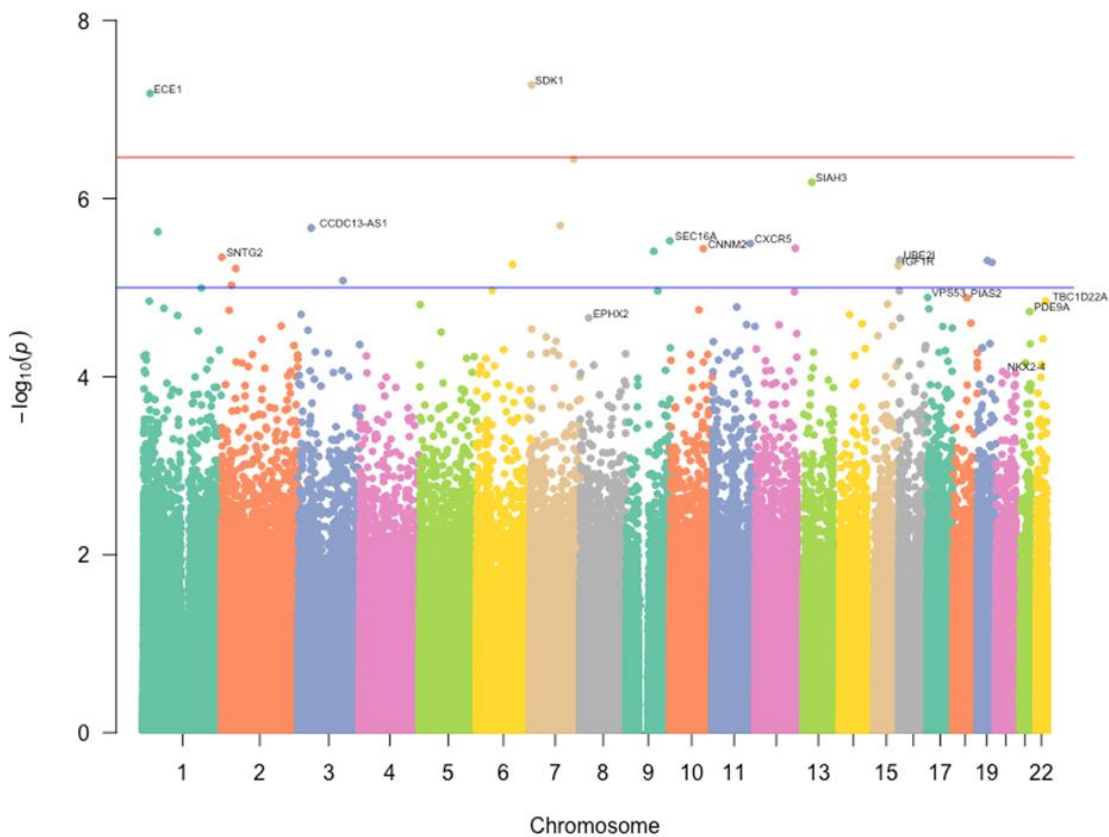


**Figure 30:** Manhattan plot for the EWAS of maximum grip strength in model 2

Model 2 adjusted for age, sex, cell composition and array with all 334 participants included. As can be seen, there are two differentially methylated CpG sites which lie beyond the False Discovery Rate (FDR) red line; which lie in the genes *ECE1* and *SDK1* respectively.

### 3.3.4.2 Sensitivity models 3 and 4

In the models 3 (adjusted for age, sex, height, weight for height residual, cell composition and array) and 4 (for 327 participants (due to 7 missing values in occupational social class) adjusted for age, sex, height, weight for height residual, occupational social class, physical activity, prudent diet score, smoking status, alcohol consumption, cell composition and array). None of the differentially methylated CpG sites met FDR criteria; however, cg00960509 in the *ECE1* gene was the site consistently observed in the lowest p-values as can be seen in **Table 20** and **Table 21**.

CpG site	p-value	Adjusted p-value	Gene name
cg04010817	1.19E-06	0.31	unclassified
cg00960509	1.62E-06	0.31	<i>ECE1</i>
cg06590119	2.12E-06	0.31	<i>VPS53</i>
cg19680388	2.80E-06	0.31	<i>THYN1</i>
cg18537410	3.41E-06	0.31	<i>DNAJC11</i>

**Table 20:** The five CpG sites with the lowest p-values (and thus highest significance) for the model 3 EWAS of maximum grip strength.

(adjusting for age, sex, height, weight for height residual, cell composition and array)

CpG site	p-value	Adjusted p-value	Gene name
cg26541517	1.22E-06	0.248123	<i>SIAH3</i>
cg16280667	1.24E-06	0.248123	<i>CXCR5</i>
cg06590119	1.37E-06	0.248123	<i>VPS53</i>
cg20424584	1.59E-06	0.248123	unclassified
cg00960509	2.03E-06	0.248123	<i>ECE1</i>

**Table 21:** The five CpG sites with the lowest p-values (and thus highest significance) for the model 4 EWAS of maximum grip strength

(adjusting for age, sex, height, weight for height residual, occupational social class, physical activity, diet, smoking status, alcohol consumption, cell composition and array).

### 3.3.5 Pathway and gene ontology for maximum grip strength

The *Enrichr* (<https://maayanlab.cloud/Enrichr/>) platform was used for pathway and gene ontology analysis.

Investigation of the CpG sites with lowest p-value ( $<1 \times 10^{-5}$ ) from model 2 was performed with the associated genes (n=17 genes) and repeated for the genes associated with 100 CpG sites with the lowest p-values (n=70 genes) to increase the pool of genes for these exploratory analyses (both listed in **Appendix 29**).

It should be noted that the number of genes in the first subset (those with a p-value  $<1 \times 10^{-5}$ ) is fairly small and that, although the second subset includes the genes with the lowest p-value, only one of these reached the pre-set, epigenome-wide threshold for significance<sup>206</sup>. The findings of these and latter, exploratory analyses should, therefore, be considered within the context of these limitations.

Model 4 (adjusted for age, sex, height, weight for height residual, occupational social class, physical activity, prudent diet score, smoking status, alcohol consumption, cell composition and array) was used for sensitivity analyses.

P-values are derived from Fisher's exact test and statistical significance in this context is represented by an adjusted p-value  $<0.05$ . This would indicate that a cluster of genes appearing in a particular pathway is not likely to have occurred by chance alone. The adjustment in this case refers to a p-value which has been adjusted for the number of tests. All quoted p-values are therefore adjusted p-values. Odds ratios in these analyses refer to the odds that a particular term (gene ontology term or pathway term) appears in a list of differentially methylated genes divided by the odds that the same term appears in a list of all genes of a given gene set.

#### 3.3.5.1 Pathway and gene ontology for maximum grip strength model 2

##### 3.3.5.1.1 Pathway analysis

In pathway analysis (KEGG 2021) for model 2 and using the  $p < 1 \times 10^{-5}$  subset, there were no significant associations, although 'caffeine metabolism' had the lowest p-value (adjusted p= 0.19). In the subset using the 100 most significant CpG sites 'caffeine metabolism' was the most strongly associated pathway but again the association was not statistically significant (adjusted p= 0.28).

##### 3.3.5.1.2 Gene ontology analysis

Examining the gene ontology of the  $p < 1 \times 10^{-5}$  subset, there were no significant associations for biological process, molecular function, cellular component or human phenotype gene ontology. When using the genes associated with the 100 CpG sites with the lowest p-value there was a

significant association for purine ribonucleotide catabolic process (adjusted  $p=0.049$ ) in the biological process gene ontology (driven by the genes *NT5E* and *XDH*) and borderline for P-type calcium transporter activity (adjusted  $p=0.049$ ) and P-type calcium ion activity (adjusted  $p=0.053$ ) (both driven by the genes *ATP2B2*, *ATP2C2*). No significant associations were observed for cellular component or human phenotype gene ontologies.

### 3.3.5.2 Pathway and gene ontology sensitivity analysis for maximum grip strength

Model 4 (including adjustments for age, sex, height, weight for height residual, occupational social class (manual vs non-manual labour), physical activity (Dallosso score<sup>157</sup>), diet (prudent diet score), smoking status (ever having smoked regularly) and alcohol consumption (an ordinal variable of units/week) was used for sensitivity analysis.

For the extended subset (including all genes associated with the 100 CpG sites with the lowest p-values,  $n=68$  genes) there were no significant findings for pathway analysis or gene ontology. Of interest, 'slender build' was the most strongly associated human phenotype gene ontology, though the association did not reach statistical significance (adjusted  $p=0.07$ ). Those relating to oxidoreductase activity, FMN, Flavin adenine dinucleotide, NADP and NADPH binding were driven by the *MTRR* gene, those relating to chemokine binding and receptor activity were driven by gene *CXCR5*, diacylglycerol kinase and phosphotransferase activity by *DGKI*, ubiquitin conjugating enzyme activity by *SIAH3* and syntaxin binding by *SCFD2*.

For the subset including only those CpG sites with a p-value  $<1 \times 10^{-5}$  ( $n=10$  genes), there were no significant associations for KEGG pathway analysis; however, there were 16 significant association with molecular functions relating to metabolism (**Table 22**). The odds ratios in this table (and in all gene ontology or pathway analyses) refer to the odds that a particular term (gene ontology term or pathway term) appears in a list of differentially methylated genes divided by the odds that the same term appears in a list of all genes of a given gene set. In this case, the large odds ratios (171 to 555) are likely due to the fact that that number of differentially methylated genes (associated with CpG sites with a p-value  $<1 \times 10^{-5}$ ) is low at a total of 10, compared to the size of the gene set (for gene ontology molecular function) which is over 20,000 genes.

CpG site	p-value	Adjusted p-	
		value	Odds Ratio
Oxidoreductase activity, acting on metal ions, NAD or NADP as acceptor	0.002	0.04	555
Oxidoreductase activity, acting on NADPH, heme protein as acceptor	0.004	0.04	371
Diacylglycerol kinase activity	0.006	0.04	222
FMN binding	0.006	0.04	222
NADPH binding	0.007	0.04	171

**Table 22:** The five most significant molecular function gene ontologies for maximum grip strength model 4  
(for genes associated with CpG sites with a  $p < 1 \times 10^{-5}$ )

Human phenotype ontology revealed a network of conditions, a large proportion of which were involved in metabolic processes (see **Figure 31**). Those relating to homocysteine, aspartate, vitamin B, methionine metabolism and megaloblastic anaemia were particularly driven by the gene *MTRR*, opisthotonus by *VPS53* and dysautonomia by *ECE1*.

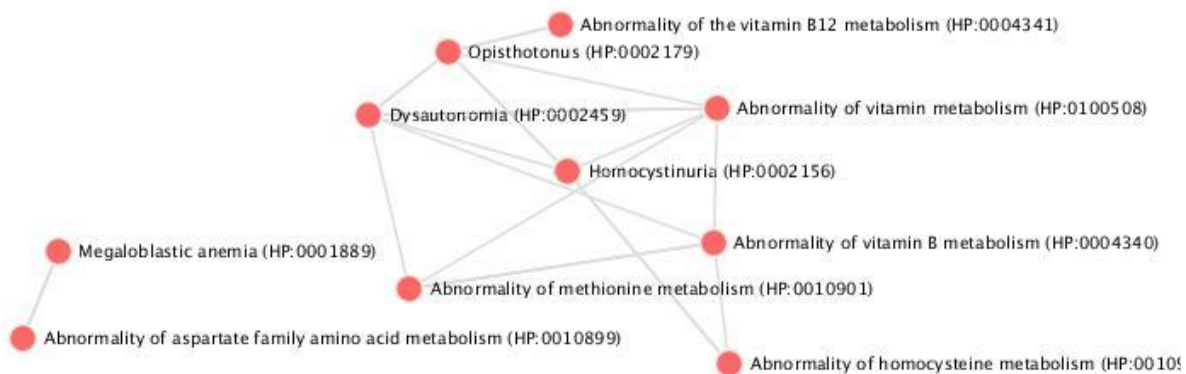


**Figure 31:** Network analysis of human phenotype gene ontology (for model 4 maximum grip strength EWAS CpG sites with  $p < 1 \times 10^{-5}$  ( $n = 10$  genes)).

Each node is representative of a phenotype term and a line linking two nodes suggests similarity between the ontology of the phenotypes.

### 3.3.6 Total femoral neck bone mineral density

In models for total hip bone mineral density, there were no differentially methylated CpG sites which met the FDR threshold; however, cg02389067 was consistently in the top 5 lowest p-values for each models 2,3 and 4, with a lowest p-value of 0.12 for model 4 (see **Table 23**, **Table 24** and



**Table 25).** cg02389067 lies in a CpG island in the promoter region at the 5` end of *GNA13* on chromosome 17 (see **Appendix 28**).

CpG site	p-value	Adjusted p-value	Gene name
cg13989810	1.80E-07	0.13	<i>DPP6</i>
cg24320640	6.79E-07	0.25	<i>ARHGEF4</i>
cg02389067	1.84E-06	0.37	<i>GNA13</i>
cg02547916	2.53E-06	0.37	unclassified
cg20668718	2.91E-06	0.37	<i>JAKMIP2</i>

**Table 23:** The five CpG sites with the lowest p-values (and thus highest significance) for the model 2 EWAS of total hip bone mineral density.  
(adjusting for age, sex, cell composition and array)

CpG site	p-value	Adjusted p-value	Gene name
cg02389067	9.84E-07	0.39	<i>GNA13</i>
cg06590119	2.58E-06	0.39	<i>JAKMIP2-AS1</i>
cg13658885	2.50E-06	0.39	<i>VPS53</i>
cg04190734	2.66E-06	0.39	<i>HSPC072</i>
cg10795509	2.51E-06	0.39	<i>MAPK8IP3</i>

**Table 24:** The five CpG sites with the lowest p-values (and thus highest significance) for the model 3 EWAS of total hip bone mineral density.  
(adjusting for age, sex, height, cell composition and array)

CpG site	p-value	Adjusted p-value	Gene name
cg02389067	2.30E-07	0.12	<i>GNA13</i>
cg13658885	3.27E-07	0.12	<i>MAPK8IP3</i>
cg10795509	1.14E-06	0.28	<i>HSPC072</i>
cg15651650	1.58E-06	0.29	unclassified
cg04190734	2.52E-06	0.31	<i>JAKMIP2-AS1</i>

**Table 25:** The five CpG sites with the lowest p-values (and thus highest significance) for the model 4 EWAS of total hip bone mineral density.  
(adjusting for age, sex, height, weight for height residual, dietary calcium, physical activity, smoking history, alcohol consumption, cell composition and array)

### 3.3.6.1 Pathway and gene ontology analysis for total femoral neck BMD

Similar to the approach used for grip strength, pathway analysis and gene ontology analysis for total femoral neck BMD focused on EWAS model 2 (adjusted for age, sex, cell composition and array) using genes associated with CpG sites which had a p-value <  $1 \times 10^{-5}$  (n=14). The majority of analyses (except molecular function gene ontology) failed to reach statistical significance so further analyses were performed using genes associated with the 100 CpG sites with the lowest p-values (see **Appendix 30** for list for genes) (n=72). Additional sensitivity analyses were performed to investigate the effect of including all covariates in the EWAS model (model 4) for genes associated with the CpG sites with p-value <  $1 \times 10^{-5}$ . These analyses are subject to the same limitations, in terms of numbers of genes and lack of statistical significance, which are described for the grip strength epigenome-wide analyses.

#### 3.3.6.1.1 Pathway and gene ontology for total femoral neck BMD model 2

##### 3.3.6.1.1.1 Pathway analysis

Pathway analysis for genes associated with CpG sites with p-value <  $1 \times 10^{-5}$  using KEGG 2021 highlighted pathways including 'cGMP-PKG signalling pathway' (due to genes *GNA14*, *PDE2A*), 'pathogenic E.coli infection' (*GNA13*, *MYO1E*) and 'regulation of actin cytoskeleton' (*GNA13*, *ARHGEF4*) though none of these reached statistical significance (adjusted p=0.058 for all).

This pathway analysis was repeated using the 100 CpG sites with the lowest p-values and demonstrated statistically significant enrichment for 'phospholipase D signalling pathway' (due to genes *GNA13*, *PDGFD*, *AKT3*, *RRAS2*, *DNM2*) (adjusted p=0.01) and 'regulation of actin cytoskeleton' (genes *GNA13*, *PDGFD*, *RRAS2*, *ARHGEF4*, *ITGA7*, *BAIAP2*) (adjusted p=0.01). Statistical significance in this case indicates that the clusters of genes appear in the particular pathway by more than would be expected due to chance alone. The pathway diagrams with the proteins expressed by the above genes are seen in **Figure 32** and **Figure 33**. These demonstrate roles for the associated genes in the cAMP signalling pathway, the Ras signalling pathway, the P13k -Akt signalling pathway, the calcium signalling pathway and endocytosis elements of the 'phospholipase D signalling pathway'. For the 'regulation of actin cytoskeleton' the key involvement of the above genes is in G-protein coupled chemotaxis, actin polymerisation and lamellipodia formation.

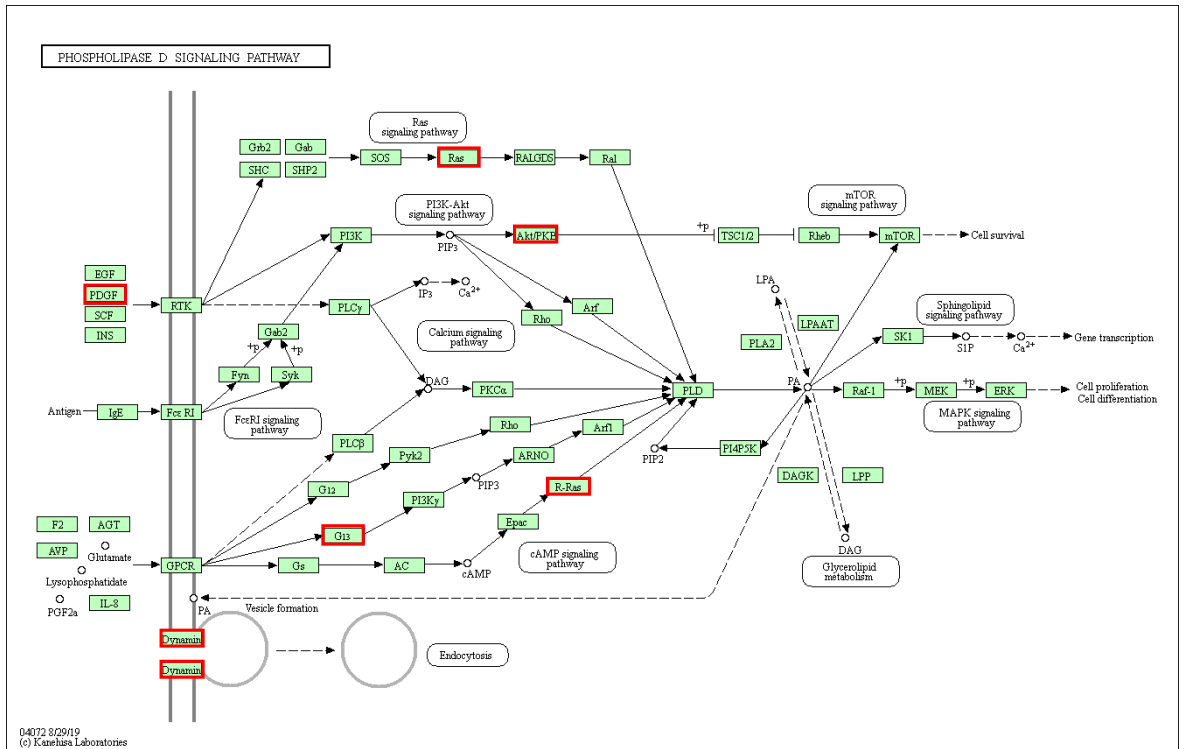


**Figure 32** The KEGG phospholipase D signalling pathway with proteins expressed from genes associated with the top 100 CpG sites associated with femoral neck BMD EWAS model 2 (highlighted in red).

These demonstrate roles for the associated genes in the cAMP signalling pathway, the Ras signalling pathway, the P13k -Akt signalling pathway, the calcium signalling pathway and endocytosis.

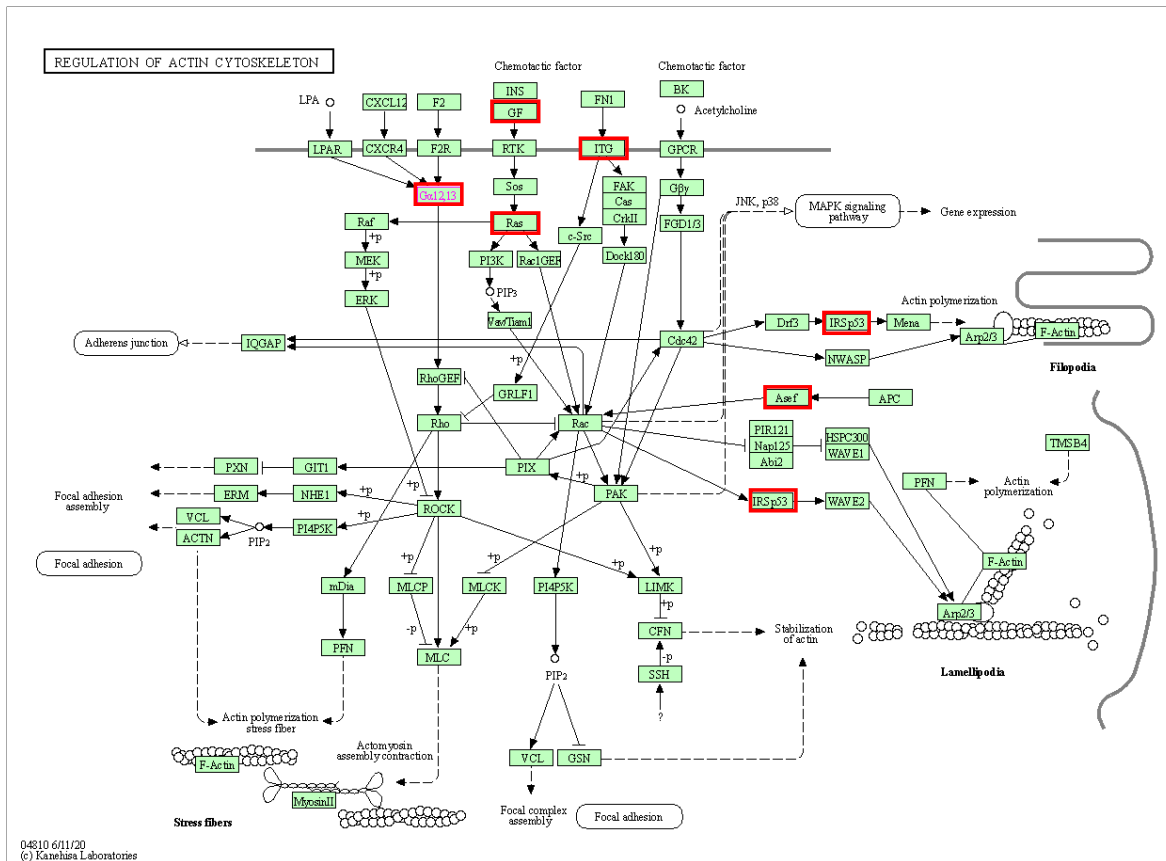


**Figure 33:** The KEGG actin cytoskeleton regulation pathway with proteins expressed from genes associated with the top 100 CpG sites associated with femoral neck BMD EWAS model 2 (highlighted in red).

These demonstrate roles for the associated genes in G-protein coupled chemotaxis, actin polymerisation and lamellipodia formation.

3.3.6.1.1.2 Gene ontology

In the genes associated with CpG sites with a  $p < 1 \times 10^{-5}$  dataset, no significant associations were observed for biological process (regulation of intracellular signal transduction, adjusted  $p=0.06$ ) or cellular component (MOZ/MORF histone acetyltransferase complex, adjusted  $p=0.1$ ) ontologies or disease ontologies; however molecular function ontologies revealed significant enrichment for the TPR binding domain, dopamine receptor binding and 3',5'-cyclic-GMP phosphodiesterase activity and other chloride channel activities (adjusted  $p=0.049$ ) as shown in **Table 26**.

In terms of human phenotype ontology, hip contracture, limited hip movement, truncal obesity and knee flexion contracture were all significantly associated when using the genes associated with CpG sites which had a  $p\text{-value} < 1 \times 10^{-5}$  (see **Table 27**)

In the larger gene group (for the top 100 CpG sites) there were no significant associations in biological process, cellular component or molecular function gene ontology; however, for human

phenotype biconcave vertebral bodies were significantly associated (adjusted  $p=0.0003$ ) as seen in the Manhattan plot below (**Figure 34**).

CpG site	p-value	Adjusted p-value	Odds Ratio
TPR domain binding	0.003	0.049	384
Dopamine receptor binding	0.004	0.049	307
3',5'-cyclic-GMP phosphodiesterase activity	0.004	0.049	256
Phosphate ion binding	0.007	0.049	171
Voltage-gated chloride channel activity	0.007	0.049	171

**Table 26:** The *biological function* gene ontology for the genes associated with CpG sites with a  $p < 1 \times 10^{-5}$  in model 2 EWAS for total femoral neck BMD.

P-values, adjusted p-values and odds ratios demonstrate the significant of the biological function gene ontology (and GO: numbers) with significance indicated by an adjusted  $p < 0.05$ .

CpG site	p-value	Adjusted p-value	Odds Ratio
Hip contracture	0.00005	0.004	238
Limited hip movement	0.0001	0.004	166
Truncal obesity	0.0001	0.004	145
Knee flexion contracture	0.0001	0.004	145
Abnormality of lateral ventricle	0.006	0.05	220

**Table 27:** The *human phenotype* gene ontology for the genes associated with CpG sites with a  $p < 1 \times 10^{-5}$  in model 2 EWAS for total femoral neck BMD.

P-values, adjusted p-values and odds ratios demonstrate the significant of the biological function gene ontology (and GO: numbers) with significance indicated by an adjusted  $p < 0.05$ .

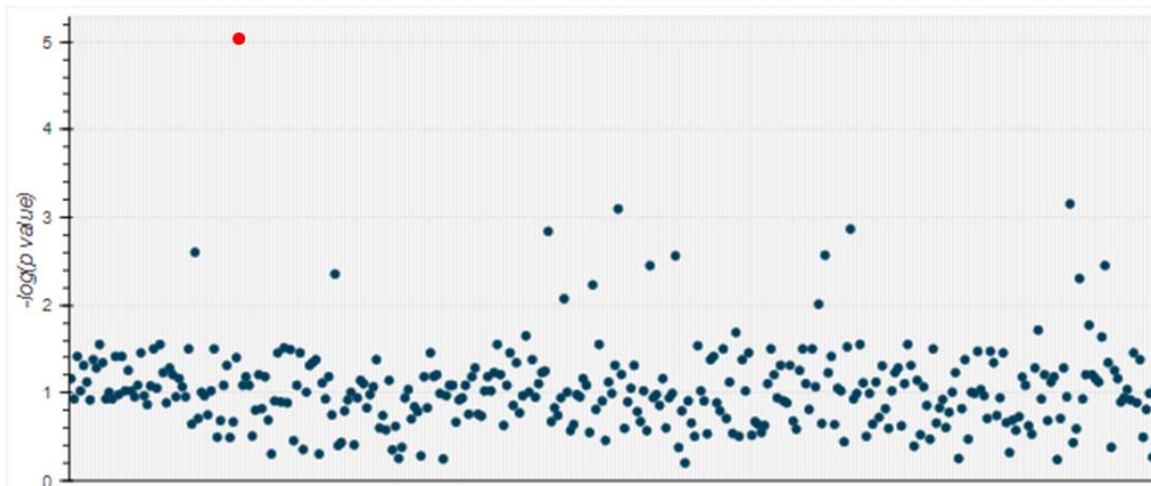


**Figure 34:** Manhattan plot demonstrating the level of significance for the association between human phenotypes and the genes associated with the top 100 CpG sites associated with femoral neck BMD EWAS model 2.

The significant result (highlighted in red) is for the phenotype 'biconcave vertebral bodies'.

### 3.3.6.2 Pathway and gene ontology sensitivity analysis for total femoral neck BMD

Model 4 (including adjustments for age, sex, height, weight for height residual, occupational social class (manual vs non-manual labour), physical activity (Dallosso score<sup>157</sup>), diet (dietary calcium for BMD analyses), smoking status (ever having smoked regularly) and alcohol consumption (an ordinal variable of units/week) was used for sensitivity analysis.

Investigation of the CpG sites with lowest p-value ( $<1 \times 10^{-5}$ ) from model 4 was performed with the associated genes (n=18) and the genes associated with the lowest 100 p-values (n=79) (see gene lists in **Appendix 30**).

No significant associations were observed for KEGG pathway analysis with either subset. Gene ontology did not demonstrate significant associations for biological process or cellular components in either set. Molecular function gene ontology was negative in the lowest 100 CpG site subset and there was a borderline association with collagen receptor activity, amidine-lyase activity and dopamine receptor activity (adjusted  $p=0.05$  for each) in the  $p < 1 \times 10^{-5}$  subset.

### 3.3.7 Summary results

#### 3.3.7.1 Maximum grip strength EWAS

The key muscle findings from this chapter are that, despite a relatively small population (n=334) we observed significant associations between grip strength and differential methylation at two CpG sites; cg08073934 (adjusted p-value = 0.02) lying in a north shore region associated with the gene *SDK1* on chromosome 7 and cg00960509 (adjusted p-value = 0.02) lying in a CpG island associated the 5' end of the gene *ECE1* on chromosome 1 (in model 2, adjusted for age, sex, cell type and array).

The finding for cg00960509 (associated with *ECE1*) was supported by the same CpG site being seen in the five most associated CpG sites in sensitivity EWAS models. The possible relevance of this finding will be addressed in the discussion chapter but the presence of the CpG in the promoter region increases the possibility that it may be involved in *ECE1* gene expression.

In downstream analyses of the maximum grip strength EWAS, there were no associations for pathway analysis, though gene ontology highlighted some potential associations with purine ribonucleotide catabolic process (adjusted p=0.049) in the biological process gene ontology (driven by the genes *NT5E*, *XDH* and *PDE9A*) and borderline for P-type calcium transporter activity (p=0.049) when using an extended gene set (taken from the 100 CpG sites with the lowest p-values).

When performing sensitivity analyses using a fully-adjusted model (including age, sex, height, weight for height residual, dietary calcium, physical activity, smoking history, alcohol consumption, cell composition and array) for the genes associated with CpG sites with a p-value <  $1 \times 10^{-5}$  significant associations were found for molecular function gene ontology (including a host of metabolic and inflammatory processes) and human phenotype ontology (including metabolic disorders).

There are two substantial factors to consider in the above findings.

The first is the issue of tissue specificity. The DNA for the EPIC (850k) array methylation analysis was extracted from peripheral blood leukocytes and so the pathways and ontologies associated are less likely to be related directly to muscle or bone but may influence the outcomes (maximum grip strength and total femoral neck bone mineral density) via systemic metabolic, signalling or inflammatory processes.

The second relates to the two subsets of genes used: the 'top 100' and the 'p <  $1 \times 10^{-5}$ '. Although a large number of significant associations for molecular function and human phenotype gene ontology were observed in sensitivity analyses, these were largely seen in the 'p <  $1 \times 10^{-5}$ ' subset. This encompasses only 10 genes and so the associations with each ontology were being driven by

only one gene. Although interesting, these findings may still be artefactual and thus will require further investigation in larger cohorts to determine whether these findings can be replicated.

### **3.3.7.2 Total femoral neck BMD EWAS**

For total femoral neck BMD, there were no significant CpG associations identified via EWAS, although cg02389067 associated with the *GNA13* gene was consistently observed to be in the 5 lowest p-values for EWAS model 2 and sensitivity models 3 and 4.

Pathway KEGG analysis demonstrated significant associations with 'phospholipase D signalling pathway' (due to genes *GNA13*, *PDGFD*, *AKT3*, *RRAS2*, *DNM2*) (adjusted p=0.01) and 'regulation of actin cytoskeleton' (genes *GNA13*, *PDGFD*, *RRAS2*, *ARHGEF4*, *ITGA7*, *BAIAP2*) (adjusted p=0.01) using EWAS model 2 and the 'top 100' subset of CpG sites.

Human phenotype gene ontology demonstrated significant associations with musculoskeletal conditions of the hip (e.g. hip contracture, limited hip movement) and biconcave vertebral bodies, which may be indicative of vertebral fracture and osteoporosis.

In the discussion chapter we will address these observations in light of biological plausibility, previous literature and the consideration of further work.



## Chapter 4 Discussion

Ageing presents one of the greatest challenges for the modern populace, with escalating health and care costs, expanding morbidity and increased mortality. The ageing of the musculoskeletal system is of particular importance as fractures and falls are associated with poor health outcomes.

This doctoral project has sought to improve our understanding of the ageing phenotype by describing changes in the musculoskeletal system in an ageing cohort in the UK, to examine associations of parameters of musculoskeletal ageing with fracture, to test whether epigenetic age acceleration (as a novel biomarker of biological ageing) is predictive of the ageing musculoskeletal phenotype, and to investigate novel methylation marks which show association with key tenets of musculoskeletal ageing.

### 4.1 Change in musculoskeletal parameters with ageing

#### 4.1.1 Change in bone microarchitecture

Let us first consider tibial bone microarchitecture. We observed decreased trabecular density with increased trabecular area together with decreased cortical area, density and thickness. In terms of cortical pores we saw increases in cortical porosity and pore diameter and, globally, a decrease in total volumetric bone density.

The above characteristics are aligned to the current theory of bone aging with trabecular bone loss and decreased cortical bone. The reason for widening trabecular area is potentially due to endocortical resorption with increases in trabecular area developing at the cost of thinning the cortex<sup>223</sup>. This process, in conjunction with failure in periosteal apposition of bone, is one of the primary causes of osteoporosis, bone fragility and increased risk of fracture<sup>224</sup>.

Our finding that total volumetric density reduces with ageing, is the first time this has been demonstrated in a mixed-sex group of older adults in the UK and this size of cohort, with annual percentage reductions of -0.5% in males and -0.8% in females. A longitudinal study in Canada which incorporated individuals across the lifecourse (aged 16-80+) showed significant 1.0% annual gain in volumetric BMD in 16-19 year old males (n=13) but significant losses for 70-79 year old males (-0.4%, n=17) and 80+ years (-0.9%, n=7), and similarly in female 70-79 year olds (-0.7%, n=59) and non-significant loss for 80+ females (-0.6%, n=9)<sup>85</sup>. In a study of peri- and post-menopausal women,

the annualised loss percentages were significant in both groups (-0.8% per-menopausal, -1.0% post-menopausal) but this was a smaller study of n=82 females in total<sup>65</sup>.

In terms of cortical parameters, the annual percentage reductions (male and female) in cortical area (-0.7%, -1.3%), thickness (-0.4%, -1.1%) and density (-0.6%, -0.7%) and increases in porosity (1.5%, 2.5%) are similar to those observed in the Canadian Multi-centre Osteoporosis Study (CAMOS) in the 70-79 year old subgroup; reduced cortical area (-1.0%, -0.3%), thickness (-1.1%, -0.4%) and density (-0.5%, -0.9%) and with greater increases in porosity (3.4%, 7.7%)<sup>85</sup>.

For trabecular parameters, again, our findings were similar to those from the CaMOS cohort with significant increases in trabecular area in HCS (0.1%, 0.2%) and CaMOS (0.3%, 0.2% for the 70-79 year subset) and a paucity of other significant findings.

#### **4.1.2 Change in grip strength**

Grip strength change across the lifecourse has been aptly described in a meta-analysis of studies performed by Dodds and colleagues which demonstrated a rise until a peak in early mid-life (approximately 35 years), followed by a gentle decline until the age of 60 when the decline is more rapid<sup>17</sup>.

In our study of community dwelling older adults, we observed absolute percentage losses of -18% (-0.80kg/year) in males and females across 5.1 years of follow-up. Previous studies of similar aged participants have demonstrated losses (in males and females) of -0.95kg/year and -0.45kg/year in Swedish Adoption/Twin Study of Aging (approximately 70 years at baseline)<sup>225</sup>, losses of -0.48kg/year and -0.30kg/year in a Japanese study (72 years at baseline)<sup>226</sup>, reduction of -0.66kg/year and -0.38kg/year in the English Longitudinal Study of Ageing (72 years at baseline)<sup>57</sup> and 0.02% and 0.01% annualised percentage loss in a Danish cohort (aged 70 years at baseline)<sup>227</sup>.

#### **4.1.3 Change in bone mineral density at the femoral neck**

Similar to the profile of grip strength across the lifecourse, bone mineral density reaches a peak in the middle of the fourth decade, before plateauing and reducing rapidly from the menopause for females and more gradually for males into older age<sup>30</sup>. Femoral neck bone mineral density losses were 2.2% in males and 3.9% across the 5.1 years of follow-up. Within the HCS a previous study utilising pQCT between 2004-05 and EPOSA (2011-12) observed a similar sex dimorphism with greater declines in cortical area for females than males at both the radius ( $p=0.006$ ) and the tibia ( $p<0.001$ )<sup>221</sup>.

This is comparable to findings from The Rotterdam Study (aged  $\geq 55$  years, 2-year follow-up) which described losses of -0.4% for males and -0.6% for females<sup>228</sup>, the Framingham Osteoporosis Study

(74 years at baseline, 4-year follow-up) which showed losses of -0.38%/year in males and -0.87%/year in females<sup>229</sup> and the MrOS cohort ( $\geq 65$  years, 4.6-year follow-up) which described losses of -1.72%<sup>230</sup>.

#### **4.1.4 Associations of musculoskeletal ageing parameters with odds of fracture**

When considering our findings with regard to fracture prediction it is important to recognise that the studies discussed below refer to incident fractures whereas our study refers to prevalent fractures. Potential confounders in the relationships observed primarily include comorbidity, poor muscle health (which could impact on bone strength and increase the risk of falls and fractures), as well as those measures included as covariates (including sex, age, height, BMI, dietary calcium, physical activity, smoking history (ever vs never), alcohol consumption and social class).

In the OFELY cohort (over 10 years of follow-up) trabecular parameters at the radius had greater predictive capacity<sup>71</sup>, as did trabecular parameters in a group taking denosumab<sup>72</sup>. In the GERICO cohort of post-menopausal females (over 5 years of follow-up), lower baseline volumetric BMD<sup>69</sup>, and in the CaMOS cohort, radial total BMD (Odds ratio (OR) per standard deviation (SD) lower baseline values: 2.1) and trabecular BMD (OR: 2.0), and lower baseline cortical thickness at the tibia (OR: 2.2)<sup>70</sup> were predictive of future fracture. An important finding from the CaMOS study was that baseline values rather than rate of change were more associated with fractures in post-menopausal females<sup>70</sup>. Similar findings were described in our study with only change in trabecular density being associated with an increased odds of fracture (OR 0.50,  $p < 0.01$ ), compared to multiple baseline parameters (including a greater odds of fracture with higher trabecular area (OR 2.18,  $p < 0.01$ ); lower total volumetric bone density (OR 0.53,  $p < 0.01$ ); lower cortical area (OR 0.53,  $p < 0.04$ ), lower cortical density (OR 0.56,  $p < 0.02$ ) and lower cortical thickness (OR 0.45,  $p < 0.01$ ). It should be noted that the odds ratios in our study were for increases in bone microarchitecture parameter whereas in CaMOS they were for reductions in bone microarchitecture<sup>70</sup>. Hence, cortical thickness in CaMOS was associated with an odds ratio of 2.2 (for each SD decrease in baseline value)<sup>70</sup> whereas, in the HCS, we reported an odds ratio of 0.45 (for each SD increase in baseline value).

In our analyses grip strength baseline level and longitudinal change had no predictive capacity for fracture and only baseline level of (and not change in) total femoral neck BMD showed any significant association with the odds of fracture reduced by 46% per standard deviation increase in BMD (OR 0.54,  $p = 0.003$ ).

The reason why associations with fracture were stronger with baseline values of musculoskeletal parameters rather than longitudinal change parameters, may imply that the genes required to form bone and muscle (in order reach a higher peak earlier in the lifecourse) have a greater influence on fracture than those associated with age-related increases in bone resorption and deteriorations in bone microarchitecture and muscle health.

We found that a SNP associated with the *ABCF2*, coding for ATP Binding Cassette Subfamily F Member 2, had a borderline association with trabecular area ( $p=0.07$ ). The protein ABCF2 plays a role in transmembrane transportation and prior work has described associations with cancer progression<sup>231,232</sup>, the molecular pathogenesis of Duchenne Muscular Dystrophy<sup>233</sup>, and down-regulation of ulcerative colitis<sup>234</sup>. The exact relevance of this gene to bone mineral density is not clear but two SNPs are implicated in skeletal health with rs7812088 associated with femoral neck BMD in the study by Estrada and colleagues<sup>219</sup>, but also rs73169678 associated with total body BMD in a separate GWAS by Medina-Gomez and colleagues<sup>235</sup>. It is possible that the observed association with trabecular area is mediated via stem cell pathways or inflammatory mechanisms which have previously been described in this cohort<sup>236</sup>.

We also recorded that a SNP (rs3801387) in the *WNT16* gene was associated with change in trabecular microarchitecture such that for each extra G allele at that locus there was a 0.28 standard deviation gain in trabecular density ( $p=0.01$ ). Wnt16 is considered to be primarily secreted by osteoblasts<sup>237</sup> (bone-forming cells) and directly suppresses osteoclastogenesis via the non-canonical JNK MAPK pathway via upregulation of osteoprotegerin. Mouse models have shown that Wnt16 is reduced by steroid administration<sup>238</sup> and rs3801387 has been associated with BMD, fracture and cortical bone thickness in previous studies<sup>171,235,239</sup>. Similar adverse effects of rs3801387 were observed in a cohort of pre-menopausal females with each additional T allele associated with lower BMD at the femoral neck ( $\beta=-0.12$ )<sup>239</sup>. Other GWAS have demonstrated associations between SNPs in *WNT16* and BMD but at alternative loci<sup>240,241</sup>.

## 4.2 Epigenetic Age Acceleration

Our investigation into whether accelerated epigenetic ageing predicts musculoskeletal ageing has highlighted some nuances of the collection of biomarkers known as epigenetic clocks. Importantly for downstream analysis we noted that epigenetic ages using the Illumina 450k array were significantly lower than those for the later iteration, the Illumina EPIC (850k) array. We also observed that the epigenetic age of HCS participants using the second-generation clocks (GrimAge and PhenoAge) were, on average, substantially lower than the first generation clock (HorvathAge). When examining the predictive capacity of epigenetic age acceleration for future musculoskeletal phenotype, we found very sex-specific relationships. GrimAge and PhenoAge acceleration, in particular, predicted future muscle outcomes (grip strength and gait speed) in males, but

associations in females were largely with bone mineral density and measures of body composition (appendicular lean mass and total fat mass) and appeared to be such that greater age acceleration was associated with greater levels of bone, muscle and fat. Indeed, in bone microarchitecture, the only significant finding was for cortical thickness and, again it was the case the greater acceleration was associated with more tissue (higher cortical thickness) which is counter to the current dogma of bone ageing.

#### **4.2.1 Differences in epigenetic clocks between 450k array and 850k array**

The 450k methylation array was superseded by the EPIC (850k) array in 2015. Although the EPIC array covers nearly twice as many CpG sites (850,000 vs 450,000) across the genome, it does not cover every CpG site found on the 450k array. In fact, 6.8% of the CpG sites from the 450k are absent from the 850k array. This is pertinent when we consider epigenetic clocks, as for the HorvathAge clock, which was designed for use on 27k (the precursor to the 450k array) and 450k array, a total of 19 CpG sites from the original 353 from which the clock is composed, are missing on the 850k array<sup>242</sup>. This has led to studies evaluating the accuracy of methylation age clocks using the 850k array.

McEwen and colleagues performed one such examination of the two arrays (450k and 850k) using monocyte DNA samples from 172 individuals<sup>243</sup>. They initially investigated the effect of three different pre-processing methods for the arrays and found a high correlation for HorvathAge clocks, concluding that chronological age to HorvathAge correlation “was largely unaffected by platform differences and normalization methods”. For between-array differences they saw a mean difference of 1.4-3.1 years across pre-processing methods. Dhingra and colleagues found similarly, with the EPIC array underestimating HorvathAge by a mean deviation of -3.4<sup>242</sup>, and suggested that the difference observed was due to the 19 missing probes despite probe imputation via the Horvath model<sup>3</sup>. However, neither of the above studies investigated the effect of ‘array type’ (i.e. 450k or 850k) on the second generation clocks (GrimAge and PhenoAge).

Absent probes may explain the inter-array differences for HorvathAge we observed; however, the same explanation cannot be the case for PhenoAge and GrimAge clocks, as each were designed using the subset of CpG sites which are common to both the 450k and 850k array. The reason for this difference remains unclear and may be artefactual.

We wanted to use both 450k and 850k data as it increased our sample size and chose a Z-score approach to combining the epigenetic age accelerations from each array. Although this has not

been employed in the specific use-case of combining 450k and 850k array datasets, it is a valid statistical approach as the epigenetic age acceleration for each array was normally distributed. Although there are not many studies which have attempted to combine 450k and 850k datasets. Rezwan and colleagues, investigating the association between epigenetic age acceleration and asthma, performed a meta-analysis of the effect estimates in order to combine their 450k and 850k regression results from different epidemiological cohorts <sup>244</sup>. This is a valid approach (particularly as the 450k arrays were performed in one cohort and 850k arrays in another cohort); however, we felt that our Z-score approach was justifiable given that our 450k and 850k samples came from the same cohort.

There is now an increasing drive to use the extended breadth of the 850k array to produce novel epigenetic clocks<sup>245,246</sup> and this could be an avenue for future work.

#### 4.2.2 Observed differences between clocks

The first generation epigenetic clocks (of which the HorvathAge clock was principle<sup>3</sup>) and second generation clocks (including GrimAge<sup>126</sup> and PhenoAge<sup>127</sup>) differ in the purpose of their original design. The first generation clocks aimed to correlate as closely as possible with chronological age, whereas the second generation clocks aimed to correlate with serum proteins known to associate with ageing<sup>127</sup> or DNA-methylation biomarkers of ageing phenotypes<sup>126</sup>, and therefore capture lifespan.

We found that GrimAge and PhenoAge were substantially lower than chronological age and HorvathAge. There are prior data suggesting that HorvathAge is systematically underestimated in older adults<sup>247</sup> but in our study mean HorvathAge was the same as mean chronological age (65.0 years). For this reason we have reviewed the chronological, HorvathAge and PhenoAge and GrimAge of a number of studies which are summarized **Table 28**.

Mean(SD)	HCS (n=415)	TILDA (n=490)	NHSD 60-64 years (n=672)		Cronje, 2021 (n=120)
	Pooled	Pooled	Males	Females	Males
Chronological age	65.0 (2.8)	62.2 (8.3)	63.0 (1.1)	63.1 (1.0)	63 (10)
HorvathAge	65.0 (4.6)	61.3 (11.0)	58.9 (4.7)	57.2 (4.1)	59 (8)
PhenoAge	56.4 (4.8)	61.2 (9.6)	48.9 (5.9)	47.7 (5.8)	47 (9)
GrimAge	58.4 (5.6)	60.8 (7.6)	64.6 (4.6)	61.1 (4.3)	64 (9)

**Table 28:** showing the mean (and standard deviation) chronological, HorvathAge, PhenoAge and GrimAge for epidemiological studies.

Including the Hertfordshire Cohort Study (HCS), the Irish Longitudinal Study on Ageing (TILDA)<sup>143</sup>, The National Survey of Health and Development (NHSD)<sup>144</sup> and a study investigating black South African males (Cronje and colleagues, 2021)<sup>248</sup>

This shows that, except for The Irish Longitudinal Study on Ageing (TILDA)<sup>143</sup>, there is a tendency for all clocks, but particularly PhenoAge, to be routinely underestimated in adults of a similar age. This, again, supports our approach to using Z-scores rather than raw values in downstream analyses.

#### **4.2.3 GrimAge acceleration and muscle outcome in males**

One of the potential utilities of epigenetic age acceleration is as a biomarker to predict future phenotypes. We observed a significant sex-specific association between GrimAge acceleration and gait speed at the HBS17 follow-up ( $\beta=-0.04$  m/s (-0.09,-0.00),  $p=0.05$  in sex-stratified models adjusted for age, height, BMI, social class, physical activity, prudent diet, ever smoked regularly and alcohol consumption) and grip strength at the EPOSA follow-up ( $\beta=-1.25$  kg (-2.24,-0.26),  $p=0.01$  in sex-stratified models adjusted for age, height and BMI).

In contrast to our study (in which there were no significant associations with first generation clocks), previous cross-sectional analyses in other cohorts have found associations between HorvathAge acceleration and gait speed in the Lothian cohort<sup>140</sup> ( $\beta= -0.05$ m/s,  $p<0.01$ ) and grip strength in a Scandinavian twin cohort ( $\beta= -5.3$  Newton-meters (kg per m/s<sup>2</sup>), Standard Error= 1.9,  $p=0.01$ )<sup>142</sup>, although both these studies pre-dated the advent of the second generation clocks and used 450k arrays only. In the Lothian cohort<sup>140</sup>, it should also be noted that the findings were cross-sectional and sex-adjusted rather than for grip strength at EPOSA follow-up and sex-specific for the HCS. Also, grip strength in this study was only assessed for the right hand<sup>140</sup>. Additional differences between the Scandinavian Twin study<sup>142</sup> and our HCS study include the fact that they used Newton-meters instead of kilograms to measure grip strength and that the study population was originally selected to include only female twin pairs who were discordant in their use of hormone replacement therapy (and thus different to our cohort, and our finding in males alone).

Latterly, studies examining GrimAge acceleration and PhenoAge acceleration have been published which have echoed our findings.

The TILDA study including 490 community dwelling older adults in Ireland, demonstrated significant cross-sectional relationships between GrimAge acceleration and grip strength ( $\beta=-0.60$  kg (-1.10,-0.1)<sup>143</sup> adjusted for age, sex and height) , and walking speed ( $\beta=-3.74$  cm/sec, (-6.03, -1.44;  $p < 0.001$ )<sup>143</sup> adjusted for age, sex, height, cell count, BMI, social class, smoking and physical activity).

These, sex-adjusted, findings are very similar to our findings in the HCS; however, it would be interesting to see the result of sex-stratified analyses to identify whether a similar pattern, of associations observed primarily in men, was present. Similar to our study, no associations with first generation clocks were identified. It should be noted that, rather than recording the maximum grip strength from 6 attempts (3 from each hand), in the TILDA study grip strength was recorded as the mean of 4 attempts (2 from each hand)<sup>143</sup> which may affect the comparison of the grip strength analyses between the two studies.

A meta-analysis by Maddock and colleagues<sup>144</sup> incorporated data from TwinsUK, National Child Development Study (NCDS) and the National Survey of Health and Development (NSHD). We will focus on the latter, as this is study of older adults, of a similar age to the HCS, who were assessed at 53 years and 69 years of age. In this group epigenetic clocks were ascertained at baseline (53 years) and relationships with grip strength were investigated cross-sectionally and longitudinally. In the NSHD (and in males alone) associations between grip strength aged 69 and GrimAge acceleration from baseline ( $\beta=-0.22$  kg (-0.37,-0.06),  $p=0.01$ ) (a similar effect size to our  $\beta=-1.25$  kg finding in the HCS, and over a similar period from baseline age acceleration measure to grip strength at EPOSA follow-up) and change in grip strength (1-year increase in GrimAge acceleration associated with a -0.25kg (-0.37, 0.14) loss in grip strength over 13 years of follow-up<sup>144</sup>. Why the GrimAge acceleration association should particularly be observed in males is not quite clear, but may be related to male-specific changes in the plasma proteins from which the GrimAge clock was created (adrenomedullin, beta-2-microglobulin, cystatin C, growth differentiation factor-15, leptin, plasminogen activator inhibitor-1, and tissue inhibitor metalloproteinase-1<sup>126</sup>) or indeed due to the effect of smoking which is incorporated into the GrimAge clock itself. The latter may be highly relevant in the HCS, as men were more likely to have ever smoked than women.

In contrast to our study, significant cross-sectional associations between grip strength and PhenoAge acceleration were seen ( $\beta=-0.12$  kg (-0.22,-0.02),  $p=0.03$ ), however, this was not robust to adjustment for covariates (including sex, BMI, height, smoking status and social class). Sensitivity analyses were performed to examine the effect of adjusting for white cell composition (as done by McCrory and colleagues in TILDA<sup>143</sup>). This is due to the theory that cell composition incorporation captures extrinsic epigenetic ageing and adjusting for (or excluding the effect of) age-related changes in cell composition captures intrinsic ageing. In our study we did not include cell composition sensitivity analyses. This may be included in future work; however, it is worth noting that Maddock and colleagues did not find a substantial effect of cell composition adjustment<sup>144</sup>.



#### **4.2.4 Epigenetic age acceleration and increased tissue measures in females**

For some parameters of body composition we observed a trend towards increased epigenetic age acceleration being associated with increased adipose and muscle tissue measures.

In a large study of Caucasian females (n=2758) in the United States with a mean age of approximately 57 years (with a range of approximately 40-80 years, being substantially broader than our HCS study), BMI was found to be significantly positively associated with PhenoAge acceleration, such that greater age acceleration was associated with higher measures of adiposity (BMI>35 vs BMI 1.5-24.9,  $\beta=3.15$  years, p for trend <0.001)<sup>249</sup>. Although these analyses were performed in quartiles of BMI (rather than a continuous variable) they support our finding that higher epigenetic age acceleration was associated with higher total fat mass in females in the HCS ( $\beta=2227$ grams, p=0.02), although our finding was for GrimAge acceleration and not PhenoAge acceleration. A similar finding was observed with PhenoAge acceleration in males, however, sensitivity analyses demonstrated that this was driven by an outlier for PhenoAge acceleration (**Appendix 26**).

The finding with GrimAge could be due to the constituent parameters which were used to devise the clocks. C-reactive protein (CRP), glucose and leukocyte count were used in devising the PhenoAge clock and have been associated with adiposity<sup>250-255</sup>. Leptin is one of the proteins used to form the GrimAge clock, and is, itself, produced by adipose tissue and associated with this element of body composition<sup>256,257</sup>. Indeed, the reason for the association between greater GrimAge acceleration and greater appendicular lean mass in females ( $\beta=119$  grams, p=0.048) may be due to fat infiltrated muscle (via the association with leptin), which would appear enlarged but may not be of as high quality. The regression coefficient for this finding is also very small and this finding would certainly require investigation in other cohorts.

#### **4.2.5 Associations of epigenetic age acceleration with bone outcomes**

Very few significant associations were observed between epigenetic age acceleration and bone outcomes and the paucity of a literature on this subject may be due to publication bias with just a single previous study by Fernandez-Rebollo and colleagues<sup>147</sup> addressing this association.

The significant cross-sectional associations we did observe were solely in females via DXA with HorvathAge acceleration ( $\beta=0.02$ g/cm<sup>2</sup>, p<0.05 at baseline and EPOSA,  $\beta=0.02$ g/cm<sup>2</sup>, p<0.02 for HBS17) and PhenoAge acceleration ( $\beta=0.02$ g/cm<sup>2</sup>, p<0.03 at baseline and EPOSA) associated with total femoral neck BMD at multiple time points and HR-pQCT scanning modalities with HorvathAge acceleration associated with cortical thickness ( $\beta=35.6$   $\mu$ m, p<0.02). This suggests that greater age

acceleration is associated with beneficial bone outcomes (thicker cortices and greater bone mineral density). Before placing too much weight on this finding it is worth noting that the effect sizes were modest; however, there are three possible explanations for these findings.

Firstly, there are data to suggest that epigenetic age acceleration remains fairly constant from early adulthood. Theoretically, a higher age acceleration at this early point of the lifecourse may be advantageous and allow an individual to reach a higher peak bone mass in the fourth decade. If the epigenetic age acceleration remains constant from that point, then a higher bone density (and cortical thickness) would be associated with a higher epigenetic age acceleration measure. This is highly speculative and future studies in young adults (and across the lifecourse) will be required to delineate this association.

Secondly, as hypothesized in the summary discussion, it is possible that, in females, the relationship between higher GrimAge acceleration and higher change in femoral neck BMD is being mediated by adiposity, as we found a similar relationship between higher GrimAge acceleration and higher fat mass (see **Figure 26**). This is unlikely to be the sole contributor to the relationship for two main reasons. Primarily, because it is increasingly accepted that adiposity is detrimental to the health of bone for hormonal, inflammatory and metabolic reasons<sup>258,259</sup>, but also because our models included body mass index as a covariate which should capture adiposity. Thirdly, although bone mineral density (and bone microarchitecture) outcomes are primarily utilised in assessing osteoporosis in clinical practice, they are also influenced by osteoarthritis. Indeed, studies show an increased bone mineral density and trabecular density in osteoarthritis patients<sup>260,261</sup>. In the case of our HCS findings, it may be that we are observing an association of increasing osteoarthritis with increasing epigenetic age acceleration. This possibility will be the subject of future research as stated in the 'Future Work' section of this discussion.

Additionally, in terms of change in bone outcomes, GrimAge acceleration was associated with a significantly greater loss of total femoral neck BMD for males across approximately 17 years of follow-up (between HCS baseline and HBS17) and females across approximately 5 years of follow-up (between EPOSA and HBS17). The finding that loss of trabecular density was associated with greater GrimAge acceleration ( $\beta=-1.09\text{mg}/\text{cm}^3$ ,  $p<0.02$ ) and HorvathAge acceleration ( $\beta=-1.17\text{mg}/\text{cm}^3$ ,  $p<0.01$ ), and that we independently found loss of trabecular density to be associated with fracture is note-worthy and may shed some insight onto the biological ageing of bone microarchitecture change. Indeed, a previous study from our group identified cross-sectional trabecular density as part of a particular phenotype of bone microarchitecture which was prone to fracture<sup>262</sup>. It may therefore be that epigenetic age acceleration (and particularly GrimAge) may provide some insight into future loss rates of bone density in the trabecular compartment and at the femur. Alternatively, as explained above, it may be a signature of health earlier in the lifecourse, the effect of adiposity or increasing joint degeneration and osteoarthritis.

The previous study by Fernandez-Rebollo and colleagues was performed in a much smaller group of 32 osteoporosis participants and 16 controls and only utilizing first generation clocks (including HorvathAge)<sup>147</sup>. Although they found a strong correlation between the epigenetic ages and chronological age (as expected given the original design of the first-generation clocks) they found no correlation between epigenetic age and osteoporosis. The lack of an association was hypothesized to be due to the fact that epigenetic age was measured in blood, thereby lacking the facets of tissue-specificity. This is supported by del Real and colleagues who had investigated the epigenetic age of skeletal tissue in patients with osteoporosis versus osteoarthritis<sup>152,263</sup>. They showed that the epigenetic age of bone tissue (acquired from bone fragments) did not display accelerated ageing. However, age acceleration was observed in bone-derived mesenchymal stem cells, suggesting that age acceleration in progenitors has a greater influence on phenotype than that seen in mature tissue. A recognized limitation of these analyses was the lack of PhenoAge and GrimAge analyses<sup>264</sup>.

### **4.3 Epigenome-wide association studies (EWAS)**

Epigenome-wide analyses of differential methylation were performed for cross-sectional associations with maximum grip strength and total femoral neck bone mineral density. The key findings for this programme of work were that there was a consistent association between maximum grip strength and differential methylation at cg00960509, lying in a CpG island associated the 5' end of the gene *ECE1* on chromosome 1. A significant association was found between grip strength and some gene ontologies, particularly the purine catabolic biological process. For total femoral neck bone mineral density there were no significant associations with individual CpG sites. However, cg02389067, associated with the *GNA13* gene, consistently appeared in the top 5 CpG sites for each model, and was also implicated (via enrichment analysis) in the significant association with the regulation of the actin cytoskeleton. The Phospholipase D signalling pathway was also significantly associated with total femoral neck BMD and there were some supporting associations with human phenotype ontologies including hip pathologies and biconcave vertebral bodies, indicative of vertebral fractures.

#### **4.3.1 Maximum grip strength EWAS**

##### **4.3.1.1 Endothelin converting enzyme-1**

A negative association was observed between methylation at cg00960509 and maximum grip strength in this group of community dwelling older adults (log<sub>2</sub> fold-change = -0.0006, adjusted p-value = 0.02). Higher methylation at this CpG site in the promoter region of *ECE1*, would potentially

lead to reduced expression of *ECE1*, and was associated with lower maximum grip strength (see **Figure 35**). The biological plausibility of this finding is examined below.

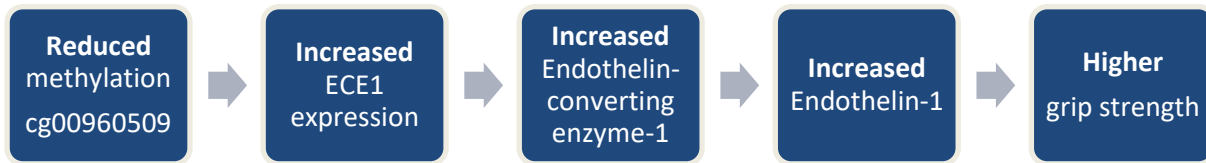


**Figure 35:** Schematic demonstrating the flow between an association between reduced methylation at cg00960509 and higher grip strength.

#### 4.3.1.1.1 Biological plausibility

The *ECE1* gene codes for endothelin converting enzyme 1; a 770 amino acid metallopeptidase which hydrolyses the 21-Trp-|-Val-2 bond in ‘big endothelin’ to produce endothelin-1<sup>265</sup>, and is located in the lysosomal membrane<sup>266</sup> and endosome<sup>267</sup>. Diseases associated with mutations in *ECE1* include Hirschsprung’s disease (a neurological condition of the bowel primarily seen in infants), cardiac defect, autonomic dysfunction and an increased risk of coronary artery disease<sup>268</sup>.

Endothelin-1 (the product of endothelin-converting enzyme 1) is one of a family of ‘endothelins’<sup>269</sup> produced by the vascular endothelium and vascular smooth muscle cells and act on endothelin receptor A (ETA) and B (ETB1 and ETB2) located on the vascular smooth muscle cells and endothelium and also on cells in other tissues including osteoblasts and adipocytes<sup>270</sup>.

Endothelin-1 is highly active in controlling vascular blood flow on the vascular endothelium. It promotes potent vasoconstriction (via ETA and ETB2)<sup>270</sup>; however it also stimulates the induction of endothelial nitric oxide synthase (eNOS or Nos3) leading to nitric oxide (NO) production with resultant profound vasodilation<sup>271,272</sup>.

Grip strength involves coordinated and sustained contraction of the muscles of the forearm and, as a form of exercise, we must consider the changes which occur in skeletal muscle blood flow in response to exercise.

Exercise leads to an increased need for skeletal blood flow. For this reason, one of the very first skeletal muscle vascular responses to exercise (which occurs very quickly, within 5 cardiac cycles<sup>273</sup>) is nitric oxide initiated vasodilation<sup>274</sup>. Additionally, noradrenaline is released which increases cardiac output and, together with endothelin-1<sup>275</sup>, leads to splanchnic vasoconstriction<sup>276</sup>. This vasoconstrictive effect is blunted in skeletal muscle blood vessels by a process of ‘functional

sympatholysis', which maintains relative, local vasodilation (involving nitric oxide<sup>277</sup> and endothelial hyperpolarization) and thus redistributes blood flow to the muscles<sup>278</sup>.

In the elderly, this local vasodilatory response may be impaired, as nitric oxide is scavenged by reactive oxygen species, leading to 45% lower nitric oxide contribution towards skeletal muscle blood flow during exercise in the elderly compared to younger adults<sup>279</sup>. Thus, in the elderly there is lower reserve in the action of nitric oxide to produce vasodilation<sup>280,281</sup>, and thus, if endothelin-1 production was reduced, there would be lower stimulation of ETB1 receptors and nitric oxide production in skeletal muscle would drop further. This, together with the endothelin-1 induced splanchnic vasoconstriction (and redistribution of blood flow to the muscles) supports our finding that lower methylation at cg00960509, via increased production of endothelin-1, could lead to better muscle performance and increased grip strength in the HCS (see **Figure 36**).

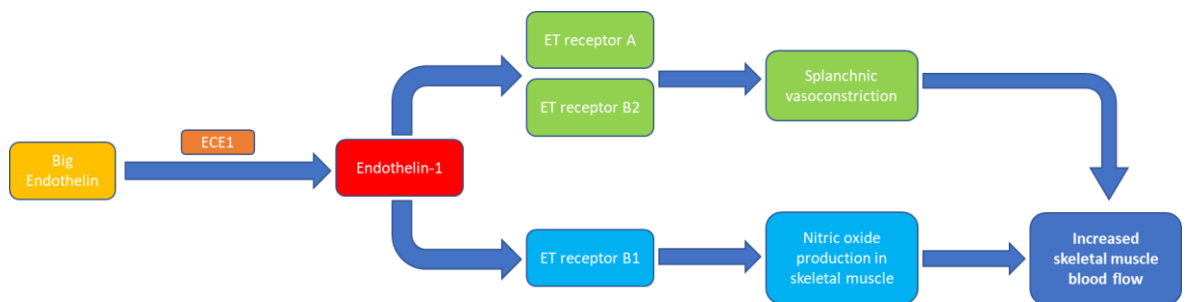


**Figure 36:** Schema depicting the hypothesised mechanism of association between lower methylation at cg00960509 and higher grip strength.

ECE1 = endothelin converting enzyme-1, ET = endothelin

This theory is supported by the finding in a rat model (of obesity) subjected to an endurance exercise programme there was a significantly greater RNA expression of *ECE1* (determined by RNA-sequencing) in the arterioles of the gastrocnemius muscle compared to a sedentary control group<sup>282</sup>. Similar to our finding, this suggests that higher endothelin-1 may be indicative of good muscle health.

The above is simply a hypothesis and comes with the caveats that the effect size in the differential methylation analyses was small, the experimental design was cross-sectional and the tissue analysed was whole blood and not muscle, and that the vascular effects in vivo for humans is still a matter of debate<sup>275</sup>.

Indeed, the scale of the methylation change in this association is very small with a 0.0003% increase in methylation (beta-value) for each kilogram increase in grip strength, and a substantial limitation is the use of a blood-based proxy for measuring a muscular outcome (when muscle tissue would be superior). In future work, it will be important to replicate this finding using an alternative technology including RNAseq or pyrosequencing.

However, we have shown that there is a plausible, biological mechanism which could explain the association observed via EWAS.

#### **4.3.1.1.2 GWAS and EWAS associations**

The *ECE1* gene has been implicated in a number of health and disease states via Genome-Wide Association Study and other methylome EWAS.

Previous GWAS associations of single-nucleotide polymorphisms (SNPs) in *ECE1* include height (for 250,000 individuals<sup>283</sup> and 450,000 individuals<sup>284</sup> of European ancestry). The latter is relevant when considering that height is strongly associated with grip strength across the lifecourse<sup>57,285,286</sup> and that short stature is associated with accelerated loss of grip strength<sup>57</sup>. However, it is unlikely that the association between methylation of cg00960509 was purely confounded by height in this study as the association persisted (despite some attenuation) when adjusting for height and weight-for-height residual.

Associations with lean (muscle) body mass were observed in a GWAS of 150,000 individuals of European ancestry<sup>287</sup> which supports the association observed in the EWAS of maximum grip strength in the HCS.

Other GWAS associations include levels of alkaline phosphatase<sup>288,289</sup>, basophil count<sup>290,291</sup>, chronotype (“ease of getting out of bed”)<sup>292,293</sup> and longevity (a case control study of individuals surviving at or beyond the age corresponding to the 90th/99th survival percentile).

Previous EWAS findings include associations between the degree of methylation at cg00960509 and HIV infection<sup>294</sup> and age (from birth to late adolescence)<sup>295</sup> (in whole blood samples). The association with age is interesting; however, may not be entirely relevant as the age range of the participants in that study (paediatric) compared to the HCS (older adults) is markedly different, and EWAS model 2 included age as a covariate which should account for any confounding effect.

Differential methylation at cg00960509 in saliva samples has been demonstrated between individuals who experienced child abuse and age-matched controls<sup>296</sup>.

Additionally, differential methylation of cg00960509 was shown to exist between blood and buccal samples<sup>297</sup>, emphasising the tissue-specific nature of methylation. Indeed, it is important to consider that the findings we see in methylation analysis of whole blood are associated with the methylation seen in white blood cells and, therefore are not expected to be directly associated with muscle-specific processes.

#### **4.3.1.2 SDK1**

We also observed a significant association between methylation at cg08073934 (log<sub>2</sub> fold-change = 0.0004, adjusted p-value = 0.02); however, this was only seen in model 2 (adjusted for age, sex, cell composition and array) and did then not appear in the list of the CpG sites with the lowest p-values. The reason for this change in level of association may be explained by previous GWAS and EWAS relating to the associated gene; *SDK1* and CpG site respectively.

As background, *SDK1* is the gene encoding the protein side-kick-1 which is a 2213 amino acid, homodimer, adhesion molecule and part of the immunoglobulin superfamily. It is located in the plasma membrane, and disease associations with the gene include brachydactyly.

Previous methylome-wide association studies (EWAS) have identified associations between cg08073934 and maternal body mass index (BMI) and obesity<sup>298</sup>, with similar body anthropometry associations with BMI adjusted waist circumference in a GWAS of asthma and obesity in 450,000 members of UK Biobank<sup>299</sup> and a global, trans-ancestral study of childhood obesity<sup>300</sup>. These associations with body composition outcomes suggest that, in our study, *SDK1* was simply a confounder for the association between body anthropometry and grip strength, which is why the association was not replicated in sensitivity models adjusting for height and weight for height residual.

This is also the likely explanation for the association being absent in sensitivity model 4 which additionally adjusted for smoking status, as *SDK1* has been associated with smoking status<sup>284,301,302</sup> and smoking initiation<sup>302-304</sup> in numerous GWAS.

The association with cg08073934 was therefore a likely confounder.

### 4.3.1.3 Pathway and gene ontology for maximum grip strength EWAS

The list of most significant CpG sites was not significantly enriched for pathway analysis; however, there were significant gene ontology associations with purine catabolism, p-type calcium transport and human phenotypes relating to homocysteine, aspartate, vitamin B and methionine metabolism.

#### 4.3.1.3.1 Purine catabolism

Purines are acquired through dietary sources (including meat, liver, kidneys, lentils) and constitute the nitrogenous bases from which DNA is formed. They have key roles as energy sources, coordinators of cellular growth and metabolic signals. They are metabolized via the purine metabolic pathway (see **Figure 37**) to form xanthine and latterly, the waste product uric acid.

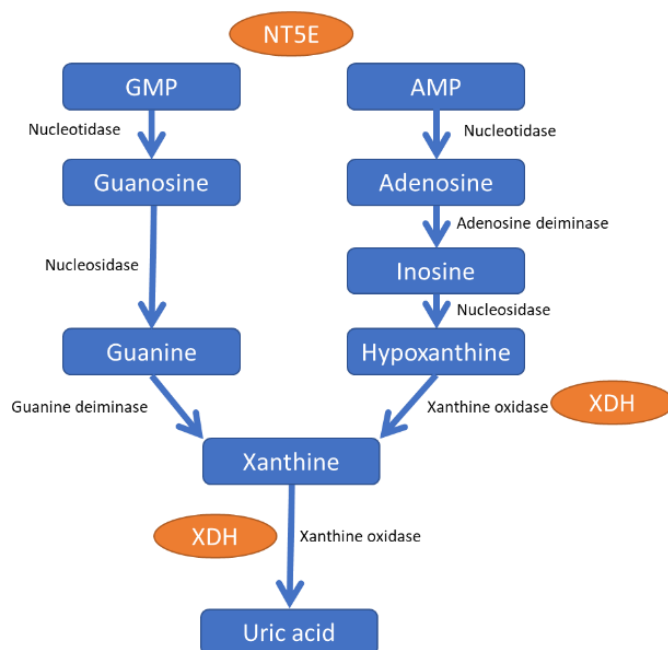


**Figure 37:** The purine metabolic pathway.

Products are in blue boxes, enzymes in black script and the products of the genes which drove the association with the biological process gene ontology are in orange (XDH – xanthine dehydroxylase, NT5E – nucleotidase ecto-5)

It is worth considering that the gene ontology ‘purine ribonucleotide catabolic process’ is fairly general, non-specific ontology defined as ‘The chemical reactions and pathways resulting in the breakdown of any purine ribonucleoside, a nucleoside in which purine base is linked to a ribose (beta-D-ribofuranose) molecule’<sup>305</sup>. The two genes which drove the association with the pathway are TE5 coding for the protein nucleotidase ecto-5 which sits in the cell membrane and catalyses the conversion of extracellular nucleotides to membrane-permeable nucleosides, ready to feed into



the purine metabolic pathway, and XDH coding for xanthine dehydroxylase, which lies at the other end of the pathway and can be converted to xanthine oxidase to produce uric acid. However, although this is a broad ontology, there is a possible reason for the association with grip strength.

The waste product of the purine metabolic pathway is uric acid, which in physiological circumstances has beneficial anti-oxidant effects and higher levels of uric acid have been associated with greater hand grip strength in a group of older individuals in South Korea<sup>306</sup> (the high serum uric acid tertile had a significantly higher mean grip strength than the lowest serum uric acid tertile ( $\beta=1.017$ , 95% CI 0.115 to 1.920)). This finding is supported by work in nonagenarians in Tuscany ( $\beta=1.24\pm SE 0.43$ ,  $p=0.005$ )<sup>307</sup> and a group of community dwelling older adults in Japan<sup>308</sup>. Thus, it may be that the association between uric acid and grip strength in these epidemiological studies of older adults is being driven by altered mechanisms and gene expression within the process of purine catabolism.

#### **4.3.1.3.2 P-type calcium transporter activity**

The other biological process which was significantly highlighted by gene ontology analysis was that of P-type calcium transporter activity. This was due to the presence of the *ATP2B2* and *ATP2C2* genes in the extended list of those CPG sites with the lowest 100 p-values.

*ATP2B2* encodes the protein ATPase plasma membrane  $Ca^{2+}$  transporting 2 which is one of a family of P-type primary ion transport ATPases that move calcium ions against concentration gradients and are involved in maintaining calcium homeostasis. They are known to play a role in platelet homeostasis and salivary secretion and genetic defects in the gene are associated with congenital deafness. Previous GWAS have demonstrated associations with height<sup>284</sup> and testosterone level<sup>309</sup>, the latter in a group of 190,000 European men and women, in which two SNPs in the *ATP2B2* gene were found (rs573833-T, rs7618363-C). There is known to be an association between testosterone and muscle ageing with systematic reviews demonstrating positive effects of testosterone on sarcopenic outcomes<sup>310,311</sup>; however, it is likely that the association with height is what drove the association in our particular EWAS as model 2, in which this particular gene ontology analysis was performed, did not include height as a covariate.

*ATP2C2* is a gene encoding ATPase secretory pathway  $Ca^{2+}$  transporting 2, and ATP driven pump which moves calcium ions across the membrane of the Golgi apparatus. There is no direct relationship to musculoskeletal health with this gene or protein, and previous GWAS have shown SNPs in *ATP2C2* to be associated with first cannabis use<sup>312</sup>.

Although calcium transport is central to muscle function, this is primarily via L-type calcium channels<sup>313</sup>.

#### **4.3.1.3.3 Human phenotype ontologies**

Some associations with particular human phenotype ontologies were observed, including those relating to homocysteine, aspartate, vitamin B, methionine metabolism and megaloblastic anaemia (driven by the gene *MTRR*), ophistonus (by *VPS53*) and dysautonomia (by *ECE1*). However, each of these phenotypic associations reached significance due to the presence of a solitary gene within an extended list of genes from the EWAS suggesting that the associations are weak and prone to artefact.

#### **4.3.2 Total femoral neck bone mineral density EWAS**

The main CpG site of interest which was highlighted by the EWAS of total femoral neck BMD was cg02389067, located in a CpG island in the promoter region at the 5' end of *GNA13* on chromosome 17. This did not reach the specified level of statistical significance; however, it was constantly observed in the top 5, most significant CpG sites in each EWAS model and is also implicated in the significantly associated pathways on enrichment analysis including The Phospholipase D signalling pathway and the regulation of actin cytoskeleton.

##### **4.3.2.1 Pathway analyses**

Before exploring the associated pathways, it is important to map out some basic elements of bone cell function. Bones are constantly undergoing a process of formation and breakdown with osteoblasts responsible for the bone production and mineralization and osteoclasts (which share many common attributes with macrophages) responsible for bone resorption. Osteoclasts have two states in which they can exist, migratory (during which they move to a site suitable for resorption) and stationary (during which resorption occurs). Both these states require specific and coordinated changes from the actin cytoskeleton and in the resorptive state this necessitates the formation of an actin ring and ruffled border which provides a sealed area around the bone (similar to a mouth) so that the lytic enzymes used to break down the bone remain localised and do not extrude into the surrounding extra-cellular matrix, leading to uncontrolled bone resorption<sup>314</sup>. As such, it is clear that the actin cytoskeleton plays a vital role in bone homeostasis.

##### **4.3.2.1.1 Regulation of the actin cytoskeleton**

Due to the inclusion of the following genes: *GNA13*, *PDGFD*, *RRAS2*, *ARHGEF4*, *ITGA7*, *BAIAP2* in the extended list of CpG sites associated with total femoral neck BMD, the pathway of regulation of the actin cytoskeleton was found to be significantly associated on enrichment analysis.

Actin, the most abundant protein in eukaryotic cells, constitutes a major part of the cytoskeleton and is found in two conformational states, G-actin (monomeric globular actin) and F-actin (polymeric fibrous actin). Actin binds to other proteins to form filamentous actin, and these filaments form two major structures within cells; bundles and networks, and are crucial to the fluctuating changes required by cells for cell division, filopodia formation and locomotion<sup>315</sup>.

Alterations in the actin cytoskeleton can be stimulated by chemokines, cytokines and fibronectin but also via G-protein coupled receptors (GPCRs) which operate via G-proteins. These are heterotrimeric proteins composed of  $\alpha$ ,  $\beta$  and  $\gamma$  subunits and are found in every tissue. GPCRs are bound by a ligand on the membrane surface and the  $\alpha$ -subunit then stimulates downstream mediators (via the Ras superfamily) to manifest intracellular effects including actin cytoskeleton reorganization, cell migration, phospholipase D and other downstream effects<sup>316</sup>. As can therefore be seen, the gene *GNA13*, which codes G-protein  $\alpha$ -subunit 13 ( $G\alpha13$ ) is integral to both pathways associated with femoral neck BMD. It has been demonstrated that  $G\alpha13$  regulates osteoclast states with downstream activation of RhoA stimulating podosome formation of the actin cytoskeleton to enable migration<sup>317</sup>, and RAC stimulating the stationary, resorptive state<sup>318</sup>. Murine studies support a key role for  $G\alpha13$  as,  $G\alpha13$  knockout animals display a severe osteoporotic phenotype, with reduced BMD, increases in osteoclast numbers and enhanced osteoclast activity<sup>319</sup>, and increased cathepsin K protease secretion<sup>320</sup>.

A previous study, conducted by Liu and colleagues, set out to specifically examine pathways linked to over 300,000 significantly associated loci in a genome-wide study of hip BMD<sup>321</sup>. They found that, together with T cell receptor and immunological pathways, the regulation of the actin cytoskeleton was a pathway that was particularly enriched in the loci associated with hip BMD, thus supporting our finding.

Genes related to actin cytoskeleton dynamics, including the *Filamin B (FLNB)* gene, have been previously implicated in bone mineral density skeletal diseases<sup>322</sup>. Filamin binds to actin providing a bridge which allows two actin filaments to join at varying angles. Murine studies have demonstrated expression of *FLNB* in embryonic vertebrae and particularly vertebral segmentation<sup>323</sup>. *FLNB*-knock out mice develop aberrations in skeletal microvasculature and bone development<sup>324</sup>, and develop profound skeletal abnormalities including scoliosis, skull malformation and fusion of the ribs and vertebrae<sup>325</sup>. In fact, there are calls amongst the community suggesting that Filamins may be a fruitful avenue for skeletal therapeutics<sup>326</sup>.

#### 4.3.2.1.2 Phospholipase D signalling pathway

The KEGG pathway enrichment analysis demonstrated an association with the Phospholipase D signalling pathway due to the presence of genes; *GNA13*, *PDGFD*, *AKT3*, *RRAS2*, *DNM2*.

Phospholipase D (PLD) is a protease enzyme which converts phosphatidylcholine to phosphatidic acid. It is activated by cytokines, hormones, growth factors and neurotransmitters via the cAMP, Ras, P13k -Akt and calcium transmission pathways and sits in the middle of the PLD signalling pathway<sup>327</sup>. PLD is expressed by osteoblasts and has been shown to peak at the onset of mineralization, suggesting that this plays a role in osteoblast maturation and stimulates mineralization of bone<sup>327</sup>. This finding is supported by the fact that PLD inhibition via halopemide, and PLD knock-out mice have reduced and less efficiently mineralizing osteoblasts<sup>327</sup>.

Not only is the whole pathway enriched for genes associated with total femoral neck BMD but individually, the genes demonstrate some associations with phenotypes of bone health. The key role of *GNA13* has already been discussed, but, also at the top of the PLD signalling pathway is the protein dynamin (produced via expression of *DNM2*) which plays a significant role in endocytosis by 'snipping' the final link of a vesicle with the phospholipid membrane. Dynamin has been shown to alter bone homeostasis, as inhibition of dynamin (by the drug *dynasore*) leads to inhibition of bone resorption by osteoclasts<sup>328</sup>. The *PDGFD* gene, encoding Platelet Derived Growth Factor D has been implicated in the initiation of bone formation<sup>329,330</sup>, the *RRAS2* gene which codes Ras-Related Protein R-Ras2 regulates the proliferation of osteoprogenitor cells, also stimulating bone formation<sup>331</sup> and the *AKT3* product plays a part in the signalling regulation of osteoporosis<sup>332</sup>.

It must be recognised that the pathway associations observed in our study related to the expression of the above genes and pathways in blood, rather than bone, and may be indicative of systemic nuances rather than findings specific to bone. Nevertheless, the associations presented above are at the very least biologically plausible, and future research will be required to further explore this area.

#### 4.3.2.2 Gene ontology

The most significantly associated human ontologies we observed included hip contracture and limited hip movement, associated with the anatomical location of the femoral neck BMD which was the phenotype of interest. It is possible that the studies on which the phenotype ontology were based were in fact picking up features of bone mineral density associated with the phenotype of interest. Truncal obesity was also included, and there are known associations between obesity and bone mineral density, even demonstrated within the HCS<sup>333,334</sup>.

It is also supportive that biconcave vertebral bodies were a human phenotype of association, as these alterations in morphology are likely indicative of vertebral fractures which are known to be epidemiologically associated with bone mineral density at the femoral neck and hip<sup>335,336</sup>.

#### 4.4 Strengths and weaknesses

There are a number of strengths to this project. The research visits and measurements were performed by trained fieldworkers (including myself) according to strict protocols and standard operating procedures providing accurate measures for downstream analyses.

The longitudinal nature of the cohort with outcomes recorded at multiple timepoints provides an important and relatively unique insight into the ageing phenotype in a group of community-dwelling older adults in the UK. The longitudinal HR-pQCT dataset is particularly unusual with the majority of previous studies focusing on wider age ranges (across the lifecourse) or either side of the menopause (in pre- and post-menopausal females).

The ability to combine the extensive musculoskeletal phenotyping with methylation and genotypic datasets leads to a broad range of research insights, and the fact that these ‘-omic’ data are available from baseline (1998-2004), allows the examination of their ability to predict future phenotypes.

However, this project has some weaknesses. In the examination of the relationship between change in musculoskeletal phenotype and fracture, the size of the cohort hindered our ability to perform site-specific fracture analyses and, in epigenome-wide analyses may have limited our power to observe some associations (particularly in the bone outcomes where the effect sizes were small).

The constitution of the Hertfordshire Cohort study is Caucasian and of a fairly narrow age range, which may impact on the generalisability of our findings. Indeed, the fact that participants had to be able to attend the research visits in person demanded a certain degree of health and mobility in order to take part. This may have introduced survival bias as only those who were survived from 1999-2004 to 2011-12 and 2017 were included and led to a healthy cohort effect. In addition, although our recorded epigenetic ages are comparable to other studies (see **Table 28**)<sup>143,144,248</sup>, it is possible that individuals involved in all studies are more involved and may therefore demonstrate a healthy selection bias. It is possible that the analyses were subject to specification error (with regard to the statistical models chosen) despite the specification checks described in the methods

section (including assessment of the linearity of relationship with a continuous outcome, normal distribution of residuals and the constant variance assumption of the residuals).

The analyses examining the relationship between change in musculoskeletal phenotype and fracture odds were hampered by the fact that we have a prevalent (rather than incident) fracture history.

Due to a paucity of significant CpG site associations from EWAS analyses, we used a selection of CpG sites for downstream, enrichment analyses which included non-significant CpG sites. The results of these analyses are purely exploratory.

There were also some potential technical weaknesses in the project, as described below.

In analyses including longitudinal change in DXA-measured bone mineral density, it should be noted that scans at EPOSA and HBS17 were performed on two different scanners which, despite capable technicians and rigorous standard operating procedures, may have introduced a degree of error. However, it is encouraging that the observed difference in bone assessments between the two scanners is minimal<sup>337</sup>.

It is possible that using data from 450k and 850k methylation arrays may have introduced a degree of measurement error; however, the use of Z-scores should have mitigated against a subsequent deleterious effect. The clocks measured the age of the DNA from whole blood leukocytes and, in order to gain a more accurate insight, it may have been necessary to measure the age acceleration of bone and muscle samples. Of course, this was not possible or appropriate in this cohort, and, if age acceleration is to be used as a biomarker in clinical practice, then blood will be a far more practical and available tissue.

In addition, the issue of tissue specificity has been previously alluded to, by which our results were more likely to highlight systemic factors associated with the phenotype of interest (metabolic or inflammatory processes) than those mechanistically related to muscle or bone, as the tissue used for methylation analyses was whole blood (leukocytes) and not muscle or bone. However, despite these limitations, we have identified individual marks, gene ontologies and pathways which are biologically plausible in their association with our musculoskeletal phenotypes of interest.

## **4.5 Overall implications of this research**

The main contributions of this work to the wider community are three-fold.

Firstly, the identification of GrimAge as a significant predictor of future muscular health is a relevant finding and has been replicated in other cohorts. It may be possible, with the development of novel methylation clocks, or biomarkers from alternative 'omic' datasets to produce a more accurate

prediction tool which could identify those at risk of adverse muscular ageing and improve their trajectories and risk of morbidity and mortality.

Secondly, although the findings from the EWAS' are preliminary, the identification of novel biochemical and physiological targets (e.g. *ECE1*) and pathways (e.g. regulation of the actin cytoskeleton), hold the potential to unlock fresh understanding of the diseases of musculoskeletal ageing and possibly provide novel interventions to promote healthy ageing and extended quality of life.

Thirdly, the precise description of change in the musculoskeletal system with age, and particularly using specialised technologies like HR-pQCT can provide new insights into how musculoskeletal ageing occurs and map responses to interventions in the future.

#### **4.5.1 Findings in relation to osteoporosis**

As previously stated, osteoporosis and fragility fractures are common in the ageing population and associated with significant morbidity and mortality. The findings of this thesis have the potential to improve our understanding of the disease and the pathology underlying it.

DXA-measured BMD is the primary imaging modality for assessing osteoporosis in clinical practice; however, it is limited to two dimensions. Bone strength is determined by three parameters; size, shape and architecture<sup>338</sup>. The two dimensions of DXA provides measures of bone size and shape but not bone microarchitecture. In describing the change in HR-pQCT over approximately 5 years, and in a specific cohort of the UK population, we are able to contribute to the overall understanding of how bone architecture (and therefore bone strength) change as we age.

Our EWAS findings for bone mineral density, although limited by a paucity of statistically significant findings and that the tissue used for methylation array was blood and not bone, did imply that the regulation of the actin cytoskeleton was associated with bone mineral density. This highlights the actin cytoskeleton as a potential avenue for further osteoporosis research and lends support to the importance of research into filamins as possible therapeutic interventions in the future<sup>326</sup>.

Our findings suggest that the current epigenetic clocks do not robustly predict future skeletal phenotypes and so the use of these biomarkers for identifying those at adverse bone health (osteoporosis and fragility fractures) may be limited.

#### 4.5.2 Findings in relation to sarcopenia

Sarcopenia can be defined according to reduced muscle mass, loss of muscle strength and impairment of muscle function<sup>11</sup>. In this research we have highlighted the potential for epigenetic clocks (particularly the second-generation clocks) to identify those at risk of lower gait speed (muscle function) and grip strength (muscle strength) at approximately 10 or even 17 years of follow-up. This suggests that, with replication and further study, methylation profiles could be used to identify those at risk of sarcopenia, so that they can be targeted with interventions to improve outcomes.

Through EWAS of grip strength we identified (within the limitation of statistical power and tissue-specificity) a locus which implicated *ECE1* and muscle blood-flow in muscle health. With further replicatory and confirmatory work this may prove to play a role in the pathogenesis of the muscle weakness associated with ageing and provide a therapeutic target for sarcopenia.

#### 4.6 Summary of findings

We have described the bone microarchitectural changes occurring within the cortical and trabecular compartments, together with the age-related changes in grip strength and femoral neck BMD in a group of community-dwelling older adults in the UK. We have demonstrated that baseline cortical and BMD levels, rather than longitudinal change (except for the case of trabecular area), were associated with prevalent fracture. We have also shown borderline associations between a SNP in the *ABCF2* gene and trabecular area, and between a SNP in the *WNT16* gene and change in trabecular density.

We have demonstrated that measures of epigenetic age acceleration have the ability in certain circumstances to predict (or are cross-sectionally associated with) elements of musculoskeletal ageing. These findings appear to have a sexual dimorphism and the most significant findings were for the prediction by GrimAge acceleration for muscle outcomes of gait speed and grip strength. Losses in bone mineral density and in the trabecular compartment were, to some extent, predicted by the GrimAge and PhenoAge measure, but cross-sectional associations seemed to demonstrate the counterintuitive finding of greater age acceleration being associated with higher bone density (though the majority of associations did not reach statistical significance). Future work in other cohorts and using novel clocks is required to further explore this field of research, and further unlock the role played by biological ageing in musculoskeletal health.



Our epigenome-wide analyses are exploratory and subject to limitations of tissue-specificity and statistical power. However, we have presented biologically plausible explanations for the association with genes, pathways and ontologies we have observed. In particular, the association observed between maximum grip strength and cg00960509 could be explained by the role played by endothelin-converting enzyme 1 in skeletal vascular manipulation, and the actin regulatory pathway associated with total femoral neck BMD may be explained by the changing motility of osteoclasts as they carry out bone resorption.

With regard to the title question of this thesis “Does accelerated epigenetic ageing predict future musculoskeletal ageing?”, it is apparent that some elements of the future musculoskeletal phenotype can be predicted (for example GrimAge acceleration and gait speed) by baseline epigenetic biomarkers. However, this is certainly not the case for all musculoskeletal parameters and neither is it the case across the sexes.

## **4.7 Future work**

The future exploration which is warranted by this thesis can be divided into two programs of work.

### *Epigenetic age acceleration and accelerated musculoskeletal ageing*

- To utilize novel methylation clocks (as they arise) to investigate their performance as predictive biomarkers of the musculoskeletal phenotype
- To develop clocks, using methods including elastic net regression, to predict future musculoskeletal phenotypes more accurately
- To examine further the relationships between epigenetic age acceleration and musculoskeletal phenotypes in the wider age range (approximately 18-85 years) in the Hertfordshire Intergenerational Study (composed of original HCS participants, their children and grandchildren)

### *Epigenome-wide exploratory analyses*

- To utilize RNAseq or pyrosequencing to investigate whether the association between grip strength and *ECE1* is replicable.
- To perform additional epigenome-wide association analyses in the HCS including cross-sectional bone microarchitecture and change in bone microarchitecture
- Having primarily examined bone and muscle outcomes, further work is planned to analyse differential methylation associations in osteoarthritis within the Hertfordshire Cohort study

## 4.8 Conclusion

With the widespread propagation of the diseases of musculoskeletal ageing and their association with increased mortality and morbidity a more precise description of the ageing of bone and muscle, novel biomarkers are required to predict those at greatest need of intervention and the discovery of new therapeutic targets is necessitated.

In response to this call to action, this doctoral thesis has described the changes in bone microarchitecture, grip strength and bone mineral density in UK cohort of older adults. It has highlighted the predictive power of the GrimAge epigenetic clock to identify those at risk of muscular ageing and deterioration and has identified potential epigenetic targets in *ECE1* and the actin cytoskeleton which warrant further research.



# Outputs from doctoral research period

## 4.8.1 Publications

- **Fuggie NR**, Westbury LD, Bevilacqua G, Titcombe P, Ó Breasail M, Harvey NC, Dennison EM, Cooper C, Ward KA. Level and change in bone microarchitectural parameters and their relationship with previous fracture and established bone mineral density loci. *Bone*. 2021 Jun;147:115937. doi: 10.1016/j.bone.2021.115937. Epub 2021 Mar 22. PMID: 33766802.
- Nevola KT, Nagarajan A, Hinton AC, Trajanoska K, Formosa MM, Xuereb-Anastasi A, van der Velde N, Stricker BH, Rivadeneira F, **Fuggie NR**, Westbury LD, Dennison EM, Cooper C, Kiel DP, Motyl KJ, Lary CW. Pharmacogenomic Effects of  $\beta$ -Blocker Use on Femoral Neck Bone Mineral Density. *J Endocr Soc*. 2021 May 15;5(8):bvab092. doi: 10.1210/jendso/bvab092. PMID: 34195528; PMCID: PMC8237849.
- **Fuggie NR**, Harrison H, MacArthur B. Will social media banish the bleep? An analysis of hospital pager activity and instant messaging patterns. *BMJ Open Qual*. 2021 Mar;10(1):e001100. doi: 10.1136/bmj-oq-2020-001100. PMID: 33771879; PMCID: PMC8006828.
- Singer AJ, **Fuggie NR**, Gill CB, Patel AR, Medeiros AP, Greenspan SL. COVID-19 and effects on osteoporosis management: the patient perspective from a National Osteoporosis Foundation survey. *Osteoporos Int*. 2021 Apr;32(4):619-622. doi: 10.1007/s00198-021-05836-3. Epub 2021 Feb 8. PMID: 33558958; PMCID: PMC7869916.
- **Fuggie NR**, Singer A, Gill C, Patel A, Medeiros A, Mlotek AS, Pierroz DD, Halbout P, Harvey NC, Reginster JY, Cooper C, Greenspan SL. How has COVID-19 affected the treatment of osteoporosis? An IOF-NOF-ESCEO global survey. *Osteoporos Int*. 2021 Apr;32(4):611-617. doi: 10.1007/s00198-020-05793-3. Epub 2021 Feb 8. Erratum in: *Osteoporos Int*. 2021 Mar 9;: PMID: 33558957; PMCID: PMC7869913.
- Lems WF, Paccou J, Zhang J, **Fuggie NR**, Chandran M, Harvey NC, Cooper C, Javaid K, Ferrari S, Akesson KE; International Osteoporosis Foundation Fracture Working Group. Vertebral fracture: epidemiology, impact and use of DXA vertebral fracture assessment in fracture liaison services. *Osteoporos Int*. 2021 Mar;32(3):399-411. doi: 10.1007/s00198-020-05804-3. Epub 2021 Jan 21. PMID: 33475820; PMCID: PMC7929949.
- **Fuggie NR**, Curtis B, Clynes M, Zhang J, Ward K, Javaid MK, Harvey NC, Dennison E, Cooper C. The treatment gap: The missed opportunities for osteoporosis therapy. *Bone*. 2021 Mar;144:115833. doi: 10.1016/j.bone.2020.115833. Epub 2020 Dec 23. PMID: 33359889; PMCID: PMC7116600.
- Westbury LD, Syddall HE, **Fuggie NR**, Dennison EM, Harvey NC, Cauley JA, Shiroma EJ, Fielding RA, Newman AB, Cooper C. Relationships Between Level and Change in Sarcopenia

and Other Body Composition Components and Adverse Health Outcomes: Findings from the Health, Aging, and Body Composition Study. *Calcif Tissue Int.* 2021 Mar;108(3):302-313. doi: 10.1007/s00223-020-00775-3. Epub 2020 Nov 15. PMID: 33191483; PMCID: PMC7881954.

- **Fuggle NR**, Kassim Javaid M, Fujita M, Halbout P, Dawson-Hughes B, Rizzoli R, Reginster JY, Kanis JA, Cooper C. Fracture Risk Assessment and How to Implement a Fracture Liaison Service. 2020 Aug 21. In: Falaschi P, Marsh D, editors. *Orthogeriatrics: The Management of Older Patients with Fragility Fractures* [Internet]. Cham (CH): Springer; 2021. Chapter 14. PMID: 33347219.
- **Fuggle NR**, Cooper C, Harvey NC, Al-Daghri N, Brandi ML, Bruyere O, Cano A, Dennison EM, Diez-Perez A, Kaufman JM, Palacios S, Prieto-Alhambra D, Rozenberg S, Thomas T, Tremollieres F, Rizzoli R, Kanis JA, Reginster JY. Assessment of Cardiovascular Safety of Anti-Osteoporosis Drugs. *Drugs.* 2020 Oct;80(15):1537-1552. doi: 10.1007/s40265-020-01364-2. PMID: 32725307; PMCID: PMC7536167.
- Clynes MA, Harvey NC, Curtis EM, **Fuggle NR**, Dennison EM, Cooper C. The epidemiology of osteoporosis. *Br Med Bull.* 2020 May 15;133(1):105-117. doi: 10.1093/bmb/ldaa005. PMID: 32282039; PMCID: PMC7115830.
- **Fuggle NR**, Cooper C, Oreffo ROC, Price AJ, Kaux JF, Maheu E, Cutolo M, Honvo G, Conaghan PG, Berenbaum F, Branco J, Brandi ML, Cortet B, Veronese N, Kurth AA, Matijevic R, Roth R, Pelletier JP, Martel-Pelletier J, Vlaskovska M, Thomas T, Lems WF, Al-Daghri N, Bruyère O, Rizzoli R, Kanis JA, Reginster JY. Alternative and complementary therapies in osteoarthritis and cartilage repair. *Aging Clin Exp Res.* 2020 Apr;32(4):547-560. doi: 10.1007/s40520-020-01515-1. Epub 2020 Mar 13. PMID: 32170710; PMCID: PMC7170824.
- Westbury LD, Syddall HE, **Fuggle NR**, Dennison EM, Cauley JA, Shiroma EJ, Fielding RA, Newman AB, Cooper C. Long-term rates of change in musculoskeletal aging and body composition: findings from the Health, Aging and Body Composition Study. *Calcif Tissue Int.* 2020 Jun;106(6):616-624. doi: 10.1007/s00223-020-00679-2. Epub 2020 Mar 3. PMID: 32125471; PMCID: PMC7188697.
- Shere C, **Fuggle NR**, Edward MH, Parsons CM, Jameson KA, Cooper C, Dennison EM, Ward KA. Jumping Joints: The Complex Relationship Between Osteoarthritis and Jumping Mechanography. *Calcif Tissue Int.* 2020 Feb;106(2):115-123. doi: 10.1007/s00223-019-00622-0. Epub 2019 Oct 26. PMID: 31655874; PMCID: PMC6994439.
- Biver E, Berenbaum F, Valdes AM, Araujo de Carvalho I, Bindels LB, Brandi ML, Calder PC, Castronovo V, Cavalier E, Cherubini A, Cooper C, Dennison E, Franceschi C, **Fuggle N**, Laslop A, Miossec P, Thomas T, Tuzun S, Veronese N, Vlaskovska M, Reginster JY, Rizzoli R. Gut microbiota and osteoarthritis management: An expert consensus of the European society

for clinical and economic aspects of osteoporosis, osteoarthritis and musculoskeletal diseases (ESCEO). *Ageing Res Rev.* 2019 Nov;55:100946. doi: 10.1016/j.arr.2019.100946. Epub 2019 Aug 19. PMID: 31437484.

- **Fuggle NR**, Curtis EM, Ward KA, Harvey NC, Dennison EM, Cooper C. Fracture prediction, imaging and screening in osteoporosis. *Nat Rev Endocrinol.* 2019 Sep;15(9):535-547. doi: 10.1038/s41574-019-0220-8. PMID: 31189982.
- **Fuggle N**, Curtis E, Shaw S, Spooner L, Bruyère O, Ntani G, Parsons C, Conaghan PG, Corp N, Honvo G, Uebelhart D, Baird J, Dennison E, Reginster JY, Cooper C. Safety of Opioids in Osteoarthritis: Outcomes of a Systematic Review and Meta-Analysis. *Drugs Aging.* 2019 Apr;36(Suppl 1):129-143. doi: 10.1007/s40266-019-00666-9. PMID: 31073926; PMCID: PMC6509215.
- Honvo G, Reginster JY, Rannou F, Rygaert X, Geerinck A, Rabenda V, McAlindon T, Charles A, **Fuggle N**, Cooper C, Curtis E, Arden N, Avouac B, Bruyère O. Safety of Intra-articular Hyaluronic Acid Injections in Osteoarthritis: Outcomes of a Systematic Review and Meta-Analysis. *Drugs Aging.* 2019 Apr;36(Suppl 1):101-127. doi: 10.1007/s40266-019-00657-w. PMID: 31073925; PMCID: PMC6509101.
- Curtis E, **Fuggle N**, Shaw S, Spooner L, Ntani G, Parsons C, Corp N, Honvo G, Baird J, Maggi S, Dennison E, Bruyère O, Reginster JY, Cooper C. Safety of Cyclooxygenase-2 Inhibitors in Osteoarthritis: Outcomes of a Systematic Review and Meta-Analysis. *Drugs Aging.* 2019 Apr;36(Suppl 1):25-44. doi: 10.1007/s40266-019-00664-x. PMID: 31073922; PMCID: PMC6509094.
- Shaw SC, Parsons CM, **Fuggle NR**, Edwards MH, Robinson SM, Dennison EM, Cooper C, Ward KA. Diet Quality and Bone Measurements Using HRpQCT and pQCT in Older Community-Dwelling Adults from the Hertfordshire Cohort Study. *Calcif Tissue Int.* 2018 Nov;103(5):494-500. doi: 10.1007/s00223-018-0445-x. Epub 2018 Jun 21. PMID: 29931462; PMCID: PMC6174074.
- Patel A, Edwards MH, Jameson KA, Ward KA, **Fuggle N**, Cooper C, Dennison EM. Longitudinal Change in Peripheral Quantitative Computed Tomography Assessment in Older Adults: The Hertfordshire Cohort Study. *Calcif Tissue Int.* 2018 Nov;103(5):476-482. doi: 10.1007/s00223-018-0442-0. Epub 2018 Jun 21. PMID: 29931460; PMCID: PMC6179140.

#### 4.8.2 Conference abstracts

- **2021**
  - IOF-ESCEO World Congress of Osteoporosis (Virtual): *Epigenetic age acceleration associations with skeletal outcomes: Differential impacts in men and women*

**NR Fuggle, MA Clynes, M O'Breasail, C Parsons, J Holloway, N Kitaba, KA Ward, C Cooper, EM Dennison**

- British Society of Rheumatology annual conference (Virtual): *Can a computer sense the symptoms of osteoarthritis from a radiograph? Initial findings from a pilot, AI approach to osteoarthritis assessment*

**NR Fuggle, D Pinto Pereira, EM Dennison, S Mahmoodi, C Cooper**

- **2020**

- British Society of Rheumatology annual conference (Virtual): *Is muscle phenotype associated with future knee osteoarthritis?*

**NR Fuggle, M Clynes, KA Jameson, C Cooper, EM Dennison**

- IOF-ESCEO World Congress of Osteoporosis (Virtual): *Alternative and complementary therapies in osteoarthritis and cartilage repair*

**Fuggle NR, Cooper C, Oreffo ROC, Price AJ, Kaux JF, Maheu E, Cutolo M, Honvo G, Conaghan PG, Berenbaum F, Branco J, Brandi ML, Cortet B, Veronese N, Kurth AA, Matijevic R, Roth R, Pelletier JP, Martel-Pelletier J, Vlaskovska M, Thomas T, Lems WF, Al-Daghri N, Bruyere O, Rizzoli R, Kanis JA, Reginster JY**

- Bone Research Society (Virtual): *How does radiographic knee osteoarthritis impact musculoskeletal aging?*

**NR Fuggle, M Clynes, KA Jameson, C Cooper, EM Dennison**

- **2019**

- British Society of Rheumatology annual conference (Birmingham): *Does knee pain or radiographic osteoarthritis better predict future muscle outcomes? Findings from the Hertfordshire Cohort Study*

**NR Fuggle, LD Westbury, KA Jameson, MH Edwards, KA Ward, C Cooper, EM Dennison**

- IOF-ESCEO World Congress of Osteoporosis (Paris): *A systematic review and metanalysis of the adverse effects of COX-2 inhibitors and opioids in osteoarthritis*

**NR Fuggle, E Curtis, G Honvo, O Bruyère, S Shaw, L Spooner, G Ntani, C Parsons, N Arden, P Conaghan, S Maggi, N Corp, D Uebelhart, J Baird, E Dennison, R Roth, N Veronese, R Chapurlat, B Avouac, V Leblanc, T McAlindon, A Migliore, O Mkinsi, F Rannou, J Kanis, R Rizzoli, JY Reginster, C Cooper**

- Bone Research Society (Cardiff): *Relationships between markers of inflammation and bone mineral density: findings from the Hertfordshire Cohort Study (Oral presentation)*

**NR Fuggle, L Westbury, HE Syddall, NA Duggal, EM Dennison, J Lord, C Cooper**

- **2018**

- Royal Osteoporosis Society: *Relationships between the hypothalamic-pituitary-adrenal axis and bone microarchitecture: findings from the Hertfordshire Cohort Study (Oral Presentation)*

**NR Fuggle**, LD Westbury, HE Syddall, K Ward, NA Duggal, J Lord, C Cooper, EM Dennison



## Appendices



**Appendix 1:** Literature review of change in bone microarchitecture. Note that not all papers quoted in this table directly relate to the research aims of this doctoral thesis but all were examined as part of a wider literature review.

Author	Year	Scan-type	Population	N	Study Design	Results and comment
Warming L <sup>339</sup>	2002	DXA	Danish men and women (20-80y)	398 females 222 males	Longitudinal (2-year follow-up)	<ul style="list-style-type: none"> <li>In women after the menopause and in men there was an age-related bone loss 0.002-0.006g/cm<sup>2</sup>/year at all sites</li> </ul>
Lauretani F <sup>340</sup>	2008	QCT	Italian men and women (21-102y)	464 females 345 males	Longitudinal (6-year follow-up)	<ul style="list-style-type: none"> <li>Tibial total volumetric BMD change between 20 year old and 90 year old:               <ul style="list-style-type: none"> <li>Males -61.1mg/cm<sup>3</sup> (-18.5%)</li> <li>Females -91.5mg/cm<sup>3</sup> (-36.4%)</li> </ul> </li> </ul>
Burt LA <sup>65</sup>	2017	HR-pQCT	Peri- and post-menopausal women (CaMOS cohort)	Perimenopausal - 26 Postmenopausal - 65	Longitudinal (6-year follow-up)	<ul style="list-style-type: none"> <li>Radial total BMD:               <ul style="list-style-type: none"> <li>Peri-menopausal 331.9mg/cm<sup>3</sup> vs postmenopausal 291.4mg/cm<sup>3</sup> (p&lt;0.01)</li> </ul> </li> <li>No significant difference in change in density across the groups</li> <li>Tibial Cortical Porosity (significant difference, p&lt;0.05)               <ul style="list-style-type: none"> <li>Peri-menopausal +9%/year</li> <li>Postmenopausal +6%/year</li> </ul> </li> <li>Tibial Total Area (significant difference p&lt;0.02)</li> </ul>

Author	Year	Scan-type	Population	N	Study Design	Results and comment
<b>Boutroy S<sup>63</sup></b>	2005	HR-pQCT	Healthy pre-menopausal, osteopenic postmenopausal, osteoporotic postmenopausal	Healthy premenopausal – 108 osteopenic postmenopausal – 113 osteoporotic postmenopausal - 35	Cross-sectional	<ul style="list-style-type: none"> <li>• Postmenopausal had significantly differences in the following parameters compared to healthy premenopausal (<math>p &lt; 0.001</math>) <ul style="list-style-type: none"> <li>○ Lower density (-36.3%)</li> <li>○ Lower Trabecular number (-20.4%)</li> <li>○ Lower cortical thickness (-41.4%)</li> </ul> </li> <li>• Osteoporotic females had significant differences in the following parameters compared to osteopenic females (<math>p &lt; 0.01</math>) <ul style="list-style-type: none"> <li>○ Lower density (-15.7%)</li> <li>○ Lower Cortical thickness (-18.1%)</li> <li>○ Higher trabecular separation (12.3%)</li> </ul> </li> </ul>
<b>Nishiyama KK<sup>67</sup></b>	2010	HR-pQCT	Pre- and postmenopausal women  (CaMOS cohort)	Normal premenopausal -63  Normal postmenopausal - 87 Osteopenic postmenopausal – 121  Osteoporotic postmenopausal - 9	Cross-sectional	<ul style="list-style-type: none"> <li>• Postmenopausal women had significant differences in the following parameters compared to healthy premenopausal women: <ul style="list-style-type: none"> <li>○ Cortical porosity (range of difference 3.2% to 12.9%, <math>p &lt; 0.001</math>)</li> </ul> </li> <li>• Osteopenic and osteoporotic women had significant differences in the following parameters compared to healthy females: <ul style="list-style-type: none"> <li>○ Lower cortical thickness (range of difference -12.8% to -30.3%, <math>p &lt; 0.01</math>)</li> <li>○ Higher cortical porosity (range of difference 2.1% to 8.1%, <math>p &lt; 0.001</math>)</li> </ul> </li> </ul>

Author	Year	Scan-type	Population	N	Study Design	Results and comment
Kawalilak CE <sup>86</sup>	2014	HR-pQCT	Postmenopausal women	N=51	Longitudinal (1-year follow-up)	<ul style="list-style-type: none"> <li>• Comparing the bone microarchitecture from baseline to 1 year follow up the following were observed: <ul style="list-style-type: none"> <li>○ Trabecularisation at the radius was noted (trabecular separation increased by 28.6%, p=0.002)</li> <li>○ In the non-medicated population changes noted over 1 year of follow-up included (mean annual percentage change, all p&lt;0.001)) <ul style="list-style-type: none"> <li>▪ Reduced Cortical area (-3.1%/year)</li> <li>▪ Increased Trabecular area (2.3%/year)</li> <li>▪ Reduced total density (-4.3%/year)</li> <li>▪ Reduced Cortical density (14.6%/year)</li> <li>▪ Reduced Cortical thickness (28.8%/year)</li> </ul> </li> </ul> </li> </ul>
Laib A <sup>341</sup>	1998	HR-pQCT	Postmenopausal women	N=17	Pilot	Prototype HR-pQCT used with an isotropic resolution of 165µm (60 slices), 9.9mm total thickness and image resolution 512 x 512
Liu CT <sup>342</sup>	2017	HR-pQCT	Framingham Osteoporosis Study	N= 710 (58% female)	Cross-sectional	<ul style="list-style-type: none"> <li>• Investigating the association between visceral adipose tissue and bone microarchitecture</li> <li>• Associations not significant when adjusting for BMI or weight</li> </ul>

Author	Year	Scan-type	Population	N	Study Design	Results and comment
Sornay-Rendu E <sup>71</sup>	2017	HR-pQCT	Postmenopausal women (OFELY cohort)	N=589	Longitudinal (9.6-year follow-up)	<ul style="list-style-type: none"> <li>• Study investigating the ability of bone microarchitecture to predict future fracture</li> <li>• Trabecular compartment of the radius is the most significant for predicting future fracture</li> <li>• Trabecular BMD: HR 1.39 (for each quartile decrease in BMD), p=0.001)</li> </ul>
Butscheidt S <sup>72</sup>	2018	HR-pQCT	Postmenopausal women on denosumab	N=182 (22 sustained fracture)	Longitudinal (>1-year follow-up)	<ul style="list-style-type: none"> <li>• Trabecular parameters at baseline best predicted future fracture</li> <li>• Trabecular and cortical parameters increased at 12 months in non-fracture group compared to fracture group</li> </ul>
Biver E <sup>69</sup>	2017	HR-pQCT	Postmenopausal women (GERICO cohort)	N=740 (68 sustained fracture)	Longitudinal (5-year follow-up)	<ul style="list-style-type: none"> <li>• Total volumetric BMD was best at predicting future fracture beyond femoral neck BMD (AUC 0.76 vs 0.70, p=0.022) and beyond FRAX® with BMD (AUC 0.76 vs 0.71, p=0.015)</li> </ul>
Shanbhogue VV <sup>66</sup>	2016	HR-pQCT	Adults across the lifecourse (aged 21-82y)	N=260	Longitudinal (3-year follow-up)	<ul style="list-style-type: none"> <li>• Annualised change in tibial volumetric BMD: <ul style="list-style-type: none"> <li>○ Premenopausal females: 0.28%/year</li> <li>○ Post-menopausal females: -0.42%/year</li> <li>○ Males aged 20-49 years: 0.13%/year</li> <li>○ Males aged over 50 years: 0.15%/year</li> </ul> </li> </ul>

Author	Year	Scan-type	Population	N	Study Design	Results and comment
de Jong JJA <sup>80</sup>	2016	HR-pQCT	Distal radius fracture in postmenopausal women	N=14	Longitudinal (2-year follow-up)	<ul style="list-style-type: none"> <li>• Comparison of fractured to non-fractured radius</li> <li>• Fractured side has increased cortical (21% higher) and trabecular (55% higher) thickness at one year</li> </ul>
de Jong JJA <sup>343</sup>	2017	HR-pQCT	Distal radius fracture in postmenopausal women	N=15	Longitudinal (2-year follow-up)	<ul style="list-style-type: none"> <li>• Significant declines in BMD in cortical but not trabecular region on contralateral (non-fracture) side at 2 years post-fracture (greater changes than would be expected simply through ageing)</li> </ul>
Gabel L <sup>88</sup>	2017	HR-pQCT	Children/adolescents	173 males 136 females	Cross-sectional	<ul style="list-style-type: none"> <li>• Study investigating the effect of physical activity (measures by accelerometer) on bone microarchitecture</li> <li>• Sedentary activity associated with detrimental effects on bone microarchitecture</li> </ul>
Burghardt AJ <sup>87</sup>	2010	HR-pQCT	Post-menopausal women randomised to alendronate or control	N=53	Randomised controlled trial (24 months follow-up)	<ul style="list-style-type: none"> <li>• Those taking alendronate had: <ul style="list-style-type: none"> <li>○ Higher cortical volumetric BMD at the tibia (p&lt;0.05)</li> <li>○ Higher trabecular BMD and cortical thickness at the radius (p&lt;0.05)</li> </ul> </li> </ul>
Gabel L <sup>68</sup>	2018	HR-pQCT	Children/adolescents	184 males 209 females	Longitudinal (2-year follow-up)	<ul style="list-style-type: none"> <li>• Growth curves presented in the paper</li> <li>• Increase in trabecular thickness (with little change in trabecular number or trabecular separation) throughout growth</li> <li>• Trabeculae thicken and remodel with each subsequent remodelling cycle</li> </ul>

Author	Year	Scan-type	Population	N	Study Design	Results and comment
Burt LA <sup>70</sup>	2018	HR-pQCT	Postmenopausal women (CaMOS cohort)	N=149 22 sustained fracture	Longitudinal (5-year follow-up)	<ul style="list-style-type: none"> <li>• Baseline values of bone microarchitecture parameters rather than rate of change plays a more significant role in predicting future fractures.</li> <li>• At baseline at the radius total BMD (OR 2.1) and trabecular BMD (OR 2.0) were best predictors of fracture</li> <li>• At baseline at the tibia total BMD (OR 2.1) and cortical thickness (OR 2.2) were best predictors of future fracture</li> </ul>
Burt LA <sup>85</sup>	2017	HR-pQCT	Lifecourse assessment (ages 16-80 y)	N=466	Longitudinal (5-year follow-up)	<ul style="list-style-type: none"> <li>• Findings presented by age group in paper</li> <li>• Gains in bone microarchitecture radius &gt; tibia</li> <li>• With advancing age: <ul style="list-style-type: none"> <li>○ Increased trabecular area and cortical porosity</li> <li>○ Reduced cortical density, thickness, area</li> <li>○ Reduced volumetric BMD in older adult subgroups</li> </ul> </li> </ul>



## Appendix 2: 2017 Hertfordshire Bone Study (HBS17) participant information leaflet

You are being invited to take part in a follow up visit for the above research study. Before you decide whether or not you wish to take part it is important that you understand why the research is being done and what it will involve. Please read this information carefully and discuss it with others if you wish. Ask us if there is anything that is not clear, or if you would like more information. Take time to decide whether or not you wish to take part. Details about the conduct of the study are on another sheet (Sheet 2 -Study Conduct Information) and this should also be read before deciding whether or not you wish to take part.

### What is the purpose of this study?

Osteoporosis is a condition caused by the thinning of bones leading to an increased risk of fracturing. It tends to affect older people and women more than men. Previous studies have shown that some of the risk of osteoporosis is determined very early in life and may be related to your weight at birth and 1 year of age. We aim to find out whether weights at time points in early life also affect the internal structure of bones.

### Why have I been chosen?

You have been chosen because you have helped us with first study visit in which you had three scans to assess your bone health. It would be very useful for us to compare information we have about you from the previous visit with information we obtain at this follow-up visit. We are hoping to find about 230 men and women aged 65-85 years old who are interested in taking part

### Do I have to take part?

No. It is up to you to decide whether or not to take part. If you do decide to take part you will be given these information sheets to

Version 1.1, 25/11/16. HNR\_F0095-01

keep and will be asked to sign a consent form. You are still free to withdraw at any time without giving a reason.

### What will happen to me if I take part?

You will be contacted by one of our researchers and an appointment will be made for you to come to the MRC Elsie Widdowson Laboratory (MRC EWL) in Cambridge on a day that is convenient for you. On that day a complimentary taxi will pick you up and take you home again. The whole session should last about half a day and during your stay, lunch and snacks will be provided.

On your arrival at the MRC EWL we will ask you to sign a consent form. Your height and weight will then be measured and we will help you to complete some questionnaires. You will have 3 scans: a DXA scan, a pQCT scan and a HRpQCT scan.

DXA stands for dual energy x-ray absorptiometry. A DXA scan involves lying on a firm table whilst an x-ray arm passes over you. A dressing gown will be provided for you to wear during the scan. The scan will last a total of about 30 minutes and will measure your body fat, lean tissue and bone density, including in the hips. You may recall having a scan like this before as part of our study. A lateral spine scan will also be performed which requires you to lay on your side for a short time.

pQCT stands for peripheral quantitative computed tomography. A pQCT scan will involve us carefully positioning your lower leg and then your forearm inside a scanner. There will be rests available to help keep the scanned limb completely still during the short procedure. This scan will take approximately 30 minutes and will produce three dimensional images of the bones in your lower leg and forearm from which we can

assess their strength. You will also have had this scan in 2005 and 2011/12.

HRpQCT stands for high resolution pQCT. This is a similar scan to a pQCT scan although it uses a slightly different machine and produces more detailed pictures. Again your lower leg and then your forearm would be scanned. This scan takes approximately 30 minutes. None of the scans would require your head or body to be enclosed within a tunnel. You will have had this scan in 2011/12.

Following the scans we will do some brief physical activities. These include standing for 10 seconds with your feet together and then with one foot in front of the other, walking 8 feet. Finally, standing up five times from sitting in a chair. You will then have your grip strength measured by squeezing an instrument 3 times with each hand.

The last test is an activity called "Up and Go". The action required for this would be demonstrated to you beforehand and you can then decide whether or not to undertake this part of the study. You would be asked to stand up from a chair, walk 3 meters away from it and then 3 meters back to it. This activity will be timed with a stop watch.

### What do I have to do?

There will not be any dietary or lifestyle restrictions around the time of the study. Your participation in the study will be completed during your one visit to the MRC EWL as described above.]

### What are the possible benefits of taking part?

The results of your DXA scan (looking at the bone density in your hips) will be sent to you

and your GP. You will have had this scan completed previously however it may be of benefit to you to know if any significant changes have occurred over the last few years.

### What are the possible disadvantages and risks of taking part?

The DXA, pQCT and HRpQCT all involve a small dose of radiation (approximately 40  $\mu$ Sv). A chest x-ray by comparison is 20 $\mu$ Sv and one trans-Atlantic flight would expose you to about 80 $\mu$ Sv.

We cannot avoid being exposed to some radiation, as natural background radiation (approximately 6  $\mu$ Sv/day) is all around us in the soil and air. Additional radiation from the scans used will expose you to the equivalent of approximately 7 days natural background radiation in Cambridge.

If a new diagnosis of osteoporosis is made, this could affect your future insurance status (e.g. for life insurance or private medical insurance).

### What will happen if anything goes wrong?

Any complaint about the way you have been dealt with during the study or any possible harm you might suffer will be addressed. The detailed information on this is given on 'Sheet 2 - study conduct information sheet'. If you wish to make a complaint you can contact Head of Operations at MRC EWL, Ms Polly Page on 01223 426356 or email [polly.page@mrc-ewl.cam.ac.uk](mailto:polly.page@mrc-ewl.cam.ac.uk).

### Will my taking part in this study be kept confidential?

Yes. All information that is collected about you during the course of the research will be kept strictly confidential. The details are

Version 1.1, 25/11/16. HNR\_F0095-01

included in 'Sheet 2 - Study Conduct Information' sheet.

### What will happen to the study results?

We will inform your GP of the result of your DXA scan (the bone density at your hips). As the scans from the study will not be processed immediately, your results may not be available for a few months.

The overall results may be presented at scientific meetings or published in a scientific journal. You will not be identified in any of these presentations or publications. A summary of the study results will be available on the MRC EWL website. We will be happy to discuss the results with you when the study is completed, and will let you know where you can obtain a copy of the published results. Details are included in 'Sheet 2 - Study Conduct Information'

### Will I be reimbursed for my time?

There will be no reimbursement for time however transport to and from the site will be arranged at no cost to you and lunch and snacks will be provided.

### Contact for further information

If you have any further questions then please contact Jennifer Woolston at MRC EWL by email [jennifer.woolston@mrc-ewl.cam.ac.uk](mailto:jennifer.woolston@mrc-ewl.cam.ac.uk) or telephone 01223 437588. Thank you for having taken the time to read this information sheet. If you do decide to take part in the study, you will be asked to sign a Consent Form and you will be given a copy of the Consent Form and the Participant Information Sheet to keep.



## Study Title: What are the determinants of the internal structure of bone?

### Information Sheet 1 for Study Participants Follow-up visit

Chief Investigator:  
Dr Nicholas Fuggle

Study Site:  
MRC Elsie Widdowson Laboratory  
Fulbourn Road  
Cambridge  
CB1 9NL

Telephone: 01223 426356  
Fax: 01223 437515  
[research@mrc-ewl.cam.ac.uk](mailto:research@mrc-ewl.cam.ac.uk)  
<http://www.mrc-ewl.cam.ac.uk>



OFFICIAL SENSITIVE

**What are the determinants of the internal structure of bone?  
Follow-up visit**

**CONSENT FORM**

**LREC Reference Number:** 11/EE/0196

**Name of Lead Investigator:** Dr Nicholas Fuggle

**Please initial boxes.**

1. I confirm that I have read and understand the information sheet dated 25th November 2016 (version 1.1) for the above study and have had the opportunity to ask questions.
2. I understand that my participation is voluntary and that I am free to withdraw at any time, without giving any reason, and without my medical care or legal rights being affected.
3. I consent to my general practitioner being notified of my participation in this research and to being informed of my results.
4. In the event that they withdraw from the study: *(delete as appropriate)*
  - a. I wish the researchers to remove all of my identifiable data collected up to that point.
  - b. I am happy for the researchers to retain my identifiable data gathered up to that point.
5. I understand relevant section of my medical notes and data collected during the study may be looked at by individuals from the Medical Research Council, or from regulatory authorities, where it is relevant to my taking part in the research. I give permission for these individuals to have access to my records.
6. I agree to take part in the above study.
7. I am willing to be contacted again in the future about the present study and any potential follow-up from it. I understand that I am under no obligation to undergo any future additional tests and can withdraw this consent at any time by notifying the study team.

\_\_\_\_\_  
Name of Volunteer (Please print)      Date      Signature

\_\_\_\_\_  
Name of Research Team Member      Date      Signature

**3 copies required:** top copy for researcher; one copy for volunteer; one copy to be kept with volunteer's notes.

**Appendix 4: Ethical approval for 2017 visit of the Hertfordshire Bone Study (HBS17)**



**Health Research Authority**

**East of England - Cambridgeshire and Hertfordshire Research Ethics Committee**

The Old Chapel  
Royal Standard Place  
Nottingham  
NG1 6FS

**Please note: This is the favourable opinion of the REC only and does not allow the amendment to be implemented at NHS sites in England until the outcome of the HRA assessment has been confirmed.**

21 December 2016

Dr Nichols Fuggle  
NIHR Academic Clinical Fellow  
MRC Lifecourse Epidemiology Unit

Dear Dr Fuggle

Study title:	Understanding the early life and environmental determinants of bone strength and structure using participants from the Hertfordshire Cohort Study.
REC reference:	11/EE/0196
Protocol number:	8012
EudraCT number:	N/A
Amendment number:	2
Amendment date:	10 November 2016
IRAS project ID:	80524

The above amendment was reviewed by the Sub-Committee in correspondence.

**Ethical opinion**

The members of the Committee taking part in the review gave a favourable ethical opinion of the amendment on the basis described in the notice of amendment form and supporting documentation.

**Discussion**

There were no ethical issues raised.

**Approved documents**

The documents reviewed and approved at the meeting were:

Document	Version	Date
GPI/consultant information sheets or letters	1.2	03 November 2016
Letters of Invitation to participant [Follow up visit ]	1.1	07 November 2016
Notice of Substantial Amendment (non-CTIMP)	2	10 November 2016
Other [Proposal for amendments]		
Other [D1 signed declarations - Dr Fuggle]		
Other [Follow-up visit study Conduct information]	1.1	07 November 2016
Other [Letter of reminder to follow-up]	1.1	07 December 2016
Other [HRpQCT follow-up Questionnaire ]	1.4	25 November 2016
Other [Revised IRAS application - Part B]		05 December 2016
Participant consent form [Follow up visit]	1	07 November 2016
Participant information sheet (PIS) [Follow up visit]	1.1	25 November 2016
Research protocol or project proposal	1.5	07 November 2016
Summary CV for Chief Investigator (CI)	Nov 2016	

#### Membership of the Committee

The members of the Committee who took part in the review are listed on the attached sheet.

#### Working with NHS Care Organisations

Sponsors should ensure that they notify the R&D office for the relevant NHS care organisation of this amendment in line with the terms detailed in the categorisation email issued by the lead nation for the study.

#### Statement of compliance

The Committee is constituted in accordance with the Governance Arrangements for Research Ethics Committees and complies fully with the Standard Operating Procedures for Research Ethics Committees in the UK.

We are pleased to welcome researchers and R & D staff at our Research Ethics Committee members' training days – see details at <http://www.hra.nhs.uk/hra-training/>

11/EE/0198: Please quote this number on all correspondence
--

Yours sincerely



pp

**Mr David Grayson**  
Chair

E-mail: [nrescommittee.eastofengland-cambsandherts@nhs.net](mailto:nrescommittee.eastofengland-cambsandherts@nhs.net)


Enclosures: *List of names and professions of members who took part in the review*



Copy to: *Diana Galpin*

Postal No.

## Early life and environmental determinants of bone microarchitecture

Follow-up Questionnaire



Today's date:  /  /

Date of birth:  /  /

Version 1.4, 25/11/16 1

### SECTION 1: HEALTH, DISEASE, MEDICATIONS, LIFESTYLE

1. Have you been told by a doctor that you have any of the following conditions? (Assume examples/conditions are *not* answered)

<input type="checkbox"/> High blood pressure	<input type="checkbox"/> <b>Stroke</b>	<input type="checkbox"/> Osteoporosis
<input type="checkbox"/> Diabetes (sugar, insulin, COVID, emphysema, chronic bronchitis)	<input type="checkbox"/> Depression	<input type="checkbox"/> Thyroid disease
<input type="checkbox"/> Rheumatoid arthritis	<input type="checkbox"/> Parkinson's disease	<input type="checkbox"/> Stroke
<input type="checkbox"/> Multiple sclerosis	<input type="checkbox"/> Heart disease (heart attack, angina, etc)	<input type="checkbox"/> Other serious illnesses (please specify below):
<input type="checkbox"/> Cancer (please specify below)	<input type="checkbox"/> Peripheral arterial disease (PAD)	<input type="checkbox"/>
<input type="checkbox"/>	<input type="checkbox"/> Operations (please specify below)	<input type="checkbox"/>
<input type="checkbox"/>	<input type="checkbox"/>	<input type="checkbox"/>

2. Have you had any falls since the age of 45 years?  Yes  No

3. Have you had any falls in the last year?  Yes  No

a. If yes, how many?  Yes  No

b. Did any of these falls result in injury?  Yes  No

c. If yes, how many?  Yes  No

4. Had you broken any bones **before** the age of 45 years?  Yes  No

a. If yes, how many?  Yes  No

5. Have you broken any bones **since** the age of 45?  Yes  No

a. Did you receive medical attention for the broken bone(s)?  Yes  No

b. If yes, where did you receive this attention?  Yes  No

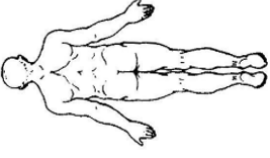
c. Was an x-ray taken of the broken bone(s)?  Yes  No

d. Complete table below

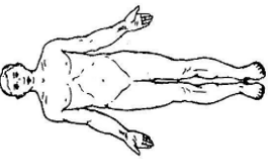
Number	How long ago when you broke the bone? Please give your age in years	Which bone did you break? Please specify as above below and also indicate on the diagram	What caused the bone to break? Please specify as above below
1			
2			
3			
4			
5			
6			
7			
8			
9			

Please put a cross on the figure (marked 1,2,3 etc.) to show where each break occurred

Right



Left



6. In the last year, have you lost more than 10 pounds unintentionally (i.e. not due to dieting or exercise)?  Yes  No

7. How often in the last week did you feel "everything I did was an effort" or "I could not get going"? Please tick one box

1. Rarely or none of the time (less than 1 day)	<input type="checkbox"/>
2. Some or a little of the time (1-2 days)	<input type="checkbox"/>
3. Most of the time (3-4 days)	<input type="checkbox"/>
4. All of the time (more than 4 days)	<input type="checkbox"/>

8. Do you or would you have any difficulty (or find it troublesome, exhausting or worrying) to do the following? Please tick one box for each difficulty

	No	Yes, unable to do alone
a. Washing down (whether in bath or not)	<input type="checkbox"/>	<input type="checkbox"/>
b. Removing a jug, sink, from an overhead shelf	<input type="checkbox"/>	<input type="checkbox"/>
c. Tying a good knot in string	<input type="checkbox"/>	<input type="checkbox"/>
d. Cutting toenails	<input type="checkbox"/>	<input type="checkbox"/>
e. Running to catch a bus	<input type="checkbox"/>	<input type="checkbox"/>
f. Going shopping and carrying a full basket of shopping in each hand	<input type="checkbox"/>	<input type="checkbox"/>
g. Doing heavy housework	<input type="checkbox"/>	<input type="checkbox"/>
h. Preparing a hot meal	<input type="checkbox"/>	<input type="checkbox"/>
9. Do you have any long-term illness, health problem or disability, which limits your activities or the work you can do?	<input type="checkbox"/>	<input type="checkbox"/>

Version 1.4, 25/11/16 3



10. Do you currently take any medicines/supplements (over-the-counter, dietary supplements, etc.)?  Yes  No  
 Please include regular pain killers such as paracetamol and over-the-counter medicines such as glucosamine

Name of the Drug	Frequency	Dosage	Unit of Drug (e.g. mg)

11. Have you ever smoked regularly? (i.e. at least once a day for a year or more)  
 If No, go to question 13

a. How old were you when you first smoked regularly?  
 b. If you added up all the years that you smoked, how many would it make in total?  
 c. What was the average amount you smoked over this time?

i. Cigarettes per day  
 ii. Roll-up tobacco (cigarettes/week)  
 iii. Cigars/week  
 iv. Pipe tobacco (couples/week)  
 d. Do you still smoke regularly?

If Yes, go to question 12

e. How old were you when you last smoked regularly?  
 f. What was the average amount you smoked over this time?

i. Cigarettes per day  
 ii. Roll-up tobacco (cigarettes/week)  
 iii. Cigars/week  
 iv. Pipe tobacco (couples/week)  
 v. If appropriate, between what ages did you cut down? (age started cutting down/age stopped cutting down)

13. Apart from your own smoking are you regularly exposed to tobacco smoke at home?  
 a. If yes, not counting yourself, how many people in your household smoke regularly?

14. Do you ever drink alcohol?  
 If No, go to question 20

15. How often do you currently drink alcohol (beer/wine/cider)? (Do not include alcohol free lager etc.)  
 Please tick one box

i. Never  
 ii. Once every 2-3 months  
 iii. Once a month  
 iv. Once a fortnight  
 v. 1-2 times per week  
 vi. 3-6 times per week  
 vii. Once a day  
 viii. More than once a day

When you drink these, how many pints would you normally have? (If a range is given then document the mid-point)  
 Note: 1 average can = 0.8 pints, 1 small can = 0.5 pints

16. How often do you currently drink beer/stock/lager/cider? (Do not include alcohol free lager etc.)  
 Please tick one box

i. Never  
 ii. Once every 2-3 months  
 iii. Once a month  
 iv. Once a fortnight  
 v. 1-2 times per week  
 vi. 3-6 times per week  
 vii. Once a day  
 viii. More than once a day

When you drink these, how many pints would you normally have? (If a range is given then document the mid-point)  
 Note: 1 average can = 0.8 pints, 1 small can = 0.5 pints

17. How often do you currently drink low alcohol wine?  
 Please tick one box

i. Never  
 ii. Once every 2-3 months  
 iii. Once a month  
 iv. Once a fortnight  
 v. 1-2 times per week  
 vi. 3-6 times per week  
 vii. Once a day  
 viii. More than once a day

When you drink these, how many glasses would you normally have? (If a range is given then document the mid-point)

18. How often do you currently drink wine/Sherry/Port/Whisky/Chateau?  
 Please tick one box

i. Never  
 ii. Once every 2-3 months  
 iii. Once a month  
 iv. Once a fortnight  
 v. 1-2 times per week  
 vi. 3-6 times per week  
 vii. Once a day  
 viii. More than once a day

When you drink these, how many glasses would you normally have? (If a range is given then document the mid-point)

19. How often do you currently drink spirits/ligueurs?  
 Please tick one box

i. Never  
 ii. Once every 2-3 months  
 iii. Once a month  
 iv. Once a fortnight  
 v. 1-2 times per week  
 vi. 3-6 times per week  
 vii. Once a day  
 viii. More than once a day

When you drink these, how many measures would you normally have? (If a range is given then document the mid-point)

20. In terms of relationships, which of the following would best describe your current status?  
 Please tick one box

i. Single  
 ii. Married  
 iii. Divorced or separated  
 iv. Widowed  
 v. Cohabiting

21. How often are you eating the following foods over the past 3 months?	AVERAGE USE IN PAST 3 MONTHS									
	Never than once/ month	1-3 times per month	Once a week	Once a 2-4 per week	Once a 2-3 per week	Once a 2-3 per day	4-5 per day	6-7 per day	8-9 per day	10-15 per day
1. White bread (one slice)	0	1	2	3	4	5	6	7	8	9
2. Brown and wholemeal bread (one slice)	0	1	2	3	4	5	6	7	8	9
3. Biscuits (one digestive (one)	0	1	2	3	4	5	6	7	8	9
4. Apples (one fruit)	0	1	2	3	4	5	6	7	8	9
5. Bananas (one fruit)	0	1	2	3	4	5	6	7	8	9
6. Melon, pineapple, kiwi and other tropical fruits (medium serving)	0	1	2	3	4	5	6	7	8	9
7. Green salad e.g. lettuce, cucumber, celery	0	1	2	3	4	5	6	7	8	9
8. Garlic - raw and cooked (finely)	0	1	2	3	4	5	6	7	8	9
9. Marrow and courgettes	0	1	2	3	4	5	6	7	8	9
10. Peppers - cooked & fresh	0	1	2	3	4	5	6	7	8	9
11. Yogurt (125g pot)	0	1	2	3	4	5	6	7	8	9
12. Eggs as boiled, fried, scrambled etc. (one egg)	0	1	2	3	4	5	6	7	8	9
13. White fish e.g. cod, haddock, salmon, sole, plaice, bass, etc. (one serving)	0	1	2	3	4	5	6	7	8	9
14. City fish, e.g. mackerel, tuna, salmon	0	1	2	3	4	5	6	7	8	9
15. Bacon and Gammon	0	1	2	3	4	5	6	7	8	9
16. Meat pies, e.g. one, one, one, steak & kidney, sausage rolls	0	1	2	3	4	5	6	7	8	9
17. Baked, mixed and liquid pastas (one egg size portion)	0	1	2	3	4	5	6	7	8	9
18. Chips	0	1	2	3	4	5	6	7	8	9
19. Pasta e.g. spaghetti, macaroni	0	1	2	3	4	5	6	7	8	9
Which is the main spreading fat you have used for example on bread, toast or vegetables and how often do you consume this?										
20. Spreading fat (optional) Please name the spreading fat you use -	0	1	2	3	4	5	6	7	8	9

22. Please detail below the type of milk you have drunk over the last 3 months	23. On average, over the past 3 months, how much milk have you consumed per day?
22. Type of milk Example: Whole	Please tick ✓
1. Whole pasteurised or UHT	0.5 pints or 1/2 pint per day
2. Semi-skimmed pasteurised (include 1% milk) or UHT	_____ pints per day
3. Skimmed pasteurised or UHT	_____ pints per day
4. Other (Please specify)	_____ pints per day
5. None	_____ pints per day

24. Have you added sugar to tea and coffee or breakfast cereals in the past 3 months?  
If no, go to question 29  Yes  No

25. Approximately how many teaspoons of sugar have you added each day?

**SECTION TWO: PATIENT REPORTED OUTCOMES**

26. In terms of quality of life, please indicate which statement best describes your quality of life (Tick one box for each statement section 1-6)

a. Mobility	i. I have no problems or walking around	<input type="checkbox"/>
	ii. I have some problems or walking around	<input type="checkbox"/>
	iii. I am confined to bed	<input type="checkbox"/>
b. Self-care	i. I have no problems with self-care	<input type="checkbox"/>
	ii. I have some problems washing or dressing myself	<input type="checkbox"/>
	iii. I am unable to wash or dress myself	<input type="checkbox"/>
c. Usual Activities (e.g. work, study, housework, family or leisure activities)	i. I have no problems with performing my usual activities	<input type="checkbox"/>
	ii. I have some problems with performing my usual activities	<input type="checkbox"/>
	iii. I am unable to perform my usual activities	<input type="checkbox"/>
d. Pain/discomfort	i. I have no pain or discomfort	<input type="checkbox"/>
	ii. I have moderate pain or discomfort	<input type="checkbox"/>
	iii. I have extreme pain or discomfort	<input type="checkbox"/>
e. Anxiety/Depression	i. I am not anxious or depressed	<input type="checkbox"/>
	ii. I am moderately anxious or depressed	<input type="checkbox"/>
	iii. I am extremely anxious or depressed	<input type="checkbox"/>



To help people compare their health state to others, we have drawn a line on the scale to show how your health state is today. Please do this by drawing a line in the box below to whichever point on the scale you think best describes your health state today.

Your own health state today



We would like to know how good or how bad your health state is today. Please do this by drawing a line in the box below to whichever point on the scale you think best describes your health state today.

**SECTION THREE: PHYSICAL FUNCTIONING**  
*(Explanation: with walking outside we mean walking to go shopping or doing other daily activities like visiting someone. We do not mean a walking tour)*

28. Did you walk during the past two weeks? <i>If no, please go to question 32</i>	<input type="checkbox"/> Yes <input type="checkbox"/> No	<input type="checkbox"/> Yes <input type="checkbox"/> No
29. How many times did you walk in the past two weeks? <i>If no, please go to question 32</i>		mins
30. How long did you usually walk for each time?		mins
31. Do you cycle? <i>(Explanation: with cycling we mean cycling to go shopping or doing other daily activities like visiting someone. We do not mean a cycling tour)</i>	<input type="checkbox"/> Yes <input type="checkbox"/> No	mins
32. Did you cycle during the past two weeks? <i>If no, please go to question 36</i>	<input type="checkbox"/> Yes <input type="checkbox"/> No	
33. How many times did you cycle in the past two weeks? <i>If no, please go to question 36</i>	<input type="checkbox"/> Yes <input type="checkbox"/> No	
34. How long did you usually cycle for each time?		mins
35. Do you have a garden (including allotment)? <i>If no, please go to question 42</i>	<input type="checkbox"/> Yes <input type="checkbox"/> No	mins
36. How many times did you work in your garden? <i>If no, please go to question 42</i>	<input type="checkbox"/> Yes <input type="checkbox"/> No	months
37. Did you work in the garden (or allotment) during the past two weeks? <i>If no, please go to question 42</i>	<input type="checkbox"/> Yes <input type="checkbox"/> No	
38. How many times did you work in the garden (or allotment) in the past two weeks?		mins
39. How long did you usually work in the garden (or allotment) for each time?		mins
40. Did you dig the earth in your garden during the past two weeks? <i>If no, please go to question 42</i>	<input type="checkbox"/> Yes <input type="checkbox"/> No	
41. Do you take part in any sporting activities? (Sports include those activities listed in question 43) <i>If no, please go to question 51</i>	<input type="checkbox"/> Yes <input type="checkbox"/> No	
42. Which sport did you take part in most during the past two weeks?		
i. Distance walking	<input type="checkbox"/>	
ii. Distance cycling	<input type="checkbox"/>	
iii. Gymnastics	<input type="checkbox"/>	
iv. Cycling on a home trainer	<input type="checkbox"/>	
v. Swimming	<input type="checkbox"/>	
vi. Dancing	<input type="checkbox"/>	
vii. Bowling	<input type="checkbox"/>	
viii. Tennis, badminton	<input type="checkbox"/>	
ix. Running, fast walking	<input type="checkbox"/>	
x. Rowing	<input type="checkbox"/>	
xi. Sailing	<input type="checkbox"/>	
xii. Play billiards	<input type="checkbox"/>	
xiii. Fishing	<input type="checkbox"/>	
xiv. Playing soccer/basketball/hockey	<input type="checkbox"/>	
xv. Playing volleyball/baseball	<input type="checkbox"/>	
xvi. Skiing	<input type="checkbox"/>	
xvii. Other (please describe):		
43. How many times did you perform the sporting activity for in the past two weeks? <i>If no, please go to question 51</i>		mins
44. For how long did you usually perform the sporting activity for each time?		mins
45. How many times did you perspire while taking part in sport during the past two weeks? <i>(Explanation: with heavy household tasks we mean washing the dishes, dusting, making the bed, doing the laundry, hanging out the laundry, mowing, drying up and cooking meals)</i>	<input type="checkbox"/> Yes <input type="checkbox"/> No	
46. For how long did you usually do light household tasks during the past two weeks? <i>(Explanation: by heavy household tasks we mean window cleaning, changing the bed, heating the mat, vacuuming, washing or scrubbing the floor, and mows with sawing, carpentry, repairing or painting)</i>	<input type="checkbox"/> Yes <input type="checkbox"/> No	
47. How many days did you usually do light household tasks during the past two weeks? <i>If no, please go to question 54</i>		mins
48. How long per day did you usually do light household tasks for?		mins
49. Do you do heavy household tasks? <i>(Explanation: by heavy household tasks we mean window cleaning, changing the bed, heating the mat, vacuuming, washing or scrubbing the floor, and mows with sawing, carpentry, repairing or painting)</i>	<input type="checkbox"/> Yes <input type="checkbox"/> No	
50. How many days did you usually do heavy household tasks during the past two weeks? <i>If no, please go to question 54</i>		mins
51. How long per day did you usually do heavy household tasks for?		mins

44. How many times did you take part in this sporting activity in the past two weeks?		
45. For how long did you usually perform this sporting activity for each time?		mins
46. Do you take part in any other sporting activities? (Sports include those activities listed in question 43) <i>If no, please go to question 50</i>	<input type="checkbox"/> Yes <input type="checkbox"/> No	
47. Which other sport did you take part in most during the past two weeks?		
i. Distance walking	<input type="checkbox"/>	
ii. Distance cycling	<input type="checkbox"/>	
iii. Gymnastics	<input type="checkbox"/>	
iv. Cycling on a home trainer	<input type="checkbox"/>	
v. Swimming	<input type="checkbox"/>	
vi. Dancing	<input type="checkbox"/>	
vii. Bowling	<input type="checkbox"/>	
viii. Tennis, badminton	<input type="checkbox"/>	
ix. Running, fast walking	<input type="checkbox"/>	
x. Rowing	<input type="checkbox"/>	
xi. Sailing	<input type="checkbox"/>	
xii. Play billiards	<input type="checkbox"/>	
xiii. Fishing	<input type="checkbox"/>	
xiv. Playing soccer/basketball/hockey	<input type="checkbox"/>	
xv. Playing volleyball/baseball	<input type="checkbox"/>	
xvi. Skiing	<input type="checkbox"/>	
xvii. Other (please describe):		
48. How many times did you perform the sporting activity for in the past two weeks? <i>If no, please go to question 51</i>		mins
49. For how long did you usually perform the sporting activity for each time?		mins
50. How many times did you perspire while taking part in sport during the past two weeks? <i>(Explanation: with heavy household tasks we mean washing the dishes, dusting, making the bed, doing the laundry, hanging out the laundry, mowing, drying up and cooking meals)</i>	<input type="checkbox"/> Yes <input type="checkbox"/> No	
51. How many days did you usually do light household tasks during the past two weeks? <i>(Explanation: by heavy household tasks we mean window cleaning, changing the bed, heating the mat, vacuuming, washing or scrubbing the floor, and mows with sawing, carpentry, repairing or painting)</i>	<input type="checkbox"/> Yes <input type="checkbox"/> No	
52. How many days did you usually do light household tasks during the past two weeks? <i>If no, please go to question 54</i>		mins
53. How long per day did you usually do light household tasks for?		mins
54. Do you do heavy household tasks? <i>(Explanation: by heavy household tasks we mean window cleaning, changing the bed, heating the mat, vacuuming, washing or scrubbing the floor, and mows with sawing, carpentry, repairing or painting)</i>	<input type="checkbox"/> Yes <input type="checkbox"/> No	
55. How many days did you usually do heavy household tasks during the past two weeks? <i>If no, please go to question 54</i>		mins
56. How long per day did you usually do heavy household tasks for?		mins

57. You just told me about your usual activities in the past two weeks. Were the past two weeks normal as compared to the rest of the last year?  
*If Yes, please go to question 59*

58. Why were the past two weeks not 'normal'?

I. Disease  Yes  No  
 II. Depression   
 III. Bad weather   
 IV. Family occasion   
 V. Holiday   
 VI. Other (please specify) \_\_\_\_\_

**SECTION FOUR: HEALTH AND SOCIAL CARE**

59. During the last year, have you been hospitalised?  
*If No, please go to question 62*

60. How many times have you been hospitalised in the last year?

61. How many days in total?

62. How many times did you visit the following in the last month:  
*If No, please go to question 65, c etc. section*

A. General practitioner (GP)

I. Daily   
 II. 3 times per week   
 III. Once a week   
 IV. Twice per month   
 V. Once per month   
 VI. Never

B. A Nurse?

I. Daily   
 II. 3 times per week   
 III. Once a week   
 IV. Twice per month   
 V. Once per month   
 VI. Never

C. A Physiotherapist?

I. Daily   
 II. 3 times per week   
 III. Once a week   
 IV. Twice per month   
 V. Once per month   
 VI. Never

D. A Psychiatrist?

I. Daily   
 II. 3 times per week   
 III. Once a week   
 IV. Twice per month   
 V. Once per month   
 VI. Never

63. How many times did you receive a visit in the last month from:  
*Please tick one box for each letter (A, B, C etc.) section*

A. A general practitioner (GP)

I. Daily   
 II. 3 times per week   
 III. Once a week   
 IV. Twice per month   
 V. Once per month   
 VI. Never

B. A Nurse?

I. Daily   
 II. 3 times per week   
 III. Once a week   
 IV. Twice per month   
 V. Once per month   
 VI. Never

C. A Physiotherapist?

I. Daily   
 II. 3 times per week   
 III. Once a week   
 IV. Twice per month   
 V. Once per month   
 VI. Never

64. How many times did you visit a medical specialist (neurology, trauma and orthopaedics) in the last year? *Please tick one box*

I. 1-5   
 II. 6-15   
 III. 16-20   
 IV. >20   
 V. Never

65. Have you gone to a Day Care Senior Centre in the last year?  
*If No, please go to question 67*

66. How often did you go to this centre? *Please tick one box*

I. Daily   
 II. 3-4 times per week   
 III. Once a week   
 IV. Twice per month   
 V. Once a month

67. Have you received formal care at home in the last year?  
*If No, please go to question 71*

68. Was this provided by social services or privately funded? *(see - social services, private - privately funded)*

I. Domestic care  Yes  No  
 II. Personal care  Soc  Private   
 III. Both

70. How often did you receive this help? *Please tick one box*

I. Daily   
 II. 3-4 times per week   
 III. Once a week   
 IV. Twice per month   
 V. Once a month

71. Have you received informal care at home in the last year?  
*If No, please go to question 75*

72. What kind of help? *Please tick one box*

I. Domestic care   
 II. Personal care   
 III. Both

73. Who gave you this help?

I. Wife or husband   
 II. Son/daughter   
 III. Other relatives   
 IV. Neighbours   
 V. Friends

74. How often did you receive this help? *Please tick one box*

I. Daily   
 II. 3-4 times per week   
 III. Once a week   
 IV. Twice per month

75. Have you been living in a residential home (RH) or nursing home (NH) in the last year? *Please tick one box*

I. No   
 II. Yes, previously   
 III. Yes, currently

SECTION FIVE: PHYSICAL EXAMINATION. TO BE COMPLETED BY RESEARCHER		
76. Height (m)		
77. Weight (kg)		
78. Waist circumference (m)		
i. 1 <sup>st</sup> measurement		
ii. 2 <sup>nd</sup> measurement		
79. Calf circumference (m)		
i. 1 <sup>st</sup> measurement		
ii. 2 <sup>nd</sup> measurement		
80. Semi-tandem stand (time in seconds)		
<i>If semi-tandem 10 seconds or more then please move to tandem stand (i.e. do not perform side-by-side stand) If under 10 seconds, please go to side-by-side stand</i>		
i. Side-by-side stand (time in seconds)		
ii. Tandem stand (time in seconds)		
81. Walking speed		
i. Walk time 1 (in seconds)		
ii. Walk time 2 (in seconds)		
82. Is patient able to stand up from sitting with arms folded?	<input type="checkbox"/> Yes	<input type="checkbox"/> No
i. Time for five repetitions (seconds)		
83. Timed up and Go (6m) – (seconds)		
84. Grip Strength (kg):	R	L
i. First attempt		
ii. Second attempt		
iii. Third attempt		



**Appendix 6:** Descriptive statistics for radial HR-pQCT parameters at baseline (2011-2012) and for changes in parameters from EPOSA to HBS17<sup>220</sup>

Parameter [Median (lower quartile, upper quartile) values shown]	Males (n=115)			Females (n=99)		
	Baseline	Annual change (%)	P-value	Baseline	Annual change (%)	P-value
Trabecular area (mm <sup>2</sup> )	332 (291, 376)	<b><u>0.1 (0.0, 0.3)</u></b>	<b>&lt;0.001</b>	226 (202, 268)	<b><u>0.1 (0.0, 0.2)</u></b>	<b>&lt;0.001</b>
Total volumetric bone density (mg/cm <sup>3</sup> )	297 (266, 339)	<b><u>-0.6 (-1.1, 0.0)</u></b>	<b>&lt;0.001</b>	244 (215, 302)	<b><u>-0.7 (-1.4, -0.2)</u></b>	<b>&lt;0.001</b>
Trabecular density (mg/cm <sup>3</sup> )	186 (163, 210)	-0.1 (-0.6, 0.2)	0.368	150 (127, 176)	-0.2 (-0.8, 0.2)	0.053
Trabecular number (mm <sup>-1</sup> )	2.4 (2.3, 2.5)	0.0 (-1.2, 0.8)	0.920	2.2 (2.0, 2.4)	<b><u>-0.5 (-1.3, 0.4)</u></b>	<b>0.004</b>
Trabecular thickness (mm)	0.066 (0.059, 0.071)	0.0 (-0.9, 0.7)	1.000	0.055 (0.051, 0.065)	0.3 (-0.8, 1.0)	0.550
Trabecular separation (mm)	0.36 (0.33, 0.38)	0.0 (-0.8, 1.4)	1.000	0.40 (0.36, 0.44)	<b><u>0.7 (-0.4, 1.4)</u></b>	<b>0.012</b>
Cortical area (mm <sup>2</sup> )	67 (57, 75)	<b><u>-1.0 (-1.8, -0.2)</u></b>	<b>&lt;0.001</b>	43 (37, 49)	<b><u>-1.0 (-1.6, 0.1)</u></b>	<b>&lt;0.001</b>
Cortical density (mg/cm <sup>3</sup> )	827 (793, 870)	<b><u>-0.4 (-0.7, -0.1)</u></b>	<b>&lt;0.001</b>	811 (775, 848)	<b><u>-0.6 (-0.8, -0.2)</u></b>	<b>&lt;0.001</b>
Cortical porosity (%)	4.1 (3.1, 5.0)	<b><u>2.0 (-0.6, 4.4)</u></b>	<b>&lt;0.001</b>	3.7 (2.5, 4.5)	1.5 (-1.3, 5.7)	0.091
Cortical thickness (mm)	0.8 (0.7, 1.0)	<b><u>-0.8 (-1.5, 0.1)</u></b>	<b>&lt;0.001</b>	0.7 (0.6, 0.8)	<b><u>-0.8 (-1.3, 0.1)</u></b>	<b>&lt;0.001</b>
Cortical pore diameter (mm)	0.15 (0.15, 0.16)	0.2 (-0.5, 1.4)	0.129	0.15 (0.15, 0.17)	<b><u>0.3 (-0.5, 1.2)</u></b>	<b>0.039</b>

P-values correspond to tests that median annual percentage changes were zero and were calculated from sign tests

Median annual percentage changes that were significantly different from zero (p<0.05) are highlighted in bold (underlined for increases and italic for decreases)

**Appendix 7:** Odds ratios for previous fracture per standard deviation difference in both baseline values and changes in parameters at the radius<sup>220</sup>

HR-pQCT (SD)	radial parameter	Baseline values in 2011-2012				Annual percentage change from 2011-2012 to 2017			
		Sex-adjusted		Fully-adjusted*		Sex-adjusted		Fully-adjusted*	
		Odds ratio (95% CI)	P-value	Odds ratio (95% CI)	P-value	Odds ratio (95% CI)	P-value	Odds ratio (95% CI)	P-value
Trabecular area		1.34 (0.84,2.13)	0.216	<b>1.86 (1.04,3.34)</b>	<b>0.038</b>	0.82 (0.57,1.17)	0.265	0.81 (0.55,1.21)	0.305
Total volumetric bone density		0.75 (0.51,1.11)	0.152	0.70 (0.44,1.12)	0.141	0.98 (0.69,1.39)	0.902	0.97 (0.65,1.43)	0.860
Trabecular density		0.85 (0.58,1.26)	0.426	0.78 (0.49,1.23)	0.284	0.69 (0.48,1.00)	0.052	0.67 (0.44,1.01)	0.059
Trabecular number		0.94 (0.65,1.36)	0.746	0.93 (0.60,1.44)	0.753	0.83 (0.58,1.18)	0.293	0.77 (0.52,1.15)	0.205
Trabecular thickness		0.82 (0.56,1.20)	0.306	0.73 (0.47,1.13)	0.161	1.02 (0.72,1.45)	0.900	1.08 (0.73,1.58)	0.707
Trabecular separation		1.11 (0.76,1.63)	0.577	1.14 (0.73,1.77)	0.576	1.22 (0.85,1.74)	0.276	1.31 (0.87,1.96)	0.195
Cortical area		0.78 (0.47,1.30)	0.342	1.11 (0.61,2.03)	0.739	1.07 (0.75,1.52)	0.703	1.01 (0.67,1.50)	0.971
Cortical density		0.78 (0.54,1.13)	0.184	0.78 (0.50,1.21)	0.260	1.04 (0.73,1.47)	0.842	1.05 (0.71,1.57)	0.800
Cortical porosity		0.94 (0.66,1.35)	0.746	0.92 (0.60,1.40)	0.685	0.93 (0.65,1.31)	0.668	0.94 (0.63,1.42)	0.780
Cortical thickness		0.71 (0.47,1.07)	0.104	0.78 (0.48,1.26)	0.308	1.02 (0.72,1.45)	0.908	0.93 (0.62,1.39)	0.733
Cortical pore diameter		<b>0.63 (0.44,0.92)</b>	<b>0.015</b>	<b>0.52 (0.34,0.80)</b>	<b>0.003</b>	1.20 (0.84,1.73)	0.318	1.40 (0.92,2.11)	0.116

HR-pQCT: High resolution peripheral quantitative computed tomography; CI: Confidence interval

\*Adjusted for sex, age, height, BMI, dietary calcium, physical activity, smoking history (ever vs never), alcohol consumption and social class

Odds ratio of less than one for annual percentage change in parameter shows that reduced declines are related to lower risk of previous fracture

Significant associations (p<0.05) are given in italics

**Appendix 8:** Odds ratios for previous fracture per standard deviation difference in both baseline values and changes in parameters for fully-adjusted models and those additionally adjusted for bisphosphonate usage.

	Fully-adjusted		Additionally adjusted for bisphosphonate use	
<b>Tibial (baseline values)</b>				
Trabecular area (mm <sup>2</sup> )	<b>2.18 (1.27,3.73)</b>	<b>0.005</b>	<b>2.17 (1.26,3.74)</b>	<b>0.005</b>
Total volumetric bone density (mg/cm <sup>3</sup> )	<b>0.53 (0.34,0.84)</b>	<b>0.007</b>	<b>0.55 (0.35,0.87)</b>	<b>0.011</b>
Trabecular density (mg/cm <sup>3</sup> )	0.72 (0.49,1.06)	0.099	0.76 (0.51,1.12)	0.164
Trabecular number (mm <sup>-1</sup> )	0.96 (0.64,1.43)	0.836	1.02 (0.67,1.54)	0.935
Trabecular thickness (mm)	0.69 (0.48,1.00)	0.052	0.71 (0.48,1.03)	0.07
Trabecular separation (um)	1.10 (0.74,1.64)	0.626	1.04 (0.69,1.57)	0.861
Cortical area (mm <sup>2</sup> )	<b>0.53 (0.30,0.95)</b>	<b>0.032</b>	<b>0.55 (0.31,0.97)</b>	<b>0.04</b>
Cortical bone mineral density (mg/cm <sup>3</sup> )	<b>0.56 (0.36,0.88)</b>	<b>0.011</b>	<b>0.57 (0.37,0.90)</b>	<b>0.015</b>
Cortical porosity (%)	0.96 (0.67,1.37)	0.808	0.93 (0.65,1.35)	0.718
Cortical thickness (mm)	<b>0.45 (0.27,0.77)</b>	<b>0.004</b>	<b>0.46 (0.27,0.79)</b>	<b>0.004</b>
Cortical pore diameter (um)	0.71 (0.49,1.03)	0.07	0.69 (0.48,1.01)	0.057
<b>Tibial (longitudinal changes)</b>				
Trabecular area % change	1.01 (0.71,1.44)	0.945	0.99 (0.69,1.42)	0.969
Total volumetric bone density % change	0.75 (0.53,1.07)	0.117	0.76 (0.53,1.09)	0.13
Trabecular density % change	<b>0.50 (0.34,0.75)</b>	<b>0.001</b>	<b>0.49 (0.33,0.74)</b>	<b>0.001</b>
Trabecular number % change	0.91 (0.64,1.29)	0.584	0.88 (0.62,1.27)	0.499
Trabecular thickness % change	0.88 (0.62,1.27)	0.502	0.90 (0.63,1.30)	0.577
Trabecular separation % change	1.13 (0.79,1.60)	0.515	1.16 (0.81,1.66)	0.431
Cortical area % change	0.98 (0.68,1.40)	0.908	0.99 (0.69,1.42)	0.966
Cortical bone mineral density % change	1.00 (0.70,1.42)	0.987	1.00 (0.70,1.42)	0.987
Cortical porosity % change	0.73 (0.51,1.05)	0.09	0.75 (0.52,1.08)	0.123
Cortical thickness % change	0.91 (0.64,1.30)	0.597	0.90 (0.63,1.29)	0.564
Cortical pore diameter % change	0.82 (0.56,1.20)	0.309	0.84 (0.57,1.24)	0.376

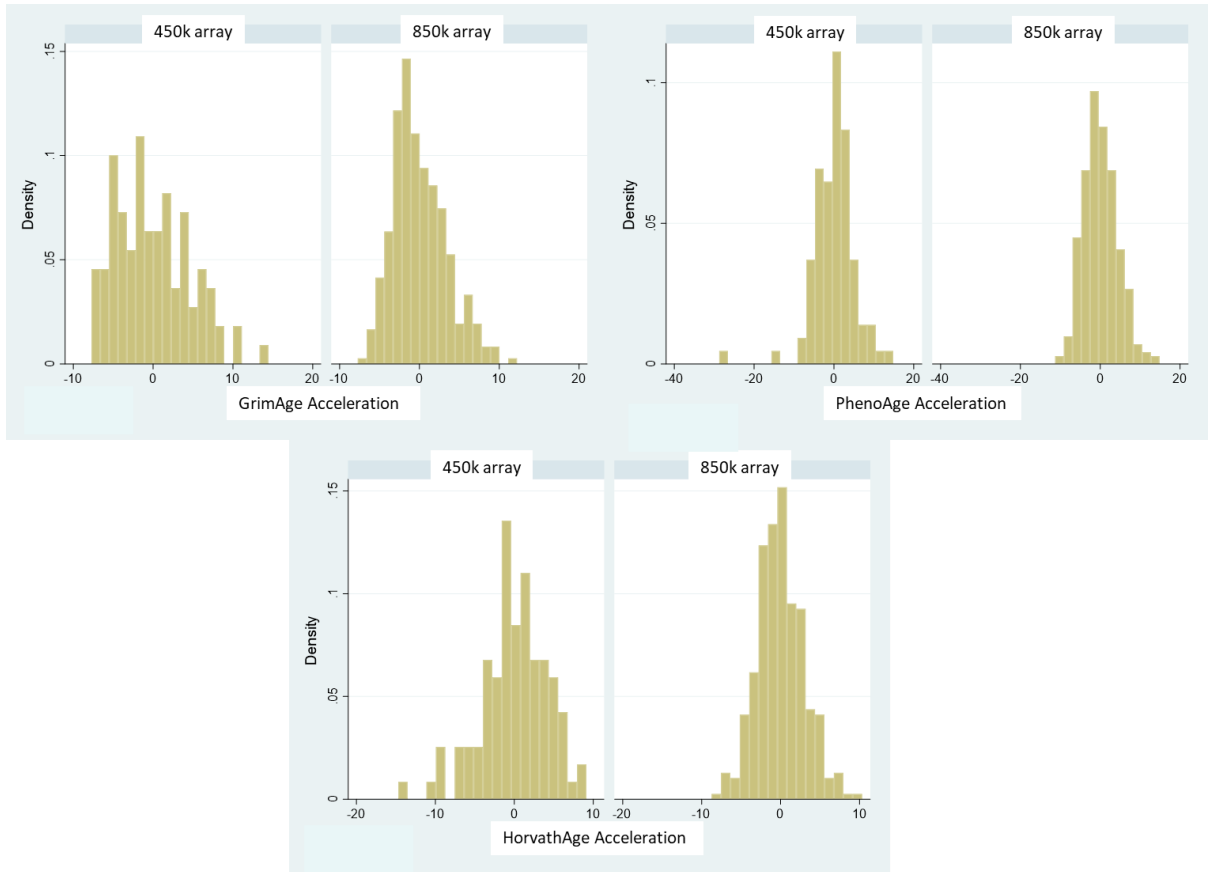
**Appendix 9:** Odds of fracture associated with Z-scores of baseline and percentage change in grip strength and baseline and percentage change in femoral neck BMD.

Unadjusted models and those adjusted for age, sex, dietary calcium, physical activity, alcohol consumption, smoking and social class are included. Change variables were additionally adjusted for follow-up time. The odds ratios and p-values for additional adjustment of bisphosphonate use for bone outcomes is shown in the columns on the right.

Z-scores	Unadjusted		Adjusted		Adjusted with bisphosphonates	
	Odds Ratio	p-value	Odds Ratio	p-value	Odds Ratio	p-value
Baseline grip strength	0.96	0.80	0.97	0.86	NA	NA
Percentage change in grip strength	0.77	0.10	0.73	0.08	NA	NA
Baseline femoral neck BMD	<b>0.61</b>	<b>0.003</b>	<b>0.54</b>	<b>0.006</b>	<b>0.60</b>	<b>0.01</b>
Percentage change in femoral neck BMD	1.30	0.14	1.42	0.09	1.35	0.18

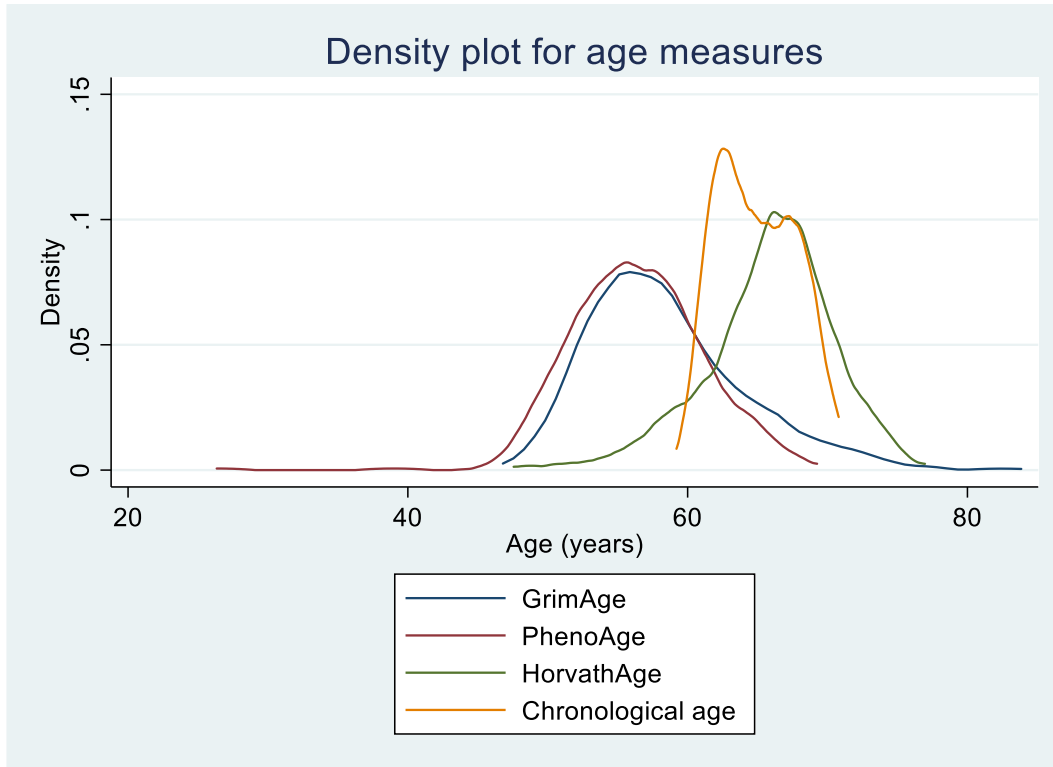


**Appendix 10:** Histograms for epigenetic age acceleration distribution for HorvathAge acceleration, PhenoAge acceleration and GrimAge acceleration within the 450k (left) and 850k (right) arrays.

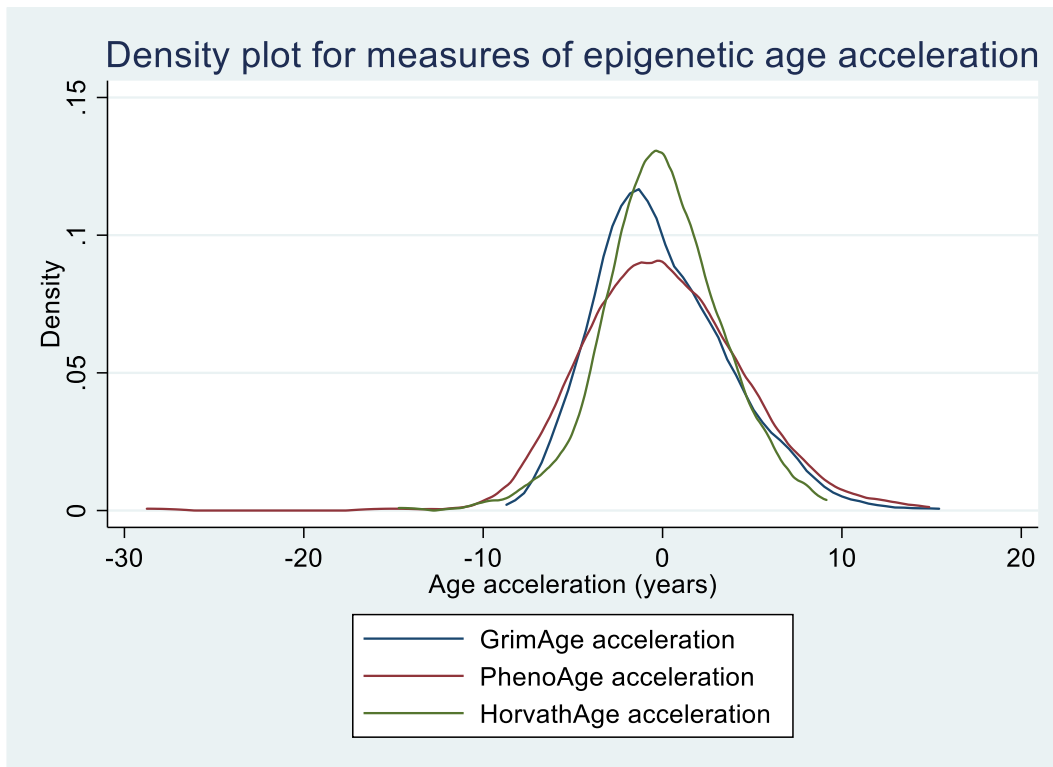


**Appendix 11:** Density plots depicting the distribution of epigenetic age and chronological age (A) and epigenetic age acceleration measures (B).

A



B



**Appendix 12:** Regression coefficients and p-values for associations between **PhenoAge** Acceleration and maximum grip strength and gait speed measured at HCS baseline (1998-2004), EPOSA (2011-12) and HBS17 (2017).

Model 1 is unadjusted, Model 2 is adjusted for age, height and BMI and Model 3 is adjusted additionally for social class, physical activity, prudent diet, ever smoked regularly and alcohol consumption. Red highlighting indicates a statistically significant result ( $p < 0.05$ ).

Grip	Model 1				Model 2				Model 3			
	Males		Females		Males		Females		Males		Females	
	beta	p	beta	p	beta	p	beta	p	beta	p	beta	p
Baseline	-0.64 (-1.56,0.27)	0.165	-0.16 (-0.87,0.55)	0.665	-0.63 (-1.42,0.16)	0.119	-0.15 (-0.86,0.56)	0.68	-0.57 (-1.39,0.26)	0.179	-0.14 (-0.86,0.57)	0.694
EPOSA	<b>-1.10 (-2.06,-0.15)</b>	<b>0.024</b>	0.25 (-0.64,1.14)	0.58	<b>-1.05 (-1.94,-0.16)</b>	<b>0.021</b>	0.36 (-0.52,1.23)	0.425	-0.88 (-1.80,0.04)	0.062	0.32 (-0.55,1.18)	0.474
HBS17	-0.87 (-2.19,0.44)	0.191	-0.18 (-1.33,0.96)	0.753	-0.69 (-1.88,0.50)	0.252	-0.07 (-1.19,1.04)	0.894	-0.56 (-1.83,0.71)	0.383	-0.12 (-1.25,1.01)	0.835
Gait	Model 1				Model 2				Model 3			
	Males		Females		Males		Females		Males		Females	
	beta	p	beta	p	beta	p	beta	p	beta	p	beta	p
Baseline	NA	NA	-0.01 (-0.04,0.02)	0.402	NA	NA	-0.00 (-0.03,0.02)	0.766	NA	NA	-0.00 (-0.03,0.02)	0.748
EPOSA	-0.02 (-0.04,0.01)	0.199	-0.01 (-0.04,0.02)	0.416	-0.01 (-0.03,0.02)	0.612	-0.01 (-0.03,0.02)	0.64	-0.01 (-0.03,0.02)	0.573	-0.00 (-0.03,0.02)	0.771
HBS17	<b>-0.04 (-0.07,-0.01)</b>	<b>0.008</b>	-0.01 (-0.05,0.03)	0.488	-0.03 (-0.06,0.00)	0.062	-0.01 (-0.05,0.03)	0.75	<b>-0.04 (-0.07,-0.00)</b>	<b>0.035</b>	-0.00 (-0.04,0.04)	0.938

**Appendix 13:** Regression coefficients and p-values for associations between **HorvathAge** Acceleration and maximum grip strength and gait speed measured at HCS baseline (1998-2004), EPOSA (2011-12) and HBS17 (2017).

Model 1 is unadjusted, Model 2 is adjusted for age, height and BMI and Model 3 is adjusted additionally for social class, physical activity, prudent diet, ever smoked regularly and alcohol consumption. Statistically significant results are highlighted in red ( $p < 0.05$ ).

Grip	Model 1				Model 2				Model 3			
	Males		Females		Males		Females		Males		Females	
	beta	p	beta	p	beta	p	beta	p	beta	p	beta	p
Baseline	-0.22 (-1.17,0.74)	0.656	0.07 (-0.63,0.76)	0.847	0.13 (-0.69,0.96)	0.748	0.07 (-0.62,0.76)	0.845	0.32 (-0.52,1.16)	0.452	-0.02 (-0.71,0.68)	0.963
EPOSA	-0.53 (-1.57,0.50)	0.313	0.10 (-0.78,0.97)	0.831	0.02 (-0.94,0.99)	0.96	0.18 (-0.69,1.04)	0.685	0.07 (-0.90,1.04)	0.886	0.09 (-0.76,0.95)	0.832
HBS17	-0.43 (-2.00,1.14)	0.588	-0.57 (-1.75,0.61)	0.338	0.02 (-1.34,1.38)	0.974	-0.58 (-1.72,0.55)	0.308	0.23 (-1.21,1.67)	0.754	-0.36 (-1.51,0.79)	0.535
Gait	Model 1				Model 2				Model 3			
	Males		Females		Males		Females		Males		Females	
	beta	p	beta	p	beta	p	beta	p	beta	p	beta	p
Baseline	NA	NA	-0.03 (-0.06,-0.00)	0.032	NA	NA	-0.03 (-0.06,-0.00)	0.027	NA	NA	-0.03 (-0.06,-0.00)	0.026
EPOSA	-0.02 (-0.04,0.01)	0.199	-0.01 (-0.04,0.02)	0.416	-0.01 (-0.03,0.02)	0.612	-0.01 (-0.03,0.02)	0.64	-0.01 (-0.03,0.02)	0.573	-0.00 (-0.03,0.02)	0.771
HBS17	-0.01 (-0.04,0.03)	0.751	0.00 (-0.04,0.04)	0.973	-0.00 (-0.04,0.04)	0.985	-0.00 (-0.04,0.04)	0.866	-0.01 (-0.05,0.03)	0.658	-0.00 (-0.05,0.04)	0.854

**Appendix 14:** Regression coefficients and p-values for associations between epigenetic age acceleration measures and percentage and absolute change in gait speed between EPOSA (2011-12) and HBS17 (2017).

Model 1 is unadjusted, Model 2 is adjusted for age, height and BMI and follow-up time and Model 3 is adjusted additionally for social class, physical activity, prudent diet, ever smoked regularly and alcohol consumption. Red highlighting indicates a statistically significant result (p<0.05).

percentage change in gait speed	Model 1				Model 2				Model 3			
	Males		Females		Males		Females		Males		Females	
	beta	p	beta	p	beta	p	beta	p	beta	p	beta	p
GrimAge Acceleration	-3.38 (-8.37,1.62)	0.183	-3.94 (-10.60,2.71)	0.242	-2.49 (-7.95,2.96)	0.366	-3.52 (-10.22,3.18)	0.3	-1.11 (-7.65,5.42)	0.735	-3.13 (-11.03,4.78)	0.434
PhenoAge Acceleration	-1.19 (-5.30,2.92)	0.566	-1.50 (-7.54,4.55)	0.624	-0.33 (-4.72,4.06)	0.883	-1.55 (-7.51,4.41)	0.605	-0.61 (-5.23,4.01)	0.793	-0.76 (-6.98,5.45)	0.808
Horvath Age Acceleration	0.19 (-4.75,5.13)	0.939	1.31 (-4.89,7.50)	0.676	0.84 (-4.20,5.88)	0.741	0.68 (-5.38,6.75)	0.823	0.18 (-5.11,5.46)	0.947	0.26 (-6.06,6.58)	0.934
absolute change in gait speed	Model 1				Model 2				Model 3			
	Males		Females		Males		Females		Males		Females	
	beta	p	beta	p	beta	p	beta	p	beta	p	beta	p
GrimAge Acceleration	0.01 (-0.02,0.05)	0.456	0.04 (-0.01,0.08)	0.103	0.01 (-0.04,0.05)	0.714	0.03 (-0.01,0.08)	0.122	-0.01 (-0.06,0.04)	0.771	0.03 (-0.02,0.08)	0.238
PhenoAge Acceleration	0.00 (-0.03,0.04)	0.836	0.01 (-0.03,0.05)	0.726	-0.00 (-0.04,0.03)	0.914	0.01 (-0.03,0.05)	0.686	-0.00 (-0.04,0.04)	0.941	-0.00 (-0.04,0.04)	0.996
Horvath Age Acceleration	-0.00 (-0.04,0.03)	0.847	-0.01 (-0.05,0.03)	0.593	-0.01 (-0.05,0.03)	0.677	-0.01 (-0.05,0.03)	0.719	-0.00 (-0.05,0.04)	0.816	-0.00 (-0.05,0.04)	0.834

**Appendix 15:** Regression coefficients and p-values for associations between epigenetic age acceleration measures and percentage and absolute change in gait speed from HCS baseline (1998-2004) to EPOSA (2011-12, upper table) or HBS17 (2017, lower table).

Model 1 is unadjusted, Model 2 is adjusted for age, height and BMI and follow-up time and Model 3 is adjusted additionally for social class, physical activity, prudent diet, ever smoked regularly and alcohol consumption. Red highlighting indicates a statistically significant result ( $p < 0.05$ ).

<b>HCS baseline to EPOSA</b>						
	Model 1		Model 2		Model 3	
	Females		Females		Females	
	beta	p	beta	p	beta	p
<b>percentage change in gait speed</b>						
GrimAge Acceleration	<b>-5.32 (-10.33,-0.31)</b>	<b>0.038</b>	-4.25 (-9.40,0.89)	0.104	-3.40 (-9.17,2.37)	0.244
PhenoAge Acceleration	-3.60 (-7.49,0.28)	0.069	-3.18 (-7.12,0.77)	0.113	-3.34 (-7.35,0.67)	0.101
Horvath Age Acceleration (residual)	-1.86 (-6.13,2.41)	0.389	-1.40 (-5.70,2.90)	0.52	-1.17 (-5.48,3.14)	0.591
	Model 1		Model 2		Model 3	
	Females		Females		Females	
	beta	p	beta	p	beta	p
<b>absolute change in gait speed</b>						
GrimAge Acceleration	0.04 (-0.01,0.09)	0.108	0.04 (-0.02,0.09)	0.178	0.03 (-0.03,0.08)	0.381
PhenoAge Acceleration	0.03 (-0.01,0.06)	0.19	0.02 (-0.02,0.06)	0.239	0.03 (-0.01,0.07)	0.212
Horvath Age Acceleration (residual)	0.01 (-0.03,0.05)	0.658	0.01 (-0.04,0.05)	0.76	0.00 (-0.04,0.05)	0.83
<b>HCS baseline to HBS17</b>						
	Model 1		Model 2		Model 3	
	Females		Females		Females	
	beta	p	beta	p	beta	p
<b>percentage change in gait speed</b>						
GrimAge Acceleration	-3.03 (-11.21,5.16)	0.459	-1.51 (-10.80,7.77)	0.743	0.75 (-8.75,10.25)	0.874
PhenoAge Acceleration	-0.24 (-6.82,6.34)	0.941	0.83 (-6.23,7.90)	0.812	1.13 (-6.36,8.63)	0.76
Horvath Age Acceleration (residual)	-0.48 (-7.13,6.17)	0.885	0.14 (-6.88,7.15)	0.969	1.54 (-5.66,8.73)	0.666
	Model 1		Model 2		Model 3	
	Females		Females		Females	
	beta	p	beta	p	beta	p
<b>absolute change in gait speed</b>						
GrimAge Acceleration	0.02 (-0.06,0.10)	0.667	0.01 (-0.08,0.10)	0.826	-0.02 (-0.11,0.07)	0.681
PhenoAge Acceleration	-0.01 (-0.07,0.06)	0.814	-0.01 (-0.08,0.06)	0.686	-0.02 (-0.09,0.05)	0.569
Horvath Age Acceleration (residual)	-0.01 (-0.07,0.06)	0.785	-0.01 (-0.08,0.05)	0.68	-0.03 (-0.10,0.04)	0.35

**Appendix 16:** GrimAge acceleration associations with total spine, total femoral and total femoral neck BMD

	Model 1				Model 2			
	Male		Female		Male		Female	
	Beta	p	Beta	p	Beta	p	Beta	p
<b>Total spinal BMD</b>								
Baseline	0.01 (-0.01,0.04)	0.172	0.03 (0.00,0.06)	0.039	0.02 (-0.01,0.04)	0.205	0.02 (-0.01,0.05)	0.203
MSFU	0.01 (-0.01,0.04)	0.335	0.04 (0.01,0.08)	0.009	0.01 (-0.02,0.04)	0.428	0.02 (-0.01,0.06)	0.184
%change baseline to MSFU	0.03 (-0.10,0.16)	0.675	0.24 (-0.04,0.52)	0.098	-0.05 (-0.19,0.10)	0.55	0.03 (-0.28,0.35)	0.843
<b>Total femoral BMD</b>								
Baseline	0.01 (-0.00,0.03)	0.129	0.02 (-0.01,0.04)	0.18	0.01 (-0.01,0.03)	0.197	0.01 (-0.02,0.03)	0.605
MSFU	0.01 (-0.01,0.03)	0.413	0.02 (0.00,0.05)	0.043	0.01 (-0.02,0.03)	0.602	0.01 (-0.01,0.03)	0.349
EPOSA	0.02 (-0.00,0.04)	0.085	0.02 (-0.01,0.04)	0.159	0.01 (-0.02,0.04)	0.46	0.01 (-0.02,0.04)	0.429
HBS17	0.00 (-0.03,0.04)	0.92	0.01 (-0.03,0.05)	0.589	-0.03 (-0.07,0.01)	0.189	-0.00 (-0.04,0.04)	0.887
<i>Change</i>								
%change baseline to MSFU	-0.10 (-0.19,-0.00)	0.04	0.16 (-0.05,0.38)	0.136	-0.12 (-0.24,-0.01)	0.031	0.15 (-0.10,0.40)	0.227
%change baseline to EPOSA	0.55 (-0.77,1.87)	0.413	-0.08 (-1.59,1.42)	0.912	0.24 (-1.30,1.79)	0.755	0.26 (-1.47,1.99)	0.769
%change baseline to HBS17	-1.11 (-3.13,0.91)	0.277	-0.97 (-3.24,1.31)	0.401	-2.68 (-5.03,-0.33)	0.026	-0.93 (-3.92,2.06)	0.538
%change EPOSA to HBS17	-0.30 (-1.10,0.51)	0.468	-1.71 (-2.91,-0.52)	0.005	-0.95 (-1.94,0.05)	0.061	-1.67 (-3.29,-0.06)	0.043
<b>Total femoral neck BMD</b>								
Baseline	0.01 (-0.01,0.03)	0.257	0.01 (-0.01,0.03)	0.266	0.01 (-0.01,0.02)	0.557	0.00 (-0.02,0.02)	0.686
MSFU	0.01 (-0.01,0.02)	0.522	0.02 (-0.00,0.04)	0.077	-0.00 (-0.02,0.02)	0.79	0.01 (-0.01,0.03)	0.459
EPOSA	0.02 (-0.00,0.04)	0.053	0.01 (-0.01,0.04)	0.3	0.01 (-0.01,0.04)	0.287	0.01 (-0.02,0.03)	0.542
HBS17	0.00 (-0.03,0.03)	0.934	0.01 (-0.02,0.04)	0.619	-0.03 (-0.07,0.01)	0.172	-0.01 (-0.04,0.03)	0.782
<i>Change</i>								
%change baseline to MSFU	-0.06 (-0.18,0.07)	0.397	0.23 (-0.03,0.49)	0.088	-0.12 (-0.28,0.03)	0.116	0.20 (-0.11,0.50)	0.201
%change baseline to EPOSA	1.60 (0.03,3.17)	0.046	-0.04 (-1.88,1.80)	0.966	1.86 (0.02,3.70)	0.048	0.18 (-1.88,2.24)	0.864
%change baseline to HBS17	-0.53 (-2.96,1.90)	0.667	-0.40 (-2.86,2.06)	0.748	-1.26 (-4.09,1.57)	0.38	-0.22 (-3.35,2.91)	0.89
%change EPOSA to HBS17	-0.33 (-1.34,0.68)	0.513	-0.91 (-2.17,0.34)	0.151	-0.87 (-2.10,0.36)	0.164	-1.11 (-2.70,0.48)	0.17

**Appendix 17: PhenoAge acceleration associations with total spine, total femoral and total femoral neck BMD**

	Model 1				Model 2			
	Male		Female		Male		Female	
	Beta	p	Beta	p	Beta	p	Beta	p
<b>Total spinal BMD</b>								
Baseline	0.01 (-0.01,0.03)	0.33	0.02 (-0.00,0.05)	0.063	0.01 (-0.02,0.03)	0.576	0.02 (-0.00,0.04)	0.101
MSFU	0.01 (-0.01,0.03)	0.446	0.01 (-0.01,0.04)	0.296	0.01 (-0.02,0.03)	0.546	0.01 (-0.01,0.03)	0.403
%change baseline to MSFU	-0.05 (-0.17,0.07)	0.447	-0.08 (-0.31,0.15)	0.479	-0.07 (-0.20,0.06)	0.311	-0.11 (-0.33,0.11)	0.326
<b>Total femoral BMD</b>								
Baseline	0.01 (-0.00,0.03)	0.157	0.02 (-0.00,0.04)	0.07	0.00 (-0.02,0.02)	0.921	0.01 (-0.00,0.03)	0.132
MSFU	0.01 (-0.01,0.03)	0.374	0.01 (-0.00,0.03)	0.127	-0.00 (-0.02,0.02)	0.899	0.01 (-0.01,0.03)	0.205
EPOSA	0.01 (-0.01,0.03)	0.397	0.02 (-0.00,0.04)	0.071	-0.00 (-0.03,0.02)	0.757	0.02 (-0.00,0.04)	0.096
HBS17	0.02 (-0.18,0.21)	0.867	-0.20 (-0.43,0.04)	0.099	-0.07 (-0.30,0.16)	0.532	-0.16 (-0.43,0.10)	0.228
Change								
%change baseline to MSFU	-0.08 (-0.16,0.01)	0.098	0.11 (-0.06,0.28)	0.21	-0.08 (-0.18,0.02)	0.107	0.10 (-0.08,0.27)	0.275
%change baseline to EPOSA	-0.41 (-1.65,0.83)	0.513	0.35 (-0.93,1.63)	0.588	-0.13 (-1.40,1.14)	0.839	0.46 (-0.85,1.76)	0.491
%change baseline to HBS17	0.19 (-1.50,1.88)	0.823	-0.87 (-3.03,1.29)	0.425	-0.22 (-2.00,1.57)	0.811	-0.86 (-3.28,1.56)	0.482
%change EPOSA to HBS17	0.02 (-0.65,0.70)	0.944	-1.06 (-2.23,0.11)	0.075	-0.35 (-1.10,0.39)	0.346	-0.98 (-2.28,0.32)	0.136
<b>Total femoral neck BMD</b>								
Baseline	0.02 (-0.00,0.03)	0.064	0.02 (0.00,0.04)	0.011	0.00 (-0.01,0.02)	0.58	0.02 (0.00,0.03)	0.012
MSFU	0.01 (-0.00,0.03)	0.149	0.02 (0.00,0.03)	0.026	0.00 (-0.01,0.02)	0.763	0.02 (0.00,0.03)	0.026
EPOSA	0.02 (-0.00,0.04)	0.127	0.02 (0.00,0.04)	0.024	0.00 (-0.02,0.03)	0.691	0.02 (0.00,0.04)	0.029
HBS17	0.07 (-0.12,0.26)	0.485	0.07 (-0.17,0.31)	0.539	-0.07 (-0.29,0.15)	0.544	0.12 (-0.14,0.38)	0.373
Change								
%change baseline to MSFU	-0.04 (-0.16,0.08)	0.526	0.09 (-0.12,0.30)	0.394	-0.05 (-0.19,0.08)	0.422	0.08 (-0.13,0.30)	0.459
%change baseline to EPOSA	-0.26 (-1.75,1.23)	0.73	-0.12 (-1.68,1.45)	0.882	0.24 (-1.28,1.77)	0.754	-0.06 (-1.62,1.50)	0.938
%change baseline to HBS17	0.52 (-1.50,2.55)	0.608	0.31 (-2.02,2.65)	0.79	0.11 (-1.99,2.20)	0.918	0.39 (-2.14,2.93)	0.757
%change EPOSA to HBS17	0.20 (-0.64,1.04)	0.639	0.09 (-1.13,1.30)	0.89	-0.25 (-1.17,0.66)	0.583	0.20 (-1.08,1.48)	0.753



**Appendix 18:** HorvathAge acceleration associations with total spine, total femoral and total femoral neck BMD

	Model 1		Female		Model 2		Female	
	Male				Male			
	Beta	p	Beta	p	Beta	p	Beta	p
<b>Total spinal BMD</b>								
Baseline	0.01 (-0.01,0.03)	0.369	0.02 (-0.01,0.04)	0.191	0.01 (-0.01,0.03)	0.238	0.01 (-0.01,0.04)	0.233
MSFU	0.01 (-0.01,0.04)	0.428	0.02 (-0.01,0.04)	0.183	0.01 (-0.01,0.04)	0.252	0.01 (-0.01,0.04)	0.288
%change baseline to MSFU	-0.00 (-0.13,0.13)	0.974	0.11 (-0.11,0.34)	0.316	0.01 (-0.12,0.13)	0.931	0.09 (-0.13,0.31)	0.439
<b>Total femoral BMD</b>								
Baseline	0.00 (-0.02,0.02)	0.771	0.01 (-0.01,0.03)	0.253	0.00 (-0.01,0.02)	0.61	0.01 (-0.01,0.03)	0.226
MSFU	-0.00 (-0.02,0.02)	0.867	0.01 (-0.00,0.03)	0.121	-0.00 (-0.02,0.02)	0.995	0.01 (-0.00,0.03)	0.14
EPOSA	-0.00 (-0.02,0.02)	0.862	0.01 (-0.01,0.03)	0.351	-0.00 (-0.02,0.02)	0.994	0.01 (-0.01,0.03)	0.378
HBS17	0.01 (-0.02,0.04)	0.593	0.02 (-0.02,0.05)	0.299	0.01 (-0.03,0.04)	0.659	0.02 (-0.01,0.05)	0.184
Change								
%change baseline to MSFU	-0.09 (-0.18,0.00)	0.057	0.14 (-0.03,0.31)	0.113	-0.08 (-0.18,0.02)	0.103	0.13 (-0.05,0.30)	0.151
%change baseline to EPOSA	-0.65 (-1.94,0.64)	0.322	0.31 (-1.02,1.63)	0.649	-0.58 (-1.87,0.71)	0.376	0.23 (-1.13,1.58)	0.744
%change baseline to HBS17	0.09 (-1.78,1.95)	0.928	-0.24 (-2.43,1.95)	0.827	0.14 (-1.75,2.02)	0.886	-0.15 (-2.50,2.21)	0.902
%change EPOSA to HBS17	0.15 (-0.59,0.90)	0.688	-1.05 (-2.22,0.13)	0.08	0.15 (-0.65,0.94)	0.717	-0.99 (-2.25,0.26)	0.12
<b>Total femoral neck BMD</b>								
Baseline	0.00 (-0.01,0.02)	0.796	<b>0.02 (0.00,0.04)</b>	<b>0.015</b>	0.00 (-0.01,0.02)	0.733	<b>0.02 (0.01,0.03)</b>	<b>0.005</b>
MSFU	0.01 (-0.00,0.03)	0.149	<b>0.02 (0.00,0.03)</b>	<b>0.026</b>	0.00 (-0.01,0.02)	0.763	<b>0.02 (0.00,0.03)</b>	<b>0.026</b>
EPOSA	0.00 (-0.02,0.02)	0.784	<b>0.02 (0.00,0.04)</b>	<b>0.043</b>	0.00 (-0.02,0.02)	0.711	<b>0.02 (0.00,0.04)</b>	<b>0.044</b>
HBS17	0.01 (-0.02,0.04)	0.448	<b>0.03 (0.00,0.06)</b>	<b>0.049</b>	0.01 (-0.02,0.04)	0.488	<b>0.04 (0.01,0.07)</b>	<b>0.011</b>
Change								
%change baseline to MSFU	-0.01 (-0.14,0.12)	0.871	0.05 (-0.16,0.26)	0.629	-0.01 (-0.15,0.12)	0.843	0.04 (-0.17,0.26)	0.685
%change baseline to EPOSA	0.06 (-1.50,1.62)	0.939	-0.14 (-1.76,1.48)	0.863	0.34 (-1.21,1.90)	0.663	0.01 (-1.61,1.62)	0.992
%change baseline to HBS17	1.32 (-0.91,3.54)	0.242	-0.24 (-2.61,2.12)	0.838	1.40 (-0.79,3.59)	0.207	0.19 (-2.27,2.65)	0.877
%change EPOSA to HBS17	0.01 (-0.92,0.94)	0.979	-0.13 (-1.35,1.09)	0.835	-0.04 (-1.01,0.94)	0.941	0.17 (-1.07,1.41)	0.786

**Appendix 19:** Epigenetic age acceleration associations with total femoral neck BMD at baseline (BL), EPOSA and HBS17 and percentage change between baseline and HBS17 and EPOSA and HBS17 in sex-stratified analyses fully-adjusted for age, height and BMI, social class, physical activity, dietary calcium, ever smoking regularly and alcohol consumption. Change analyses were additionally adjusted for follow-up time. Fully-adjusted models with the additional adjusted of bisphosphonate usage are shown on the right.

Total Femoral Neck BMD		Fully-adjusted						Fully adjusted with bisphosphonates		
		Male		Female		Male		Female		
		beta	p	beta	p	beta	p	beta	p	
<b>BL</b>	GrimAge Acceleration	0.00 (-0.03,0.03)	0.945	-0.01 (-0.04,0.02)	0.613	0.00 (-0.03,0.03)	0.95	-0.01 (-0.04,0.02)	0.662	
	PhenoAge Acceleration	0.00 (-0.02,0.03)	0.639	0.02 (-0.01,0.04)	0.128	0.00 (-0.02,0.03)	0.657	0.01 (-0.01,0.04)	0.252	
	Horvath Age Acceleration (residual)	-0.00 (-0.03,0.02)	0.736	<b>0.02 (0.00,0.05)</b>	<b>0.033</b>	-0.00 (-0.03,0.02)	0.705	<b>0.03 (0.00,0.05)</b>	<b>0.03</b>	
<b>HBS17</b>	GrimAge Acceleration	-0.03 (-0.07,0.01)	0.19	-0.01 (-0.05,0.03)	0.555	-0.03 (-0.07,0.01)	0.144	-0.01 (-0.05,0.03)	0.704	
	PhenoAge Acceleration	0.01 (-0.02,0.04)	0.628	0.02 (-0.01,0.05)	0.108	0.01 (-0.02,0.04)	0.675	0.02 (-0.01,0.06)	0.124	
	Horvath Age Acceleration (residual)	0.01 (-0.02,0.04)	0.481	<b>0.03 (0.00,0.06)</b>	<b>0.047</b>	0.01 (-0.02,0.04)	0.521	<b>0.04 (0.01,0.07)</b>	<b>0.014</b>	
<b>%change BL to HBS17</b>	GrimAge Acceleration	-1.26 (-4.09,1.57)	0.38	-0.22 (-3.35,2.91)	0.89	-1.10 (-3.97,1.76)	0.447	0.37 (-2.54,3.27)	0.801	
	PhenoAge Acceleration	0.11 (-1.99,2.20)	0.918	0.39 (-2.14,2.93)	0.757	0.22 (-1.90,2.34)	0.837	0.86 (-1.50,3.23)	0.469	
	Horvath Age Acceleration (residual)	1.40 (-0.79,3.59)	0.207	0.19 (-2.27,2.65)	0.877	1.48 (-0.71,3.67)	0.182	0.24 (-2.08,2.56)	0.84	
<b>EPOSA</b>	GrimAge Acceleration	0.00 (-0.03,0.04)	0.807	0.00 (-0.03,0.04)	0.958	0.00 (-0.04,0.04)	0.996	-0.00 (-0.04,0.04)	0.989	
	PhenoAge Acceleration	0.01 (-0.02,0.03)	0.675	0.02 (-0.01,0.04)	0.236	0.00 (-0.02,0.03)	0.784	0.01 (-0.01,0.04)	0.299	
	Horvath Age Acceleration (residual)	0.01 (-0.03,0.04)	0.717	<b>0.03 (0.00,0.06)</b>	<b>0.02</b>	0.00 (-0.03,0.03)	0.808	<b>0.04 (0.01,0.07)</b>	<b>0.005</b>	
<b>%change EPOSA to HBS17</b>	GrimAge Acceleration	-0.87 (-2.10,0.36)	0.164	-1.11 (-2.70,0.48)	0.17	-0.83 (-2.03,0.38)	0.177	-0.99 (-2.48,0.51)	0.191	
	PhenoAge Acceleration	-0.25 (-1.17,0.66)	0.583	0.20 (-1.08,1.48)	0.753	-0.13 (-1.03,0.77)	0.769	0.28 (-0.92,1.49)	0.64	
	Horvath Age Acceleration (residual)	-0.04 (-1.01,0.94)	0.941	0.17 (-1.07,1.41)	0.786	0.14 (-0.80,1.08)	0.761	0.01 (-1.17,1.19)	0.984	

**Appendix 20:** Epigenetic age acceleration associations with total femoral BMD at baseline (BL), EPOSA and HBS17 and percentage change between baseline and HBS17 and EPOSA and HBS17 in sex-stratified analyses fully- adjusted for age, height and BMI, social class, physical activity, dietary calcium, ever smoking regularly and alcohol consumption. Change analyses were additionally adjusted for follow-up time. Fully-adjusted models with the additional adjusted of bisphosphonate usage are shown on the right. BL = baseline

Total Femoral BMD		Fully-adjusted				Fully adjusted with bisphosphonates			
		Male		Female		Male		Female	
		beta	p	beta	p	beta	p	beta	p
<b>BL</b>	GrimAge Acceleration	0.01 (-0.02,0.04)	0.486	0.00 (-0.03,0.04)	0.809	0.01 (-0.02,0.04)	0.504	0.01 (-0.03,0.04)	0.779
	PhenoAge Acceleration	-0.01 (-0.03,0.02)	0.659	0.01 (-0.02,0.04)	0.394	-0.01 (-0.03,0.02)	0.626	0.01 (-0.02,0.04)	0.591
	Horvath Age Acceleration (residual)	0.00 (-0.02,0.03)	0.716	0.02 (-0.01,0.04)	0.233	0.00 (-0.02,0.03)	0.818	0.02 (-0.01,0.05)	0.246
<b>HBS17</b>	GrimAge Acceleration	-0.03 (-0.07,0.02)	0.195	-0.01 (-0.05,0.03)	0.671	-0.03 (-0.08,0.01)	0.108	-0.01 (-0.05,0.04)	0.781
	PhenoAge Acceleration	-0.01 (-0.04,0.03)	0.74	0.01 (-0.02,0.04)	0.516	-0.01 (-0.04,0.02)	0.667	0.01 (-0.02,0.04)	0.579
	Horvath Age Acceleration (residual)	0.01 (-0.03,0.04)	0.628	0.01 (-0.02,0.05)	0.391	0.01 (-0.02,0.04)	0.641	0.02 (-0.01,0.05)	0.201
<b>%change BL to HBS17</b>	GrimAge Acceleration	<b>-2.68 (-5.03,-0.33)</b>	<b>0.026</b>	-0.93 (-3.92,2.06)	0.538	<b>-2.80 (-5.18,-0.42)</b>	<b>0.022</b>	-0.46 (-3.35,2.43)	0.752
	PhenoAge Acceleration	-0.22 (-2.00,1.57)	0.811	-0.86 (-3.28,1.56)	0.482	-0.17 (-1.98,1.63)	0.849	-0.88 (-3.23,1.48)	0.46
	Horvath Age Acceleration (residual)	0.14 (-1.75,2.02)	0.886	-0.15 (-2.50,2.21)	0.902	0.25 (-1.64,2.14)	0.792	-0.27 (-2.58,2.03)	0.814
<b>EPOSA</b>	GrimAge Acceleration	-0.00 (-0.04,0.04)	0.957	0.01 (-0.02,0.05)	0.505	-0.01 (-0.05,0.03)	0.607	0.01 (-0.03,0.05)	0.577
	PhenoAge Acceleration	-0.00 (-0.03,0.03)	0.858	0.02 (-0.01,0.04)	0.257	-0.00 (-0.03,0.02)	0.736	0.01 (-0.01,0.04)	0.32
	Horvath Age Acceleration (residual)	0.00 (-0.03,0.04)	0.849	0.02 (-0.00,0.05)	0.106	0.00 (-0.03,0.03)	0.864	<b>0.03 (0.01,0.06)</b>	<b>0.02</b>
<b>%change EPOSA to HBS17</b>	GrimAge Acceleration	-0.95 (-1.94,0.05)	0.061	<b>-1.67 (-3.29,-0.06)</b>	<b>0.043</b>	-0.91 (-1.90,0.08)	0.07	<b>-1.57 (-3.11,-0.03)</b>	<b>0.045</b>
	PhenoAge Acceleration	-0.35 (-1.10,0.39)	0.346	-0.98 (-2.28,0.32)	0.136	-0.27 (-1.01,0.47)	0.471	-0.83 (-2.09,0.42)	0.19
	Horvath Age Acceleration (residual)	0.15 (-0.65,0.94)	0.717	-0.99 (-2.25,0.26)	0.12	0.23 (-0.55,1.00)	0.56	-1.20 (-2.41,0.01)	0.051

**Appendix 21:** Age acceleration associations with bone microarchitecture outcomes (trabecular density, volumetric BMD and cortical thickness)

<b>Tibial</b>				
	Males		Females	
	beta	p	beta	p
<b>Tibial trabecular density</b>				
GrimAge Acceleration	3.54 (-2.70,9.78)	0.264	-1.74 (-10.09,6.60)	0.681
PhenoAge Acceleration	-0.29 (-5.50,4.92)	0.913	0.59 (-5.63,6.80)	0.852
Horvath Age Acceleration (residual)	0.23 (-4.98,5.44)	0.93	1.00 (-5.41,7.42)	0.757
<b>Tibial total vBMD</b>				
GrimAge Acceleration	5.08 (-3.76,13.91)	0.258	0.94 (-9.57,11.44)	0.86
PhenoAge Acceleration	-2.10 (-9.47,5.27)	0.574	3.43 (-4.37,11.23)	0.386
Horvath Age Acceleration (residual)	-0.02 (-7.40,7.35)	0.995	6.03 (-1.98,14.04)	0.139
<b>Tibial cortical thickness</b>				
GrimAge Acceleration	16.07 (-26.59,58.72)	0.458	17.88 (-20.05,55.82)	0.353
PhenoAge Acceleration	-24.58 (-59.91,10.75)	0.171	12.05 (-16.19,40.30)	0.401
Horvath Age Acceleration (residual)	-15.39 (-50.84,20.07)	0.393	<b>35.56 (6.91,64.21)</b>	<b>0.015</b>
<b>Radial</b>				
	Males		Females	
	beta	p	beta	p
<b>Radial Trabecular density</b>				
GrimAge Acceleration	3.21 (-3.76,10.18)	0.364	2.13 (-6.51,10.76)	0.627
PhenoAge Acceleration	0.63 (-5.22,6.48)	0.832	4.11 (-2.38,10.59)	0.213
Horvath Age Acceleration (residual)	-1.74 (-7.61,4.13)	0.559	2.92 (-3.83,9.66)	0.395
<b>Radial total vBMD</b>				
GrimAge Acceleration	1.49 (-9.40,12.39)	0.787	6.43 (-5.81,18.67)	0.301
PhenoAge Acceleration	-1.00 (-10.13,8.13)	0.829	5.14 (-4.09,14.37)	0.273
Horvath Age Acceleration (residual)	-1.33 (-10.50,7.83)	0.774	5.06 (-4.53,14.64)	0.299
<b>Radial cortical thickness</b>				
GrimAge Acceleration	-7.15 (-41.20,26.90)	0.679	29.35 (-4.25,62.94)	0.086
PhenoAge Acceleration	-6.30 (-34.83,22.23)	0.663	4.14 (-21.45,29.72)	0.75
Horvath Age Acceleration (residual)	-6.11 (-34.76,22.54)	0.674	5.65 (-20.89,32.19)	0.675

**Appendix 22:** Age acceleration associations with pQCT cortical thickness at the 14%, 38% and 66% slices

Tibial	Fully adjusted				Fully-adjusted with bisphosphonate usage			
	Males		Females		Males		Females	
	beta	p	beta	p	beta	p	beta	p
<b>Tibial cortical thickness 14%</b>								
GrimAge Acceleration	-0.01 (-0.08,0.07)	0.855	0.01 (-0.07,0.09)	0.821	0.00 (-0.08,0.09)	0.93	0.04 (-0.05,0.12)	0.415
PhenoAge Acceleration	-0.05 (-0.11,0.01)	0.123	0.02 (-0.04,0.08)	0.499	-0.03 (-0.09,0.04)	0.423	-0.00 (-0.07,0.06)	0.948
Horvath Age Acceleration	-0.04 (-0.10,0.02)	0.226	<b>0.09 (0.03,0.15)</b>	<b>0.004</b>	-0.05 (-0.12,0.02)	0.136	<b>0.10 (0.03,0.16)</b>	<b>0.004</b>
<b>Tibial cortical thickness 38%</b>								
GrimAge Acceleration	0.00 (-0.11,0.11)	0.981	-0.04 (-0.17,0.10)	0.576	0.01 (-0.12,0.13)	0.933	-0.01 (-0.15,0.12)	0.868
PhenoAge Acceleration	-0.04 (-0.14,0.05)	0.338	0.05 (-0.05,0.15)	0.303	-0.04 (-0.13,0.06)	0.41	0.00 (-0.10,0.11)	0.942
Horvath Age Acceleration	-0.05 (-0.14,0.05)	0.323	<b>0.11 (0.01,0.21)</b>	<b>0.033</b>	-0.04 (-0.14,0.06)	0.483	<b>0.12 (0.01,0.22)</b>	<b>0.032</b>
<b>Tibial cortical thickness 66%</b>								
GrimAge Acceleration	0.00 (-0.11,0.11)	0.987	0.09 (-0.05,0.22)	0.214	-0.01 (-0.11,0.10)	0.928	0.13 (-0.01,0.27)	0.065
PhenoAge Acceleration	-0.03 (-0.12,0.05)	0.441	0.08 (-0.02,0.18)	0.13	-0.03 (-0.11,0.06)	0.54	0.06 (-0.04,0.17)	0.249
HorvathAge Acceleration	-0.01 (-0.10,0.08)	0.748	0.09 (-0.02,0.19)	0.099	-0.03 (-0.12,0.06)	0.509	0.07 (-0.04,0.18)	0.206

## Appendix 23: Age acceleration associations with change in bone microarchitecture

	Unadjusted		Adjusted					
	Males	p	Females		Males	Females		
	beta		beta	p	beta	p	beta	p
<b>Tibia trabecular density</b>								
GrimAge Acceleration	0.31 (-0.27,0.89)	0.288	0.03 (-1.01,1.06)	0.962	0.14 (-0.57,0.84)	0.702	0.11 (-1.22,1.44)	0.87
PhenoAge Acceleration	0.41 (-0.12,0.94)	0.126	-0.12 (-1.05,0.81)	0.796	0.33 (-0.29,0.95)	0.294	-0.51 (-1.49,0.46)	0.297
Horvath Age Acceleration (residual)	-0.07 (-0.63,0.50)	0.815	0.62 (-0.33,1.58)	0.199	-0.05 (-0.64,0.53)	0.853	0.15 (-0.88,1.19)	0.772
<b>Tibial vBMD</b>								
GrimAge Acceleration	0.39 (-0.43,1.21)	0.347	-0.70 (-1.85,0.44)	0.227	0.29 (-0.73,1.32)	0.571	-0.42 (-1.94,1.10)	0.586
PhenoAge Acceleration	0.53 (-0.23,1.29)	0.169	-0.46 (-1.49,0.56)	0.375	0.40 (-0.50,1.30)	0.379	-0.55 (-1.67,0.56)	0.327
Horvath Age Acceleration (residual)	0.14 (-0.66,0.95)	0.722	0.14 (-0.93,1.22)	0.792	0.20 (-0.64,1.04)	0.645	0.02 (-1.16,1.21)	0.969
<b>Tibial cortical thickness</b>								
GrimAge Acceleration	0.84 (-0.42,2.09)	0.188	-1.44 (-3.19,0.31)	0.105	0.21 (-1.36,1.79)	0.789	-0.31 (-2.57,1.94)	0.783
PhenoAge Acceleration	0.60 (-0.57,1.76)	0.311	-0.31 (-1.88,1.27)	0.7	0.22 (-1.15,1.58)	0.754	-0.05 (-1.72,1.61)	0.948
Horvath Age Acceleration (residual)	-0.13 (-1.37,1.10)	0.83	0.37 (-1.27,2.01)	0.655	-0.15 (-1.41,1.11)	0.813	0.75 (-1.00,2.50)	0.397
<b>Radius trabecular density</b>								
GrimAge Acceleration	-0.42 (-1.30,0.45)	0.338	-0.39 (-1.78,1.00)	0.576	<b>-1.09 (-2.15,-0.02)</b>	<b>0.045</b>	-0.87 (-2.68,0.95)	0.343
PhenoAge Acceleration	0.34 (-0.33,1.00)	0.32	-0.50 (-1.77,0.77)	0.437	0.08 (-0.77,0.94)	0.846	-0.74 (-2.18,0.69)	0.304
Horvath Age Acceleration (residual)	<b>-1.05 (-1.84,-0.25)</b>	<b>0.01</b>	-1.22 (-2.56,0.13)	0.076	<b>-1.17 (-1.99,-0.36)</b>	<b>0.005</b>	-1.43 (-2.94,0.09)	0.065
<b>Radial vBMD</b>								
GrimAge Acceleration	-0.33 (-1.38,0.72)	0.532	-0.55 (-1.80,0.69)	0.379	-0.86 (-2.12,0.40)	0.178	-0.54 (-2.19,1.11)	0.515
PhenoAge Acceleration	0.21 (-0.59,1.02)	0.596	-0.24 (-1.39,0.90)	0.676	-0.02 (-1.03,0.98)	0.967	-0.22 (-1.53,1.09)	0.735
Horvath Age Acceleration (residual)	-0.94 (-1.91,0.02)	0.055	-0.71 (-1.94,0.51)	0.25	-0.90 (-1.88,0.08)	0.071	-0.94 (-2.34,0.45)	0.181
<b>Radial cortical thickness</b>								
GrimAge Acceleration	-0.17 (-1.74,1.40)	0.832	-1.30 (-3.12,0.51)	0.156	-0.04 (-1.85,1.78)	0.969	-1.11 (-3.35,1.14)	0.326
PhenoAge Acceleration	-0.19 (-1.38,1.01)	0.758	-0.04 (-1.76,1.68)	0.96	-0.48 (-1.90,0.94)	0.504	0.41 (-1.45,2.26)	0.661
Horvath Age Acceleration (residual)	-0.97 (-2.42,0.48)	0.187	0.00 (-1.83,1.84)	0.999	-0.88 (-2.29,0.52)	0.215	-0.10 (-2.04,1.84)	0.917

**Appendix 24:** Associations between epigenetic age acceleration variable and appendicular lean mass (ALM) at the EPOSA (2011-12) and HBS17 (2017) timepoints.

Adjusted models are adjusted for age, height, occupational social class, physical activity, diet, smoking, alcohol consumption

<b>EPOSA</b>								
<b>ALM</b>	<b>Unadjusted Male <i>beta</i></b>	<i>p</i>	<b>Female <i>beta</i></b>	<i>p</i>	<b>Adjusted Male <i>beta</i></b>	<i>p</i>	<b>Female <i>beta</i></b>	<i>p</i>
Horvath Age Acceleration	-62.20 (-187.20,62.80)	0.327	-1.17 (-99.28,96.95)	0.981	-16.28 (-124.21,91.65)	0.766	-25.12 (-117.31,67.07)	0.591
GrimAge Acceleration	-25.18 (-153.88,103.52)	0.7	105.00 (-9.09,219.09)	0.071	-10.03 (-138.73,118.67)	0.878	<b>118.84 (1.23,236.45)</b>	<b>0.048</b>
PhenoAge Acceleration	4.50 (-114.23,123.23)	0.94	9.89 (-87.74,107.52)	0.842	4.42 (-98.31,107.14)	0.932	-0.85 (-91.87,90.18)	0.985
<b>HBS17</b>								
<b>ALM</b>	<b>Unadjusted Male <i>beta</i></b>	<i>p</i>	<b>Female <i>beta</i></b>	<i>p</i>	<b>Adjusted Male <i>beta</i></b>	<i>p</i>	<b>Female <i>beta</i></b>	<i>p</i>
Horvath Age Acceleration	-84.52 (-305.63,136.58)	0.449	-104.67 (-259.33,49.98)	0.182	16.40 (-183.94,216.73)	0.871	-74.39 (-228.28,79.50)	0.339
GrimAge Acceleration	-16.63 (-256.86,223.59)	0.891	14.93 (-152.37,182.23)	0.859	-25.55 (-276.08,224.97)	0.84	-15.09 (-207.07,176.89)	0.876
PhenoAge Acceleration	-3.34 (-194.28,187.61)	0.972	-30.17 (-185.11,124.77)	0.699	-12.07 (-185.24,161.10)	0.89	38.21 (-116.90,193.32)	0.625

**Appendix 25:** Associations between epigenetic age acceleration variable and total fat mass at the EPOSA (2011-12) and HBS17 (2017) timepoints.

Adjusted models are adjusted for age, height, occupational social class, physical activity, diet, smoking, alcohol consumption

<b>EPOSA</b>									
<b>Fat mass</b>	<b>Unadjusted Male beta</b>	<b>p</b>	<b>Female beta</b>	<b>p</b>	<b>Adjusted Male beta</b>	<b>p</b>	<b>Female beta</b>	<b>p</b>	
Horvath Age Acceleration	-158.36 (-1492.69,1175.97)	0.815	-55.29 (-1553.82,1443.24)	0.942	296.63 (-1003.27,1596.54)	0.653	-174.46 (-1645.11,1296.19)	0.815	
GrimAge Acceleration	903.20 (-417.71,2224.12)	0.179	1503.84 (-217.51,3225.18)	0.086	220.93 (-1332.00,1773.86)	0.779	<b>2226.51 (377.93,4075.09)</b>	<b>0.019</b>	
PhenoAge Acceleration	<b>1980.99 (739.93,3222.04)</b>	<b>0.002</b>	1106.30 (-375.83,2588.42)	0.142	<b>1513.14 (275.04,2751.24)</b>	<b>0.017</b>	1378.30 (-80.59,2837.19)	0.064	
<b>HBS17</b>									
<b>Fat mass</b>	<b>Unadjusted Male beta</b>	<b>p</b>	<b>Female beta</b>	<b>p</b>	<b>Adjusted Male beta</b>	<b>p</b>	<b>Female beta</b>	<b>p</b>	
Horvath Age Acceleration	-378.77 (-2405.49,1647.94)	0.711	-1369.97 (-3526.71,786.78)	0.21	-10.57 (-2052.64,2031.49)	0.992	-1179.07 (-3458.05,1099.91)	0.305	
GrimAge Acceleration	695.74 (-1439.76,2831.23)	0.518	689.95 (-1612.77,2992.67)	0.552	1449.46 (-1297.43,4196.35)	0.296	1859.00 (-857.51,4575.51)	0.177	
PhenoAge Acceleration	1389.52 (-509.02,3288.07)	0.149	65.48 (-2094.29,2225.26)	0.952	1131.02 (-824.50,3086.54)	0.252	724.96 (-1572.71,3022.64)	0.531	



**Appendix 26:** Table demonstrating the associations between PhenoAge acceleration and musculoskeletal outcomes with the outlier for PhenoAge included (on the left) and excluded (on the right). The outlier was a male so only sex-specific, male analyses are shown for unadjusted and fully adjusted analyses. Statistically significant results are highlighted in red.

		Outlier included				Outlier excluded			
		Unadjusted		Fully-adjusted		Unadjusted		Fully-adjusted	
		beta	p	beta	p	beta	p	beta	p
<b>Baseline</b>	Maximum grip (kg)	-0.64 (-1.56,0.27)	0.165	-0.57 (-1.39,0.26)	0.179	-0.60 (-1.58,0.38)	0.229	-0.52 (-1.41,0.37)	0.247
	Total femoral est. bmd (g/cm2)	0.01 (-0.00,0.03)	0.157	0.00 (-0.02,0.02)	0.921	0.01 (-0.01,0.03)	0.263	0.00 (-0.02,0.02)	0.915
	Total femoral neck est. bmd (g/cm2)	0.02 (-0.00,0.03)	0.064	0.00 (-0.01,0.02)	0.58	0.01 (-0.00,0.03)	0.133	0.00 (-0.01,0.02)	0.57
<b>EPOSA</b>	Maximum grip (kg)	<b>-1.10 (-2.06,-0.15)</b>	<b>0.024</b>	-0.88 (-1.80,0.04)	0.062	-0.88 (-2.02,0.25)	0.127	-0.70 (-1.77,0.36)	0.195
	Gait speed (m/s)	-0.02 (-0.04,0.01)	0.199	-0.01 (-0.03,0.02)	0.573	-0.02 (-0.04,0.01)	0.248	-0.01 (-0.03,0.02)	0.703
	Total femoral est. bmd (g/cm2)	0.01 (-0.01,0.03)	0.397	-0.00 (-0.03,0.02)	0.757	0.01 (-0.01,0.03)	0.388	-0.00 (-0.03,0.02)	0.972
	Total femoral neck est. bmd (g/cm2)	0.02 (-0.00,0.04)	0.127	0.00 (-0.02,0.03)	0.691	0.02 (-0.01,0.04)	0.135	0.01 (-0.02,0.03)	0.473
	Tibia total volumetric bone density (mg/cm3)	-0.57 (-7.75,6.61)	0.876	-2.10 (-9.47,5.27)	0.574	-0.96 (-8.78,6.87)	0.81	-0.73 (-8.67,7.21)	0.856
	Tibia apparent cortical thickness(microm)	-0.94 (-37.17,35.28)	0.959	-24.58 (-59.91,10.75)	0.171	4.97 (-34.46,44.41)	0.804	-5.66 (-44.51,33.18)	0.774
	Tibia trabecular density (mg/cm3)	-0.53 (-5.47,4.41)	0.832	-0.29 (-5.50,4.92)	0.913	-1.64 (-7.00,3.72)	0.547	-1.01 (-6.63,4.62)	0.724
	Whole body dxa total fat mass (g)	<b>1994 (732,3256)</b>	<b>0.002</b>	<b>1513 (275,2751)</b>	<b>0.017</b>	<b>1895 (497,3294)</b>	<b>0.008</b>	68 (-953,1089)	0.895
	Whole body dxa arms lean mass (g)	9 (-114,132)	0.886	-68 (-165,28)	0.166	12 (-122,147)	0.852	-75 (-181,31)	0.164
	<b>HBS17</b>	Maximum grip strength (kg)	-0.87 (-2.19,0.44)	0.191	-0.56 (-1.83,0.71)	0.383	-0.80 (-2.30,0.69)	0.288	-0.55 (-1.95,0.86)
Gait speed (m/s)		<b>-0.04 (-0.07,-0.01)</b>	<b>0.008</b>	<b>-0.04 (-0.07,-0.00)</b>	<b>0.035</b>	<b>-0.04 (-0.08,-0.01)</b>	<b>0.009</b>	<b>-0.04 (-0.08,-0.00)</b>	<b>0.027</b>
Total femoral est. bmd (g/cm2)		0.02 (-0.18,0.21)	0.867	-0.07 (-0.30,0.16)	0.532	0.01 (-0.02,0.05)	0.481	-0.00 (-0.04,0.04)	0.917
Total femoral neck est. bmd (g/cm2)		0.07 (-0.12,0.26)	0.485	-0.07 (-0.29,0.15)	0.544	0.02 (-0.01,0.06)	0.144	0.01 (-0.03,0.05)	0.549
Tibia total volumetric bone density (mg/cm3)		3.13 (-8.18,14.44)	0.584	-0.19 (-12.39,12.02)	0.976	3.13 (-8.18,14.44)	0.584	-0.19 (-12.39,12.02)	0.976
Tibia apparent cortical thickness (mm)		0.02 (-0.04,0.07)	0.584	-0.02 (-0.07,0.04)	0.597	0.02 (-0.04,0.07)	0.584	-0.02 (-0.07,0.04)	0.597
Tibia trabecular density (mg/cm3)		3.03 (-4.70,10.76)	0.438	2.02 (-6.38,10.42)	0.634	3.03 (-4.70,10.76)	0.438	2.02 (-6.38,10.42)	0.634
Whole body DXA total fat mass (g)		1787 (-161,3736)	0.072	430 (-1120,1979)	0.581	1784 (-698,4266)	0.156	-49 (-2039,1940)	0.961
Whole body DXA arms lean mass (g)		-4.39 (-201,193)	0.965	-131 (-269,6)	0.061	-9 (-241,222)	0.936	<b>-162 (-323,-1)</b>	<b>0.049</b>

*Grip strength and gait speed* covariates included age, height, BMI, social class, physical activity, prudent diet, ever smoked regularly and alcohol consumption

*Femoral neck BMD* covariates included age, height, BMI, social class, physical activity, dietary calcium, smoking, alcohol

*Total fat mass* covariates included age, height, occupational social class, physical activity, prudent diet, smoking, alcohol consumption

**Appendix 27:** Genome browser output demonstrating the location of the cg00960509 and the geographic location in a CpG island associated the 5' end of the gene *ECE1* on chromosome 1



**Appendix 28:** Genome browser output demonstrating the location of the cg02389067 lying in a CpG island at in the promoter region at the 5' end of GNA13 on chromosome 17



**Appendix 29:** Genes associated with the 100 CpG sites with the lowest p-values associated with the maximum grip strength in model 2 EWAS

(adjusted for age, sex, cell composition and array). Those in red highlight are those with a p-value <  $1 \times 10^{-5}$

<i>SDK1</i>	<i>AXIN1</i>	<i>CMTM8</i>	<i>PLD5</i>
<i>ECE1</i>	<i>NCOR2</i>	<i>TNN</i>	<i>TRIM37</i>
<i>KIAA1549</i>	<i>VPS53</i>	<i>SFSWAP</i>	<i>CLIP2</i>
<i>SIAH3</i>	<i>PIAS2</i>	<i>SLC12A6</i>	<i>ERC2</i>
<i>CCDC13-AS1</i>	<i>PAX7</i>	<i>SLC16A8</i>	<i>GUCY1B2</i>
<i>NASP</i>	<i>TBC1D22A</i>	<i>MYO7B</i>	<i>C18orf22</i>
<i>SEC16A</i>	<i>AK3L1</i>	<i>MUC5B</i>	<i>GRB10</i>
<i>CXCR5</i>	<i>SPNS3</i>	<i>KRTAP12-3</i>	<i>CRYBG3</i>
<i>CNNM2</i>	<i>SF3B14</i>	<i>DLG1</i>	<i>ZC3H3</i>
<i>AGTPBP1</i>	<i>PDE9A</i>	<i>TRIP12</i>	<i>PDZD8</i>
<i>SNTG2</i>	<i>ATP2B2</i>	<i>ATP2C2</i>	<i>ZNF365</i>
<i>UBE2I</i>	<i>PRPF38B</i>	<i>PRKACA</i>	<i>INTS1</i>
<i>SIX5</i>	<i>EPHX2</i>	<i>CACNA1B</i>	<i>TMEM131</i>
<i>IGF1R</i>	<i>CCBE1</i>	<i>OR10H2</i>	<i>LOC102724539</i>
<i>SIX2</i>	<i>FAM108C1</i>	<i>MEG8</i>	<i>PLEK2</i>
<i>C3orf58</i>	<i>THYN1</i>	<i>TSPAN9</i>	<i>SHANK2</i>
<i>XDH</i>	<i>RPTOR</i>	<i>MPHOSPH6</i>	<i>SFRS8</i>
<i>CRISP3</i>	<i>SDK1</i>	<i>NT5E</i>	

**Appendix 30:** Genes associated with the 100 CpG sites with the lowest p-values associated with the maximum grip strength in model 4 EWAS.

(adjusted for age, sex, height, weight for height residual, occupational social class (manual vs non-manual labour), physical activity (Dallosso score<sup>1</sup>), diet (prudent diet score), smoking status (ever having smoked regularly) and alcohol consumption (an ordinal variable of units/week cell composition and array). Those in red highlight are those with a p-value<1x10<sup>-5</sup>

<i>SIAH3</i>	<i>EEF1A2</i>	<i>RFC5</i>	<i>PSMB9</i>
<i>CXCR5</i>	<i>CRISP3</i>	<i>SFRS8</i>	<i>C18orf1</i>
<i>VPS53</i>	<i>COL6A3</i>	<i>C21orf29</i>	<i>TXNL4A</i>
<i>ECE1</i>	<i>TBC1D22A</i>	<i>FBXL7</i>	<i>CACNA2D2</i>
<i>SEC16A</i>	<i>RPTOR</i>	<i>DHRS7B</i>	<i>SDK1</i>
<i>MTRR</i>	<i>COPA</i>	<i>FAM13C</i>	<i>RHOBTB1</i>
<i>DGKI</i>	<i>TPT1-AS1</i>	<i>MUC5B</i>	<i>MAP3K12</i>
<i>THYN1</i>	<i>SLC6A15</i>	<i>TRIP12</i>	<i>VPS11</i>
<i>LINC01237</i>	<i>MUC5B</i>	<i>SLC6A19</i>	<i>ERAP1</i>
<i>SCFD2</i>	<i>ARHGAP24</i>	<i>ADORA2B</i>	<i>FAM188A</i>
<i>CNNM2</i>	<i>NCOR2</i>	<i>NKX2-4</i>	<i>ENOX1</i>
<i>TGFB1</i>	<i>KIAA1549</i>	<i>IGF2BP2</i>	<i>GUCY1B2</i>
<i>CARD14</i>	<i>CATSPERG</i>	<i>CCDC13-AS1</i>	<i>LOC100506457</i>
<i>NASP</i>	<i>FBL</i>	<i>SPECC1</i>	<i>XDH</i>
<i>CCBE1</i>	<i>RHBDD1</i>	<i>OR10H2</i>	<i>AHRR</i>
<i>MYH15</i>	<i>SIX2</i>	<i>C1orf89</i>	
<i>PRPF38B</i>	<i>IGF1R</i>	<i>SPNS3</i>	
<i>DNAJC11</i>	<i>KRTAP12-3</i>	<i>PRRG2</i>	

## List of References

- 1 Cooper, C., Campion, G. & Melton, L. J., 3rd. Hip fractures in the elderly: a world-wide projection. *Osteoporos Int* **2**, 285-289 (1992).
- 2 Kern, L. M. *et al.* Association between screening for osteoporosis and the incidence of hip fracture. *Annals of internal medicine* **142**, 173-181 (2005).
- 3 Horvath, S. DNA methylation age of human tissues and cell types. *Genome Biol* **14**, R115, doi:10.1186/gb-2013-14-10-r115 (2013).
- 4 Teschendorff, A. E. *et al.* Age-dependent DNA methylation of genes that are suppressed in stem cells is a hallmark of cancer. *Genome Res* **20**, 440-446, doi:gr.103606.109 [pii] 10.1101/gr.103606.109 (2010).
- 5 Rakyan, V. K. *et al.* Human aging-associated DNA hypermethylation occurs preferentially at bivalent chromatin domains. *Genome Res* **20**, 434-439, doi:gr.103101.109 [pii] 10.1101/gr.103101.109 (2010).
- 6 Cruz-Jentoft, A. J. *et al.* Sarcopenia: revised European consensus on definition and diagnosis. *Age Ageing*, doi:10.1093/ageing/afy169 (2018).
- 7 Anker, S. D., Morley, J. E. & von Haehling, S. Welcome to the ICD-10 code for sarcopenia. *J Cachexia Sarcopenia Muscle* **7**, 512-514, doi:10.1002/jcsm.12147 (2016).
- 8 Pinedo-Villanueva, R. *et al.* Health Care Costs Associated With Muscle Weakness: A UK Population-Based Estimate. doi:10.1007/s00223-018-0478-1 (2018).
- 9 Cruz-Jentoft, A. J. *et al.* Sarcopenia: European consensus on definition and diagnosis: Report of the European Working Group on Sarcopenia in Older People. *Age and ageing* **39**, 412-423, doi:10.1093/ageing/afq034 (2010).
- 10 Shafiee, G. *et al.* Prevalence of sarcopenia in the world: a systematic review and meta-analysis of general population studies. *J Diabetes Metab Disord* **16**, 21, doi:10.1186/s40200-017-0302-x (2017).
- 11 Cruz-Jentoft, A. J. & Sayer, A. A. Sarcopenia. *The Lancet* **393**, 2636-2646, doi:[https://doi.org/10.1016/S0140-6736\(19\)31138-9](https://doi.org/10.1016/S0140-6736(19)31138-9) (2019).
- 12 Gielen, E. *et al.* Endocrine determinants of incident sarcopenia in middle-aged and elderly European men. *J Cachexia Sarcopenia Muscle* **6**, 242-252, doi:10.1002/jcsm.12030 (2015).
- 13 Yu, R. *et al.* Incidence, reversibility, risk factors and the protective effect of high body mass index against sarcopenia in community-dwelling older Chinese adults. *Geriatr Gerontol Int* **14 Suppl 1**, 15-28, doi:10.1111/ggi.12220 (2014).
- 14 Dodds, R. M. *et al.* Prevalence and incidence of sarcopenia in the very old: findings from the Newcastle 85+ Study. *J Cachexia Sarcopenia Muscle* **8**, 229-237, doi:10.1002/jcsm.12157 (2017).
- 15 Liu, X. *et al.* Prevalence of sarcopenia in multi ethnics adults and the association with cognitive impairment: findings from West-China health and aging trend study. *BMC Geriatrics* **20**, 63, doi:10.1186/s12877-020-1468-5 (2020).

- 16 Beard, J. R. *et al.* The World report on ageing and health: a policy framework for healthy ageing. *Lancet* **387**, 2145-2154, doi:10.1016/s0140-6736(15)00516-4 (2016).
- 17 Dodds, R. M. *et al.* Grip strength across the life course: normative data from twelve British studies. *PLoS One* **9**, e113637, doi:10.1371/journal.pone.0113637 (2014).
- 18 Dam, T. T. *et al.* An evidence-based comparison of operational criteria for the presence of sarcopenia. *J Gerontol A Biol Sci Med Sci* **69**, 584-590, doi:10.1093/gerona/glu013 (2014).
- 19 Studenski, S. A. *et al.* The FNIH sarcopenia project: rationale, study description, conference recommendations, and final estimates. *J Gerontol A Biol Sci Med Sci* **69**, 547-558, doi:10.1093/gerona/glu010 (2014).
- 20 Barazzoni, R. *et al.* Sarcopenic Obesity: Time to Meet the Challenge. *Obesity Facts* **11**, 294-305, doi:10.1159/000490361 (2018).
- 21 von Berens, Å. *et al.* Sarcopenic obesity and associations with mortality in older women and men – a prospective observational study. *BMC Geriatrics* **20**, 199, doi:10.1186/s12877-020-01578-9 (2020).
- 22 Yeung, S. S. Y. *et al.* Sarcopenia and its association with falls and fractures in older adults: A systematic review and meta-analysis. *Journal of cachexia, sarcopenia and muscle* **10**, 485-500, doi:10.1002/jcsm.12411 (2019).
- 23 Frost, H. M. The mechanostat: a proposed pathogenic mechanism of osteoporoses and the bone mass effects of mechanical and nonmechanical agents. *Bone Miner* **2**, 73-85 (1987).
- 24 Frost, H. M. Bone's mechanostat: a 2003 update. *Anat Rec A Discov Mol Cell Evol Biol* **275**, 1081-1101, doi:10.1002/ar.a.10119 (2003).
- 25 Kanis, J. A., Johnell, O., Oden, A., Johansson, H. & McCloskey, E. FRAX and the assessment of fracture probability in men and women from the UK. *Osteoporos Int* **19**, 385-397, doi:10.1007/s00198-007-0543-5 (2008).
- 26 Assessment of fracture risk and its application to screening for postmenopausal osteoporosis. Report of a WHO Study Group. *World Health Organ Tech Rep Ser* **843**, 1-129 (1994).
- 27 Hernlund, E. *et al.* Osteoporosis in the European Union: medical management, epidemiology and economic burden. A report prepared in collaboration with the International Osteoporosis Foundation (IOF) and the European Federation of Pharmaceutical Industry Associations (EFPIA). *Arch Osteoporos* **8**, 136, doi:10.1007/s11657-013-0136-1 (2013).
- 28 Broken Bones, Broken Lives: a roadmoap to solve the fragility fracture crisis in Europe. *International Osteoporosis Foundation* (2018).
- 29 Harvey, N., Dennison, E. & Cooper, C. Osteoporosis: a lifecourse approach. *J Bone Miner Res* **29**, 1917-1925, doi:10.1002/jbmr.2286 (2014).
- 30 Cooper, C. & Melton, L. J., 3rd. Epidemiology of osteoporosis. *Trends Endocrinol Metab* **3**, 224-229, doi:10.1016/1043-2760(92)90032-v (1992).
- 31 Sambrook, P. & Cooper, C. Osteoporosis. *Lancet* **367**, 2010-2018, doi:10.1016/s0140-6736(06)68891-0 (2006).
- 32 Cruz-Jentoft, A. J. *et al.* Prevalence of and interventions for sarcopenia in ageing adults: a systematic review. Report of the International Sarcopenia Initiative (EWGSOP and IWGS). *Age and ageing* **43**, 748-759, doi:10.1093/ageing/afu115 (2014).



- 33 Janssen, I., Shepard, D. S., Katzmarzyk, P. T. & Roubenoff, R. The healthcare costs of sarcopenia in the United States. *Journal of the American Geriatrics Society* **52**, 80-85 (2004).
- 34 van Staa, T. P., Dennison, E. M., Leufkens, H. G. & Cooper, C. Epidemiology of fractures in England and Wales. *Bone* **29**, 517-522, doi:10.1016/s8756-3282(01)00614-7 (2001).
- 35 Bliuc, D., Alarkawi, D., Nguyen, T. V., Eisman, J. A. & Center, J. R. Risk of subsequent fractures and mortality in elderly women and men with fragility fractures with and without osteoporotic bone density: the Dubbo Osteoporosis Epidemiology Study. *J Bone Miner Res* **30**, 637-646, doi:10.1002/jbmr.2393 (2015).
- 36 *Osteoporosis: clinical guidelines for the prevention and treatment.* (Royal College of Physicians, 1999).
- 37 Eddy, D. M. *et al.* Osteoporosis: Review of the evidence for prevention, diagnosis, and treatment and cost-effectiveness analysis. Status report. *Osteoporosis International* **8**, I-S82 (1998).
- 38 Carmona, R. H. in *Bone Health and Osteoporosis: A Report of the Surgeon General* (Office of the Surgeon General (US), 2004).
- 39 van der Velde, R. Y. *et al.* Secular trends in fracture incidence in the UK between 1990 and 2012. *Osteoporosis Int* **27**, 3197-3206, doi:10.1007/s00198-016-3650-3 (2016).
- 40 Gullberg, B., Johnell, O. & Kanis, J. A. World-wide projections for hip fracture. *Osteoporosis Int* **7**, 407-413 (1997).
- 41 Cooper, C., Atkinson, E. J., O'Fallon, W. M. & Melton, L. J., 3rd. Incidence of clinically diagnosed vertebral fractures: a population-based study in Rochester, Minnesota, 1985-1989. *J Bone Miner Res* **7**, 221-227, doi:10.1002/jbmr.5650070214 (1992).
- 42 Burge, R. *et al.* Incidence and economic burden of osteoporosis-related fractures in the United States, 2005-2025. *J Bone Miner Res* **22**, 465-475, doi:10.1359/jbmr.061113 (2007).
- 43 Johnell, O. & Kanis, J. A. An estimate of the worldwide prevalence and disability associated with osteoporotic fractures. *Osteoporosis Int* **17**, 1726-1733, doi:10.1007/s00198-006-0172-4 (2006).
- 44 Fuggle, N. R. *et al.* The treatment gap: The missed opportunities for osteoporosis therapy. *Bone* **144**, 115833, doi:10.1016/j.bone.2020.115833 (2021).
- 45 Kanis, J. A. *et al.* Case finding for the management of osteoporosis with FRAX--assessment and intervention thresholds for the UK. *Osteoporosis Int* **19**, 1395-1408, doi:10.1007/s00198-008-0712-1 (2008).
- 46 Fuggle, N. R. *et al.* Fracture prediction, imaging and screening in osteoporosis. *Nature Reviews Endocrinology* **15**, 535-547, doi:10.1038/s41574-019-0220-8 (2019).
- 47 Paccou, J., Edwards, M., Moss, C., Dennison, E. & Cooper, C. High-resolution imaging of bone and joint architecture in rheumatoid arthritis. *Br Med Bull* **112**, 107-118, doi:10.1093/bmb/ldu033 (2014).
- 48 Cameron, J. R. & Sorenson, J. MEASUREMENT OF BONE MINERAL IN VIVO: AN IMPROVED METHOD. *Science* **142**, 230-232 (1963).

- 49 Lotz, J. C., Cheal, E. J. & Hayes, W. C. Fracture prediction for the proximal femur using finite element models: Part I--Linear analysis. *J Biomech Eng* **113**, 353-360 (1991).
- 50 Nielson, C. M. *et al.* BMI and fracture risk in older men: the osteoporotic fractures in men study (MrOS). *J Bone Miner Res* **26**, 496-502, doi:10.1002/jbmr.235 (2011).
- 51 Shepherd, J. A., Schousboe, J. T., Broy, S. B., Engelke, K. & Leslie, W. D. Executive Summary of the 2015 ISCD Position Development Conference on Advanced Measures From DXA and QCT: Fracture Prediction Beyond BMD. *J Clin Densitom* **18**, 274-286, doi:10.1016/j.jocd.2015.06.013 (2015).
- 52 Beaudart, C. *et al.* Sarcopenia in daily practice: assessment and management. *BMC Geriatr* **16**, 170, doi:10.1186/s12877-016-0349-4 (2016).
- 53 Bridge, P. *et al.* Validation of longitudinal DXA changes in body composition from pre- to mid-adolescence using MRI as reference. *J Clin Densitom* **14**, 340-347, doi:10.1016/j.jocd.2011.04.005 (2011).
- 54 Tavoian, D., Ampomah, K., Amano, S., Law, T. D. & Clark, B. C. Changes in DXA-derived lean mass and MRI-derived cross-sectional area of the thigh are modestly associated. *Scientific Reports* **9**, 10028, doi:10.1038/s41598-019-46428-w (2019).
- 55 Cameron, J., McPhee, J. S., Jones, D. A. & Degens, H. Five-year longitudinal changes in thigh muscle mass of septuagenarian men and women assessed with DXA and MRI. *Aging Clinical and Experimental Research* **32**, 617-624, doi:10.1007/s40520-019-01248-w (2020).
- 56 Westbury, L. D. *et al.* Relationships Between Level and Change in Sarcopenia and Other Body Composition Components and Adverse Health Outcomes: Findings from the Health, Aging, and Body Composition Study. *Calcif Tissue Int* **108**, 302-313, doi:10.1007/s00223-020-00775-3 (2021).
- 57 Syddall, H. E. *et al.* Correlates of Level and Loss of Grip Strength in Later Life: Findings from the English Longitudinal Study of Ageing and the Hertfordshire Cohort Study. *Calcif Tissue Int* **102**, 53-63, doi:10.1007/s00223-017-0337-5 (2018).
- 58 *Dual Energy X Ray Absorptiometry for Bone Mineral Density and Body Composition Assessment.* (INTERNATIONAL ATOMIC ENERGY AGENCY, 2011).
- 59 Krug, R., Burghardt, A. J., Majumdar, S. & Link, T. M. High-resolution imaging techniques for the assessment of osteoporosis. *Radiol Clin North Am* **48**, 601-621, doi:10.1016/j.rcl.2010.02.015 (2010).
- 60 van den Bergh, J. P. *et al.* The clinical application of high-resolution peripheral computed tomography (HR-pQCT) in adults: state of the art and future directions. *Osteoporos Int* **32**, 1465-1485, doi:10.1007/s00198-021-05999-z (2021).
- 61 Burghardt, A. J., Kazakia, G. J., Ramachandran, S., Link, T. M. & Majumdar, S. Age- and gender-related differences in the geometric properties and biomechanical significance of intracortical porosity in the distal radius and tibia. *J Bone Miner Res* **25**, 983-993, doi:10.1359/jbmr.091104 (2010).
- 62 Liu, X. S. *et al.* High-resolution peripheral quantitative computed tomography can assess microstructural and mechanical properties of human distal tibial bone. *J Bone Miner Res* **25**, 746-756, doi:10.1359/jbmr.090822 (2010).
- 63 Boutroy, S., Bouxsein, M. L., Munoz, F. & Delmas, P. D. In vivo assessment of trabecular bone microarchitecture by high-resolution peripheral quantitative computed tomography. *J Clin Endocrinol Metab* **90**, 6508-6515, doi:10.1210/jc.2005-1258 (2005).

- 64 Boutroy, S. *et al.* Finite element analysis based on in vivo HR-pQCT images of the distal radius is associated with wrist fracture in postmenopausal women. *Journal of Bone and Mineral Research* **23**, 392-399 (2008).
- 65 Burt, L. A., Bhatla, J. L., Hanley, D. A. & Boyd, S. K. Cortical porosity exhibits accelerated rate of change in peri- compared with post-menopausal women. *Osteoporos Int* **28**, 1423-1431, doi:10.1007/s00198-016-3900-4 (2017).
- 66 Shanbhogue, V. V., Brixen, K. & Hansen, S. Age- and Sex-Related Changes in Bone Microarchitecture and Estimated Strength: A Three-Year Prospective Study Using HRpQCT. *J Bone Miner Res* **31**, 1541-1549, doi:10.1002/jbmr.2817 (2016).
- 67 Nishiyama, K. K., Macdonald, H. M., Buie, H. R., Hanley, D. A. & Boyd, S. K. Postmenopausal women with osteopenia have higher cortical porosity and thinner cortices at the distal radius and tibia than women with normal aBMD: an in vivo HR-pQCT study. *J Bone Miner Res* **25**, 882-890, doi:10.1359/jbmr.091020 (2010).
- 68 Gabel, L., Macdonald, H. M., Nettlefold, L. A. & McKay, H. A. Sex-, Ethnic-, and Age-Specific Centile Curves for pQCT- and HR-pQCT-Derived Measures of Bone Structure and Strength in Adolescents and Young Adults. *J Bone Miner Res* **33**, 987-1000, doi:10.1002/jbmr.3399 (2018).
- 69 Biver, E. *et al.* Evaluation of Radius Microstructure and Areal Bone Mineral Density Improves Fracture Prediction in Postmenopausal Women. *J Bone Miner Res* **33**, 328-337, doi:10.1002/jbmr.3299 (2018).
- 70 Burt, L. A., Manske, S. L., Hanley, D. A. & Boyd, S. K. Lower Bone Density, Impaired Microarchitecture, and Strength Predict Future Fragility Fracture in Postmenopausal Women: 5-Year Follow-up of the Calgary CaMos Cohort. *J Bone Miner Res* **33**, 589-597, doi:10.1002/jbmr.3347 (2018).
- 71 Sornay-Rendu, E., Boutroy, S., Duboeuf, F. & Chapurlat, R. D. Bone Microarchitecture Assessed by HR-pQCT as Predictor of Fracture Risk in Postmenopausal Women: The OFELY Study. *J Bone Miner Res* **32**, 1243-1251, doi:10.1002/jbmr.3105 (2017).
- 72 Butscheidt, S., Rolvien, T., Vettorazzi, E. & Fieling, I. Trabecular bone microarchitecture predicts fragility fractures in postmenopausal women on denosumab treatment. *Bone* **114**, 246-251, doi:10.1016/j.bone.2018.06.022 (2018).
- 73 Szulc, P., Boutroy, S. & Chapurlat, R. Prediction of Fractures in Men Using Bone Microarchitectural Parameters Assessed by High-Resolution Peripheral Quantitative Computed Tomography-The Prospective STRAMBO Study. *J Bone Miner Res* **33**, 1470-1479, doi:10.1002/jbmr.3451 (2018).
- 74 Langsetmo, L. *et al.* Volumetric Bone Mineral Density and Failure Load of Distal Limbs Predict Incident Clinical Fracture Independent HR-pQCT BMD and Failure Load Predicts Incident Clinical Fracture of FRAX and Clinical Risk Factors Among Older Men. *J Bone Miner Res* **33**, 1302-1311, doi:10.1002/jbmr.3433 (2018).
- 75 Ohlsson, C. *et al.* Cortical Bone Area Predicts Incident Fractures Independently of Areal Bone Mineral Density in Older Men. *J Clin Endocrinol Metab* **102**, 516-524, doi:10.1210/jc.2016-3177 (2017).
- 76 Sundh, D. *et al.* Increased Cortical Porosity in Older Men With Fracture. *J Bone Miner Res* **30**, 1692-1700, doi:10.1002/jbmr.2509 (2015).

- 77 Szulc, P. *et al.* Cross-sectional analysis of the association between fragility fractures and bone microarchitecture in older men: the STRAMBO study. *J Bone Miner Res* **26**, 1358-1367, doi:10.1002/jbmr.319 (2011).
- 78 Litwic, A. E. *et al.* Bone Phenotype Assessed by HRpQCT and Associations with Fracture Risk in the GLOW Study. *Calcif Tissue Int* **102**, 14-22, doi:10.1007/s00223-017-0325-9 (2018).
- 79 Mikolajewicz, N. *et al.* HR-pQCT Measures of Bone Microarchitecture Predict Fracture: Systematic Review and Meta-Analysis. *J Bone Miner Res* **35**, 446-459, doi:10.1002/jbmr.3901 (2020).
- 80 de Jong, J. J. A. *et al.* Fracture Repair in the Distal Radius in Postmenopausal Women: A Follow-Up 2 Years Postfracture Using HRpQCT. *J Bone Miner Res* **31**, 1114-1122, doi:10.1002/jbmr.2766 (2016).
- 81 Macdonald, H. M., Nishiyama, K. K., Kang, J., Hanley, D. A. & Boyd, S. K. Age-related patterns of trabecular and cortical bone loss differ between sexes and skeletal sites: a population-based HR-pQCT study. *J Bone Miner Res* **26**, 50-62, doi:10.1002/jbmr.171 (2011).
- 82 Dalzell, N. *et al.* Bone micro-architecture and determinants of strength in the radius and tibia: age-related changes in a population-based study of normal adults measured with high-resolution pQCT. *Osteoporos Int* **20**, 1683-1694, doi:10.1007/s00198-008-0833-6 (2009).
- 83 Khosla, S. *et al.* Effects of sex and age on bone microstructure at the ultradistal radius: a population-based noninvasive in vivo assessment. *J Bone Miner. Res.* **21**, 124-131, doi:10.1359/JBMR.050916 [doi] (2006).
- 84 Hansen, S., Shanbhogue, V., Folkestad, L., Nielsen, M. M. & Brixen, K. Bone microarchitecture and estimated strength in 499 adult Danish women and men: a cross-sectional, population-based high-resolution peripheral quantitative computed tomographic study on peak bone structure. *Calcif Tissue Int* **94**, 269-281, doi:10.1007/s00223-013-9808-5 (2014).
- 85 Burt, L. A., Hanley, D. A. & Boyd, S. K. Cross-sectional Versus Longitudinal Change in a Prospective HR-pQCT Study. **32**, 1505-1513, doi:10.1002/jbmr.3129 (2017).
- 86 Kawalilak, C. E., Johnston, J. D., Olszynski, W. P. & Kontulainen, S. A. Characterizing microarchitectural changes at the distal radius and tibia in postmenopausal women using HR-pQCT. *Osteoporos Int* **25**, 2057-2066, doi:10.1007/s00198-014-2719-0 (2014).
- 87 Burghardt, A. J. *et al.* A longitudinal HR-pQCT study of alendronate treatment in postmenopausal women with low bone density: Relations among density, cortical and trabecular microarchitecture, biomechanics, and bone turnover. *J Bone Miner Res* **25**, 2558-2571, doi:10.1002/jbmr.157 (2010).
- 88 Gabel, L., Macdonald, H. M., Nettlefold, L. & McKay, H. A. Physical Activity, Sedentary Time, and Bone Strength From Childhood to Early Adulthood: A Mixed Longitudinal HR-pQCT study. *J Bone Miner Res* **32**, 1525-1536, doi:10.1002/jbmr.3115 (2017).
- 89 Greenberg, M. V. C. & Bourc'his, D. The diverse roles of DNA methylation in mammalian development and disease. *Nat Rev Mol Cell Biol* **20**, 590-607, doi:10.1038/s41580-019-0159-6 (2019).
- 90 Teschendorff, A. E. & Relton, C. L. Statistical and integrative system-level analysis of DNA methylation data. *Nat Rev Genet*, doi:10.1038/nrg.2017.86 (2017).

- 91 Zhang, Y. *et al.* Overview of Histone Modification. *Adv Exp Med Biol* **1283**, 1-16, doi:10.1007/978-981-15-8104-5\_1 (2021).
- 92 Kouzarides, T. Chromatin modifications and their function. *Cell* **128**, 693-705, doi:10.1016/j.cell.2007.02.005 (2007).
- 93 Sims, R. J., 3rd, Nishioka, K. & Reinberg, D. Histone lysine methylation: a signature for chromatin function. *Trends Genet* **19**, 629-639, doi:10.1016/j.tig.2003.09.007 (2003).
- 94 Seto, E. & Yoshida, M. Erasers of histone acetylation: the histone deacetylase enzymes. *Cold Spring Harb Perspect Biol* **6**, a018713-a018713, doi:10.1101/cshperspect.a018713 (2014).
- 95 Meister, G. & Tuschl, T. Mechanisms of gene silencing by double-stranded RNA. *Nature* **431**, 343-349, doi:10.1038/nature02873 (2004).
- 96 Statello, L., Guo, C.-J., Chen, L.-L. & Huarte, M. Gene regulation by long non-coding RNAs and its biological functions. *Nature Reviews Molecular Cell Biology* **22**, 96-118, doi:10.1038/s41580-020-00315-9 (2021).
- 97 Wang, W. *et al.* Biological Function of Long Non-coding RNA (LncRNA) Xist. *Frontiers in Cell and Developmental Biology* **9**, doi:10.3389/fcell.2021.645647 (2021).
- 98 Woodcock, D. M., Crowther, P. J. & Diver, W. P. The majority of methylated deoxycytidines in human DNA are not in the CpG dinucleotide. *Biochem Biophys Res Commun* **145**, 888-894, doi:10.1016/0006-291x(87)91048-5 (1987).
- 99 Lock, L. F., Takagi, N. & Martin, G. R. Methylation of the Hprt gene on the inactive X occurs after chromosome inactivation. *Cell* **48**, 39-46, doi:10.1016/0092-8674(87)90353-9 (1987).
- 100 Holliday, R. & Grigg, G. W. DNA methylation and mutation. *Mutat Res* **285**, 61-67, doi:10.1016/0027-5107(93)90052-h (1993).
- 101 Illingworth, R. S. & Bird, A. P. CpG islands – ‘A rough guide’. *FEBS Letters* **583**, 1713-1720, doi:10.1016/j.febslet.2009.04.012 (2009).
- 102 Jones, P. A. Functions of DNA methylation: islands, start sites, gene bodies and beyond. *Nat Rev Genet* **13**, 484-492, doi:10.1038/nrg3230 (2012).
- 103 Chen, P. Y., Feng, S., Joo, J. W., Jacobsen, S. E. & Pellegrini, M. A comparative analysis of DNA methylation across human embryonic stem cell lines. *Genome Biol* **12**, R62, doi:10.1186/gb-2011-12-7-r62 (2011).
- 104 Leonhardt, H., Page, A. W., Weier, H. U. & Bestor, T. H. A targeting sequence directs DNA methyltransferase to sites of DNA replication in mammalian nuclei. *Cell* **71**, 865-873, doi:10.1016/0092-8674(92)90561-p (1992).
- 105 Okano, M., Xie, S. & Li, E. Cloning and characterization of a family of novel mammalian DNA (cytosine-5) methyltransferases. *Nat Genet* **19**, 219-220, doi:10.1038/890 (1998).
- 106 Li, D., Guo, B., Wu, H., Tan, L. & Lu, Q. TET Family of Dioxygenases: Crucial Roles and Underlying Mechanisms. *Cytogenet Genome Res* **146**, 171-180, doi:10.1159/000438853 (2015).
- 107 Hashimoto, H. *et al.* Recognition and potential mechanisms for replication and erasure of cytosine hydroxymethylation. *Nucleic Acids Res* **40**, 4841-4849, doi:10.1093/nar/gks155 (2012).

- 108 Branco, M. R., Ficz, G. & Reik, W. Uncovering the role of 5-hydroxymethylcytosine in the epigenome. *Nat Rev Genet* **13**, 7-13, doi:10.1038/nrg3080 (2011).
- 109 Naveh-Many, T. & Cedar, H. Active gene sequences are undermethylated. *Proc Natl Acad Sci U S A* **78**, 4246-4250, doi:10.1073/pnas.78.7.4246 (1981).
- 110 Watt, F. & Molloy, P. L. Cytosine methylation prevents binding to DNA of a HeLa cell transcription factor required for optimal expression of the adenovirus major late promoter. *Genes Dev* **2**, 1136-1143, doi:10.1101/gad.2.9.1136 (1988).
- 111 Yin, Y. *et al.* Impact of cytosine methylation on DNA binding specificities of human transcription factors. *Science* **356**, doi:10.1126/science.aaj2239 (2017).
- 112 Gal-Yam, E. N. *et al.* Frequent switching of Polycomb repressive marks and DNA hypermethylation in the PC3 prostate cancer cell line. *Proc Natl Acad Sci U S A* **105**, 12979-12984, doi:10.1073/pnas.0806437105 (2008).
- 113 Jones, P. A. The DNA methylation paradox. *Trends Genet* **15**, 34-37, doi:10.1016/s0168-9525(98)01636-9 (1999).
- 114 Wolf, S. F., Jolly, D. J., Lunnen, K. D., Friedmann, T. & Migeon, B. R. Methylation of the hypoxanthine phosphoribosyltransferase locus on the human X chromosome: implications for X-chromosome inactivation. *Proc Natl Acad Sci U S A* **81**, 2806-2810, doi:10.1073/pnas.81.9.2806 (1984).
- 115 Fraga, M. F. & Esteller, M. Epigenetics and aging: the targets and the marks. *Trends Genet* **23**, 413-418, doi:10.1016/j.tig.2007.05.008 (2007).
- 116 Martin, E. M. & Fry, R. C. Environmental Influences on the Epigenome: Exposure-Associated DNA Methylation in Human Populations. *Annual Review of Public Health* **39**, 309-333, doi:10.1146/annurev-publhealth-040617-014629 (2018).
- 117 Lillycrop, K. A., Hoile, S. P., Grenfell, L. & Burdge, G. C. DNA methylation, ageing and the influence of early life nutrition. *Proceedings of the Nutrition Society* **73**, 413-421, doi:10.1017/S0029665114000081 (2014).
- 118 Issa, J.-P. Aging and epigenetic drift: a vicious cycle. *The Journal of Clinical Investigation* **124**, 24-29, doi:10.1172/JCI69735 (2014).
- 119 Talens, R. P. *et al.* Epigenetic variation during the adult lifespan: cross-sectional and longitudinal data on monozygotic twin pairs. *Aging Cell* **11**, 694-703, doi:10.1111/j.1474-9726.2012.00835.x (2012).
- 120 Horvath, S. *et al.* Aging effects on DNA methylation modules in human brain and blood tissue. *Genome Biology* **13**, R97, doi:10.1186/gb-2012-13-10-r97 (2012).
- 121 Kananen, L. *et al.* The trajectory of the blood DNA methylome ageing rate is largely set before adulthood: evidence from two longitudinal studies. *AGE* **38**, 65, doi:10.1007/s11357-016-9927-9 (2016).
- 122 Simpkin, A. J. *et al.* Prenatal and early life influences on epigenetic age in children: a study of mother-offspring pairs from two cohort studies. *Human Molecular Genetics* **25**, 191-201, doi:10.1093/hmg/ddv456 (2015).
- 123 Hannum, G. *et al.* Genome-wide Methylation Profiles Reveal Quantitative Views of Human Aging Rates. *Molecular Cell* **49**, 359-367, doi:<https://doi.org/10.1016/j.molcel.2012.10.016> (2013).
- 124 Horvath, S. *et al.* An epigenetic clock analysis of race/ethnicity, sex, and coronary heart disease. *Genome biology* **17**, 171 (2016).

- 125 Horvath, S. *et al.* Decreased epigenetic age of PBMCs from Italian semi-supercentenarians and their offspring. *Aging* **7**, 1159-1170, doi:10.18632/aging.100861 (2015).
- 126 Lu, A. T. *et al.* DNA methylation GrimAge strongly predicts lifespan and healthspan. *Aging (Albany NY)* **11**, 303-327, doi:10.18632/aging.101684 (2019).
- 127 Levine, M. E. *et al.* An epigenetic biomarker of aging for lifespan and healthspan. *Aging (Albany NY)* **10**, 573-591, doi:10.18632/aging.101414 (2018).
- 128 Marioni, R. E. *et al.* DNA methylation age of blood predicts all-cause mortality in later life. *Genome Biology* **16**, 25, doi:10.1186/s13059-015-0584-6 (2015).
- 129 Marioni, R. E. *et al.* The epigenetic clock and telomere length are independently associated with chronological age and mortality. *International journal of epidemiology* **45**, 424-432 (2016).
- 130 Chen, B. H. *et al.* DNA methylation-based measures of biological age: Meta-analysis predicting time to death. *Aging* **8**, 1844-1865, doi:10.18632/aging.101020 (2016).
- 131 Zheng, Y. *et al.* Blood Epigenetic Age may Predict Cancer Incidence and Mortality. *EBioMedicine* **5**, 68-73, doi:<https://doi.org/10.1016/j.ebiom.2016.02.008> (2016).
- 132 Levine, M. E. *et al.* DNA methylation age of blood predicts future onset of lung cancer in the women's health initiative. *Aging* **7**, 690-700, doi:10.18632/aging.100809 (2015).
- 133 Gao, X., Zhang, Y., Breitling, L. P. & Brenner, H. Relationship of tobacco smoking and smoking-related DNA methylation with epigenetic age acceleration. *Oncotarget* **7**, 46878-46889, doi:10.18632/oncotarget.9795 (2016).
- 134 Breitling, L. P. *et al.* Frailty is associated with the epigenetic clock but not with telomere length in a German cohort. *Clinical Epigenetics* **8**, 21, doi:10.1186/s13148-016-0186-5 (2016).
- 135 Fried, L. P. *et al.* Frailty in older adults: evidence for a phenotype. *J Gerontol A Biol Sci Med Sci* **56**, M146-156, doi:10.1093/gerona/56.3.m146 (2001).
- 136 Gale, C. R., Marioni, R. E., Harris, S. E., Starr, J. M. & Deary, I. J. DNA methylation and the epigenetic clock in relation to physical frailty in older people: the Lothian Birth Cohort 1936. *Clin Epigenetics* **10**, 101, doi:10.1186/s13148-018-0538-4 (2018).
- 137 Quach, A. *et al.* Epigenetic clock analysis of diet, exercise, education, and lifestyle factors. *Aging (Albany NY)* **9**, 419-446, doi:10.18632/aging.101168 (2017).
- 138 Gale, C. R. *et al.* The epigenetic clock and objectively measured sedentary and walking behavior in older adults: the Lothian Birth Cohort 1936. *Clin Epigenetics* **10**, 4, doi:10.1186/s13148-017-0438-z (2018).
- 139 Belsky, D. W. *et al.* Eleven Telomere, Epigenetic Clock, and Biomarker-Composite Quantifications of Biological Aging: Do They Measure the Same Thing? *Am J Epidemiol* **187**, 1220-1230, doi:10.1093/aje/kwx346 (2018).
- 140 Marioni, R. E. *et al.* The epigenetic clock is correlated with physical and cognitive fitness in the Lothian Birth Cohort 1936. *Int J Epidemiol* **44**, 1388-1396, doi:10.1093/ije/dyu277 (2015).
- 141 Simpkin, A. J. *et al.* Are objective measures of physical capability related to accelerated epigenetic age? Findings from a British birth cohort. *BMJ Open* **7**, e016708, doi:10.1136/bmjopen-2017-016708 (2017).

- 142 Sillanpää, E. *et al.* Biological clocks and physical functioning in monozygotic female twins. *BMC Geriatr* **18**, 83, doi:10.1186/s12877-018-0775-6 (2018).
- 143 McCrory, C. *et al.* GrimAge Outperforms Other Epigenetic Clocks in the Prediction of Age-Related Clinical Phenotypes and All-Cause Mortality. *J Gerontol A Biol Sci Med Sci* **76**, 741-749, doi:10.1093/gerona/glaa286 (2021).
- 144 Maddock, J. *et al.* DNA Methylation Age and Physical and Cognitive Aging. *J Gerontol A Biol Sci Med Sci* **75**, 504-511, doi:10.1093/gerona/glz246 (2020).
- 145 Voisin, S. *et al.* An epigenetic clock for human skeletal muscle. *J Cachexia Sarcopenia Muscle*, doi:10.1002/jcsm.12556 (2020).
- 146 Yu, F. *et al.* Mendelian Randomization Identifies CpG Methylation Sites With Mediation Effects for Genetic Influences on BMD in Peripheral Blood Monocytes. *Front Genet* **11**, 60, doi:10.3389/fgene.2020.00060 (2020).
- 147 Fernandez-Rebollo, E. *et al.* Primary Osteoporosis Is Not Reflected by Disease-Specific DNA Methylation or Accelerated Epigenetic Age in Blood. *J Bone Miner Res* **33**, 356-361, doi:10.1002/jbmr.3298 (2018).
- 148 Delgado-Calle, J. *et al.* Genome-wide profiling of bone reveals differentially methylated regions in osteoporosis and osteoarthritis. *Arthritis Rheum* **65**, 197-205, doi:10.1002/art.37753 (2013).
- 149 Reppe, S. *et al.* Distinct DNA methylation profiles in bone and blood of osteoporotic and healthy postmenopausal women. *Epigenetics* **12**, 674-687, doi:10.1080/15592294.2017.1345832 (2017).
- 150 Reppe, S. *et al.* Eight genes are highly associated with BMD variation in postmenopausal Caucasian women. *Bone* **46**, 604-612, doi:10.1016/j.bone.2009.11.007 (2010).
- 151 Cheishvili, D. *et al.* Identification of an Epigenetic Signature of Osteoporosis in Blood DNA of Postmenopausal Women. *J Bone Miner Res* **33**, 1980-1989, doi:10.1002/jbmr.3527 (2018).
- 152 Del Real, A. *et al.* Differential analysis of genome-wide methylation and gene expression in mesenchymal stem cells of patients with fractures and osteoarthritis. *Epigenetics* **12**, 113-122, doi:10.1080/15592294.2016.1271854 (2017).
- 153 Morris, J. A. *et al.* Epigenome-wide Association of DNA Methylation in Whole Blood With Bone Mineral Density. *J Bone Miner Res* **32**, 1644-1650, doi:10.1002/jbmr.3148 (2017).
- 154 Soerensen, M. *et al.* Epigenome-wide exploratory study of monozygotic twins suggests differentially methylated regions to associate with hand grip strength. *Biogerontology* **20**, 627-647, doi:10.1007/s10522-019-09818-1 (2019).
- 155 Bell, J. T. *et al.* Epigenome-wide scans identify differentially methylated regions for age and age-related phenotypes in a healthy ageing population. *PLoS Genet* **8**, e1002629, doi:10.1371/journal.pgen.1002629 (2012).
- 156 Syddall, H. E. *et al.* The Hertfordshire Cohort Study: an overview. **8**, 82, doi:10.12688/f1000research.17457.1 (2019).
- 157 Dallosso, H. M. *et al.* Levels of customary physical activity among the old and the very old living at home. *Journal of Epidemiology and Community Health* **42**, 121-127, doi:10.1136/jech.42.2.121 (1988).
- 158 Shepherd, J. A. *et al.* Comparison of BMD precision for Prodigy and Delphi spine and femur scans. *Osteoporos Int* **17**, 1303-1308, doi:10.1007/s00198-006-0127-9 (2006).



- 159 Morrison, S. A., Petri, R. M., Hunter, H. L., Raju, D. & Gower, B. Comparison of the Lunar Prodigy and iDXA Dual-Energy X-ray Absorptiometers for Assessing Total and Regional Body Composition. *J Clin Densitom* **19**, 290-297, doi:10.1016/j.jocd.2015.06.003 (2016).
- 160 Boutroy, S., Buxsein, M. L., Munoz, F. & Delmas, P. D. In vivo assessment of trabecular bone microarchitecture by high-resolution peripheral quantitative computed tomography. *J. Clin. Endocrinol. Metab.* **90**, 6508-6515 (2005).
- 161 Pauchard, Y., Liphardt, A.-M., Macdonald, H. M., Hanley, D. A. & Boyd, S. K. Quality control for bone quality parameters affected by subject motion in high-resolution peripheral quantitative computed tomography. *Bone* **50**, 1304-1310 (2012).
- 162 MacNeil, J. A. & Boyd, S. K. Accuracy of high-resolution peripheral quantitative computed tomography for measurement of bone quality. *Med. Eng. Phys.* **29**, 1096-1105 (2007).
- 163 Laib, A., Hauselmann, H. J. & Ruegsegger, P. In vivo high resolution 3D-QCT of the human forearm. *Technol.Health Care* **6**, 329-337 (1998).
- 164 Vilayphiou, N. *et al.* Finite element analysis performed on radius and tibia HR-pQCT images and fragility fractures at all sites in men. *J. Bone Miner. Res.* **26**, 965-973 (2011).
- 165 Burghardt, A. J., Buie, H. R., Laib, A., Majumdar, S. & Boyd, S. K. Reproducibility of direct quantitative measures of cortical bone microarchitecture of the distal radius and tibia by HR-pQCT. *Bone* **47**, 519-528, doi:10.1016/j.bone.2010.05.034 (2010).
- 166 Whittier, D. E. *et al.* Guidelines for the assessment of bone density and microarchitecture in vivo using high-resolution peripheral quantitative computed tomography. doi:10.1007/s00198-020-05438-5 (2020).
- 167 Paggiosi, M. A., Eastell, R. & Walsh, J. S. Precision of high-resolution peripheral quantitative computed tomography measurement variables: influence of gender, examination site, and age. *Calcif Tissue Int* **94**, 191-201, doi:10.1007/s00223-013-9798-3 (2014).
- 168 *Infinium® Genotyping Data Analysis, A guide for analyzing Infinium genotyping data using the GenomeStudio® Genotyping Module,*  
<[https://www.illumina.com/Documents/products/technotes/technote\\_infinium\\_genotyping\\_data\\_analysis.pdf](https://www.illumina.com/Documents/products/technotes/technote_infinium_genotyping_data_analysis.pdf)> (
- 169 Purcell, S. *et al.* PLINK: a tool set for whole-genome association and population-based linkage analyses. *Am J Hum Genet* **81**, 559-575, doi:10.1086/519795 (2007).
- 170 Loh, P.-R. *et al.* Reference-based phasing using the Haplotype Reference Consortium panel. *Nature genetics* **48**, 1443-1448, doi:10.1038/ng.3679 (2016).
- 171 Estrada, K. *et al.* Genome-wide meta-analysis identifies 56 bone mineral density loci and reveals 14 loci associated with risk of fracture. *Nat. Genet.* **44**, 491-501 (2012).
- 172 McCall, M. N. & Irizarry, R. A. Thawing Frozen Robust Multi-array Analysis (fRMA). *BMC Bioinformatics* **12**, 369, doi:10.1186/1471-2105-12-369 (2011).
- 173 Ritchie, M. E. *et al.* limma powers differential expression analyses for RNA-sequencing and microarray studies. *Nucleic Acids Res* **43**, e47, doi:10.1093/nar/gkv007 (2015).
- 174 Bibikova, M. *et al.* High density DNA methylation array with single CpG site resolution. *Genomics* **98**, 288-295, doi:10.1016/j.ygeno.2011.07.007 (2011).

- 175 Pidsley, R. *et al.* Critical evaluation of the Illumina MethylationEPIC BeadChip microarray for whole-genome DNA methylation profiling. *Genome Biol* **17**, 208, doi:10.1186/s13059-016-1066-1 (2016).
- 176 Min, J. L., Hemani, G., Davey Smith, G., Relton, C. & Suderman, M. Meffil: efficient normalization and analysis of very large DNA methylation datasets. *Bioinformatics* **34**, 3983-3989, doi:10.1093/bioinformatics/bty476 (2018).
- 177 Aryee, M. J. *et al.* Minfi: a flexible and comprehensive Bioconductor package for the analysis of Infinium DNA methylation microarrays. *Bioinformatics* **30**, 1363-1369, doi:10.1093/bioinformatics/btu049 (2014).
- 178 Houseman, E. A. *et al.* DNA methylation arrays as surrogate measures of cell mixture distribution. *BMC Bioinformatics* **13**, 86, doi:10.1186/1471-2105-13-86 (2012).
- 179 Nordlund, J. *et al.* Genome-wide signatures of differential DNA methylation in pediatric acute lymphoblastic leukemia. *Genome Biology* **14**, r105, doi:10.1186/gb-2013-14-9-r105 (2013).
- 180 Zhou, W., Laird, P. W. & Shen, H. Comprehensive characterization, annotation and innovative use of Infinium DNA methylation BeadChip probes. *Nucleic Acids Research* **45**, e22-e22, doi:10.1093/nar/gkw967 (2016).
- 181 Gagnon-Bartsch, J. A. & Speed, T. P. Using control genes to correct for unwanted variation in microarray data. *Biostatistics* **13**, 539-552, doi:10.1093/biostatistics/kxr034 (2012).
- 182 Tian, Y. *et al.* ChAMP: updated methylation analysis pipeline for Illumina BeadChips. *Bioinformatics* **33**, 3982-3984, doi:10.1093/bioinformatics/btx513 (2017).
- 183 Leek, J. T., Johnson, W. E., Parker, H. S., Jaffe, A. E. & Storey, J. D. The sva package for removing batch effects and other unwanted variation in high-throughput experiments. *Bioinformatics* **28**, 882-883, doi:10.1093/bioinformatics/bts034 (2012).
- 184 Ong, M. L. & Holbrook, J. D. Novel region discovery method for Infinium 450K DNA methylation data reveals changes associated with aging in muscle and neuronal pathways. *Aging Cell* **13**, 142-155, doi:10.1111/accel.12159 (2014).
- 185 McGregor, R. A., Cameron-Smith, D. & Poppitt, S. D. It is not just muscle mass: a review of muscle quality, composition and metabolism during ageing as determinants of muscle function and mobility in later life. *Longev Healthspan* **3**, 9, doi:10.1186/2046-2395-3-9 (2014).
- 186 Sayer, A. A. *et al.* The developmental origins of sarcopenia. *J Nutr Health Aging* **12**, 427-432, doi:10.1007/bf02982703 (2008).
- 187 Patel, H. P. *et al.* Prevalence of sarcopenia in community-dwelling older people in the UK using the European Working Group on Sarcopenia in Older People (EWGSOP) definition: findings from the Hertfordshire Cohort Study (HCS). *Age Ageing* **42**, 378-384, doi:10.1093/ageing/afs197 (2013).
- 188 De Laet, C. *et al.* Body mass index as a predictor of fracture risk: a meta-analysis. *Osteoporos Int* **16**, 1330-1338, doi:10.1007/s00198-005-1863-y (2005).
- 189 Marcell, T. J. Sarcopenia: causes, consequences, and preventions. *J Gerontol A Biol Sci Med Sci* **58**, M911-916, doi:10.1093/gerona/58.10.m911 (2003).
- 190 Szulc, P., Duboeuf, F., Marchand, F. & Delmas, P. D. Hormonal and lifestyle determinants of appendicular skeletal muscle mass in men: the MINOS study. *Am J Clin Nutr* **80**, 496-503, doi:10.1093/ajcn/80.2.496 (2004).

- 191 Curtis, E., Litwic, A., Cooper, C. & Dennison, E. Determinants of Muscle and Bone Aging. *J Cell Physiol* **230**, 2618-2625, doi:10.1002/jcp.25001 (2015).
- 192 Xu, L., McElduff, P., D'Este, C. & Attia, J. Does dietary calcium have a protective effect on bone fractures in women? A meta-analysis of observational studies. *Br J Nutr* **91**, 625-634, doi:10.1079/bjn20031085 (2004).
- 193 Dawson-Hughes, B., Harris, S. S., Krall, E. A. & Dallal, G. E. Effect of calcium and vitamin D supplementation on bone density in men and women 65 years of age or older. *N Engl J Med* **337**, 670-676, doi:10.1056/nejm199709043371003 (1997).
- 194 Wilson, M. M. & Morley, J. E. Invited review: Aging and energy balance. *J Appl Physiol (1985)* **95**, 1728-1736, doi:10.1152/jappphysiol.00313.2003 (2003).
- 195 Volpi, E., Kobayashi, H., Sheffield-Moore, M., Mittendorfer, B. & Wolfe, R. R. Essential amino acids are primarily responsible for the amino acid stimulation of muscle protein anabolism in healthy elderly adults. *Am J Clin Nutr* **78**, 250-258, doi:10.1093/ajcn/78.2.250 (2003).
- 196 Kortebein, P., Ferrando, A., Lombeida, J., Wolfe, R. & Evans, W. J. Effect of 10 days of bed rest on skeletal muscle in healthy older adults. *Jama* **297**, 1772-1774, doi:10.1001/jama.297.16.1772-b (2007).
- 197 Bérard, A., Bravo, G. & Gauthier, P. Meta-analysis of the effectiveness of physical activity for the prevention of bone loss in postmenopausal women. *Osteoporos Int* **7**, 331-337, doi:10.1007/bf01623773 (1997).
- 198 Zampieri, S. *et al.* Lifelong physical exercise delays age-associated skeletal muscle decline. *J Gerontol A Biol Sci Med Sci* **70**, 163-173, doi:10.1093/gerona/glu006 (2015).
- 199 Law, M. R. & Hackshaw, A. K. A meta-analysis of cigarette smoking, bone mineral density and risk of hip fracture: recognition of a major effect. *Bmj* **315**, 841-846, doi:10.1136/bmj.315.7112.841 (1997).
- 200 Kanis, J. A. *et al.* Smoking and fracture risk: a meta-analysis. *Osteoporos Int* **16**, 155-162, doi:10.1007/s00198-004-1640-3 (2005).
- 201 Kanis, J. A. *et al.* Alcohol intake as a risk factor for fracture. *Osteoporos Int* **16**, 737-742, doi:10.1007/s00198-004-1734-y (2005).
- 202 Clark, E. M., Ness, A. & Tobias, J. H. Social position affects bone mass in childhood through opposing actions on height and weight. *J Bone Miner Res* **20**, 2082-2089, doi:10.1359/jbmr.050808 (2005).
- 203 Brennan, S. L. *et al.* Association between socioeconomic status and bone mineral density in adults: a systematic review. *Osteoporos Int* **22**, 517-527, doi:10.1007/s00198-010-1261-y (2011).
- 204 Dorosty, A., Arero, G., Chamar, M. & Tavakoli, S. Prevalence of Sarcopenia and Its Association with Socioeconomic Status among the Elderly in Tehran. *Ethiop J Health Sci* **26**, 389-396, doi:10.4314/ejhs.v26i4.11 (2016).
- 205 Swan, L., Warters, A. & O'Sullivan, M. Socioeconomic Inequality and Risk of Sarcopenia in Community-Dwelling Older Adults. *Clin Interv Aging* **16**, 1119-1129, doi:10.2147/cia.S310774 (2021).

- 206 Mansell, G. *et al.* Guidance for DNA methylation studies: statistical insights from the Illumina EPIC array. *BMC Genomics* **20**, 366, doi:10.1186/s12864-019-5761-7 (2019).
- 207 Peters, T. J. *et al.* De novo identification of differentially methylated regions in the human genome. *Epigenetics & Chromatin* **8**, 6, doi:10.1186/1756-8935-8-6 (2015).
- 208 Benjamini, Y. & Hochberg, Y. Controlling the False Discovery Rate: A Practical and Powerful Approach to Multiple Testing. *Journal of the Royal Statistical Society. Series B (Methodological)* **57**, 289-300 (1995).
- 209 Phipson, B., Maksimovic, J. & Oshlack, A. missMethyl: an R package for analyzing data from Illumina's HumanMethylation450 platform. *Bioinformatics* **32**, 286-288, doi:10.1093/bioinformatics/btv560 (2016).
- 210 Kuleshov, M. V. *et al.* Enrichr: a comprehensive gene set enrichment analysis web server 2016 update. *Nucleic Acids Res* **44**, W90-97, doi:10.1093/nar/gkw377 (2016).
- 211 Reimand, J. *et al.* Pathway enrichment analysis and visualization of omics data using g:Profiler, GSEA, Cytoscape and EnrichmentMap. *Nat Protoc* **14**, 482-517, doi:10.1038/s41596-018-0103-9 (2019).
- 212 Kanehisa, M., Furumichi, M., Sato, Y., Ishiguro-Watanabe, M. & Tanabe, M. KEGG: integrating viruses and cellular organisms. *Nucleic Acids Res* **49**, D545-d551, doi:10.1093/nar/gkaa970 (2021).
- 213 Kanehisa, M. Toward understanding the origin and evolution of cellular organisms. *Protein Sci* **28**, 1947-1951, doi:10.1002/pro.3715 (2019).
- 214 Kanehisa, M. & Goto, S. KEGG: kyoto encyclopedia of genes and genomes. *Nucleic Acids Res* **28**, 27-30, doi:10.1093/nar/28.1.27 (2000).
- 215 Ashburner, M. *et al.* Gene ontology: tool for the unification of biology. The Gene Ontology Consortium. *Nat Genet* **25**, 25-29, doi:10.1038/75556 (2000).
- 216 The Gene Ontology resource: enriching a GOld mine. *Nucleic Acids Res* **49**, D325-d334, doi:10.1093/nar/gkaa1113 (2021).
- 217 Köhler, S. *et al.* The Human Phenotype Ontology in 2017. *Nucleic Acids Res* **45**, D865-d876, doi:10.1093/nar/gkw1039 (2017).
- 218 Chen, E. Y. *et al.* Enrichr: interactive and collaborative HTML5 gene list enrichment analysis tool. *BMC Bioinformatics* **14**, 128, doi:10.1186/1471-2105-14-128 (2013).
- 219 Estrada, K. *et al.* Genome-wide meta-analysis identifies 56 bone mineral density loci and reveals 14 loci associated with risk of fracture. *Nat Genet* **44**, 491-501, doi:10.1038/ng.2249 (2012).
- 220 Fuggle, N. R. *et al.* Level and change in bone microarchitectural parameters and their relationship with previous fracture and established bone mineral density loci. *Bone* **147**, 115937, doi:10.1016/j.bone.2021.115937 (2021).
- 221 Patel, A. *et al.* Longitudinal Change in Peripheral Quantitative Computed Tomography Assessment in Older Adults: The Hertfordshire Cohort Study. *Calcif Tissue Int* **103**, 476-482, doi:10.1007/s00223-018-0442-0 (2018).
- 222 Rivadeneira, F. & Uitterlinden, A. G. in *Marcus and Feldman's Osteoporosis (Fifth Edition)* (eds David W. Dempster, Jane A. Cauley, Mary L. Bouxsein, & Felicia Cosman) 405-451 (Academic Press, 2021).

- 223 Bala, Y. *et al.* Trabecular and cortical microstructure and fragility of the distal radius in women. *J Bone Miner Res* **30**, 621-629, doi:10.1002/jbmr.2388 (2015).
- 224 Szulc, P., Seeman, E., Duboeuf, F., Sornay-Rendu, E. & Delmas, P. D. Bone fragility: failure of periosteal apposition to compensate for increased endocortical resorption in postmenopausal women. *J Bone Miner Res* **21**, 1856-1863, doi:10.1359/jbmr.060904 (2006).
- 225 Sternäng, O. *et al.* Factors associated with grip strength decline in older adults. *Age Ageing* **44**, 269-274, doi:10.1093/ageing/afu170 (2015).
- 226 Botosaneanu, A. *et al.* Cardiometabolic Risk, Socio-Psychological Factors, and Trajectory of Grip Strength Among Older Japanese Adults. *J Aging Health* **27**, 1123-1146, doi:10.1177/0898264315577587 (2015).
- 227 Frederiksen, H. *et al.* Age trajectories of grip strength: cross-sectional and longitudinal data among 8,342 Danes aged 46 to 102. *Ann Epidemiol* **16**, 554-562, doi:10.1016/j.annepidem.2005.10.006 (2006).
- 228 Burger, H. *et al.* Risk factors for increased bone loss in an elderly population: the Rotterdam Study. *Am J Epidemiol* **147**, 871-879, doi:10.1093/oxfordjournals.aje.a009541 (1998).
- 229 Hannan, M. T. *et al.* Risk factors for longitudinal bone loss in elderly men and women: the Framingham Osteoporosis Study. *J Bone Miner Res* **15**, 710-720, doi:10.1359/jbmr.2000.15.4.710 (2000).
- 230 Cawthon, P. M. *et al.* Loss of hip BMD in older men: the osteoporotic fractures in men (MrOS) study. *J Bone Miner Res* **24**, 1728-1735, doi:10.1359/jbmr.090419 (2009).
- 231 Karatas, O. F., Guzel, E., Duz, M. B., Ittmann, M. & Ozen, M. The role of ATP-binding cassette transporter genes in the progression of prostate cancer. *Prostate* **76**, 434-444, doi:10.1002/pros.23137 (2016).
- 232 Gao, J., Dai, C., Yu, X., Yin, X. B. & Zhou, F. Circ-TCF4.85 silencing inhibits cancer progression through microRNA-486-5p-targeted inhibition of ABCF2 in hepatocellular carcinoma. **14**, 447-461, doi:10.1002/1878-0261.12603 (2020).
- 233 Xiu, M. X., Zeng, B. & Kuang, B. H. Identification of hub genes, miRNAs and regulatory factors relevant for Duchenne muscular dystrophy by bioinformatics analysis. *Int J Neurosci*, 1-10, doi:10.1080/00207454.2020.1810030 (2020).
- 234 Verma, N., Ahuja, V. & Paul, J. Profiling of ABC transporters during active ulcerative colitis and in vitro effect of inflammatory modulators. *Dig Dis Sci* **58**, 2282-2292, doi:10.1007/s10620-013-2636-7 (2013).
- 235 Medina-Gomez, C. *et al.* Meta-analysis of genome-wide scans for total body BMD in children and adults reveals allelic heterogeneity and age-specific effects at the WNT16 locus. *PLoS Genet* **8**, e1002718, doi:10.1371/journal.pgen.1002718 (2012).
- 236 Fuggle, N. R. *et al.* Relationships between markers of inflammation and bone density: findings from the Hertfordshire Cohort Study. *Osteoporos Int* **29**, 1581-1589, doi:10.1007/s00198-018-4503-z (2018).
- 237 Movérare-Skrtic, S. *et al.* Osteoblast-derived WNT16 represses osteoclastogenesis and prevents cortical bone fragility fractures. *Nature medicine* **20**, 1279-1288, doi:10.1038/nm.3654 (2014).

- 238 Hildebrandt, S. *et al.* Glucocorticoids suppress Wnt16 expression in osteoblasts in vitro and in vivo. *Scientific reports* **8**, 8711-8711, doi:10.1038/s41598-018-26300-z (2018).
- 239 Koller, D. L. *et al.* Meta-analysis of genome-wide studies identifies WNT16 and ESR1 SNPs associated with bone mineral density in premenopausal women. *J Bone Miner Res* **28**, 547-558, doi:10.1002/jbmr.1796 (2013).
- 240 Zheng, H. F. *et al.* WNT16 influences bone mineral density, cortical bone thickness, bone strength, and osteoporotic fracture risk. *PLoS Genet* **8**, e1002745, doi:10.1371/journal.pgen.1002745 (2012).
- 241 Kemp, J. P. *et al.* Identification of 153 new loci associated with heel bone mineral density and functional involvement of GPC6 in osteoporosis. *Nature genetics* **49**, 1468-1475, doi:10.1038/ng.3949 (2017).
- 242 Dhingra, R. *et al.* Evaluating DNA methylation age on the Illumina MethylationEPIC Bead Chip. *PLoS One* **14**, e0207834, doi:10.1371/journal.pone.0207834 (2019).
- 243 McEwen, L. M. *et al.* Systematic evaluation of DNA methylation age estimation with common preprocessing methods and the Infinium MethylationEPIC BeadChip array. *Clin Epigenetics* **10**, 123, doi:10.1186/s13148-018-0556-2 (2018).
- 244 Rezwan, F. I. *et al.* Association of adult lung function with accelerated biological aging. *Aging (Albany NY)* **12**, 518-542, doi:10.18632/aging.102639 (2020).
- 245 Lee, Y. *et al.* Blood-based epigenetic estimators of chronological age in human adults using DNA methylation data from the Illumina MethylationEPIC array. *BMC Genomics* **21**, 747, doi:10.1186/s12864-020-07168-8 (2020).
- 246 Alsaleh, H. & Hadrill, P. R. Identifying blood-specific age-related DNA methylation markers on the Illumina MethylationEPIC® BeadChip. *Forensic Science International* **303**, 109944, doi:<https://doi.org/10.1016/j.forsciint.2019.109944> (2019).
- 247 El Khoury, L. Y. *et al.* Systematic underestimation of the epigenetic clock and age acceleration in older subjects. *Genome Biol* **20**, 283, doi:10.1186/s13059-019-1810-4 (2019).
- 248 Cronjé, H. T. *et al.* Comparison of DNA methylation clocks in Black South African men. *Epigenomics* **13**, 437-449, doi:10.2217/epi-2020-0333 (2021).
- 249 Kresovich, J. K. *et al.* Associations of Body Composition and Physical Activity Level With Multiple Measures of Epigenetic Age Acceleration. *Am J Epidemiol* **190**, 984-993, doi:10.1093/aje/kwaa251 (2021).
- 250 Pannacciulli, N. *et al.* C-reactive protein is independently associated with total body fat, central fat, and insulin resistance in adult women. *Int J Obes Relat Metab Disord* **25**, 1416-1420, doi:10.1038/sj.ijo.0801719 (2001).
- 251 Park, H. S., Park, J. Y. & Yu, R. Relationship of obesity and visceral adiposity with serum concentrations of CRP, TNF-alpha and IL-6. *Diabetes Res Clin Pract* **69**, 29-35, doi:10.1016/j.diabres.2004.11.007 (2005).
- 252 Ross, R., Fortier, L. & Hudson, R. Separate associations between visceral and subcutaneous adipose tissue distribution, insulin and glucose levels in obese women. *Diabetes Care* **19**, 1404-1411, doi:10.2337/diacare.19.12.1404 (1996).
- 253 Brochu, M. *et al.* Visceral adipose tissue is an independent correlate of glucose disposal in older obese postmenopausal women. *J Clin Endocrinol Metab* **85**, 2378-2384, doi:10.1210/jcem.85.7.6685 (2000).

- 254 Nieman, D. C. *et al.* Influence of obesity on immune function. *J Am Diet Assoc* **99**, 294-299, doi:10.1016/s0002-8223(99)00077-2 (1999).
- 255 Church, T. S. *et al.* Relative associations of fitness and fatness to fibrinogen, white blood cell count, uric acid and metabolic syndrome. *Int J Obes Relat Metab Disord* **26**, 805-813, doi:10.1038/sj.ijo.0802001 (2002).
- 256 Havel, P. J. Role of adipose tissue in body-weight regulation: mechanisms regulating leptin production and energy balance. *Proc Nutr Soc* **59**, 359-371, doi:10.1017/s0029665100000410 (2000).
- 257 Van Harmelen, V. *et al.* Leptin secretion from subcutaneous and visceral adipose tissue in women. *Diabetes* **47**, 913-917, doi:10.2337/diabetes.47.6.913 (1998).
- 258 Sharma, S., Tandon, V. R., Mahajan, S., Mahajan, V. & Mahajan, A. Obesity: Friend or foe for osteoporosis. *J Midlife Health* **5**, 6-9, doi:10.4103/0976-7800.127782 (2014).
- 259 Bauer, J. M. *et al.* Is There Enough Evidence for Osteosarcopenic Obesity as a Distinct Entity? A Critical Literature Review. *Calcif Tissue Int* **105**, 109-124, doi:10.1007/s00223-019-00561-w (2019).
- 260 Tamimi, I. *et al.* Composition and characteristics of trabecular bone in osteoporosis and osteoarthritis. *Bone* **140**, 115558, doi:<https://doi.org/10.1016/j.bone.2020.115558> (2020).
- 261 Burnett, W. D. *et al.* Proximal tibial trabecular bone mineral density is related to pain in patients with osteoarthritis. *Arthritis Research & Therapy* **19**, 200, doi:10.1186/s13075-017-1415-9 (2017).
- 262 Edwards, M. H. *et al.* Cluster analysis of bone microarchitecture from high resolution peripheral quantitative computed tomography demonstrates two separate phenotypes associated with high fracture risk in men and women. *Bone* **88**, 131-137, doi:10.1016/j.bone.2016.04.025 (2016).
- 263 Del Real, A., Riancho-Zarrabeitia, L. & Riancho, J. A. Epigenetic Aging in Osteoporosis. *J Bone Miner Res* **33**, 1902-1903, doi:10.1002/jbmr.3567 (2018).
- 264 Jakob, F., Ebert, R., Fernandez-Rebollo, E., Bischof, O. & Wagner, W. Response to Letter to the Editor: Epigenetic Aging in Osteoporosis. *J Bone Miner Res* **33**, 1904-1905, doi:10.1002/jbmr.3569 (2018).
- 265 Schweizer, A. *et al.* Human endothelin-converting enzyme (ECE-1): three isoforms with distinct subcellular localizations. *Biochem J* **328 ( Pt 3)**, 871-877, doi:10.1042/bj3280871 (1997).
- 266 Schröder, B. *et al.* Integral and associated lysosomal membrane proteins. *Traffic* **8**, 1676-1686, doi:10.1111/j.1600-0854.2007.00643.x (2007).
- 267 Padilla, B. E. *et al.* Endothelin-converting enzyme-1 regulates endosomal sorting of calcitonin receptor-like receptor and beta-arrestins. *J Cell Biol* **179**, 981-997, doi:10.1083/jcb.200704053 (2007).
- 268 Wang, L. S. *et al.* Endothelin-converting enzyme-1b C-338A polymorphism is associated with the increased risk of coronary artery disease in Chinese population. *Clin Chim Acta* **384**, 75-79, doi:10.1016/j.cca.2007.06.003 (2007).

- 269 Kowalczyk, A., Kleniewska, P., Kolodziejczyk, M., Skibska, B. & Goraca, A. The role of endothelin-1 and endothelin receptor antagonists in inflammatory response and sepsis. *Arch Immunol Ther Exp (Warsz)* **63**, 41-52, doi:10.1007/s00005-014-0310-1 (2015).
- 270 Hynynen, M. M. & Khalil, R. A. The vascular endothelin system in hypertension--recent patents and discoveries. *Recent Pat Cardiovasc Drug Discov* **1**, 95-108, doi:10.2174/157489006775244263 (2006).
- 271 Herrera, M. & Garvin, J. L. Endothelin stimulates endothelial nitric oxide synthase expression in the thick ascending limb. *Am J Physiol Renal Physiol* **287**, F231-235, doi:10.1152/ajprenal.00413.2003 (2004).
- 272 Marsen, T. A., Egink, G., Suckau, G. & Baldamus, C. A. Tyrosine-kinase-dependent regulation of the nitric oxide synthase gene by endothelin-1 in human endothelial cells. *Pflugers Arch* **438**, 538-544, doi:10.1007/s004249900079 (1999).
- 273 Tschakovsky, M. E. *et al.* Immediate exercise hyperemia in humans is contraction intensity dependent: evidence for rapid vasodilation. *J Appl Physiol (1985)* **96**, 639-644, doi:10.1152/jappphysiol.00769.2003 (2004).
- 274 Wray, D. W. *et al.* Progressive handgrip exercise: evidence of nitric oxide-dependent vasodilation and blood flow regulation in humans. *Am J Physiol Heart Circ Physiol* **300**, H1101-1107, doi:10.1152/ajpheart.01115.2010 (2011).
- 275 Rapoport, R. M. & Merkus, D. Endothelin-1 Regulation of Exercise-Induced Changes in Flow: Dynamic Regulation of Vascular Tone. *Frontiers in Pharmacology* **8**, doi:10.3389/fphar.2017.00517 (2017).
- 276 Hearon, C. M., Jr. & Dinunno, F. A. Regulation of skeletal muscle blood flow during exercise in ageing humans. *J Physiol* **594**, 2261-2273, doi:10.1113/jp270593 (2016).
- 277 Jendzjowsky, N. G. & Delorey, D. S. Short-term exercise training enhances functional sympatholysis through a nitric oxide-dependent mechanism. *The Journal of physiology* **591**, 1535-1549, doi:10.1113/jphysiol.2012.238998 (2013).
- 278 Crecelius, A. R., Kirby, B. S., Luckasen, G. J., Larson, D. G. & Dinunno, F. A. Mechanisms of rapid vasodilation after a brief contraction in human skeletal muscle. *Am J Physiol Heart Circ Physiol* **305**, H29-40, doi:10.1152/ajpheart.00298.2013 (2013).
- 279 Schrage, W. G., Eisenach, J. H. & Joyner, M. J. Ageing reduces nitric-oxide- and prostaglandin-mediated vasodilatation in exercising humans. *J Physiol* **579**, 227-236, doi:10.1113/jphysiol.2006.124313 (2007).
- 280 Trinity, J. D. *et al.* Contribution of nitric oxide to brachial artery vasodilation during progressive handgrip exercise in the elderly. *Am J Physiol Regul Integr Comp Physiol* **305**, R893-899, doi:10.1152/ajpregu.00311.2013 (2013).
- 281 Crecelius, A. R., Kirby, B. S., Voyles, W. F. & Dinunno, F. A. Nitric oxide, but not vasodilating prostaglandins, contributes to the improvement of exercise hyperemia via ascorbic acid in healthy older adults. *Am J Physiol Heart Circ Physiol* **299**, H1633-1641, doi:10.1152/ajpheart.00614.2010 (2010).
- 282 Laughlin, M. H. *et al.* Exercise-induced differential changes in gene expression among arterioles of skeletal muscles of obese rats. *J Appl Physiol (1985)* **119**, 583-603, doi:10.1152/jappphysiol.00316.2015 (2015).
- 283 Wood, A. R. *et al.* Defining the role of common variation in the genomic and biological architecture of adult human height. *Nature genetics* **46**, 1173-1186, doi:10.1038/ng.3097 (2014).



- 284 Kichaev, G. *et al.* Leveraging Polygenic Functional Enrichment to Improve GWAS Power. *Am J Hum Genet* **104**, 65-75, doi:10.1016/j.ajhg.2018.11.008 (2019).
- 285 Whipp, B. J. & Sargeant, A. *Physiological Determinants of Exercise Tolerance in Humans*. (Ashgate Publishing, 1999).
- 286 Ploegmakers, J. J., Hepping, A. M., Geertzen, J. H., Bulstra, S. K. & Stevens, M. Grip strength is strongly associated with height, weight and gender in childhood: a cross sectional study of 2241 children and adolescents providing reference values. *J Physiother* **59**, 255-261, doi:10.1016/s1836-9553(13)70202-9 (2013).
- 287 Hübel, C. *et al.* Genomics of body fat percentage may contribute to sex bias in anorexia nervosa. *Am J Med Genet B Neuropsychiatr Genet* **180**, 428-438, doi:10.1002/ajmg.b.32709 (2019).
- 288 Kanai, M. *et al.* Genetic analysis of quantitative traits in the Japanese population links cell types to complex human diseases. *Nature genetics* **50**, 390-400, doi:10.1038/s41588-018-0047-6 (2018).
- 289 Sinnott-Armstrong, N. *et al.* Genetics of 35 blood and urine biomarkers in the UK Biobank. *Nature genetics* **53**, 185-194, doi:10.1038/s41588-020-00757-z (2021).
- 290 Vuckovic, D. *et al.* The Polygenic and Monogenic Basis of Blood Traits and Diseases. *Cell* **182**, 1214-1231.e1211, doi:10.1016/j.cell.2020.08.008 (2020).
- 291 Chen, M. H. *et al.* Trans-ethnic and Ancestry-Specific Blood-Cell Genetics in 746,667 Individuals from 5 Global Populations. *Cell* **182**, 1198-1213.e1114, doi:10.1016/j.cell.2020.06.045 (2020).
- 292 Jansen, P. R. *et al.* Genome-wide analysis of insomnia in 1,331,010 individuals identifies new risk loci and functional pathways. *Nature genetics* **51**, 394-403, doi:10.1038/s41588-018-0333-3 (2019).
- 293 Jones, S. E. *et al.* Genome-wide association analyses of chronotype in 697,828 individuals provides insights into circadian rhythms. *Nat Commun* **10**, 343 (2019).  
<<http://europepmc.org/abstract/MED/30696823>
- <https://doi.org/10.1038/s41467-018-08259-7>
- <https://europepmc.org/articles/PMC6351539>
- <https://europepmc.org/articles/PMC6351539?pdf=render>>.
- 294 Gross, A. M. *et al.* Methylome-wide Analysis of Chronic HIV Infection Reveals Five-Year Increase in Biological Age and Epigenetic Targeting of HLA. *Mol Cell* **62**, 157-168, doi:10.1016/j.molcel.2016.03.019 (2016).
- 295 Mulder, R. H. *et al.* Epigenome-wide change and variation in DNA methylation in childhood: trajectories from birth to late adolescence. *Hum Mol Genet* **30**, 119-134, doi:10.1093/hmg/ddaa280 (2021).
- 296 Yang, B. Z. *et al.* Child abuse and epigenetic mechanisms of disease risk. *Am J Prev Med* **44**, 101-107, doi:10.1016/j.amepre.2012.10.012 (2013).
- 297 Islam, S. A. *et al.* Integration of DNA methylation patterns and genetic variation in human pediatric tissues help inform EWAS design and interpretation. *Epigenetics Chromatin* **12**, 1, doi:10.1186/s13072-018-0245-6 (2019).

- 298 Sharp, G. C. *et al.* Maternal BMI at the start of pregnancy and offspring epigenome-wide DNA methylation: findings from the pregnancy and childhood epigenetics (PACE) consortium. *Hum Mol Genet* **26**, 4067-4085, doi:10.1093/hmg/ddx290 (2017).
- 299 Zhu, Z. *et al.* Shared genetic and experimental links between obesity-related traits and asthma subtypes in UK Biobank. *J Allergy Clin Immunol* **145**, 537-549, doi:10.1016/j.jaci.2019.09.035 (2020).
- 300 Bradfield, J. P. *et al.* A trans-ancestral meta-analysis of genome-wide association studies reveals loci associated with childhood obesity. *Hum Mol Genet* **28**, 3327-3338, doi:10.1093/hmg/ddz161 (2019).
- 301 Cai, N. *et al.* Minimal phenotyping yields genome-wide association signals of low specificity for major depression. *Nat Genet* **52**, 437-447, doi:10.1038/s41588-020-0594-5 (2020).
- 302 Liu, M. *et al.* Association studies of up to 1.2 million individuals yield new insights into the genetic etiology of tobacco and alcohol use. *Nat Genet* **51**, 237-244, doi:10.1038/s41588-018-0307-5 (2019).
- 303 Brazel, D. M. *et al.* Exome Chip Meta-analysis Fine Maps Causal Variants and Elucidates the Genetic Architecture of Rare Coding Variants in Smoking and Alcohol Use. *Biol Psychiatry* **85**, 946-955, doi:10.1016/j.biopsych.2018.11.024 (2019).
- 304 Erzurumluoglu, A. M. *et al.* Meta-analysis of up to 622,409 individuals identifies 40 novel smoking behaviour associated genetic loci. *Mol Psychiatry* **25**, 2392-2409, doi:10.1038/s41380-018-0313-0 (2020).
- 305 *Gene Ontology: Unifying Biology*, <<http://geneontology.org/>> (
- 306 Lee, J., Hong, Y. S., Park, S.-H. & Kang, K. Y. High serum uric acid level is associated with greater handgrip strength in the aged population. *Arthritis research & therapy* **21**, 73-73, doi:10.1186/s13075-019-1858-2 (2019).
- 307 Molino-Lova, R. *et al.* Higher uric acid serum levels are associated with better muscle function in the oldest old: Results from the Mugello Study. *Eur J Intern Med* **41**, 39-43, doi:10.1016/j.ejim.2017.03.014 (2017).
- 308 Kawamoto, R. *et al.* Serum Uric Acid Is Positively Associated with Handgrip Strength among Japanese Community-Dwelling Elderly Women. *PLoS One* **11**, e0151044, doi:10.1371/journal.pone.0151044 (2016).
- 309 Ruth, K. S. *et al.* Using human genetics to understand the disease impacts of testosterone in men and women. *Nat Med* **26**, 252-258, doi:10.1038/s41591-020-0751-5 (2020).
- 310 Parahiba, S. M. *et al.* Effect of testosterone supplementation on sarcopenic components in middle-aged and elderly men: A systematic review and meta-analysis. *Exp Gerontol* **142**, 111106, doi:10.1016/j.exger.2020.111106 (2020).
- 311 Falqueto, H. *et al.* Can conditions of skeletal muscle loss be improved by combining exercise with anabolic-androgenic steroids? A systematic review and meta-analysis of testosterone-based interventions. *Rev Endocr Metab Disord* **22**, 161-178, doi:10.1007/s11154-021-09634-4 (2021).
- 312 Minică, C. C. *et al.* Genome-wide association meta-analysis of age at first cannabis use. *Addiction* **113**, 2073-2086, doi:10.1111/add.14368 (2018).
- 313 Agrawal, A., Suryakumar, G. & Rathor, R. Role of defective Ca(2+) signaling in skeletal muscle weakness: Pharmacological implications. *J Cell Commun Signal* **12**, 645-659, doi:10.1007/s12079-018-0477-z (2018).

- 314 Soysa, N. S. & Alles, N. Osteoclast function and bone-resorbing activity: An overview. *Biochem Biophys Res Commun* **476**, 115-120, doi:10.1016/j.bbrc.2016.05.019 (2016).
- 315 Lee, S. H. & Dominguez, R. Regulation of actin cytoskeleton dynamics in cells. *Mol Cells* **29**, 311-325, doi:10.1007/s10059-010-0053-8 (2010).
- 316 Syrovatkina, V. & Huang, X. Y. Signaling mechanisms and physiological functions of G-protein G $\alpha$ (13) in blood vessel formation, bone homeostasis, and cancer. *Protein Sci* **28**, 305-312, doi:10.1002/pro.3531 (2019).
- 317 Georgess, D., Machuca-Gayet, I., Blangy, A. & Jurdic, P. Podosome organization drives osteoclast-mediated bone resorption. *Cell Adh Migr* **8**, 191-204, doi:10.4161/cam.27840 (2014).
- 318 Weivoda, M. M. & Oursler, M. J. The Roles of Small GTPases in Osteoclast Biology. *Orthop Muscular Syst* **3**, doi:10.4172/2161-0533.1000161 (2014).
- 319 Wu, M. *et al.* G $\alpha$ 13 negatively controls osteoclastogenesis through inhibition of the Akt-GSK3 $\beta$ -NFATc1 signalling pathway. *Nat Commun* **8**, 13700, doi:10.1038/ncomms13700 (2017).
- 320 Troen, B. R. The role of cathepsin K in normal bone resorption. *Drug News Perspect* **17**, 19-28, doi:10.1358/dnp.2004.17.1.829022 (2004).
- 321 Liu, X., Zhang, Y., Tian, J. & Gao, F. Analyzing Genome-Wide Association Study Dataset Highlights Immune Pathways in Lip Bone Mineral Density. *Front Genet* **11**, 4, doi:10.3389/fgene.2020.00004 (2020).
- 322 Mullin, B. H. *et al.* Conditional testing of multiple variants associated with bone mineral density in the FLNB gene region suggests that they represent a single association signal. *BMC Genet* **14**, 107-107, doi:10.1186/1471-2156-14-107 (2013).
- 323 Krakow, D. *et al.* Mutations in the gene encoding filamin B disrupt vertebral segmentation, joint formation and skeletogenesis. *Nat Genet* **36**, 405-410, doi:10.1038/ng1319 (2004).
- 324 Zhou, X. *et al.* Filamin B deficiency in mice results in skeletal malformations and impaired microvascular development. *Proc Natl Acad Sci U S A* **104**, 3919-3924, doi:10.1073/pnas.0608360104 (2007).
- 325 Lu, J. *et al.* Filamin B mutations cause chondrocyte defects in skeletal development. *Hum Mol Genet* **16**, 1661-1675, doi:10.1093/hmg/ddm114 (2007).
- 326 Xu, Q., Wu, N., Cui, L., Wu, Z. & Qiu, G. Filamin B: The next hotspot in skeletal research? *J Genet Genomics* **44**, 335-342, doi:10.1016/j.jgg.2017.04.007 (2017).
- 327 Abdallah, D. *et al.* Effects of phospholipase D during cultured osteoblast mineralization and bone formation. *J Cell Biochem* **120**, 5923-5935, doi:10.1002/jcb.27881 (2019).
- 328 Thirukonda, G. J. *et al.* The dynamin inhibitor dynasore inhibits bone resorption by rapidly disrupting actin rings of osteoclasts. *J Bone Miner Metab* **34**, 395-405, doi:10.1007/s00774-015-0683-1 (2016).
- 329 Caplan, A. I. & Correa, D. PDGF in bone formation and regeneration: new insights into a novel mechanism involving MSCs. *J Orthop Res* **29**, 1795-1803, doi:10.1002/jor.21462 (2011).

- 330 Davies, O. G., Grover, L. M., Lewis, M. P. & Liu, Y. PDGF is a potent initiator of bone formation in a tissue engineered model of pathological ossification. *J Tissue Eng Regen Med* **12**, e355-e367, doi:10.1002/term.2320 (2018).
- 331 Papaioannou, G., Mirzamohammadi, F. & Kobayashi, T. Ras signaling regulates osteoprogenitor cell proliferation and bone formation. *Cell Death Dis* **7**, e2405-e2405, doi:10.1038/cddis.2016.314 (2016).
- 332 Xi, J. C. *et al.* The PI3K/AKT cell signaling pathway is involved in regulation of osteoporosis. *J Recept Signal Transduct Res* **35**, 640-645, doi:10.3109/10799893.2015.1041647 (2015).
- 333 Litwic, A. E., Westbury, L. D., Ward, K., Cooper, C. & Dennison, E. M. Adiposity and bone microarchitecture in the GLOW study. *Osteoporos Int* **32**, 689-698, doi:10.1007/s00198-020-05603-w (2021).
- 334 Dennison, E. M., Syddall, H. E., Aihie Sayer, A., Martin, H. J. & Cooper, C. Lipid profile, obesity and bone mineral density: the Hertfordshire Cohort Study. *Qjm* **100**, 297-303, doi:10.1093/qjmed/hcm023 (2007).
- 335 Watt, J. & Crilly, R. Location of Vertebral Fractures is Associated with Bone Mineral Density and History of Traumatic Injury. *Calcif Tissue Int* **100**, 412-419, doi:10.1007/s00223-017-0244-9 (2017).
- 336 Lems, W. F. *et al.* Vertebral fracture: epidemiology, impact and use of DXA vertebral fracture assessment in fracture liaison services. *Osteoporos Int* **32**, 399-411, doi:10.1007/s00198-020-05804-3 (2021).
- 337 Crabtree, N. J. *et al.* Amalgamated Reference Data for Size-Adjusted Bone Densitometry Measurements in 3598 Children and Young Adults-the ALPHABET Study. *J Bone Miner Res* **32**, 172-180, doi:10.1002/jbmr.2935 (2017).
- 338 Choksi, P., Jepsen, K. J. & Clines, G. A. The challenges of diagnosing osteoporosis and the limitations of currently available tools. *Clinical Diabetes and Endocrinology* **4**, 12, doi:10.1186/s40842-018-0062-7 (2018).
- 339 Warming, L., Hassager, C. & Christiansen, C. Changes in bone mineral density with age in men and women: a longitudinal study. *Osteoporos Int* **13**, 105-112, doi:10.1007/s001980200001 (2002).
- 340 Lauretani, F. *et al.* Longitudinal changes in BMD and bone geometry in a population-based study. *J Bone Miner Res* **23**, 400-408, doi:10.1359/jbmr.071103 (2008).
- 341 Laib, A., Hauselmann, H. J. & Ruegsegger, P. In vivo high resolution 3D-QCT of the human forearm. *Technol Health Care* **6**, 329-337 (1998).
- 342 Liu, C. T. *et al.* Visceral Adipose Tissue Is Associated With Bone Microarchitecture in the Framingham Osteoporosis Study. *J Bone Miner Res* **32**, 143-150, doi:10.1002/jbmr.2931 (2017).
- 343 de Jong, J. J. A. *et al.* Contra-lateral bone loss at the distal radius in postmenopausal women after a distal radius fracture: A two-year follow-up HRpQCT study. *Bone* **101**, 245-251, doi:10.1016/j.bone.2017.05.011 (2017).